Doctoral theses at NTNU, 2017:201

Xiaolong Lin

Systematics and evolutionary history of *Tanytarsus* van der Wulp, 1874 (Diptera: Chironomidae)

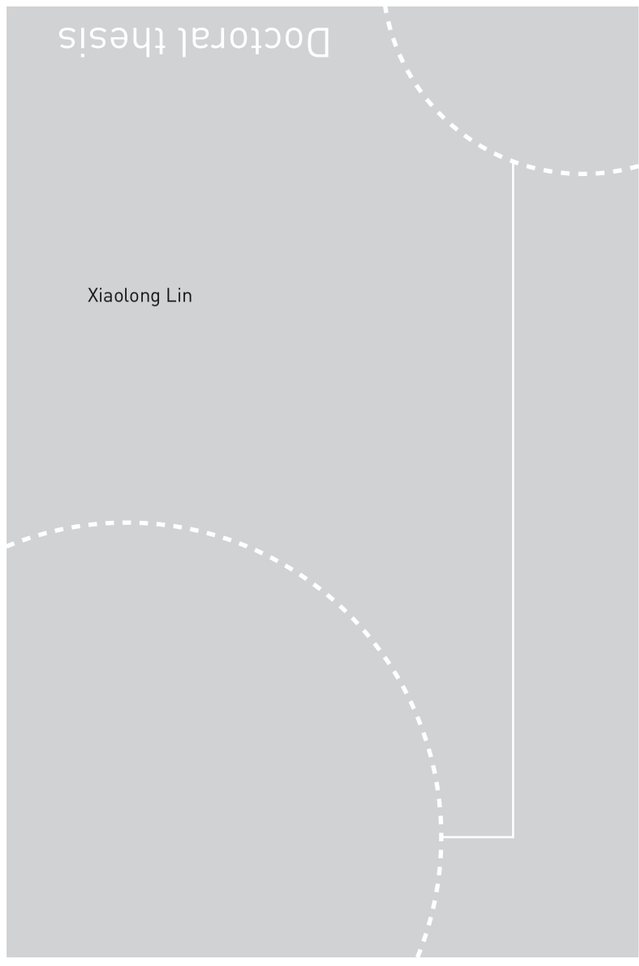

ISBN 978-82-326-2474-4 (printed ver.)
ISBN 978-82-326-2475-1 (electronic ver.)
ISSN 1503-8181

NTNU
Norwegian University of
Science and Technology

NTNU
Norwegian University of Science and Technology
Thesis for the Degree of
Philosophiae Doctor
Faculty of Natural Sciences
Department of Biology

Doctoral theses at NTNU, 2017:201

NTNU
Norwegian University of
Science and Technology

Xiaolong Lin

Systematics and evolutionary history of *Tanytarsus* van der Wulp, 1874 (Diptera: Chironomidae)

Thesis for the Degree of Philosophiae Doctor

Trondheim, June 2017

Norwegian University of Science and Technology
Faculty of Natural Sciences
Department of Biology

NTNU
Norwegian University of
Science and Technology

NTNU
Norwegian University of Science and Technology

Thesis for the Degree of Philosophiae Doctor

Faculty of Natural Sciences
Department of Biology

ISBN 978-82-326-2474-4 (printed ver.)
ISBN 978-82-326-2475-1 (electronic ver.)
ISSN 1503-8181

Doctoral theses at NTNU, 2017:201

Printed by NTNU Grafisk senter

Acknowledgements

When I tell my friends that I am working with non-biting midges, they find it both strange and interesting. Undertaking this PhD has been a truly life-changing experience for me and it would not have been possible without the support and guidance that I received from many people.

I have had great support and help from a lot of people, making the hard journey of finishing a PhD-thesis possible. First of all I would like to say a very big thank you to my supervisors, Torbjørn Ekrem and Elisabeth Stur, for all the support and encouragement they gave me. Without their guidance and constant feedback, I could not have finished this PhD thesis.

There are several people at the Department of Natural History I owe a great deal of thanks to too: Narcis Yousefi and Anders Lorentzen Kolstad for sharing offices, Hans K. Stenøien for teaching the phylogenetic courses, Renate Kvernberg and Torkild Bakken for administrative help, Aina Mærk Aspaas for photography guidance, Maria Capa and Erik Boström for assistance and recommendations. To all PhD and Master students at the museum, thank you so much for improving my workdays.

Many thanks to Xin-Hua Wang, Xin Qi, Chao Song, Wen-Bin Liu, Viktor Baranov, Wojciech Giłka, Natsuko Kondo, Richard Cornette, Koichiro Kawai, Yeon Jae Bae, Hyojeong Kang, Han-Il Ree Bing-Jiao Sun and Qiang Wang for sending material and sharing data. Many thanks to Akihiko Shinohara, Alan Lanford, Allison Brown, David Yeates, and Pol Limbourg for the loan of specimens. Also thanks to ForBio providing relevant courses.

Furthermore, I would like to say a heartfelt thank you to my family and friends for always believing in me and encourage me to follow my dreams.

The research in this thesis was funded by the NTNU University Museum.

Xiaolong Lin

Trondheim, April 2017

Contents

List of papers

I. Exploring genetic divergence in a species-rich insect genus using 2790 DNA barcodes. *Plos One* 2015, 10, e0138993.

II. DNA barcodes and morphology reveal new semi-cryptic species of Chironomidae (Diptera). (Submitted to *Insect Systematics & Evolution*)

III. Exploring species boundaries with multiple genetic loci using empirical data from non-biting midges. (Manuscript)

IV. Molecular phylogeny and temporal diversification of *Tanytarsus* (Diptera: Chironomidae) suggest generic synonyms, new classifications, and place of origin. (Manuscript)

All new taxonomic names and nomenclatorial decisions in this thesis are not to be regarded as valid until the individual papers are published in official journals.

Declaration of contributions

I performed all work on which this thesis is based. Torbjørn Ekrem and Elisabeth Stur contributed significantly to the initiating and planning of all papers and were involved in the writing of all papers. Conceived and designed the experiments: XL ES TE. Performed the experiments: XL. Analyzed the data: XL. Contributed reagents/materials/analysis tools: XL ES TE. Wrote the papers: XL ES TE.

Introduction

Biodiversity is important to our planet. This includes species diversity, genetic diversity and ecosystem diversity. As species is the fundamental unit of biodiversity, accurate species identification and delimitation are crucial in studying evolution, ecology, agriculture and conservation biology. Insect diversity and evolution has fascinated biologists for at least 260 years. Their enormous capacity for adaptation and radiation is unmatched by other multicellular organisms and makes many insect groups excellent models for studies of evolution and speciation. For instance, among the 271 papers have been published in the Molecular Phylogenetics and Evolution in 2016–2017, 20% are about insects.

The dipteran family Chironomidae, also called non-biting midges, is the most ubiquitous and most abundant insect group in all types of freshwater and even saltwater, sometimes inhabiting terrestrial and semi-terrestrial environments (Armitage et al. 1995). At present, there are more than 6,000 described species within eleven subfamilies worldwide (P. Ashe pers. comm.), and estimated up to 10–15,000 species (Armitage et al. 1995). Due to their high abundance and diversity, they are important as freshwater indicator organisms (Rosenberg 1992). Chironomids are an important food source for fishes, birds and bats. As some species can live in eutrophic water, chironomids can be biological filters of wastewaters (Armitage et al. 1995). A recent study shows that some flower-visiting chironomids are also potential pollinators (Kevan 2007). Since chironomids dates back to the Upper Triassic period (Cranston et al. 2012), they have also traditionally been used in studies of biogeography, most famously by Brundin (1966) in his classical study on transantarctic relationships.

This thesis focuses on systematics and evolutionary history of the genus *Tanytarsus* van der Wulp, 1874 within the Chironomidae.

Tanytarsus belongs to the tribe Tanytarsini within the subfamily Chironominae of family Chironomidae (Fig. 1). The genus contains more than 400 described species worldwide, which make it one of the most diverse genera in Chironomidae. Most immature stages of *Tanytarsus* occur in freshwater, but some species also populate marine or terrestrial environments (Epler et al. 2013; Sugimaru et al. 2008; Tokunaga 1933). One species is known to be dwelling in phytotelmata in bromeliads (Cranston 2007).

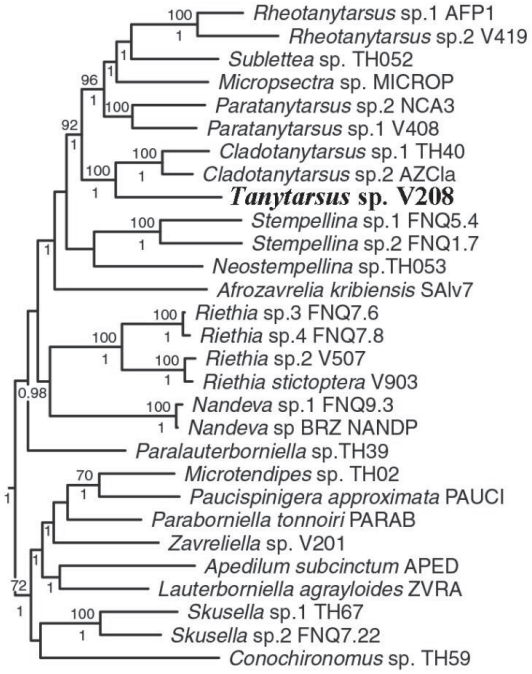

Figure 1. Subtree of Bayesian tree of Chironominae from Cranston et al. (2012). Branch support refers to ML bootstrap value over 70% (above branch) and posterior probability over 0.95 (below branch).

The genus *Tanytarsus* was erected by van der Wulp (1874) with *Tanytarsus signatus* (van der Wulp, 1859) as type species. *Tanytarsus* has nine generic synonyms: *Calopsectra* Kieffer, 1909; *Clinotanytarsus* Kieffer, 1921; *Ditanytarsus* Kieffer, 1921; *Fournieria* Kieffer, 1924; *Gymnotanytarsus* Goetghebuer, 1934; *Halotanytarsus* Tourenq, 1975; *Hexatanytarsus* Kieffer, 1921; *Tetratanytarsus* Kieffer, 1922; *Xenotanytarsus* Kieffer, 1921 (Ashe 1983). Most

Tanytarsus species have been described from the Holarctic region. Reiss and Fittkau (1971) revised the western Palaearctic *Tanytarsus*, and divided them into 13 species groups based on the morphological characters of adult males. Species belonging to the *eminulus*-, *gregarius*-, *lugens*- and *mendax*- species groups from Europe, North America and Japan were reviewed (Ekrem 2002, 2004; Ekrem et al. 2003). More comprehensive taxonomic revisions of *Tanytarsus* from Africa (Ekrem 2001b; Freeman 1958), Australia (Cranston 2000; Ekrem 2001a; Glover 1973) and the Neotropical region (Sanseverino 2006), have also been carried out as well as descriptions of single species (e.g. Chaudhuri et al. 1984; Ghonaim et al. 2004; Giłka & Paasivirta 2007, 2008, 2009; Sasa 1980; Sasa & Kawai 1987; Sublette 1964; Trivinho-Strixino & Strixino 2007; Trivinho-Strixino et al. 2015; Vinogradova et al. 2009). Despite all these studies, there are still many unknown and cryptic species to detect and describe, both in poorly explored parts like the eastern Palearctic and Oriental region but also in relatively well investigated areas.

Since the association between adults and immature stages through rearing is time-consuming, often with low success rates, *Tanytarsus* species have been defined and separated generally based on adult males only (Fig. 2). Cryptic species which are highly similar in adult males, may be separated by the morphological features of immature stages. Over the last decade, advancements in DNA sequencing technologies, bioinformatics and computational biology have provided large amounts of molecular data and improved the tools used to analyze them (Cristescu 2014; Garber et al. 2011; Goodwin et al. 2016; Mardis 2008; Metzker 2010; Scholz et al. 2012; van Dijk et al. 2014; Wagner et al. 2013). For instance, DNA barcoding (Hebert et al. 2003a; Hebert et al. 2003b), using short standardized genetic markers for species identification, has proven useful in biodiversity assessments (Hajibabaei et al. 2016; Lee et al. 2016) and taxonomic revisions (Miller et al. 2016). DNA barcoding can also demonstrate species community compositions, food webs and genetic variation within species (Baker et al.

2016; Littlefair & Clare 2016; Roslin & Majaneva 2016). Furthermore, DNA barcoding can play an important role in biosecurity (Ashfaq & Hebert 2016; Hodgetts et al. 2016) and biomonitoring of freshwater ecosystems (Brodin et al. 2013; Carew et al. 2013). Likewise, DNA barcodes can detect cryptic species diversity in many cases (Macher et al. 2016; Witt et al. 2006; Yang et al. 2012), and indicate species boundaries with additional morphological and ecological data. In Chironomidae, DNA barcodes have been proven efficient in species separation and uncovered several cryptic species (Anderson et al. 2013; Carew et al. 2011; Lin et al. 2015; Song et al. 2016; Stur & Ekrem 2015). Therefore, a continuously improved DNA barcode reference library of would immensely benefit our knowledge of life stages, species diversity and species boundaries as well as ecology and biogeography of this family.

Figure 2. *Tanytarsus occultus* Brundini, 1949, adult male.

Although DNA barcodes have improved our understanding of Chironomidae diversity, there are several biological processes that can obscure the evolutionary signal of a single marker. For instance, introgression (Gay et al. 2007; Martinsen et al. 2001) and incomplete lineage sorting (Ballard & Whitlock 2004; Heckman et al. 2007; Willyard et al. 2009) might lead to inaccurate conclusions on species boundaries. In addition, deep mitochondrial genetic

divergence is not always accompanied by correspondingly deep nuclear separation. For these reasons, the use of multiple loci can provide more convincing evidence for species boundaries, and validate cryptic lineages that are otherwise difficult to discern based on morphological characters.

There are several species delimitation methods that can be used to investigate species boundaries using genetic data. For example, in DNA barcoding one often focus on the so-called "barcode gap" which assumes that interspecific genetic distance should larger than intraspecific distance. Although some studies show that barcode gaps can disappear with increased geographical coverage (Bergsten et al. 2012), the Automatic Barcode Gap Discovery (ABGD) (Puillandre et al. 2012) has been proposed to sort the sequences into hypothetical species based on the barcode gap. Standard phylogenetic analyses relying on dichotomous splitting of ancestral branches can also be used to recognize species as phylogenetic monophyletic groups. Character-based, rigorously tested approaches include maximum parsimony (MP), maximum likelihood (ML) and Bayesian inference (BI). While these methods produce results that are based on similarities analyzed in a strictly framework, coalescent-based species delimitation methods combine population genetic and phylogenetic theory to provide objective means for delineating evolutionary significant units of diversity. For single genetic loci, the Generalized Mixed Yule Coalescent model (GMYC) (Pons et al. 2006; Zhang et al. 2013), the Poisson Tree Processes (PTP) are widely used to apply the phylogenetic species concept with assumed reciprocal monophyly in gene trees. However, gene trees can be different from each other and are not same as species trees due to processes like incomplete lineage sorting. Using coalescent-based methods on multiple loci can be therefore beneficial as it uncouples gene trees and species trees, and the gene tree coalescences are allowed to be older than species tree coalescences. It is recognized that coalescent-based Bayesian Phylogenetics and Phylogeography (BPP) method (Zhang et al.

2013) using multiple loci adopts the biological species concept, and can delineate closely related species (Yang 2015; Yang & Rannala 2010, 2017). Currently, only a few studies have compared the performance of these analytical methods for different genetic markers, especially considering the delineation of potentially cryptic species in insects.

Several molecular phylogenies on various groups in Chironomidae have been hypothesized (Allegrucci et al. 2006; Cranston & Krosch 2015; Ekrem et al. 2010; Huang & Cheng 2011; Martin et al. 2007; Papoucheva et al. 2003) and Cranston et al. (2012) have presented an evolutionary history for critical genera in all subfamilies using multiple DNA markers.

However, the phylogenetic relationships among *Tanytarsus* species and its closely related genera (*Caladomyia* Säwedal, 1981, *Corynocera* Zetterstedt, 1838, *Sublettea* Roback, 1975 and *Virgatanytarsus* Pinder, 1982) remain ambiguous. The only previous phylogenetic study on *Tanytarsus* conclude that morphology alone could not resolve the phylogeny of genus (Ekrem 2003), as missing data from immature life stages and high levels of homoplasy in available characters obscure the phylogenetic signal in parsimony analyses. Molecular phylogenetic analyses of the tribe Tanytarsini has been carried out using a single mitochondrial gene (COII), but the authors did not resolve the relationship between *Tanytarsus* and all the morphologically most similar genera (Ekrem & Willassen 2004). Nor was the taxonomic sampling sufficient to address the evolutionary relationships within *Tanytarsus* (Ekrem & Willassen 2004). Thus, a molecular phylogeny of *Tanytarsus* sensu lato using multiple molecular loci would provide considerable new knowledge on the evolutionary history of this species rich, widely distributed group of chironomids.

Aims of the thesis

The purpose of this thesis was to study the systematic and evolutionary history of *Tanytarsus* non-biting midges. Specifically, the aims of the thesis were:

(1) Build and improve the DNA barcode reference library of *Tanytarsus*, and detect misidentifications and cryptic species (Paper I).

(2) Explore the efficiency of DNA barcodes to delimit species in the diverse chironomid genus *Tanytarsus* by using 2790 DNA barcodes and different analytical tools (Paper I).

(3) Review species of the *T. curticornis* and *T. heusdensis* species complexes, diagnose and describe them based on morphology and DNA barcodes, and provide keys to adult males and known immatures (Paper II).

(4) Investigate if different molecular markers and analytical tools give similar results when applied to a set of morphologically similar species of Chironomidae, and see if the results are comparable to those achieved from DNA barcodes or morphological characters (Paper III).

(5) Test the monophyly of the species-rich genus *Tanytarsus* using multiple nuclear genetic markers (Paper IV).

(6) Infer the relationships among species of *Tanytarsus*, *Caladomyia*, *Corynocera*, *Sublettea* and *Virgatanytarsus* (Paper IV).

(7) Explore the biogeographical history of *Tanytarsus*, determine its likely place of origin and tempo of diversification (Paper IV).

Material and Methods

The specimens of *Tanytarsus* and related genera used in this study were obtained from many different parts of the world. My own field work was conducted with light traps, malaise traps and hand net mainly in Europe and China, but some fresh material from Canada, Japan, South Africa and South America was obtained by the help of various colleagues. Types of several *Tanytarsus* from Australia, Belgium, Canada, South Korea, and Japan were loaned for comparison with collected material. Most voucher specimens are deposited at the Department of Natural History, NTNU University Museum, Trondheim, Norway, while the remaining vouchers are deposited at the Department of Natural History, Bergen University Museum, Bergen, Norway and the College of Life and Sciences, Nankai University, Tianjin, China.

A dataset including 2790 COI sequences was generated in 2015 by combining own data with data available in BOLD and GenBank. The dataset was used to explore genetic divergence within and among species in *Tanytarsus* (Paper I). Moreover, a total of 67 specimens of *T. curticornis* and *T. heusdensis* species complexes were used for the analyses of species boundaries based on both morphological and molecular data (Paper II, III). Finally, a dataset including 111 *Tanytarsus* species, and 19 species from six related genera (*Caladomyia*, *Cladotanytarsus*, *Corynocera*, *Paratanytarsus*, *Rheotanytarsus Sublettea* and *Virgatanytarsus*) was used to explore the molecular phylogeny of *Tanytarsus* sensu lato (Paper IV).

Morphological analyses (Paper II)

For the morphological analyses of adults, pupae and larvae, the examined specimens were slide-mounted in Euparal following the procedures outlined by Sæther (1969). This ensured comparable measurements and observation of morphological characters. The morphological terminology and abbreviations used follow Sæther (1980) and specimens were identified under compound microscope using available taxonomic revisions and species descriptions

(Cranston 2000, 2007; Ekrem 2001b, 2002; Ekrem et al. 2003; Glover 1973; Lindeberg 1963, 1967; Reiss & Fittkau 1971; Sanseverino 2006; Sasa 1980; Sasa & Kawai 1987; Sublette & Sasa 1994; Trivinho-Strixino 2012; Trivinho-Strixino et al. 2015; Vinogradova et al. 2009). Taxonomic descriptions of Chironomidae most often include and refer to line drawings of characteristic body parts. However, digital photography of diagnostic characters, including male genitalia, has proven effective in some recent studies on Chironomidae (Przhiboro & Ekrem 2011; Stur & Ekrem 2011; Stur & Ekrem 2015). Thus, I used this approach to accurately display body coloration, wing setation and genitalia structures. Photo were taken using a Leica DFC420 camera mounted on a Leica DM6000 B compound microscope.

Molecular analyses (Paper I, III, IV)

I used a few different approaches to retrieve and analyze molecular data of *Tanytarsus* specimens in my possession: Genomic DNA was extracted no-destructively from thorax and head using QIAGEN® and GeneMole® DNA Tissue Kits. The standard COI barcode sequences of sampled specimens were amplified to contribute the barcode reference library of chironomids, while additional five nuclear markers (18S, AATS1, CAD, PGD and TPI) of selected specimens were amplified to address the phylogenetic questions and species boundaries. Raw sequences were assembled and edited using Sequencher 4.8 (Gene Codes Corp., Ann Arbor, Michigan, USA). The protein-coding gene sequences were aligned the Muscle algorithm (Edgar 2004) on the amino acids in MEGA 6 (Tamura et al. 2013). Detected introns of nuclear genes were removed using GT-AT rule (Rogers & Wall 1980). The 18S sequences were aligned with the Muscle algorithm in MEGA, and then the high variable regions were excluded using GBlocks v0.91b (Castresana 2000).

Substitution saturation tests of each gene were assessed using DAMBE v.5.5.25 (Xia 2013; Xia & Lemey 2009; Xia et al. 2003). PartitionFinder v1.1.1 (Lanfear et al. 2012) and

jModelTest 2.17 were used to find the best fitting nucleotide model for each gene and partitions of the concatenated datasets.

MEGA 6 was used to calculate K2P pairwise distances of COI barcode sequences to assess the intraspecific- and interspecific divergence as well as to generate the neighbor joining tree (Paper I). In paper I, I also analyzed the COI-dataset with Objective Clustering, ABGD, GMYC and PTP to estimate the number of molecular operational taxonomic units (OTUs). This was compared with the number of generated BINs in BOLD.

To delineate potential cryptic species detected by DNA barcodes of the *T. curticornis* and *T. heusdensis* species complexes, I added three additional nuclear markers (AATS1, CAD1 and PGD) to explore species boundaries using different analytical methods (ABGD, PTP, networks, GMYC and BPP models) and compared the performances of both markers and analytical approaches.

A concatenated nuclear gene dataset (18S, AATS1, CAD, PGD and TPI) was used to reconstruct the phylogeny of *Tanytarsus* sensu lato based on three methods: 1) Maximum likelihood (ML) using the software RAxML v8.2.X (Stamatakis 2006, 2014); 2) Maximum parsimony (MP) using PAUP 4.0b10 (Swofford 2002); 3) Bayesian inference using MrBayes 3.2.6 (Ronquist et al. 2012) and BEAST v1.8.2 (Drummond et al. 2012). Phylogenetic divergence times of *Tanytarsus* sensu lato were also estimated and calibrated using BEAST v1.8.2. The event-based method S-DIVA (statistical dispersal-vicariance analysis) (Yu et al. 2010) was used to infer the biogeographical history of the included taxa and to estimate the most likely ancestral area.

Results and Discussion

Over the last four years, I have collected a large material of *Tanytarsus* from the eastern Palaearctic and Oriental Regions. Among these new specimens and previous collections from China, 52 *Tanytarsus* species were identified, including ten species new to science, eight junior synonyms, five misidentifications and six new combinations. Ideally, this new information could have been included as a fifth taxonomic revisionary paper in the present PhD thesis, but the task was just too large to be completed within the time frame of the study. However, as it is important for the advancement of Chironomidae taxonomy, particularly in the eastern Palearctic and Oriental Regions, I do intend to complete this work after finishing the PhD.

DNA barcode analyses of *Tanytarsu*s (Paper I)

In general, the discrimination of *Tanytarsus* species by 2790 DNA barcodes was highly successful with unambiguous grouping of 94.6% of the species recognized by prior morphological study. A neighbor joining tree of DNA barcodes (Fig. 3) comprised131 well separated clusters representing 121 morphological species of *Tanytarsus*, and also revealed some misidentifications or synonyms. The average intraspecific K2P divergence was 2.14%, while the average interspecific divergence was 15.9%. Deep intraspecific divergence existed in eleven morphospecies complexes, indicating potential cryptic species. Therefore, no clear 'barcode gap' was observed in the large dataset. The DNA barcodes clustered into 120–242 molecular OTUs depending on whether Objective Clustering, ABGD, GMYC, PTP, subjective evaluation of the neighbor joining tree or BINs was used. The ABGD and Objective Clustering more accurately reflected the morphological species in the large dataset. Our result revealed that a fixed threshold for delineating species using COI sequences is inappropriate for many *Tanytarsus* non-biting midges. While a 2% threshold has proven

effective in identifications at the species level of Ephemeroptera (Schmidt et al. 2015; Webb et al. 2012; Zhou et al. 2010), Lepidoptera (Zahiri et al. 2014) and Trichoptera (Zhou et al. 2016), a 2.2% threshold of Heteroptera (Knebelsberger et al. 2014), a 2.5% threshold of aquatic beetles (Monaghan et al. 2005), and a >3% threshold for several dipteran groups (Nzelu et al. 2015; Renaud et al. 2012), our results suggest that a 4–5% threshold is more appropriate for species delimitation in genus *Tanytarsus*. This corresponds well with previous findings for other chironomids.

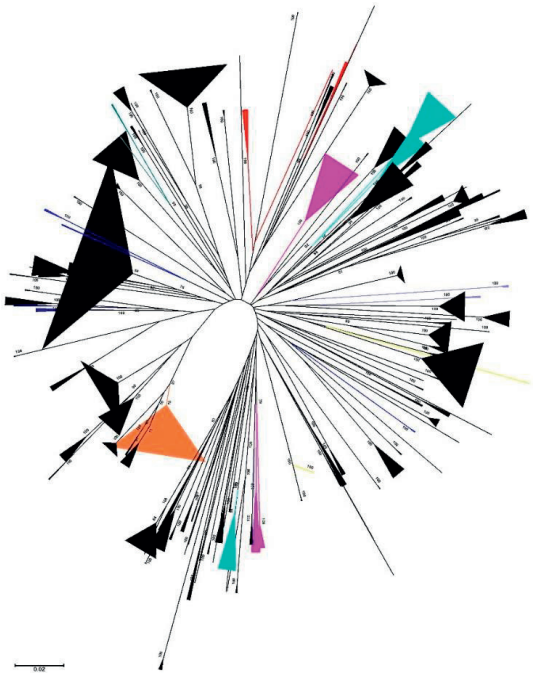

Figure 3. Neighbor joining bootstrap consensus tree for 2790 *Tanytarsus* barcodes. Numbers on branches are bootstrap support (>70%) using 500 bootstrap replicates. The colourized clusters indicate cryptic species or misidentifications.

Previous to our study, there were 84 morphospecies with 2036 DNA barcodes of *Tanytarsus* in the Barcode of Life Data System (June 2014, Fig. 4). Including our efforts as well as those of many colleagues, there are now 147 morphospecies with 13974 DNA barcodes of *Tanytarsus* in BOLD (April 2017, Fig. 5). Thus, within few years, the number of species have nearly doubled. However, taxon sampling is biased towards northwestern Europe, China and

North America, while few species from the eastern Palearctic and Afrotropical regions have been barcoded. There is a long way to go before a complete DNA barcode reference of *Tanytarsus* is available.

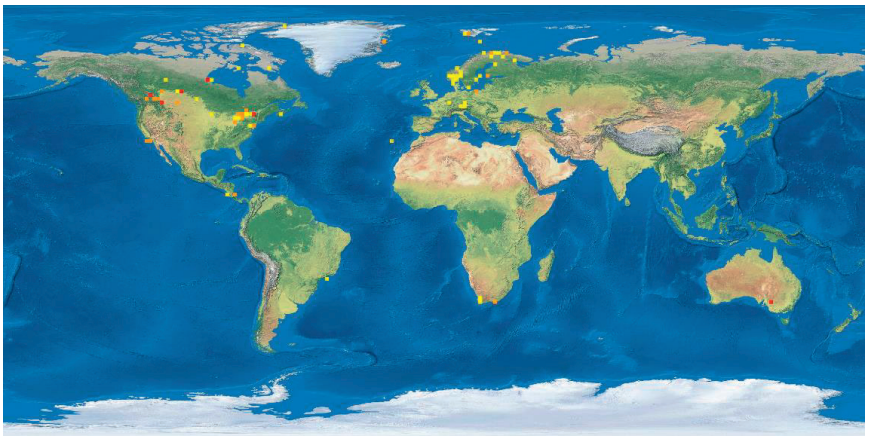

Figure 4. Collection sites of barcoded *Tanytarsus* specimens on BOLD as of June 11, 2014.

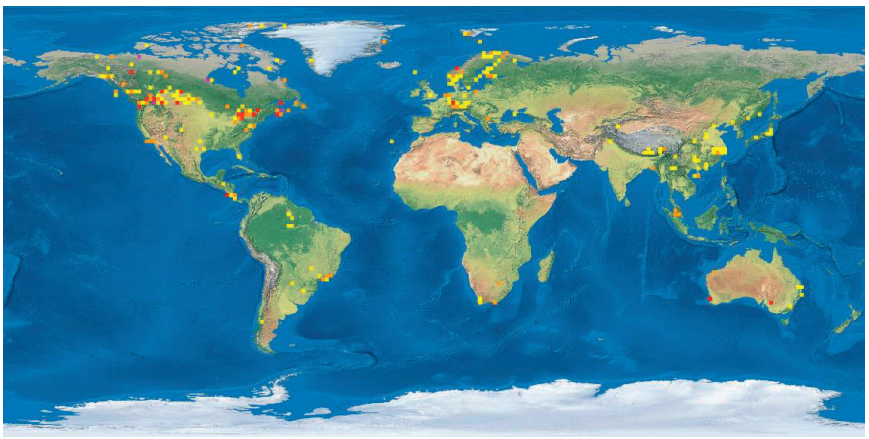

Figure 5. Collection sites of barcoded *Tanytarsus* specimens on BOLD as of April 24, 2017.

Species boundaries in *Tanytarsus* (Paper II, III)

Based on COI barcodes of species within the *T. curticornis* species complex, the neighbor joining tree (Fig. 6) indicated nine distinct genetic lineages, of which six could not be assigned to any described morphospecies. The neighbor joining tree based on COI barcodes of species of the *T. heusdensis* species complex (Fig. 7) revealed five genetic different

lineages. However, unusual deep intraspecific K2P divergence in COI barcodes existed in both species complexes. The maximum intraspecific divergence was 9.8% in the *T. curticornis* species complex, and 8.6% in the *T. heusdensis* species complex.

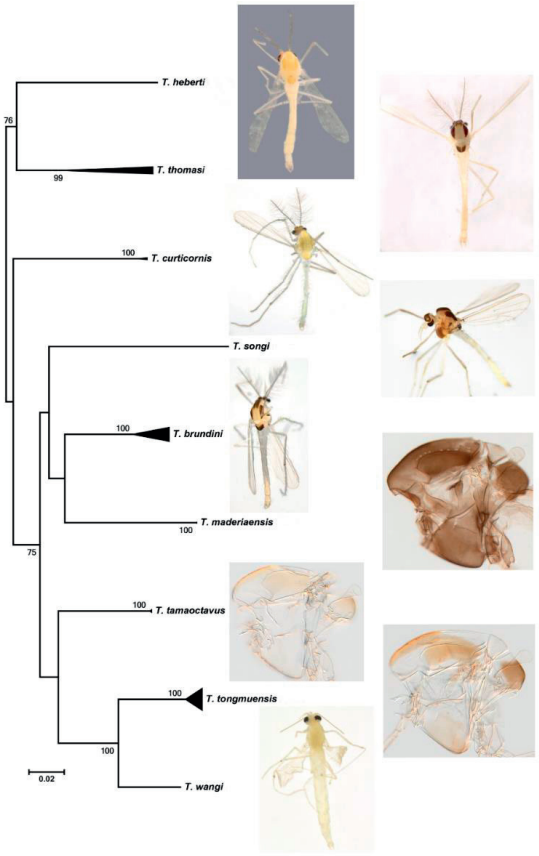

Figure 6. Neighbor joining tree for nine morphospecies of the *Tanytarsus curticornis* species complex based on K2P distances in DNA barcodes. Numbers on branches represent bootstrap support (>70%) based on 1000 replicates; scale equals K2P genetic distance; figures show the full body or thorax of adult males of each corresponding morphospecies.

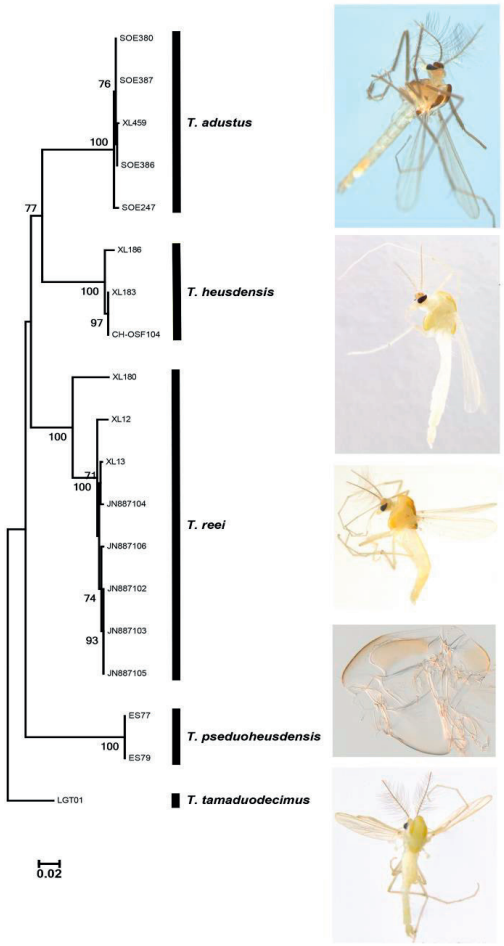

Figure 7. Neighbor joining tree for five species of the *Tanytarsus heusdensis* species complex based on K2P distances in DNA barcodes. Numbers on branches represent bootstrap support (>70%) based on 1000 replicates; scale equals K2P genetic distance; figures show the full body or thorax of adult males of each corresponding morphospecies.

Species delimitation based on COI alone can lead to inaccurate species delimitation as a result of recent speciation and incomplete lineage sorting (Meier et al. 2006). Thus, I compared the results from analyses of COI with those of three selected nuclear markers (AATS1, CAD1 and PGD) using ABGD, GMYC, PTP, parsimony networks and BPP approaches. The results revealed that species delimitation based on multiple nuclear DNA markers performed more

accurately (relative to identified morphospecies) than those based on a single locus. Moreover, ABGD, GMYC, PTP and network models arrived at conflicting results based on a single locus and delineated species differently than morphology. Results from BPP analyses on multiple loci corresponded best with the current morphological species concept. A conflicting result between mitochondrial and nuclear genes was found in populations of *Tanytarsus brundini*. The populations showed deep divergence in all nuclear markers while their COI sequences were close to identical. This pattern might have a result of recent hybridization between cryptic species, but a wider geographical sampling of *Tanytarsus* brundini is needed to explore this phenomenon in detail.

Based on the observed genetic divergences, we discussed the diagnostic characters of these complexes, and found that some previously ignored morphological characters (e.g. body coloration and wing setation) can be used separate the semi-cryptic species in the species complex. Thus, after taxonomic revision of the species belonging to the *T. curticornis* and *T. heusdensis* species complexes, eight species new to science were described and illustrated: *T. adustus* sp. n., *T. heberti* sp. n., *T. madeiraensis* sp. n., *T. pseudoheusdensis* sp. n., *T. song* sp. n., *T. thomasi* sp. n., *T. tongmuensis* sp. n. and *T. wangi* sp. n.. Additionally, *Tanytarsus reei* and *T. tamaoctavus* were re-described, and the remaining species within complexes were also discussed. *Tanytarsus tusimatneous* was synonymized with *T. tamaduodecimus* and keys to males and known pupae of the two species complexes were developed.

An even more comprehensive sampling of species in the *T. curticornis* and *T. heusdensis* species complexes, in particular of the immature life stages, could provide more morphological characters to separate species in these groups. Nevertheless, our results show that integrative taxonomy combing morphological and molecular provides more accurate results in species delimitation of closely related taxa.

Phylogeny of *Tanytarsus* sensu lato (Paper IV)

Our results revealed that *Tanytarsus* is paraphyletic with *Caladomyia* placed among South American *Tanytarsus*, *Virgatanytarsus* within a Gondwanan clade (Fig. 8), and *Corynocera* within the *T. norvegicus* species group, indicating three generic synonyms. As expected, *T. rhabdomantis* grouped with other Neotropical *Tanytarsus* and confirmed the synonymy of *Nimbocera* within *Tanytarsus*, and *Sublettea* remained valid. According to the genetic and morphological data, eight new monophyletic species groups (the *aterrimus*-, *curticornis*-, *giovannii*-, *heusdensis*-, *kiche*-, *motosuensis*-, *tamakutibasi*- and *thaicus* species groups) were proposed. Moreover, some previously postulated *Tanytarsus* species groups (*aculeatus*-, *excavatus*-, *norvegicus*-, *pallidicornis*-, *signatus*- and *verralli*- species groups) are recovered as monophyletic. The species previously placed in the *eminulus*-, *gregarius*-, *lugens*-, *mcmillani*- and *mendax* species groups are well supported and sister to the *motosuensis* + *norvegicus* species groups. However, the phylogenetic relationships between these groups remain uncertain, suggesting that they perhaps should be regarded as one group.

The results of molecular divergence time estimates revealed that genus *Tanytarsus* diverged from its sister group *Cladotanytarsus* during the late Cretaceous and early Paleogene (61.28–78.54 Mya). According to the results of S-DIVA analyses under three different division schemes for zoogeographical regions, the genus most likely originated in the Old World (Oriental- and Palearctic regions) with subsequent dispersal and vicariance events leading to radiation across most continents in the word.

The analyses were likely influenced by some sampling bias as more species from the Palearctic than from other biogeographical regions were included. Thus, differences in phylogenetic diversity could have obscured some of the true evolutionary and biogeographic

history of *Tanytarsus*. A broader geographical sampling in the future will reveal if the biogeographical hypotheses presented are supported or refused.

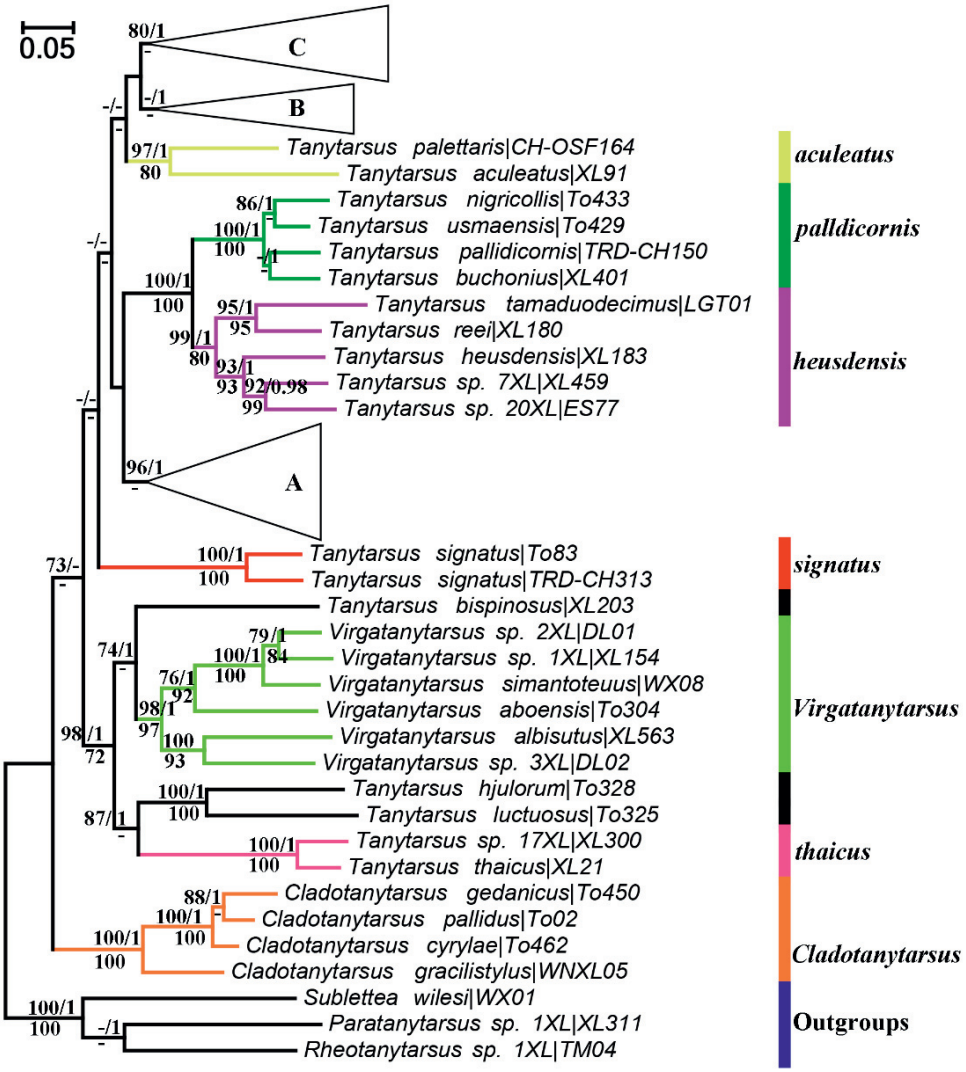

Figure 8. Maximum likelihood tree based on the concatenated DNA dataset (18S, AATS1, CAD1, CAD4, PGD and TPI) of *Tanytarsus* sensu lato showing *Virgatanytarsus* placed among basal *Tanytarsus* species. Branch support refers to ML bootstrap value over 70% and posterior probability over 0.95 (above branches), MP bootstrap values over 70% below branches.

Conclusion

The results presented in this thesis contribute to an increased knowledge of the systematic and evolutionary history of *Tanytarsus* non-biting midges on different levels. My findings indicate that the paraphyletic genus *Tanytarsus* diverged from *Cladotanytarsus* during the late Cretaceous and early Paleogene (61.28–78.54 Mya), and most likely originated in the Oriental and Palearctic regions. Consecutive radiation in all geographical regions except Antarctica has led to the widely distributed diversity we see today. While DNA barcodes are very useful in detecting and documenting this species diversity, natural processes can obscure species boundaries when only one marker is used. Likewise, cryptic species cannot be easily separated from each other based on morphology alone. Thus, an integrative approach that combines morphology and genetic data from multiple loci is sometimes needed to improve our understanding of species boundaries in *Tanytarsus*. Although increased geographical sampling will contribute to a more comprehensive DNA barcode reference library and an even better understanding of speciation and evolutionary history in *Tanytarsus*, my results provide well-supported hypotheses for future testing.

References

Allegrucci, G., Carchini, G., Todisco, V., Convey, P. & Sbordoni, V. (2006) A molecular phylogeny of Antarctic Chironomidae and its implications for biogeographical history. *Polar Biology* **29:** 320–326.

Anderson, A.M., Stur, E. & Ekrem, T. (2013) Molecular and morphological methods reveal cryptic diversity and three new species of Nearctic *Micropsectra* (Diptera: Chironomidae). *Freshwater Science* **32:** 892–921.

Armitage, P.D., Cranston, P.S. & Pinder, L.C.V. (1995) The Chironomidae: Biology and ecology of non-biting midges: Chapman & Hall, London. XII, 572.

Ashe, P. (1983) A catalog of chironomid genera and subgenera of the world including synonyms (Diptera, Chironomidae). *Entomologica Scandinavica, Supplement* **17:** 1–68.
Ashfaq, M. & Hebert, P.D.N. (2016) DNA barcodes for bio-surveillance: regulated and economically important arthropod plant pests. *Genome* **59:** 933–945.
Baker, C.C., Bittleston, L.S., Sanders, J.G. & Pierce, N.E. (2016) Dissecting host-associated communities with DNA barcodes. *Philosophical Transactions of the Royal Society B: Biological Sciences* **371:** 20150328.
Ballard, J.W.O. & Whitlock, M.C. (2004) The incomplete natural history of mitochondria. *Molecular Ecology* **13:** 729–744.
Bergsten, J., Bilton, D.T., Fujisawa, T., Elliott, M., Monaghan, M.T., Balke, M., Hendrich, L., Geijer, J., Herrmann, J., Foster, G.N., Ribera, I., Nilsson, A.N., Barraclough, T.G. & Vogler, A.P. (2012) The effect of geographical scale of sampling on DNA barcoding. *Systematic Biology* **61:** 851–869.
Brodin, Y., Ejdung, G., Strandberg, J. & Lyrholm, T. (2013) Improving environmental and biodiversity monitoring in the Baltic Sea using DNA barcoding of Chironomidae (Diptera). *Molecular Ecology Resources* **13:** 996–1004.
Brundin, L. (1966) Transantarctic relationships and their significance, as evidenced by chironomid midges with a monograph of the subfamilies Podonominae and Aphroteniinae and the austral Heptagynae. *Kongliga Svenska Vetenskaps Academiens nya Handlingar* **11:** 1–472.
Carew, M.E., Marshall, S.E. & Hoffmann, A.A. (2011) A combination of molecular and morphological approaches resolves species in the taxonomically difficult genus *Procladius* Skuse (Diptera: Chironomidae) despite high intra-specific morphological variation. *Bulletin of Entomological Research* **101:** 505–519.
Carew, M.E., Pettigrove, V.J., Metzeling, L. & Hoffmann, A.A. (2013) Environmental monitoring using next generation sequencing: rapid identification of macroinvertebrate bioindicator species. *Frontiers in Zoology* **10:** 45.
Castresana, J. (2000) Selection of conserved blocks from multiple alignments for their use in phylogenetic analysis. *Molecular Biology and Evolution* **17:** 540–552.
Chaudhuri, P.K., Guha, D.K. & Ghosh, M. (1984) Tanytarsini (Diptera, Chironomidae) from India. *Oriental Insects* **18:** 31–41.
Cranston, P.S. (2000) Monsoonal tropical *Tanytarsus* van der Wulp (Diptera: Chironomidae) reviewed: New species, life histories and significance as aquatic environmental indicators. *Australian Journal of Entomology* **39:** 138–159.
Cranston, P.S. (2007) A new species for a bromeliad phytotelm-dwelling *Tanytarsus* (Diptera: Chironomidae). *Annals of the Entomological Society of America* **100:** 617–622.
Cranston, P.S., Hardy, N.B. & Morse, G.E. (2012) A dated molecular phylogeny for the Chironomidae (Diptera). *Systematic Entomology* **37:** 172–188.
Cranston, P.S. & Krosch, M.N. (2015) DNA sequences and austral taxa indicate generic synonymy of *Paratrichocladius* Santos-Abreu with *Cricotopus* Wulp (Diptera: Chironomidae). *Systematic Entomology* **40:** 719–732.
Cristescu, M.E. (2014) From barcoding single individuals to metabarcoding biological communities: towards an integrative approach to the study of global biodiversity. *Trends in Ecology & Evolution* **29:** 566–571.
Drummond, A.J., Suchard, M.A., Xie, D. & Rambaut, A. (2012) Bayesian phylogenetics with BEAUti and the BEAST 1.7. *Molecular Biology and Evolution* **29:** 1969–1973.
Edgar, R.C. (2004) MUSCLE: multiple sequence alignment with high accuracy and high throughput. *Nucleic Acids Research* **32:** 1792–1797.

Ekrem, T. (2001a) Diagnoses and immature stages of some Australian *Tanytarsus* van der Wulp (Diptera : Chironomidae). *Australian Journal of Entomology* **40:** 312–325.
Ekrem, T. (2001b) A Review of Afrotropical *Tanytarsus* van der Wulp (Diptera: Chironomidae). *Tijdschrift voor Entomologie* **144:** 5–40.
Ekrem, T. (2002) A review of selected South- and East Asian *Tanytarsus* v.d. Wulp (Diptera: Chironomidae). *Hydrobiologia* **474:** 1–39.
Ekrem, T. (2003) Towards a phylogeny of *Tanytarsus* van der Wulp (Diptera: Chironomidae). Is morphology alone sufficient to reconstruct the genealogical relationship? *Insect Systematics & Evolution* **34:** 199–219.
Ekrem, T. (2004) Immature stages of European *Tanytarsus* species I. The *eminulus*-, *gregarius*-, *lugens*- and *mendax* species groups (Diptera, Chironomidae). *Deutsche Entomologische Zeitschrift* **51:** 97–146.
Ekrem, T., Sublette, M.F. & Sublette, J.E. (2003) North American *Tanytarsus* I. Descriptions and Keys to Species in the *eminulus*, *gregarius*, *lugens* and *mendax* Species Groups (Diptera : Chironomidae). *Annals of the Entomological Society of America* **96:** 265–328.
Ekrem, T. & Willassen, E. (2004) Exploring Tanytarsini relationships (Diptera : Chironomidae) using mitochondrial COII gene sequences. *Insect Systematics & Evolution* **35:** 263–276.
Ekrem, T., Willassen, E. & Stur, E. (2010) Phylogenetic utility of five genes for dipteran phylogeny: A test case in the Chironomidae leads to generic synonymies. *Molecular Phylogenetics and Evolution* **57:** 561–571.
Epler, J.H., Ekrem, T. & Cranston, P.S. (2013) The larvae of Chironominae (Diptera: Chironomidae) of the Holarctic region—keys and diagnoses. In: Cederholm L, ed. Chironomidae of the Holarctic Region: Keys and Diagnoses, Part 1: Larvae. Lund, Sweden: Insect Systematics and Evolution, Supplement **66:** 387–556.
Freeman, P. (1958) A study of the Chironomidae (Diptera) of Africa South of the Sahara. Part IV. *Bulletin of the British Museum (Natural History). Entomology* **6:** 263–363.
Garber, M., Grabherr, M.G., Guttman, M. & Trapnell, C. (2011) Computational methods for transcriptome annotation and quantification using RNA-seq. *Nature Methods* **8:** 469–477.
Gay, L., Neubauer, G., Zagalska-Neubauer, M., Debain, C., Pons, J.M., David, P. & Crochet, P.A. (2007) Molecular and morphological patterns of introgression between two large white-headed gull species in a zone of recent secondary contact. *Molecular Ecology* **16:** 3215–3227.
Ghonaim, M., Ali, A. & Salem, M. (2004) *Tanytarsus* (Diptera : Chironomidae) from Egypt with description of a new species. *Florida Entomologist* **87:** 571–575.
Giłka, W. & Paasivirta, L. (2007) Two new species of the genus *Tanytarsus* van der Wulp (Diptera: Chironomidae) from Fennoscandia. In: Andersen T, ed. Contributions to the systematics and ecology of aquatic Diptera–A tribute to Ole A. Sæther. Columbus, Ohio: The Caddis Press. 107–113.
Giłka, W. & Paasivirta, L. (2008) On the systematics of the tribe Tanytarsini (Diptera: Chironomidae) - three new species from Finland. *Entomologica Fennica* **19:** 41–48.
Giłka, W. & Paasivirta, L. (2009) Evaluation of diagnostic characters of the *Tanytarsus chinyensis* group (Diptera: Chironomidae), with description of a new species from Lapland. *Zootaxa* **2197:** 31–42.
Glover, B. (1973) The Tanytarsini (Diptera: Chironomidae) of Australia. *Australian Journal of Zoology Supplementary Series* **21:** 403–478.
Goodwin, S., McPherson, J.D. & McCombie, W.R. (2016) Coming of age: ten years of next-generation sequencing technologies. *Nature Reviews Genetics* **17:** 333–351.

Hajibabaei, M., Baird, D.J., Fahner, N.A., Beiko, R. & Golding, G.B. (2016) A new way to contemplate Darwin's tangled bank: how DNA barcodes are reconnecting biodiversity science and biomonitoring. *Philosophical Transactions of the Royal Society B: Biological Sciences* **371:** 20150330.

Hebert, P.D.N., Cywinska, A. & Ball, S.L. (2003a) Biological identifications through DNA barcodes. *Proceedings of the Royal Society of London B: Biological Sciences* **270:** 313–321.

Hebert, P.D.N., Ratnasingham, S. & de Waard, J.R. (2003b) Barcoding animal life: cytochrome c oxidase subunit 1 divergences among closely related species. *Proceedings of the Royal Society of London B: Biological Sciences* **270:** S96–S99.

Heckman, K.L., Mariani, C.L., Rasoloarison, R. & Yoder, A.D. (2007) Multiple nuclear loci reveal patterns of incomplete lineage sorting and complex species history within western mouse lemurs (*Microcebus*). *Molecular Phylogenetics and Evolution* **43:** 353–367.

Hodgetts, J., Ostojá-Starzewski, J.C., Prior, T., Lawson, R., Hall, J. & Boonham, N. (2016) DNA barcoding for biosecurity: case studies from the UK plant protection program 1. *Genome* **59:** 1033–1048.

Huang, D.W. & Cheng, L.N. (2011) The flightless marine midge *Pontomyia* (Diptera: Chironomidae): ecology, distribution, and molecular phylogeny. *Zoological Journal of the Linnean Society* **162:** 443–456.

Kevan, P.G. (2007) Diaheliotaxis and ombrophobia in an anthophilous high arctic midge *Smitta velutina*. *Chironomus Newsletter on Chironomidae Research* **20:** 29–31.

Knebelsberger, T., Landi, M., Neumann, H., Kloppmann, M., Sell, A.F., Campbell, P.D., Laakmann, S., Raupach, M.J., Carvalho, G.R. & Costa, F.O. (2014) A reliable DNA barcode reference library for the identification of the North European shelf fish fauna. *Molecular Ecology Resources* **14:** 1060–1071.

Lanfear, R., Calcott, B., Ho, S.Y.W. & Guindon, S. (2012) PartitionFinder: Combined Selection of Partitioning Schemes and Substitution Models for Phylogenetic Analyses. *Molecular Biology and Evolution* **29:** 1695–1701.

Lee, P.S., Gan, H.M., Clements, G.R. & Wilson, J.J. (2016) Field calibration of blowfly-derived DNA against traditional methods for assessing mammal diversity in tropical forests. *Genome* **59:** 1008–1022.

Lin, X.L., Stur, E. & Ekrem, T. (2015) Exploring genetic divergence in a species-rich insect genus using 2790 DNA Barcodes. *PloS One* **10:** e0138993.

Lindeberg, B. (1963) Taxonomy, biology and biometry of *Tanytarsus curticornis* Kieff. and *T. brundini* n. sp. (Dipt., Chironomidae). *Annales Entomologici Fennici* **29:** 118–130.

Lindeberg, B. (1967) Sibling species delimitation in the *Tanytarsus lestagei* aggregate Diptera, Chironomidae. *Annales Zoologici Fennici* **4:** 45–86.

Littlefair, J.E. & Clare, E.L. (2016) Barcoding the food chain: from Sanger to high-throughput sequencing. *Genome* **59:** 946–958.

Macher, J.N., Salis, R.K., Blakemore, K.S., Tollrian, R., Matthaei, C.D. & Leese, F. (2016) Multiple-stressor effects on stream invertebrates: DNA barcoding reveals contrasting responses of cryptic mayfly species. *Ecological Indicators* **61:** 159–169.

Mardis, E.R. (2008) Next-generation DNA sequencing methods. *Annual Review of Genomics and Human Genetics* **9:** 387–402.

Martin, J., Blinov, A., Alieva, E. & Hirabayashi, K. (2007) A molecular phylogenetic investigation of the genera closely related to *Chironomus* Meigen (Diptera: Chironomidae). In: Andersen T, ed. Contributions to the systematics and ecology of aquatic Diptera. A tribute to Ole A. Sæther. Columbus, Ohio: Caddis Press. 193–203.

Martinsen, G.D., Whitham, T.G., Turek, R.J. & Keim, P. (2001) Hybrid populations selectively filter gene introgression between species. *Evolution* **55:** 1325–1335.
Meier, R., Shiyang, K., Vaidya, G. & Ng, P.K. (2006) DNA barcoding and taxonomy in Diptera: a tale of high intraspecific variability and low identification success. *Systematic Biology* **55:** 715–728.
Metzker, M.L. (2010) Sequencing technologies—the next generation. *Nature Reviews Genetics* **11:** 31–46.
Miller, S.E., Hausmann, A., Hallwachs, W. & Janzen, D.H. (2016) Advancing taxonomy and bioinventories with DNA barcodes. *Philosophical Transactions of the Royal Society B: Biological Sciences* **371:** 20150339.
Monaghan, M.T., Balke, M., Gregory, T.R. & Vogler, A.P. (2005) DNA-based species delineation in tropical beetles using mitochondrial and nuclear markers. *Philosophical Transactions of the Royal Society of London B: Biological Sciences* **360:** 1925–1933.
Nzelu, C.O., Caceres, A.G., Arrunategui-Jimenez, M.J., Lanas-Rosas, M.F., Yanez-Trujillano, H.H., Luna-Caipo, D.V., Holguin-Mauricci, C.E., Katakura, K., Hashiguchi, Y. & Kato, H. (2015) DNA barcoding for identification of sand fly species (Diptera: Psychodidae) from leishmaniasis-endemic areas of Peru. *Acta Tropica* **145:** 45–51.
Papoucheva, E., Proviz, V., Lambkin, C., Goddeeris, B. & Blinov, A. (2003) Phylogeny of the endemic baikalian *Sergentia* (Chironomidae, Diptera). *Molecular Phylogenetics and Evolution* **29:** 120–125.
Pons, J., Barraclough, T.G., Gomez-Zurita, J., Cardoso, A., Duran, D.P., Hazell, S., Kamoun, S., Sumlin, W.D. & Vogler, A.P. (2006) Sequence-based species delimitation for the DNA taxonomy of undescribed insects. *Systematic Biology* **55:** 595–609.
Przhiboro, A.A. & Ekrem, T. (2011) Taxonomy and bionomics of *Tanytarsus recurvatus* Brundin, 1947. In: X.H. W and Liu W, eds. Contemporary chironomid studies. Proceedings of the 17th International Symposium on Chironomidae. Tianjin, China: Nankai University Press. 159–183.
Puillandre, N., Lambert, A., Brouillet, S. & Achaz, G. (2012) ABGD, Automatic Barcode Gap Discovery for primary species delimitation. *Molecular Ecology* **21:** 1864–1877.
Reiss, F. & Fittkau, E.J. (1971) Taxonomie und Ökologie europäisch verbreiteter *Tanytarsus*-Arten (Chironomidae, Diptera). *Archiv für Hydrobiologie, Supplement* **40:** 75–200.
Renaud, A.K., Savage, J. & Adamowicz, S.J. (2012) DNA barcoding of Northern Nearctic Muscidae (Diptera) reveals high correspondence between morphological and molecular species limits. *BMC Ecology* **12:** 24.
Rogers, J. & Wall, R. (1980) A mechanism for RNA splicing. *Proceedings of the National Academy of Sciences* **77:** 1877–1879.
Ronquist, F., Teslenko, M., van der Mark, P., Ayres, D.L., Darling, A., Höhna, S., Larget, B., Liu, L., Suchard, M.A. & Huelsenbeck, J.P. (2012) MrBayes 3.2: efficient bayesian phylogenetic inference and model choice across a large model space. *Systematic Biology* **61:** 539–542.
Rosenberg, D. (1992) Freshwater biomonitoring and Chironomidae. *Netherlands Journal of Aquatic Ecology* **26:** 101–122.
Roslin, T. & Majaneva, S. (2016) The use of DNA barcodes in food web construction—terrestrial and aquatic ecologists unite! 1. *Genome* **59:** 603–628.
Sæther, O.A. (1969) Some Nearctic Pondonominae, Diamesinae, and Orthocladiinae (Diptera: Chironomidae). *Bulletin of the Fisheries Research Board of Canada* **170:** 1–154.
Sæther, O.A. (1980) Glossary of chironomid morphology terminology (Diptera: Chironomidae). *Entomologica scandinavica, Supplements* **14:** 1–51.
Sanseverino, A.M. (2006) A review of the genus *Tanytarsus* van der Wulp, 1874 (Insecta, Diptera, Chironomidae) from the Neotropical region. *Dissertation zur Erlangung des*

*Doktorgrades der Fakultät für Biologie der Ludwig-Maximilians-Universität, München***:** pp. 306.
Sasa, M. (1980) Studies on chironomid midges of the Tama River. Part 2. Description of 20 species of Chironominae recovered from a tributary. *Research Report from the National Institute for Environmental Studies, Japan* **13:** 9–107.
Sasa, M. & Kawai, K. (1987) Studies on chironomid midges of Lake Biwa (Diptera, Chironomidae). *Lake Biwa Research Institute, Otsu, Japan* **3:** 1–119.
Schmidt, S., Schmid-Egger, C., Morinière, J., Haszprunar, G. & Hebert, P.D. (2015) DNA barcoding largely supports 250 years of classical taxonomy: identifications for Central European bees (Hymenoptera, Apoidea *partim*). *Molecular Ecology Resources* **15:** 985–1000.
Scholz, M.B., Lo, C.C. & Chain, P.S.G. (2012) Next generation sequencing and bioinformatic bottlenecks: the current state of metagenomic data analysis. *Current Opinion in Biotechnology* **23:** 9–15.
Song, C., Wang, Q., Zhang, R.L., Sun, B.J. & Wang, X.H. (2016) Exploring the utility of DNA barcoding in species delimitation of *Polypedilum* (*Tripodura*) non-biting midges (Diptera: Chironomidae). *Zootaxa* **4079:** 534–550.
Stamatakis, A. (2006) RAxML-VI-HPC: maximum likelihood-based phylogenetic analyses with thousands of taxa and mixed models. *Bioinformatics* **22:** 2688–2690.
Stamatakis, A. (2014) RAxML version 8: a tool for phylogenetic analysis and post-analysis of large phylogenies. *Bioinformatics* **30:** 1312–1313.
Stur, E. & Ekrem, T. (2011) Exploring unknown life stages of Arctic Tanytarsini (Diptera: Chironomidae) with DNA barcoding. *Zootaxa* **2743:** 27–39.
Stur, E. & Ekrem, T. (2015) A review of Norwegian *Gymnometriocnemus* (Diptera, Chironomidae) including the description of two new species and a new name for *Gymnometriocnemus volitans* (Goetghebuer) sensu Brundin. *ZooKeys* **508:** 127–142.
Sublette, J. & Sasa, M. (1994) Chironomidae collected in Onchocerciasis endemic areas of Guatemala (Insecta, Diptera). *Spixiana Supplement* **20:** 1–60.
Sublette, J.E. (1964) Chironomidae (Diptera) of Louisiana. I. Systematics and immature stages of some lentic chironomids of west-central Louisiana. *Tulane Studies in Zoology* **11:** 109–150.
Sugimaru, K., Kawai, K. & Imabayashi, H. (2008) A new marine chironomid species of the genus *Tanytarsus* (Diptera: Chironomidae) from Okinawa, Japan. *Plankton and Benthos Research* **3:** 240–242.
Swofford, D.L. (2002) PAUP*: Phylogenetic Analysis Using Parsimony (* and Other Methods), Version 4.0 b10. *Sinauer Associates. Sunderland, MA*.
Tamura, K., Stecher, G., Peterson, D., Filipski, A. & Kumar, S. (2013) MEGA6: molecular evolutionary genetics analysis version 6.0. *Molecular Biology and Evolution* **30:** 2725–2729.
Tokunaga, M. (1933) Chironomidae from Japan (Diptera). II. Marine *Tanytarsus*. *The Philippine Journal of Science* **51:** 357–367.
Trivinho-Strixino, S. (2012) A systematic review of Neotropical *Caladomyia* SÄWEDAL (Diptera: Chironomidae). *Zootaxa* **3495:** 1–41.
Trivinho-Strixino, S. & Strixino, G. (2007) A new Neotropical species of *Tanytarsus* van der Wulp, 1874 (Diptera : Chironomidae), with an unusual anal process. *Zootaxa* **1654:** 61–67.
Trivinho-Strixino, S., Wiedenbrug, S. & da Silva, F.L. (2015) New species of *Tanytarsus* van der Wulp (Diptera: Chironomidae: Tanytarsini) from Brazil. *European Journal of Environmental Sciences* **5:** 92–100.

van Dijk, E.L., Auger, H., Jaszczyszyn, Y. & Thermes, C. (2014) Ten years of next-generation sequencing technology. *Trends in Genetics* **30:** 418–426.
Vinogradova, E.M., Riss, H.W. & Spies, M. (2009) New species of *Tanytarsus* van der Wulp, 1874 (Diptera: Chironomidae) from Central America. *Aquatic Insects* **31:** 11–17.
Wagner, C.E., Keller, I., Wittwer, S., Selz, O.M., Mwaiko, S., Greuter, L., Sivasundar, A. & Seehausen, O. (2013) Genome-wide RAD sequence data provide unprecedented resolution of species boundaries and relationships in the Lake Victoria cichlid adaptive radiation. *Molecular Ecology* **22:** 787–798.
Webb, J.M., Jacobus, L.M., Funk, D.H., Zhou, X., Kondratieff, B., Geraci, C.J., DeWalt, R.E., Baird, D.J., Richard, B., Phillips, I. & Hebert, P.D. (2012) A DNA barcode library for North American Ephemeroptera: progress and prospects. *PloS One* **7:** e38063.
Willyard, A., Cronn, R. & Liston, A. (2009) Reticulate evolution and incomplete lineage sorting among the ponderosa pines. *Molecular Phylogenetics and Evolution* **52:** 498–511.
Witt, J.D., Threloff, D.L. & Hebert, P.D. (2006) DNA barcoding reveals extraordinary cryptic diversity in an amphipod genus: implications for desert spring conservation. *Molecular Ecology* **15:** 3073–3082.
Wulp, F.M. (1874) Dipterologische aanteekeningen. *Tijdschrift voor Entomologie* **17:** 109–148.
Xia, X.H. (2013) DAMBE5: a comprehensive software package for data analysis in molecular biology and evolution. *Molecular Biology and Evolution* **30:** 1720–1728.
Xia, X.H. & Lemey, P. (2009) Assessing substitution saturation with DAMBE. *The phylogenetic handbook: a practical approach to DNA and protein phylogeny* **2:** 615–630.
Xia, X.H., Xie, Z., Salemi, M., Chen, L. & Wang, Y. (2003) An index of substitution saturation and its application. *Molecular Phylogenetics and Evolution* **26:** 1–7.
Yang, Z. (2015) The BPP program for species tree estimation and species delimitation. *Current Zoology* **61:** 854–865.
Yang, Z. & Rannala, B. (2010) Bayesian species delimitation using multilocus sequence data. *Proceedings of the National Academy of Sciences* **107:** 9264–9269.
Yang, Z. & Rannala, B. (2017) Bayesian species identification under the multispecies coalescent provides significant improvements to DNA barcoding analyses. *Molecular Ecology***:** http://dx.doi.org/10.1111/mec.14093.
Yang, Z.F., Landry, J.F., Handfield, L., Zhang, Y.L., Alma Solis, M., Handfield, D., Scholtens, B.G., Mutanen, M., Nuss, M. & Hebert, P.D.N. (2012) DNA barcoding and morphology reveal three cryptic species of *Anania* (Lepidoptera: Crambidae: Pyraustinae) in North America, all distinct from their European counterpart. *Systematic Entomology* **37:** 686–705.
Yu, Y., Harris, A. & He, X.J. (2010) S-DIVA (Statistical Dispersal-Vicariance Analysis): a tool for inferring biogeographic histories. *Molecular Phylogenetics and Evolution* **56:** 848–850.
Zahiri, R., Lafontaine, J.D., Schmidt, B.C., Dewaard, J.R., Zakharov, E.V. & Hebert, P.D. (2014) A transcontinental challenge–a test of DNA barcode performance for 1,541 species of Canadian Noctuoidea (Lepidoptera). *PloS One* **9:** e92797.
Zhang, J., Kapli, P., Pavlidis, P. & Stamatakis, A. (2013) A general species delimitation method with applications to phylogenetic placements. *Bioinformatics* **29:** 2869–2876.
Zhou, X., Frandsen, P.B., Holzenthal, R.W., Beet, C.R., Bennett, K.R., Blahnik, R.J., Bonada, N., Cartwright, D., Chuluunbat, S. & Cocks, G.V. (2016) The Trichoptera barcode initiative: a strategy for generating a species-level Tree of Life. *Philosophical Transactions of the Royal Society B: Biological Sciences* **371:** 20160025.

Zhou, X., Jacobus, L.M., DeWalt, R.E., Adamowicz, S.J. & Hebert, P.D.N. (2010) Ephemeroptera, Plecoptera, and Trichoptera fauna of Churchill (Manitoba, Canada): insights into biodiversity patterns from DNA barcoding. *Journal of the North American Benthological Society* **29:** 814–837.

PLOS | ONE

RESEARCH ARTICLE

Exploring Genetic Divergence in a Species-Rich Insect Genus Using 2790 DNA Barcodes

Xiaolong Lin*, Elisabeth Stur, Torbjørn Ekrem

Department of Natural History, NTNU University Museum, Norwegian University of Science and Technology, Trondheim, Norway

* xiaolong.lin@ntnu.no

OPEN ACCESS

Citation: Lin X, Stur E, Ekrem T (2015) Exploring Genetic Divergence in a Species-Rich Insect Genus Using 2790 DNA Barcodes. PLoS ONE 10(9): e0138993. doi:10.1371/journal.pone.0138993

Editor: Diego Fontaneto, Consiglio Nazionale delle Ricerche (CNR), ITALY

Received: May 15, 2015

Accepted: September 7, 2015

Published: September 25, 2015

Data Availability Statement: All relevant data are within the paper and its Supporting Information files. Collection data, sequences, and trace files are available on BOLD (www.boldsystems.org) in public dataset "Tanytarsus DNA barcoding 2015 (DS-TABAC)", DOI: dx.doi.org/10.5883/DS-TABAC.

Funding: Part of the DNA barcode data in this publication was generated in collaboration with the Norwegian Barcode of Life Network (NorBOL) funded by the Research Council of Norway (226134/F50) and the Norwegian Biodiversity Information Centre (14-14, 70184209). The funders had no role in study design, data collection and analysis, decision to publish, or preparation of the manuscript.

Abstract

DNA barcoding using a fragment of the mitochondrial cytochrome *c* oxidase subunit 1 gene (COI) has proven to be successful for species-level identification in many animal groups. However, most studies have been focused on relatively small datasets or on large datasets of taxonomically high-ranked groups. We explore the quality of DNA barcodes to delimit species in the diverse chironomid genus *Tanytarsus* (Diptera: Chironomidae) by using different analytical tools. The genus *Tanytarsus* is the most species-rich taxon of tribe Tanytarsini (Diptera: Chironomidae) with more than 400 species worldwide, some of which can be notoriously difficult to identify to species-level using morphology. Our dataset, based on sequences generated from own material and publicly available data in BOLD, consist of 2790 DNA barcodes with a fragment length of at least 500 base pairs. A neighbor joining tree of this dataset comprises 131 well separated clusters representing 121 morphological species of *Tanytarsus*: 77 named, 16 unnamed and 28 unidentified theoretical species. For our geographically widespread dataset, DNA barcodes unambiguously discriminate 94.6% of the *Tanytarsus* species recognized through prior morphological study. Deep intraspecific divergences exist in some species complexes, and need further taxonomic studies using appropriate nuclear markers as well as morphological and ecological data to be resolved. The DNA barcodes cluster into 120–242 molecular operational taxonomic units (OTUs) depending on whether Objective Clustering, Automatic Barcode Gap Discovery (ABGD), Generalized Mixed Yule Coalescent model (GMYC), Poisson Tree Process (PTP), subjective evaluation of the neighbor joining tree or Barcode Index Numbers (BINs) are used. We suggest that a 4–5% threshold is appropriate to delineate species of *Tanytarsus* non-biting midges.

Introduction

Genetic variation between species in cytochrome c oxidase subunit 1 (COI) gene sequences has been proven informative for species identification in many animal taxa, including non-biting midges, the Chironomidae (Insecta, Diptera) [1–5]. The mutation rate in COI can be fast enough to provide informative characters for delineation of closely related and sibling species

Competing Interests: The authors have declared that no competing interests exist.

and even to analyze phylogeographic patterns within a single species [6–9]. Many chironomid species, especially in the larval life stage (Fig 1), are difficult to identify and partial COI gene sequences as DNA barcodes have been shown appropriate to delimit and identify species as well as associate life stages in this family [3, 10–14]. In general, partial COI sequences show a high-level of divergence between species in Chironomidae, so high that the marker performs poorly in phylogenetic reconstructions [3, 15]. Nevertheless, COI has been used to infer the phylogenetic relationship within family Chironomidae [16, 17].

The dipteran family Chironomidae is the most ubiquitous and usually most abundant insect group in all types of freshwater and even saltwater [18]. At present, there are more than 6000 described species worldwide (P. Ashe pers comm.) and certain species can reach densities up to 15600 individuals per m^2 at favorable conditions [19]. Due to their high abundance and diversity, chironomid larvae occupy a key position among benthic macroinvertebrates, they are important as freshwater indicator organisms [20] and as food items for fish. In addition, larval head capsules are preserved in lake sediments and have been shown to be useful in climate reconstructions since species composition varies with water temperature as well as other environmental factors. However, identification of chironomid larvae to species-level via morphology usually is arduous, time-consuming and expensive, and more effective identification techniques such as DNA barcoding can greatly improve the use of chironomids in biological-assessments of freshwater ecosystems [21–23]. Recently, this was exemplified with a next-generation sequencing protocol analyzing 1015 tropical chironomids at a cost of less than $1 per specimens [24]. At present, there are few publications that investigate the performance of DNA barcoding in species-rich genera. A couple of studies are known from plants [25–27], but there are currently no papers that explore how efficient DNA barcodes are in delineation of species in larger genera (>200 species) of insects.

The genus *Tanytarsus* van der Wulp, 1874 is the most species-rich genus of the tribe Tanytarsini in subfamily Chironominae with more than 400 described species worldwide. Species of the genus *Tanytarsus* (Fig 2) are eurytopic, and immatures occur in all types of freshwater. There are even species with larvae and pupae in marine or terrestrial environments[28]. The genus was erected by van der Wulp [29] and various species groups and regionally distributed species have been revised over the last few decades [30–37]. A morphological determination of some *Tanytarsus* species group can be extremely challenging. Moreover, there are many unknown and cryptic species in *Tanytarsus* and it is difficult to associate the immature stages with adults through rearing since it is time-consuming and not always successful. In general, identification at the species-level strongly relies on the morphological characters of adult males. However, diagnostic characters might be unreliable due to intraspecific morphological variation even for this life stage and phenotypic plasticity [38] in morphometric ratios and hypopygial structures caused by different temperature regimes and food quality has been observed in several chironomid species [39]. Moreover, artifacts created in the slide-mounting process can also obscure species specific characteristics.

Currently, there are several approaches to analyze how DNA barcode data form separate genetic clusters potentially corresponding to biological species. In this context, evaluation of neighbor joining [40] ID-trees perhaps represents the most widely used method for the direct comparison of DNA barcodes. In general, neighbor joining trees are easy and fast to compute with appropriate bootstraps replicates even for big datasets. Furthermore, methods such as Automatic Barcode Gap Discovery (ABGD) [41], the Generalized Mixed Yule Coalescent model (GMYC) [42–44], the Poisson Tree Process (PTP) [45], Objective Clustering [46], and the Barcode Index Numbers Algorithm (BINs) [47] also have been proven to represent effective approaches to group hypothetical species in a sequence alignment. ABGD aims to assign sequences into Operational Taxonomic Units (OTUs) based on a statistically inferred barcode

Fig 1. *Tanytarsus* sp.10XL, larva.

doi:10.1371/journal.pone.0138993.g001

gap in an initial partitioning, conducting a second round of splitting through recursive partitioning [41, 48]. ABGD performs well for standard prior maximum intraspecific divergences except for datasets including less than three sequences per species [41]. The GMYC model is a likelihood method for delimiting species by fitting within and between species branching models to gene trees [43] while the Poisson Tree Process (PTP) is a method for species delimitation based on rooted phylogenetic trees [45]. The PTP-model assumes that intra- and interspecific substitutions follow two distinct Poisson processes, and that intraspecific substitutions are discernibly fewer than interspecific substitutions [44]. The Objective Clustering method of the software Species Identifier aims to explore intra- and interspecific genetic distances of cluster sequences based on pairwise distances [46]. Species Identifier allows the comparison of clusters generated using preset thresholds by users with existing taxonomy [49–51]. The Barcode Index Numbers Algorithm (BIN) is incorporated in the Barcode of Life Data Systems (BOLD, www.boldsystems.org) [47, 52]. BIN analysis generates one number of OTUs for each set of DNA barcode sequences using the Refined Single Linkage algorithm [48]. The BIN algorithm has been effectively tested on numerous taxonomic groups and shows potential for applications in

Fig 2. *Tanytarsus occultus* Brundin, 1949, adult male.

doi:10.1371/journal.pone.0138993.g002

species abundance studies and environmental barcoding [47]. Nevertheless, few studies have compared the performance of the novel analytical methods for the DNA barcode-based delineation of OTUs [48].

In this study, we have used 2790 *Tanytarsus* DNA barcodes to test the utility of COI barcodes for species identification in *Tanytarsus*. Furthermore, we used DNA barcodes and morphology to evaluate potentially cryptic species within this genus. Finally, we compared the number of OTUs using ABGD, GMYC, PTP, Objective Clustering and the BIN algorithm to see which of these methods correspond best to morphological species concepts in *Tanytarsus* and which level of intraspecific divergence we should expect within this genus.

Materials and Methods

Taxon sampling and data collection

The *Tanytarsus* sequences used in this study originated from specimens that were collected in many different parts of the world. Own field work was conducted mainly in Northern Europe, China and Canada during recent years, but chironomids were also collected in Central Europe, North and Central America, Africa and Australia. Specimens were identified morphologically using taxonomic revisions and species description [31, 32, 34–36, 53–64].

In addition to own data, we searched for public COI barcodes in BOLD belonging to genus *Tanytarsus* that were longer than 500 base pairs and lacked stop codons, indicating absence of dysfunctional copies of mitochondrial genes (NUMTs). Searches were done January 17, 2015.

Hits were combined with own data and are available through the dataset "*Tanytarsus* DNA barcoding 2015 (DS-TABAC)" on BOLD, DOI: dx.doi.org/10.5883/DS-TABAC.

The complete dataset includes 2790 COI sequences of which 164 originated from GenBank, 340 from our own lab at the Department of Natural History, NTNU University Museum, and the remaining 2286 sequences from various projects in BOLD. In our dataset, 1242 of 2790 specimens were not examined by us and only identified to genus-level. Since this would make analyses of intra- and interspecific distances difficult, we re-named the 1242 sequences by the clusters they belonged to in a standard neighbor joining tree based on Kimura 2-Parameter (K2P) [65] distances (S1 File). In cases where unidentified sequences matched named morphospecies, we gave them this name; in cases where there was no matching morphospecies name, we gave all sequences in that cluster the same distinguishable group name.

DNA extraction, PCR amplification, sequencing and alignment

Sampled specimens were preserved in 75–96% ethanol and stored dark at 4°C before molecular analyses. Depending on size, a single or three legs were removed from the majority of specimens and sent to Canadian Centre for DNA Barcoding, the Biodiversity Institute of Ontario (Guelph, Ontario, Canada) for DNA extraction, PCR and bi-directional Sanger sequencing as part of the International Barcode of Life project. In addition, DNA of 102 specimens was extracted from the thorax and head using GeneMole DNA Tissue Kit on a GeneMole® instrument (Mole Genetics, Lysaker, Norway) at the Department of Natural History, NTNU University Museum. The standard protocol was followed with exception that 4 μl Proteinase K was mixed with 100 μl buffer for overnight lysis at 56°C. The final elution volume was 100 μl. After DNA extraction, the exoskeleton was washed with 96% ethanol and mounted in Euparal on the same microscope slide as its corresponding antennae, wings, legs and abdomen following the procedure outlined by Sæther [66]. Vouchers are deposited at the Department of Natural History, NTNU University Museum, Trondheim, Norway and College of Life Sciences, Nankai University, Tianjin, China (Chinese specimens).

A 658 bp fragment of the COI region was PCR-amplified using the universal primers LCO1490 and HCO2198 [67]. DNA amplification was carried out in 25 μl reactions using 2.5 μl 10x Takara ExTaq pcr buffer (CL), 2 μl 2.5 mM dNTP mix, 2 μl 25 mM $MgCl_2$, 0.2 μl Takara Ex Taq HS, 1 μl 10 μM of each primer, 2 μl template DNA and 14.3 μl ddH_2O. Amplification cycles were performed on a Biorad C1000 Thermal Cycler (Bio-Rad, California, USA) and followed a program with an initial denaturation step of 95°C for 5 min, then followed by 34 cycles of 94°C for 30 s, 51°C for 30 s, 72°C for 1 min and 1 final extension at 72°C for 3 min. PCR products were purified using illustra ExoProStar 1-Step (GE Healthcare Life Sciences, Buckinghamshire, UK) and shipped to MWG Eurofins (Ebersberg, Germany) for bidirectional sequencing using BigDye 3.1 (Applied Biosystems, Foster City, CA, USA) termination.

Sequences were assembled and edited using Sequencher 4.8 (Gene Codes Corp., Ann Arbor, Michigan, USA). Sequence information was uploaded on BOLD (www.boldsystems.org) along with an image and collateral information for each voucher specimen.

The sequences names were edited using MESQUITE 2.50 [68]. Alignment of the sequences was carried out using the Muscle algorithm [69] on amino acids in MEGA 6 [70] (S2 File).

The nucleotide statistics and pairwise distances using the K2P model were calculated in MEGA 6 (S1 Table). The neighbor joining tree was conducted using K2P substitution model with 500 bootstrap replications and the "pairwise deletion" option of missing data in MEGA 6. The K2P model was used to make our results comparable with most other DNA barcode studies on insects.

To estimate the number of OTUs, the aligned sequences were subjected to Objective Clustering at 2–7% threshold in Species Identifier (TaxonDNA 1.6.2) [46]. In addition, the aligned sequences were sorted into hypothetical species using ABGD method with a prior *P* that ranges from 0.005 to 0.1, and the K2P model, following the default settings. The number of BINs in the dataset was counted as they appeared in BOLD on March 28th, 2015. Furthermore, a reduced dataset with 1250 unique sequences (haplotypes) was generated using ElimDupes (https://hcv.lanl.gov/content/sequence/ELIMDUPES/elimdupes.html) and manual inspection for use in both GMYC and PTP. The ultrametric tree required for the GMYC method was obtained using BEAST 1.8 [71] on the reduced dataset. The MCMC chain was run for 50 million generations under the HKY substitution model with two partitions (positions 1+2; position 3) and the Yule speciation model. Runs using more complex and fit models of substitution (e.g. GTR+I+G) was also attempted, but MCMC failed to start in BEAST due to low initial likelihoods even with UPGMA and ML starting trees. Prior settings are available from the authors. The MCMC log on prior and posterior values was examined in Tracer 1.6 [72] and a burn-in of 10 million generations was used to avoid suboptimal trees in the final consensus tree. The single-threshold GMYC method was applied using the *splits* package [73] in R [74] with step-by-step guides available on Tomochika Fujisawa's blog (https://tmfujis.wordpress.com/2013/04/23/how-to-run-gmyc/). For PTP-based OTU estimation, the needed rooted phylogenetic input-tree was constructed with RAxML [75] using raxmlGUI v1.3 [76] with the GTR+G+I substitution model. The PTP model was implemented following the default parameters and 500 000 generations on the bPTP web server (http://species.h-its.org/ptp/) [45] as well as 1 000 000 generations on the stand-alone version in a Linux environment.

Results and Discussion

Barcode analysis

The aligned 2790 sequences ranged from 507 to 658 base pairs, including 798 sequences with full barcode length. In total, there were 338 variable sites (51.4%), of which 301 (89.1%) were parsimony informative. Most variable sites occurred in the third codon-position. The sequences were heavily AT-biased specifically in the third position with an average AT-composition of 87.6% (Table 1).

Our dataset included 1548 barcode sequences which before analysis were identified to species-level and 1242 barcodes which were identified to the genus-level. The number of DNA barcodes per morphospecies (n = 93) and DNA barcode cluster (n = 131) ranged from 1 to 430 (Fig 3).

Average intraspecific divergence was 2.14% (S2 Table) with maximum intraspecific divergence observed in *Tanytarsus brundini* Lindeberg (21.1%). This was even beyond the average interspecific divergence (15.9%) and sequences belonging to this morphospecies clustered clearly in four genetically divergent groups, indicating cryptic species. A similar situation was also observed for other morphospecies (see below). When disregarding obvious cryptic species complexes, the maximum intraspecific divergence was 8.5% (for *Tanytarsus occultus* Brundin).

Table 1. Variable and informative sites, and average nucleotide composition in the aligned COI gene sequences.

Nucleotide Position	Variable Site (%)	Informative Site (%)	T (%)	C (%)	A (%)	G (%)	AT (%)	GC (%)
1st	25.7	22.6	26	17.3	29.2	27.4	55.2	44.7
2nd	9.2	4.9	43	27.2	13.3	16.5	56.3	43.7
3rd	65.1	72.4	45	8.9	42.6	3.1	87.6	12.4
All	51.4	89.1	38.1	17.8	28.4	15.7	66.5	33.5

doi:10.1371/journal.pone.0138993.t001

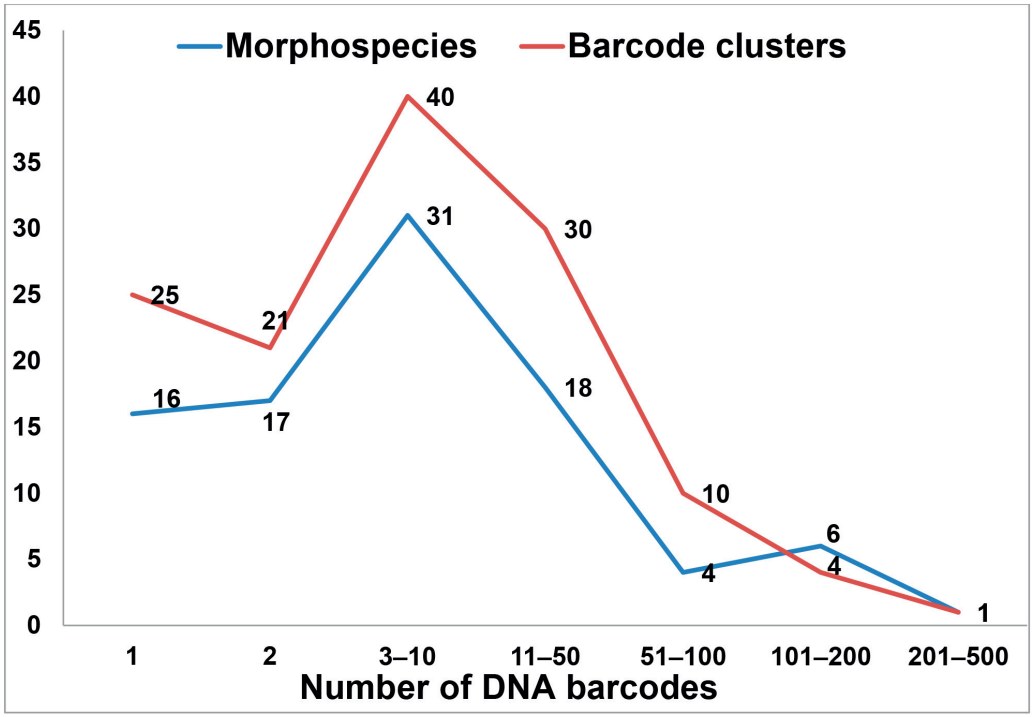

Fig 3. Number of DNA barcodes per morphospecies and barcode clusters based on the neighbor joining tree.

doi:10.1371/journal.pone.0138993.g003

The maximum interspecific divergence was 26.7% between *Tanytarsus mendax* Kieffer and *Tanytarsus nigricollis* Goetghebuer. The minimum interspecific divergence was 0.9% between *Tanytarsus unagiseptimus* Sasa and *Tanytarsus kiseogi* Ree & Jeong, but this case probably was due to a misidentification of specimens not available to us for morphological examination and might also indicate a taxonomic synonym (see below).

In general, our data showed distinctly larger interspecific (S3 Table) than intraspecific divergences, but due to the presence of cryptic species diversity and a few misidentifications, there was no clear "barcode gap" in the pairwise K2P distances (Fig 4). In addition, there are some cases of low genetic divergence between morphologically distinguishable species, likely due to recent speciation. For instance, three related morphospecies in the *lugens* species group, *Tanytarsus lugens* Kieffer, *Tanytarsus bathophilus* Kieffer and *Tanytarsus heliomesonyctios* Langton cannot be well-differentiated by DNA barcodes having interspecific pairwise distance up to about 3.2% (Fig 5).

Species discrimination

The neighbor joining tree based on 2790 DNA barcodes comprises 131 well separated clusters, representing 77 named and 44 unnamed morphological species of *Tanytarsus* (S1 File). Among these unnamed species, 16 identified morphological species might be new to science, while 28 barcode clusters were not otherwise assignable to valid morphospecies. The results

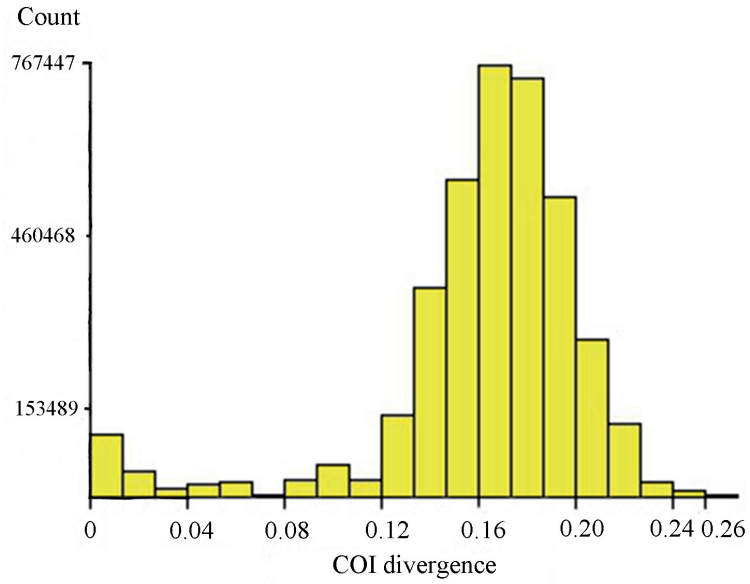

Fig 4. Histogram of pairwise K2P distances of 2790 aligned sequences. The figure was a result of analysis with ABGD using the K2P model. The horizontal axis shows the pairwise K2P-distance, and the vertical axis shows the number of pairwise sequence comparisons.

doi:10.1371/journal.pone.0138993.g004

showed that DNA barcode clusters in general corresponded well with morphological species concepts in *Tanytarsus*; 94.6% (88/93) of the species identified based on morphology matched divergent barcode clusters.

However, DNA barcodes were not sufficient for identification in all cases. Previous studies have shown that the presences of NUMTs [77–79], symbiotic bacteria [80], incomplete lineage sorting [81–83], introgression [84, 85] and distant geographic areas can present obstacles in

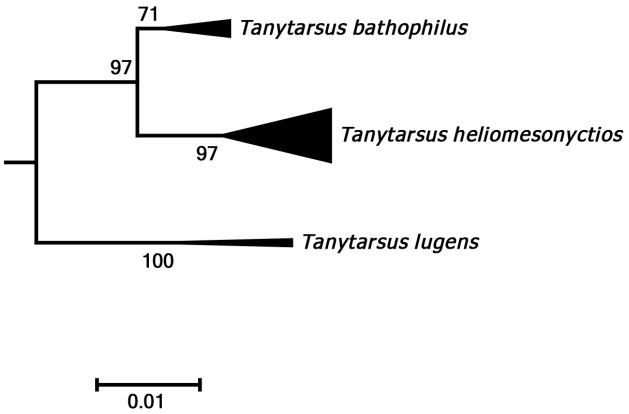

Fig 5. Neighbor joining subtree of the *Tanytarsus lugens* species group. Numbers on branches represent bootstrap support (>70%) based on 500 replicates; scale represents K2P genetic distance.

doi:10.1371/journal.pone.0138993.g005

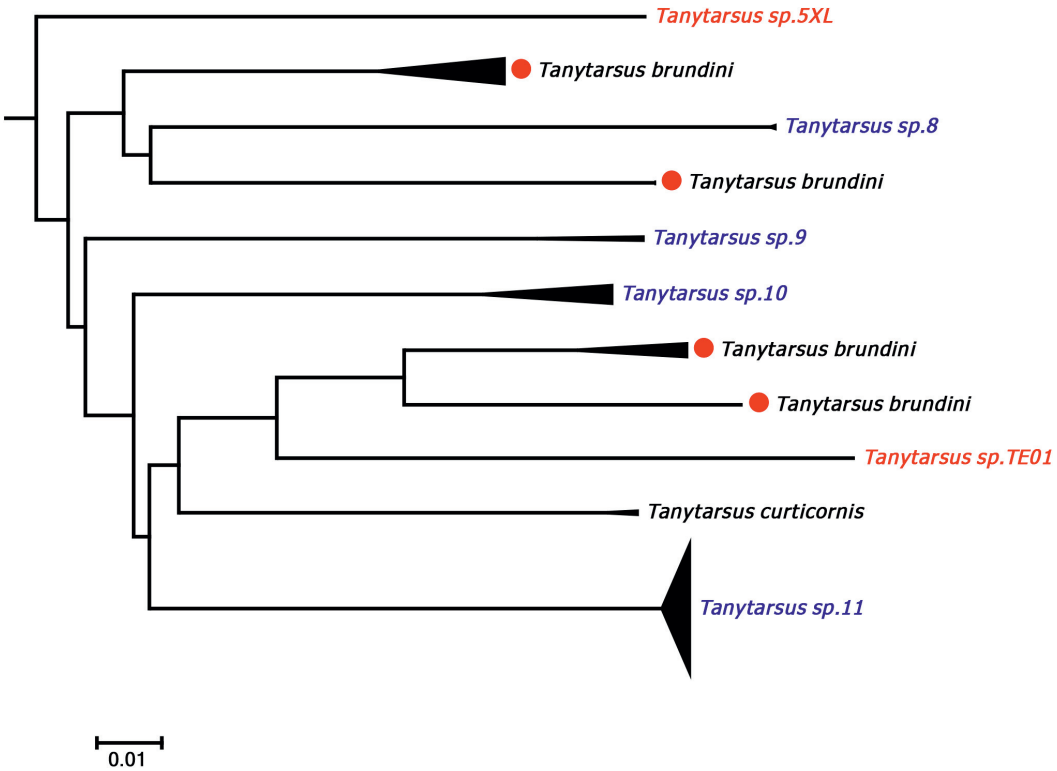

Fig 6. Neighbor joining subtree of the *Tanytarsus brundini* species complex. Numbers on branches represent bootstrap support (>70%) based on 500 replicates; scale represents K2P genetic distance.

doi:10.1371/journal.pone.0138993.g006

species delimitation [86, 87] using DNA barcoding. NUMTs and symbiotic bacteria, like *Wolbachia* have to our knowledge not yet been recorded in Chironomidae, but the three other causes are possible explanations for the observed inconsistencies between morphological and molecular species clusters.

A few examples of deep COI sequence divergence among specimens assigned to a single morphospecies were detected. There were at least two divergent barcode clusters in *Tanytarsus aterrimus* Freeman, *Tanytarsus bathophilus* Kieffer, *Tanytarsus brundini*, *Tanytarsus glabrescens* Edwards, *Tanytarsus guerlus* (Roback), *Tanytarsus heusdensis* Goetghebuer, *T. lestagei* Lindeberg, *Tanytarsus occultus*, *Tanytarsus takahashii* Kawai & Sasa and *Tanytarsus telmaticus* Lindeberg (S1 File).

For *T. brundini*, intraspecific pairwise K2P distances ranged from 0 to 21.1% and a total of four well separated barcode clusters Western Europe and Canada were observed (Fig 6). Examination of the voucher specimens did not reveal any distinct morphological characters corresponding with the clustering in COI sequences although some zoogeographical structure is present. We therefore suspect that this morphological species contains several cryptic species. A similar situation is present in *T. heusdensis*, another member of the *Tanytarsus chinyensis* Goetghebuer species group. There were three distinct barcode clusters of *T. heusdensis* in the result from our analyses, but no obvious morphological characters that will separate adult

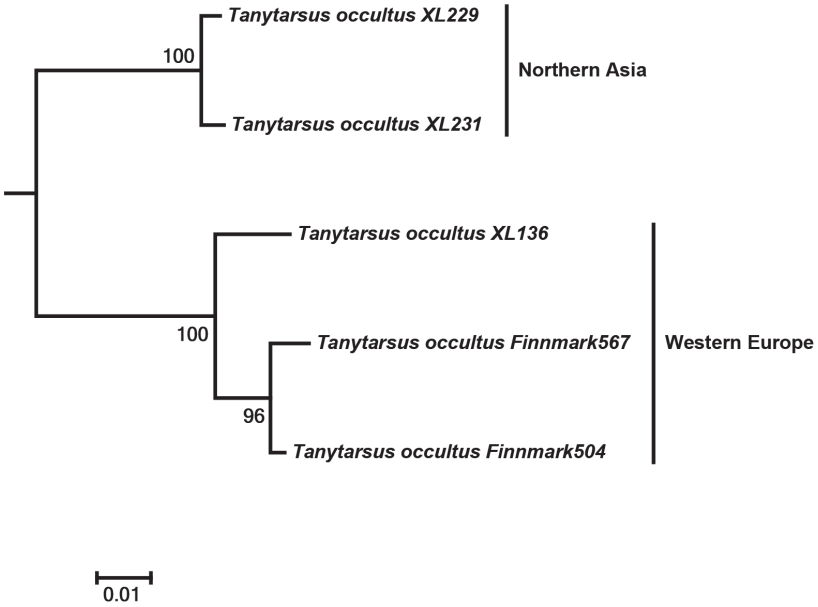

Fig 7. Neighbor joining subtree of *Tanytarsus occultus*. Numbers on branches represent bootstrap support (>70%) based on 500 replicates; scale represents K2P genetic distance.

doi:10.1371/journal.pone.0138993.g007

males from Germany and Norway (S1 File). Thus, it appears that geographically separated populations of some species in the *T. chinyensis* group are genetically divergent, but difficult to separate based on morphology. Identification of species in this group has also previously been acknowledged as challenging [36, 55, 57], thus it is perhaps not surprising that hidden genetic diversity is detected among members in the *T. chinyensis* group.

Members of the South African *T. aterrimus* also showed high intraspecific divergences with pairwise K2P-distances of up to 13.9%. The DNA barcodes clustered into 3 groups (S1 File) that so far could not be differentiated via morphology.

Another interesting case was observed in *T. occultus* where specimens from Northeastern Asia and Western Europe separated into two distinct clusters with sequence divergences from 7% to 8.5% (Fig 7). The adult male vouchers examined are as far as we can observe at present morphologically indistinguishable. Also, DNA barcodes of a hitherto undescribed morphospecies from Tibet, *Tanytarsus* sp.3XL, showed high intraspecific divergences and might be more than one species (Fig 8).

In addition to this previously undetected diversity, our results also suggest some new taxonomic synonyms on the species-level. For example, three closely related species in *Tanytarsus eminulus* species group, *Tanytarsus oscillans* Johannsen, *T. unagiseptimus* and *T. kiseogi*, distributed in China, Japan, South Korea, the Russian Fast East and Singapore, are differentiated by subtle morphological differences in the adult male genitalia [32, 60]. DNA barcode data indicate that *T. kiseogi* should be regarded as a junior synonym of *T. unagiseptimus* as the maximum interspecific divergence between specimens of these species was 1.5%. It is not clear if the *T. kiseogi* specimens from which the COI-sequences in GenBank originates are part of the type material, but they were possibly identified by one of the authors from the original species description since he is co-authoring the DNA barcode paper that published these sequences.

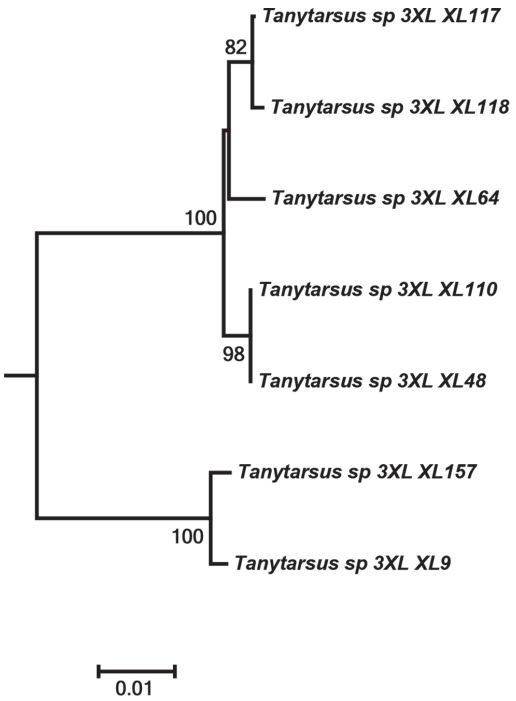

Fig 8. Neighbor joining subtree of *Tanytarsus* sp.3XL from Tibet, China. Numbers on branches represent bootstrap support (>70%) based on 500 replicates; scale represents K2P genetic distance.

doi:10.1371/journal.pone.0138993.g008

However, a formal synonymy should await comparison of type material. *Tanytarsus oscillans* and *Tanytarsus unagiseptimus*, on the other hand, probably are two valid species with a minimum interspecific divergence at 7% (Fig 9). In this case, the subtle morphological difference (i.e. extensively distributed microtrichia between the crests of the anal point in *T. oscillans* compared to a smooth surface in *T. unagiseptimus*) was perfectly mirrored by COI divergence.

Some mismatches between barcode clusters and identifications might be a result of misidentifications or differences in opinion between identifiers. This is to be expected because there are several groups in *Tanytarsus* with challenging taxonomy. Moreover, this type of mismatch can also occur if a reference database is used to identify unknown specimens but the identifications of these are not updated at the same time as the original reference sequences(s) if these change name. We found that *T. glabrescens* together with some unnamed *Tanytarsus* sequences grouped into three well-differentiated barcode clusters, which might demonstrate potential cryptic species within this species complex. One of the clusters was particularly interesting as single individuals of both *T. glabrescens* and *Tanytarsus buckleyi* Sublette were present together with many sequences from unidentified specimens (Fig 10). In case like this it is tempting to regard the one *T. glabrescens* as a misidentification since the species name already is present in two other clusters. However, it can only be clarified through examination of voucher specimens and collaboration between identifiers. It is therefore a great advantage for the taxonomy of challenging groups to deposit reference data in a database that facilitates communication

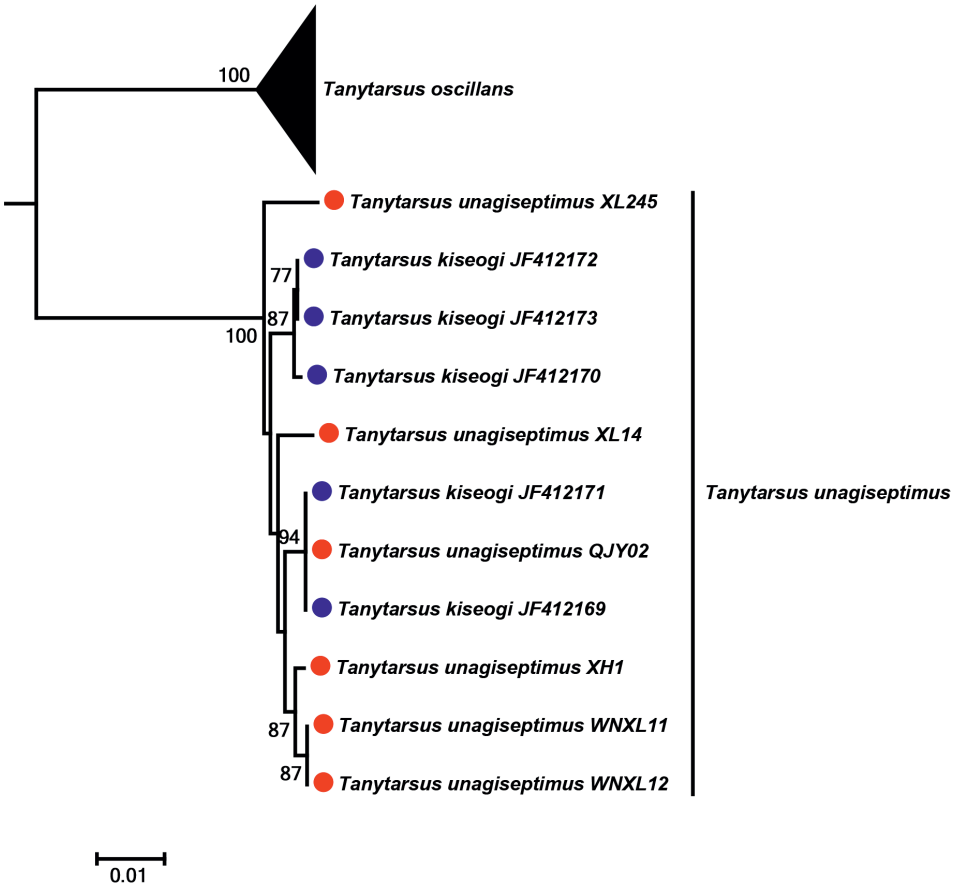

Fig 9. Neighbor joining subtree of *Tanytarsus kiseogi*, *Tanytarsus oscillans* and *Tanytarsus unagiseptimus*. Numbers on branches represent bootstrap support (>70%) based on 500 replicates; scale represents K2P genetic distance.

doi:10.1371/journal.pone.0138993.g009

between contributors and identifiers, such as BOLD, and voucher specimens of the sequences in an accessible collection [88].

A very similar situation was observed in the *Tanytarsus lestagei* aggregate which consists of several almost identical species [36, 58]. Within the European populations, some specimens of *T. lestagei*, *T. telmaticus and Tanytarsus* cf. *longitarsis* Kieffer grouped into the same cluster, while remaining specimens of *T. telmaticus*, *T. lestagei* and *Tanytarsus* cf. *dispar* Lindeberg could be well differentiated by DNA barcodes (Fig 11). However, there are currently several species with multiple synonyms within this group. Thus, perhaps Lindeberg's [58] separation of sympatric species turns out to be closer to the true species boundaries within this aggregate than Ekrem's [32] interpretation (and synonymization) of species in the same group.

The Asian members of the *T. lestagei* aggregate, *T. takahashii* and *Tanytarsus yunosecundus* Sasa previously have been distinguished from each other based on characters found in adult males, e.g. differences in the fore leg ratio and the shape of the superior volsella [32]. Recently,

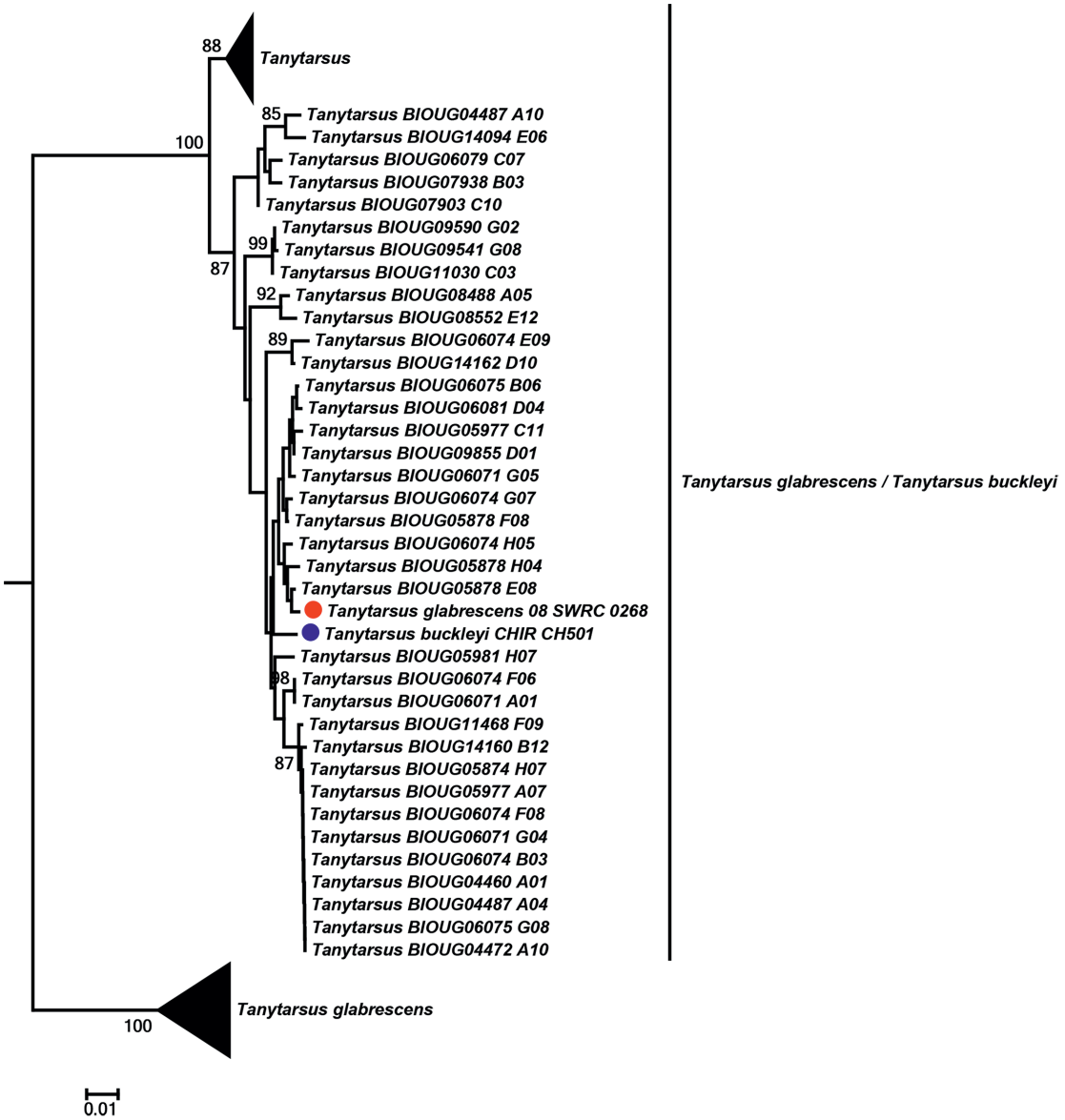

Fig 10. Neighbor joining subtree of *Tanytarsus buckleyi* and *Tanytarsus glabrescens*. Numbers on branches represent bootstrap support (>70%) based on 500 replicates; the dots indicate the specimens identified morphologically; scale represents K2P genetic distance.

doi:10.1371/journal.pone.0138993.g010

Tadashi Kobayashi (pers comm.) suggested *T. takahashii* to be a junior synonym of *T. yunosecundus*. DNA barcodes of populations from China and South Korea revealed low interspecific

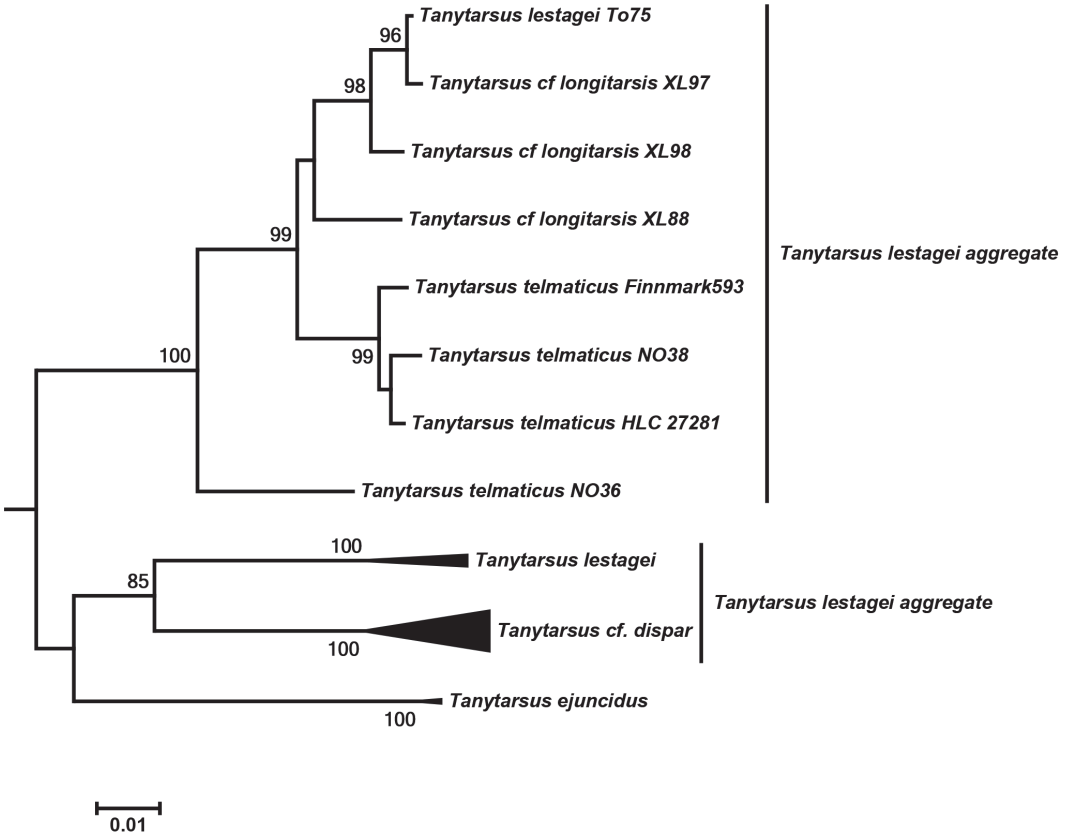

Fig 11. Neighbor joining subtree of European *Tanytarsus lestagei* aggregate. Numbers on branches represent bootstrap support (>70%) based on 500 replicates; scale represents K2P genetic distance.

doi:10.1371/journal.pone.0138993.g011

pairwise distance (2%) (Fig 12). However, a single DNA barcode of *T. takahashii* from Japan downloaded from GenBank did not group with these sequences and was more than 13% divergent based on K2P-distances. The single, divergent sequence was obtained from a pooled sample of male individuals (Richard Cornette pers comm.) and it is not unlikely that the barcode of *T. takahashii* from Japan in GenBank belong to another species. We have examined specimens from the same collection sample and can confirm that there are two superficially similar *Tanytarsus* and one *Cladotanytarsus* species present. Nevertheless, a synonymy of *T. takahashii* and *T. yunosecundus* should be avoided until more specimens of these species are examined and analyzed, especially from Japanese populations.

It should be kept in mind that there are no shortcuts to resolve the taxonomy of morphologically and genetically challenging species. Thus, further study using nuclear markers and more thorough morphological analyses are needed to sort out species boundaries and conclude on the potentially cryptic species within the different group treated above.

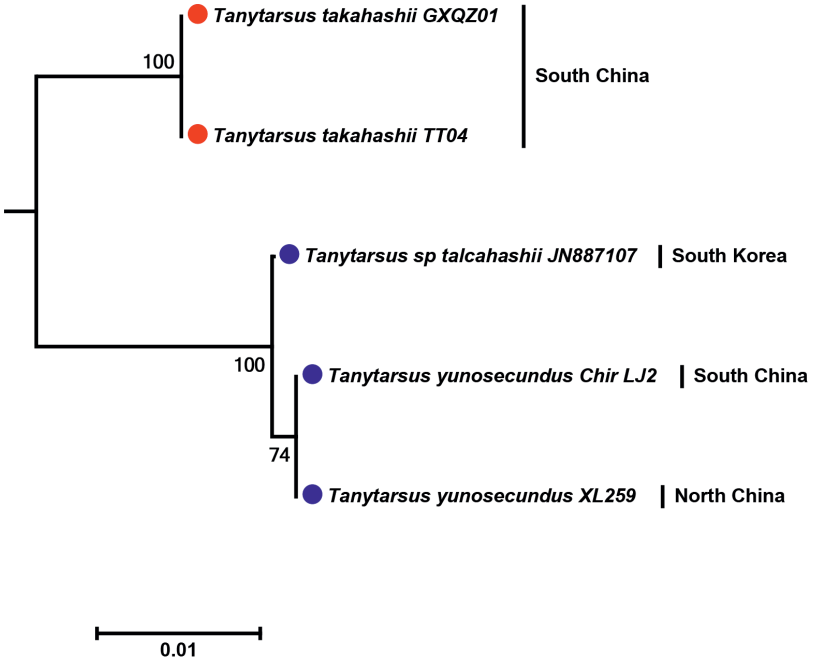

Fig 12. Neighbor joining subtree of Asian *Tanytarsus lestagei* aggregate (*Tanytarsus takahashii* and *Tanytarsus yunosecundus*). Numbers on branches represent bootstrap support (>70%) based on 500 replicates. It should be noted that "*Tanytarsus talcahashii*" is a misspelling of "*Tanytarsus takahashii*" in GenBank; scale represents K2P genetic distance.

doi:10.1371/journal.pone.0138993.g012

We based our study on taxon samples from around the world, particularly from Australia, China, Northern America and Western Europe. As there are more than 200 described *Tanytarsus* species from Africa, Australia, Eastern Asia and Southern America [32, 37], we have only about 1/3 of the known diversity of this genus. As shown above, a single or a few barcodes may not represent the putative species as whole, especially for geographically widespread species. Thus, restricted taxon sampling in many cases probably have led to an underrepresentation of the complete genetic range and inaccuracies in estimation of species [89]. As mentioned above, geographically separated populations of *T. occultus* showed high intraspecific variability. Without morphological taxonomic consideration, the two geographically separated populations would be regarded as cryptic species. In this and other sister group cases in *Tanytarsus*, a more detailed analysis is required to determine the current rate of gene flow between populations and if there is speciation in progress. Despite several challenging and biologically interesting incidents, DNA barcoding generally is effective for species identification in *Tanytarsus*, even when taxa are sampled from multiple and large geographic areas. This is similar to what has been recorded for Lepidoptera [90, 91] but opposite to findings for aquatic beetles [92]. Our data and results also show that traditional taxonomic considerations and comprehensive sampling are highly important for correct identification [87, 93] and that DNA barcodes in reference libraries provide an excellent starting point for taxonomic considerations and discussion on the identity of challenging taxa.

OTU estimation

Any particularly set threshold value for species separation will affect taxon diversity in any taxonomic group. Moreover, studies indicate that the same threshold is not appropriate for all groups. In insects for instance, a 2% threshold provides effective identification at the species-level of Ephemeroptera [94–96], Lepidoptera [97, 98], Plecoptera and Trichoptera [97]. While a 2.2% threshold has been found appropriate for Heteroptera [99, 100], a 2.5% threshold has been found suitable for aquatic beetles [101], a >3% threshold has been registered for several dipteran groups [46, 102, 103].

In Chironomidae, average intraspecific divergences range from 0.9% to 2.32% [3, 104] and when disregarding obvious cryptic species clusters, maximum intraspecific K2P distances can be as high as 8.5%, considerably higher than comparable rates in Heteroptera, Hymenoptera and Lepidoptera. In our study, morphologically determined *Tanytarsus* species had average intraspecific divergences of 2.14% (S2 Table). This was the case even for heavily sampled species such as *T. mendax*, where 430 sequences showed a mean pairwise divergence of 2.1%.

The number of OTUs in a DNA barcode dataset relies on both the method and threshold value used. Thus, we tested different methods for OTU calculation to explore what might be an appropriate threshold for *Tanytarsus* species.

Using Objective Clustering at threshold 2% yielded 217 clusters, while thresholds ranging from 3% to 7% yielded 120–156 clusters (Fig 13). Applying the ABGD method with prior

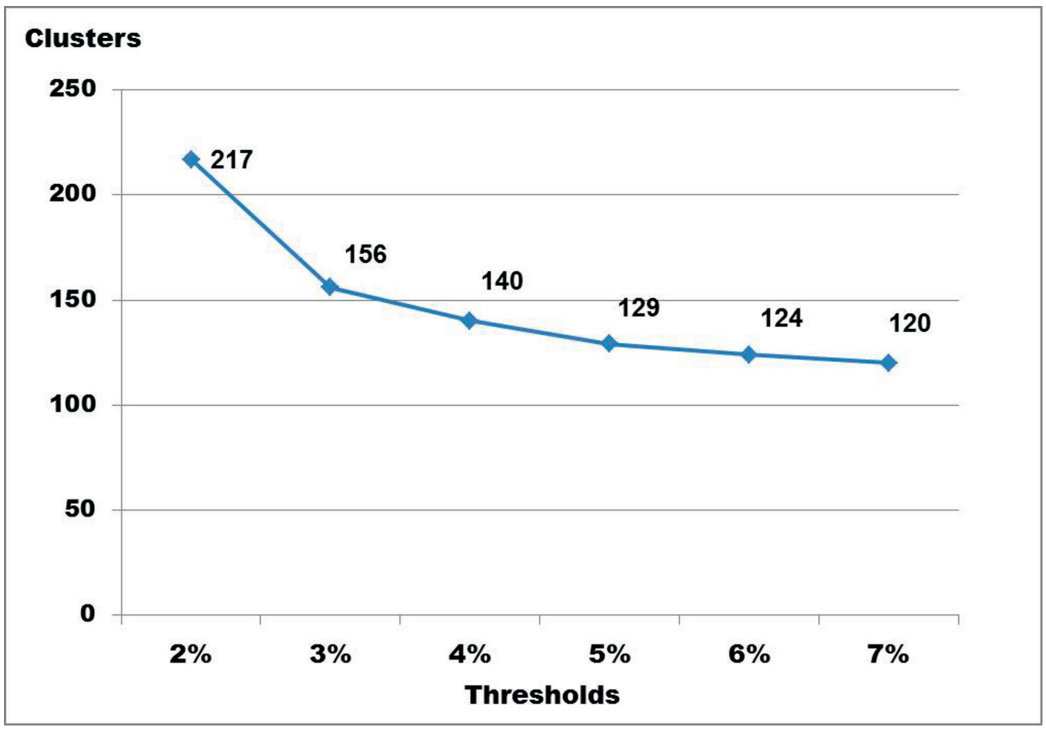

Fig 13. The number of DNA clusters according to Objective Clustering at different thresholds.

doi:10.1371/journal.pone.0138993.g013

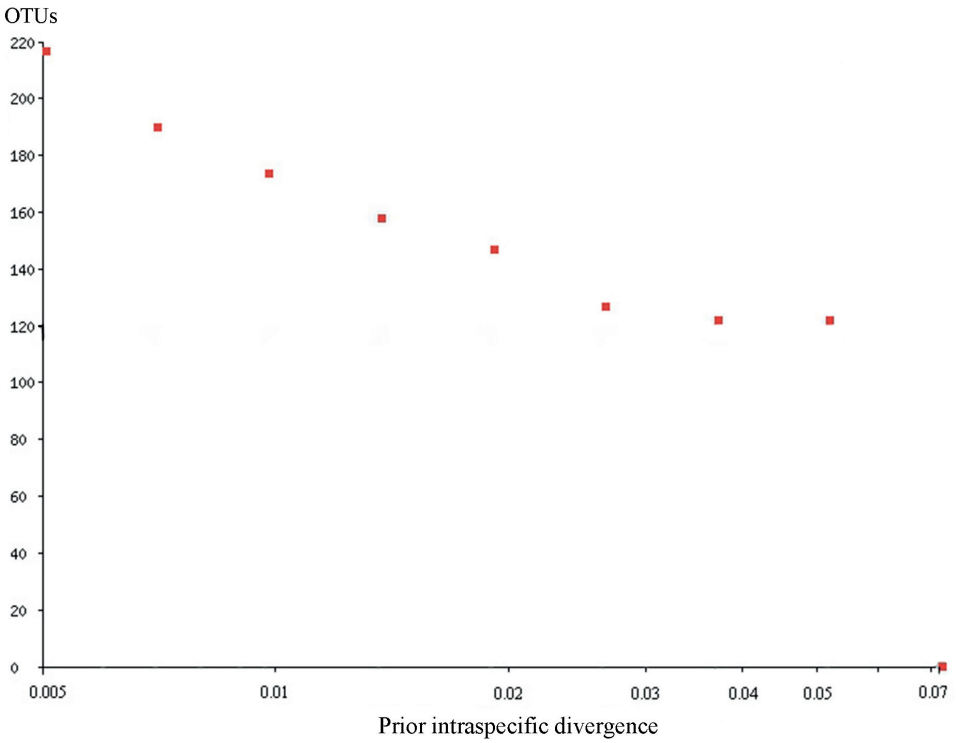

Fig 14. The number of the OTUs by the prior intraspecific divergence calculated with ABGD online.

doi:10.1371/journal.pone.0138993.g014

intraspecific divergence ranging from 3%–5% yielded 123–129 OTUs (Fig 14). This is similar to the number of divergent barcode clusters seen when subjectively evaluating the neighbor joining tree. Analyses of the reduced dataset containing only unique haplotype sequences yielded 180 clusters with a confidence interval ranging from 164–193 using GMYC (Fig 15) and 224–225

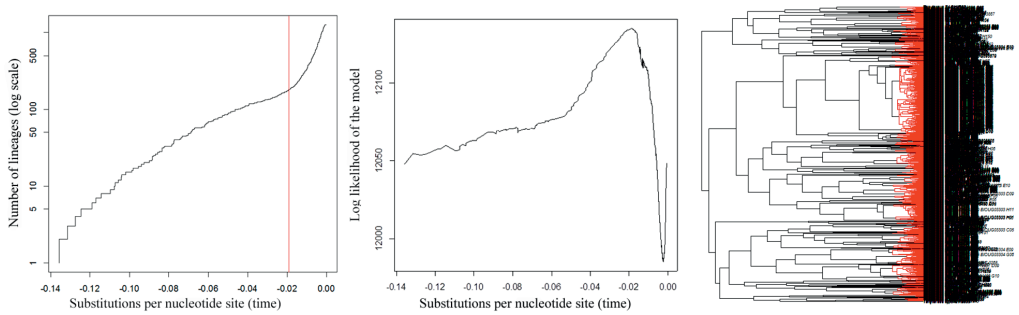

Fig 15. Results of the GMYC analysis. The red vertical line (left) indicates the single threshold time between inter-intraspecific branching; y axis (left) equals the number of lineages; y axis (center) equals the log likelihood of the single threshold GMYC model; the x axes (left and center) show substitutions per nucleotide site; the red branches (right) on the gene tree indicate estimated delimited species.

doi:10.1371/journal.pone.0138993.g015

clusters with PTP and bPTP (S3 File). Thus, GMYC yielded a more conservative number of species than PTP, but still considerably higher than what was obtained with Objective Clustering and ABGD using higher thresholds and our subjective evaluation of the neighbor joining tree. The observed difference in the species estimate for PTP may be associated with the unbalanced number of individuals sampled per species as this can affect the species delimitation [45].

Examining the dataset in BOLD, 2749 of 2790 barcodes were assigned a barcode index number and represented 242 BINs. In total, 2250 barcodes matched with morphospecies, representing 166 BINs, and 63 barcodes were singletons representing 63 BINs. Surprisingly, the 242 BINs in BOLD were approximately twice the number of divergent barcode clusters observed in the neighbor joining tree (131) and even higher than the number of species estimated by PTP. Thus, for *Tanytarsus*, the number of BINs generated by the BIN algorithm did not represent morphological species well. One reason might be that numerous identical haplotypes move the BIN-boundary upwards (Sujeevan Ratnasingham pers comm.). However, since BINs in BOLD have been shown to coincide strongly with known species boundaries in other insect groups, i.e. Coleoptera and Lepidoptera [97, 105], we suspect that it also is the starting threshold for the BIN algorithm that is too low for Chironomidae. Comparison of the results of ABGD, GMYC, PTP and objective clustering indicate that a 4–5% threshold is more appropriate for species delimitation in genus *Tanytarsus*.

Conclusion and Future Prospects

The discrimination of *Tanytarsus* species by DNA barcodes was highly successful with unambiguous grouping of 94.6% of the species recognized through prior morphological study. Deep intraspecific divergence existed in some species complexes, and further taxonomic studies are required to resolve these issues. Such studies preferably should involve morphological examination of all life stages as well as analysis of relationships using nuclear markers. Morphological re-examination of voucher specimens, in particular nominal types will be crucial to sort out taxonomic challenges and provide the best barcode reference library possible. We suggest that a 4–5% threshold on average is an appropriate level for species separation in *Tanytarsus* non-biting midges. This threshold is considerably higher than it is for certain other insect groups as well as the basis for the BIN-algorithm used in BOLD.

Supporting Information

S1 File. Neighbor joining bootstrap consensus tree for 2790 *Tanytarsus* barcodes. Numbers on branches are bootstrap support (>70%) using 500 bootstrap replicates. The clade names in blue represent 28 groups morphologically unidentified to the species-level, but clustering together. The clade names in red represent 16 identified morphospecies which likely are new to science but unpublished. The clade names in black represent morphospecies. For named species with more than two clusters, indicating cryptic species or misidentifications, we have used symbols with the same color and shape in front of the sequence names.
(PDF)

S2 File. Original alignment of 2790 *Tanytarsus* barcode sequences. Alignment of the 2790 sequences based on the Muscle algorithm (Edgar 2004) in MEGA6. Final length 658 bp.
(FAS)

S3 File. Maximum likelihood tree based on the PTP model.
(PDF)

S1 Table. Estimates of evolutionary divergence between sequences. Pairwise distance between 2790 nucleotide sequences based on the K2P model calculated in MEGA6. The

analysis included all codon positions and pairwise deletion of gaps for each sequence pair.
(XLS)

S2 Table. Estimates of average evolutionary divergence over sequence pairs within groups. Average pairwise distances within species based on the K2P substitution model calculated in MEGA6. The analysis included all codon positions and pairwise deletion of gaps for each sequence pair. In order to calculate the intra- and interspecific distances including sequences without species names in public databases, species names were added to 1242 DNA barcodes if they matched named sequences in the neighbor joining tree.
(XLS)

S3 Table. Estimates of evolutionary divergence over sequence pairs between groups. Average pairwise distance between species based on the K2P substitution model calculated in MEGA6. The analysis included all codon positions and pairwise deletion of gaps for each sequence pair. In order to calculate the intra- and interspecific distances including sequences without species names in public databases, species names were added to 1242 DNA barcodes if the matched named sequence in the neighbor joining tree.
(XLS)

Acknowledgments

This paper is part of the first author's thesis for the partial fulfilment of a PhD degree of the Norwegian University of Science and Technology, Norway, entitled "Systematics and Evolutionary history of *Tanytarsus* van der Wulp, 1874 (Diptera: Chironomidae)".

Thanks to the team at the Canadian Centre for DNA Barcoding for help with DNA barcode analysis. We are grateful to Professor Xinhua Wang (College of Life Sciences, Nankai University, China), who provided us with many important specimens from China. We also thank Dr. Wojciech Giłka (Department of Invertebrate Zoology and Parasitology, University of Gdańsk, Poland) and Chinese colleagues including Xin Qi (College of Life Sciences, Taizhou University, China), Chao Song and Wenbin Liu (College of Life Sciences, Nankai University, China) for providing material and Richard Cornette (National Institute of Agrobiological Sciences, Ibaraki, Japan) for valuable information on published COI sequences and material of *Tanytarsus takahashii*.Thanks also to Diego Fontaneto, Bruno Rossaro and Michael Raupach for valuable input on the manuscript.

Author Contributions

Conceived and designed the experiments: XL ES TE. Performed the experiments: XL TE. Analyzed the data: XL TE. Contributed reagents/materials/analysis tools: XL ES TE. Wrote the paper: XL ES TE.

References

1. Hebert PDN, Stoeckle MY, Zemlak TS, Francis CM. Identification of birds through DNA barcodes. PLoS Biol. 2004; 2(10):e312. doi: 10.1371/journal.pbio.0020312 PMID: 15455034; PubMed Central PMCID: PMC518999.
2. Hogg ID, Hebert PDN. Biological identification of springtails (Hexapoda: Collembola) from the Canadian Arctic, using mitochondrial DNA barcodes. Can J Zool. 2004; 82(5):749–754. doi: 10.1139/Z04-041 PMID: WOS:000225021400010.
3. Ekrem T, Willassen E, Stur E. A comprehensive DNA sequence library is essential for identification with DNA barcodes. Mol Phylogenet Evol. 2007; 43(2):530–542. doi: 10.1016/j.ympev.2006.11.021 PMID: WOS:000246918800015.

4. Oba Y, Ohira H, Murase Y, Moriyama A, Kumazawa Y. DNA barcoding of Japanese click beetles (Coleoptera, Elateridae). Plos One. 2015; 10(1):e0116612. doi: 10.1371/journal.pone.0116612 PMID: 25636000; PubMed Central PMCID: PMC4312051.
5. Smith PJ, Mcveagh SM, Allain V, Sanchez C. DNA identification of gut contents of large pelagic fishes. J Fish Biol. 2005; 67(4):1178–1183. doi: 10.1111/j.0022-1112.2005.00804.x PMID: WOS:000232787400025.
6. Hebert PDN, Cywinska A, Ball SL, deWaard JR. Biological identifications through DNA barcodes. Proc Biol Sci. 2003; 270(1512):313–321. doi: 10.1098/rspb.2002.2218 PMID: 12614582; PubMed Central PMCID: PMC1691236.
7. Hebert PDN, Ratnasingham S, deWaard JR. Barcoding animal life: cytochrome c oxidase subunit 1 divergences among closely related species. Proc Biol Sci. 2003; 270 Suppl 1:S96–99. doi: 10.1098/rsbl.2003.0025 PMID: 12952648; PubMed Central PMCID: PMC1698023.
8. Hunter SJ, Goodall TI, Walsh KA, Owen R, Day JC. Nondestructive DNA extraction from blackflies (Diptera: Simuliidae): retaining voucher specimens for DNA barcoding projects. Mol Ecol Resour. 2008; 8(1):56–61. doi: 10.1111/j.1471-8286.2007.01879.x PMID: 21585718.
9. Ilmonen J, Adler PH, Malmqvist B, Cywinska A. The *Simulium vernum* group (Diptera: Simuliidae) in Europe: multiple character sets for assessing species status. Zool J Linn Soc. 2009; 156(4):847–863. doi: 10.1111/j.1096-3642.2009.00500.x PMID: WOS:000269395300006.
10. Carew ME, Pettigrove V, Hoffmann AA. The utility of DNA markers in classical taxonomy: Using cytochrome oxidase I markers to differentiate Australian *Cladopelma* (Diptera: Chironomidae) midges. Ann Entomol Soc Am. 2005; 98(4):587–594. doi: 10.1603/0013-8746(2005)098[0587:Tuodmi]2.0.Co;2 PMID: WOS:000230359800020.
11. Ekrem T, Stur E, Hebert PDN. Females do count: Documenting Chironomidae (Diptera) species diversity using DNA barcoding. Org Divers Evol. 2010; 10(5):397–408. doi: 10.1007/s13127-010-0034-y PMID: WOS:000284364300004.
12. Silva FL, Wiedenbrug S. Integrating DNA barcodes and morphology for species delimitation in the *Corynoneura* group (Diptera: Chironomidae: Orthocladiinae). B Entomol Res. 2014; 104(1):65–78. doi: 10.1017/S0007485313000515 PMID: WOS:000332950800008.
13. Silva FL, Fonseca-Gessner AA, Ekrem T. A taxonomic revision of genus *Labrundinia* Fittkau, 1962 (Diptera: Chironomidae: Tanypodinae). Zootaxa. 2014; 3769(1):1–185. doi: 10.11646/zootaxa.3769.1.1 PMID: WOS:000332070000001.
14. Stur E, Ekrem T. Exploring unknown life stages of Arctic Tanytarsini (Diptera: Chironomidae) with DNA barcoding. Zootaxa. 2011;(2743:):27–39. PMID: WOS:000286330700002.
15. Silva FL, Ekrem T, Fonseca-Gessner AA. Out of South America: phylogeny of non-biting midges in the genus *Labrundinia* suggests multiple dispersal events to Central and North America. Zool Scr. 2015; 44(1):59–71. doi: 10.1111/Zsc.12089 PMID: WOS:000346161200005.
16. Demin AG, Polukonova NV, Mugue NS. Molecular phylogeny and the time of divergence of minges (Chironomidae, Nematocera, Diptera) inferred from a partial nucleotide sequence of the cytochrome oxidase I gene (COI). Russ J Genet+. 2011; 47(10):1168–1180. doi: 10.1134/S1022795411100061 PMID: WOS:000297849700004.
17. Sari A, Duran M, Sen A, Bardakci F. Investigation of Chironomidae (Diptera) relationships using mitochondrial COI gene. Biochem Sys Ecol. 2015; 59(0):229–238. doi: 10.1016/j.bse.2015.01.005
18. Armitage PD, Cranston PS, Pinder LCV. The Chironomidae: biology and ecology of non-biting midges. London: Chapman & Hall; 1995. XII, 572 p.
19. Ali A, Majori G, Ceretti G, Dandrea F, Scattolin M, Ferrarese U. A chironomid (Diptera, Chironomidae) midge population study and laboratory evaluation of larvicides against midges inhabiting the Lagoon of Venice, Italy. J Am Mosquito Contr. 1985; 1(1):63–68. PMID: WOS:A1985AFX6500014.
20. Rosenberg D. Freshwater biomonitoring and Chironomidae. Neth J Aquat Ecol. 1992; 26(2–4):101–122. doi: 10.1007/BF02255231
21. Carew ME, Pettigrove VJ, Metzeling L, Hoffmann AA. Environmental monitoring using next generation sequencing: rapid identification of macroinvertebrate bioindicator species. Front Zool. 2013; 10. doi: 10.1186/1742-9994-10-45 PMID: WOS:000322907500001.
22. Brodin Y, Ejdung G, Strandberg J, Lyrholm T. Improving environmental and biodiversity monitoring in the Baltic Sea using DNA barcoding of Chironomidae (Diptera). Mol Ecol Resour. 2013; 13(6):996–1004. doi: 10.1111/1755-0998.12053 PMID: 23280321.
23. Cranston PS, Ang YC, Heyzer A, Lim RBH, Wong WH, Woodford JM, et al. The nuisance midges (Diptera: Chironomidae) of Singapore's Pandan and Bedok Reservoirs. Raffles B Zool. 2013; 61 (2):779–793. PMID: WOS:000323694800027.

24. Meier R, Wong W, Srivathsan A, Foo M. $1 DNA barcodes for reconstructing complex phenomes and finding rare species in specimen-rich samples. Cladistics. 2015:1–11. doi: 10.1111/cla.12115

25. Edwards D, Horn A, Taylor D, Savolain V, Hawkins JA. DNA barcoding of a large genus, *Aspalathus* L. (Fabaceae). Taxon. 2008; 57(4):1317–1327. PMID: WOS:000261283000021.

26. Xu S, Li D, Li J, Xiang X, Jin W, Huang W, et al. Evaluation of the DNA barcodes in *Dendrobium* (Orchidaceae) from mainland Asia. Plos One. 2015; 10(1):e0115168. doi: 10.1371/journal.pone.0115168 PMID: 25602282; PubMed Central PMCID: PMC4300225.

27. Yan L, Liu J, Moller M, Zhang L, Zhang X, Li D, et al. DNA barcoding of *Rhododendron* (Ericaceae), the largest Chinese plant genus in biodiversity hotspots of the Himalaya-Hengduan Mountains. Mol Ecol Resour. 2014. doi: 10.1111/1755-0998.12353 PMID: 25469426.

28. Epler JH, Ekrem T, Cranston PS. The larvae of Chironominae (Diptera: Chironomidae) of the Holarctic region–keys and diagnoses. In: Cederholm L, editor. Chironomidae of the Holarctic Region: Keys and Diagnoses, Part 1: Larvae. 66. Lund, Sweden: Insect Systematics and Evolution Supplements 2013. p. 387–556.

29. Wulp FM. Dipterologische aanteekeningen. Tijdschr Ent. 1874; 17:109–148.

30. Ekrem T. Diagnoses and immature stages of some Australian *Tanytarsus* van der Wulp (Diptera: Chironomidae). Aust J Entomol. 2001; 40:312–325. doi: 10.1046/j.1440-6055.2001.00246.x PMID: WOS:000179821100002.

31. Ekrem T. A Review of Afrotropical *Tanytarsus* Van Der Wulp (Diptera: Chironomidae). Tijdschr Ent. 2001; 144(1):5–40. doi: 10.1163/22119434-99900054

32. Ekrem T. A review of selected south-and east Asian *Tanytarsus* vd Wulp (Diptera: Chironomidae). Hydrobiologia. 2002; 474(1–3):1–39. doi: 10.1023/A:1016527603086

33. Ekrem T. Immature stages of European *Tanytarsus* species I. The *eminulus*-, *gregarius*-, *lugens*- and *mendax* species groups (Diptera, Chironomidae). Dtsch entomol Z. 2004; 51(1):97–146. doi: 10.1002/mmnd.20040510110 PMID: WOS:000222263900009.

34. Ekrem T, Sublette MF, Sublette JE. North American *Tanytarsus* I. Descriptions and keys to species in the *eminulus*, *gregarius*, *lugens* and *mendax* species groups (Diptera: Chironomidae). Ann Entomol Soc Am. 2003; 96(3):265–328. doi: 10.1603/0013-8746(2003)096[0265:Natida]2.0.Co;2 PMID: WOS:000183079900011.

35. Glover B. The Tanytarsini (Diptera, Chironomidae) of Australia. Aust J Zool Suppl Ser. 1973; 25:403–478. doi: 10.1071/AJZS023

36. Reiss F, Fittkau EJ. Taxonomie und Ökologie europäisch verbreiteter *Tanytarsus*-Arten (Chironomidae, Diptera). Arch Hydrobiol Suppl. 1971; 40:75–200.

37. Sanseverino AM. A review of the genus *Tanytarsus* van der Wulp, 1874 (Insecta, Diptera, Chironomidae) from the Neotropical Region [Dissertation, LMU Munich]. München2006.

38. Price TD, Qvarnstrom A, Irwin DE. The role of phenotypic plasticity in driving genetic evolution. Proc Biol Sci. 2003; 270(1523):1433–1440. Epub 2003/09/11. doi: 10.1098/rspb.2003.2372 PMID: 12965006; PubMed Central PMCID: PMCPmc1691402.

39. McKie BG, Cranston PS. Size matters: systematic and ecological implications of allometry in the responses of chironomid midge morphological ratios to experimental temperature manipulations. Can J Zool. 2005; 83(4):553–568. doi: 10.1139/z05-051

40. Saitou N, Nei M. The neighbor-joining method: a new method for reconstructing phylogenetic trees. Mol Bio Evol. 1987; 4(4):406–425.

41. Puillandre N, Lambert A, Brouillet S, Achaz G. ABGD, Automatic Barcode Gap Discovery for primary species delimitation. Mol Ecol. 2012; 21(8):1864–1877. doi: 10.1111/j.1365-294X.2011.05239.x PMID: WOS:000302616200008.

42. Pons J, Barraclough TG, Gomez-Zurita J, Cardoso A, Duran DP, Hazell S, et al. Sequence-based species delimitation for the DNA taxonomy of undescribed insects. Syst Biol. 2006; 55(4):595–609. PMID: 16967577.

43. Fujisawa T, Barraclough TG. Delimiting Species Using Single-Locus Data and the Generalized Mixed Yule Coalescent Approach: A Revised Method and Evaluation on Simulated Data Sets. Syst Biol. 2013; 62(5):707–724. doi: 10.1093/sysbio/syt033 PMID: 23681854

44. Fontaneto D, Flot J-F, Tang C. Guidelines for DNA taxonomy, with a focus on the meiofauna. Mar Biodiv. 2015:1–19. doi: 10.1007/s12526-015-0319-7

45. Zhang J, Kapli P, Pavlidis P, Stamatakis A. A general species delimitation method with applications to phylogenetic placements. Bioinformatics. 2013; 29(22):2869–2876. doi: 10.1093/bioinformatics/btt499 PMID: 23990417

46. Meier R, Shiyang K, Vaidya G, Ng PK. DNA barcoding and taxonomy in Diptera: a tale of high intraspecific variability and low identification success. Syst Biol. 2006; 55(5):715–728. doi: 10.1080/10635150600969864 PMID: 17060194.

47. Ratnasingham S, Hebert PD. A DNA-based registry for all animal species: the barcode index number (BIN) system. Plos One. 2013; 8(7):e66213. doi: 10.1371/journal.pone.0066213 PMID: 23861743; PubMed Central PMCID: PMC3704603.

48. Kekkonen M, Mutanen M, Kaila L, Nieminen M, Hebert PD. Delineating species with DNA barcodes: a case of taxon dependent method performance in moths. Plos One. 2015; 10(4):e0122481. doi: 10.1371/journal.pone.0122481 PMID: 25849083.

49. Hendrich L, Pons J, Ribera I, Balke M. Mitochondrial cox1 sequence data reliably uncover patterns of insect diversity but suffer from high lineage-idiosyncratic error rates. Plos One. 2010; 5(12):e14448. doi: 10.1371/journal.pone.0014448 PMID: 21203427

50. Tänzler R, Sagata K, Surbakti S, Balke M, Riedel A. DNA barcoding for community ecology-how to tackle a hyperdiverse, mostly undescribed Melanesian fauna. Plos One. 2012; 7(1):e28832. doi: 10.1371/journal.pone.0028832 PMID: 22253699

51. Hawlitschek O, Nagy ZT, Berger J, Glaw F. Reliable DNA barcoding performance proved for species and island populations of comoran squamate reptiles. Plos One. 2013; 8(9):e73368. doi: 10.1371/journal.pone.0073368 PMID: 24069192

52. Ratnasingham S, Hebert PDN. BOLD: The Barcode of Life Data System (www.barcodinglife.org). Mol Ecol Notes. 2007; 7(3):355–364. doi: 10.1111/j.1471-8286.2006.01678.x PMID: WOS:000246244300001.

53. Ekrem T, Stur E. Description of *Tanytarsus hjulorum*, new species, with notes and DNA barcodes of some South African *Tanytarsus* (Diptera: Chironomidae). In: Andersen T, editor. Contributions to the systematics and ecology of aquatic Diptera. A tribute to Ole A. Sæther. Columbus, Ohio: Caddis Press; 2007. p. 87–92.

54. Giłka W, Paasivirta L. On the systematics of the tribe Tanytarsini (Diptera: Chironomidae)—three new species from Finland. Entomol Fennica. 2008; 19(1):41–48. PMID: WOS:000254116100006.

55. Giłka W, Paasivirta L. Evaluation of diagnostic characters of the *Tanytarsus chinyensis* group (Diptera: Chironomidae), with description of a new species from Lapland. Zootaxa. 2009;(2197:):31–42. PMID: WOS:000268906300003.

56. Langton PH. *Micropsectra silvesterae* n. sp and *Tanytarsus heliomesonyctios* n. sp., (Diptera: Chironomidae), two parthenogenetic species from Ellesmere Island, Arctic Canada. J Kansas Entomol Soc. 1998; 71(3):208–215. PMID: WOS:000083304900003.

57. Lindeberg B. Taxonomy, biology and biometry of *Tanytarsus curticornis* Kieff. and *T. brundini* n. sp. (Dipt., Chironomidae). Annls Zool Fennici. 1963; 29:118–130.

58. Lindeberg B. Sibling species delimitation in the *Tanytarsus lestagei* aggregate Diptera, Chironomidae. Annls Zool Fennici. 1967; 4(1):45–86.

59. Moubayed Z. Chironomids from running waters of Thailand: description of *Rheotanytarsus thailandensis* sp.n. and *Tanytarsus thaicus* sp.n. (Dipt., Chironomidae). Hydrobiologia. 1990; 203(1–2):29–33. doi: 10.1007/BF00005610

60. Ree HI, Jeong KY. Fauna of non-biting midges (Diptera, Chironomidae) from Soyang River in Chuncheon-si, Gangwon-do, Korea. Korean J Syst Zool. 2010; 26(2):115–140. doi: 10.5635/KJSZ.2010.26.2.115

61. Sasa M, Kawai K. Studies on chironomid midges of Lake Biwa (Diptera, Chironomidae): Lake Biwa Research Institute, Otsu, Japan; 1987. 119 p.

62. Sasa M, Suzuki H, Sakai T. Studies on the chironomid midges collected on the shore of Shimanto River in April, 1998. Part 1. Description of species of the subfamily Chironominae. Trop Med. 1998; 40(2):47–89.

63. Sasa M, Suzuki H. Stuidies on the chironomid species collected on Ishigaki and Iriomote Islands, Southwestern Japan. Trop Med. 2000; 42(1):1–37.

64. Sublette JE, Sasa M. Chironomidae collected in onchocerciasis endemic areas of Guatemala (Insecta, Diptera). Spixiana Suppl. 1994; 20.

65. Kimura M. A simple method for estimating evolutionary rates of base substitutions through comparative studies of nucleotide sequences. J Mol Evol. 1980; 16(2):111–120. Epub 1980/12/01. PMID: 7463489.

66. Sæther OA. Some Nearctic Pondonominae, Diamesinae, and Orthocladiinae (Diptera: Chironomidae). Ottawa: Department of Fisheries and Oceans; 1969. 154 p.

67. Folmer O, Black M, Hoeh W, Lutz R, Vrijenhoek R. DNA primers for amplification of mitochondrial cytochrome c oxidase subunit I from diverse metazoan invertebrates. Mol Mar Biol Biotechnol. 1994; 3(5):294–299. PMID: 7881515.

68. Maddison WP, Maddison DR. Mesquite: a modular system for evolutionary analysis 2.5 ed. 2008.

69. Edgar RC. MUSCLE: multiple sequence alignment with high accuracy and high throughput. Nucleic Acids Res. 2004; 32(5):1792–1797. doi: 10.1093/Nar/Gkh340 PMID: WOS:000220487200025.

70. Tamura K, Stecher G, Peterson D, Filipski A, Kumar S. MEGA6: Molecular Evolutionary Genetics Analysis version 6.0. Mol Biol Evol. 2013; 30(12):2725–2729. doi: 10.1093/molbev/mst197 PMID: 24132122; PubMed Central PMCID: PMC3840312.

71. Drummond AJ, Suchard MA, Xie D, Rambaut A. Bayesian phylogenetics with BEAUti and the BEAST 1.7. Mol Bio Evol. 2012; 29(8):1969–1973. Epub 2012/03/01. doi: 10.1093/molbev/mss075 PMID: 22367748; PubMed Central PMCID: PMCPmc3408070.

72. Rambaut A, Suchard MA, Xie D, Drummond AJ. Tracer v1.6, Available: http://beast.bio.ed.ac.uk/Tracer. 2014.

73. Ezard T, Fujisawa T, Barraclough T. Splits: SPecies' LImits by Threshold Statistics, R package version 1.0-11/r29. 2009.

74. Team RC. R: A language and environment for statistical computing. R Foundation for Statistical Computing, Vienna, Austria, 2012. ISBN 3-900051-07-0; 2014.

75. Stamatakis A. RAxML-VI-HPC: maximum likelihood-based phylogenetic analyses with thousands of taxa and mixed models. Bioinformatics. 2006; 22(21):2688–2690. PMID: 16928733

76. Silvestro D, Michalak I. raxmlGUI: a graphical front-end for RAxML. Org Divers Evol. 2012; 12 (4):335–337. doi: 10.1007/s13127-011-0056-0

77. Lopez JV, Yuhki N, Masuda R, Modi W, O'Brien SJ. Numt, a recent transfer and tandem amplification of mitochondrial DNA to the nuclear genome of the domestic cat. J Mol Evol. 1994; 39(2):174–190. Epub 1994/08/01. PMID: 7932781.

78. Bensasson D, Zhang D, Hartl DL, Hewitt GM. Mitochondrial pseudogenes: evolution's misplaced witnesses. Trends Ecol Evol. 2001; 16(6):314–321. Epub 2001/05/23. PMID: 11369110.

79. Richly E, Leister D. NUMTs in sequenced eukaryotic genomes. Mol Biol Evol. 2004; 21(6):1081–1084. Epub 2004/03/12. doi: 10.1093/molbev/msh110 PMID: 15014143.

80. Smith MA, Bertrand C, Crosby K, Eveleigh ES, Fernandez-Triana J, Fisher BL, et al. *Wolbachia* and DNA Barcoding Insects: Patterns, Potential, and Problems. Plos One. 2012; 7(5):e36514. doi: 10.1371/journal.pone.0036514 PMID: 22567162

81. Ballard JWO, Whitlock MC. The incomplete natural history of mitochondria. Mol Ecol. 2004; 13 (4):729–744. PMID: WOS:000220153000002.

82. Heckman KL, Mariani CL, Rasoloarison R, Yoder AD. Multiple nuclear loci reveal patterns of incomplete lineage sorting and complex species history within western mouse lemurs (Microcebus). Mol Phylogenet Evol. 2007; 43(2):353–367. doi: 10.1016/j.ympev.2007.03.005 PMID: WOS:000246918800001.

83. Willyard A, Cronn R, Liston A. Reticulate evolution and incomplete lineage sorting among the ponderosa pines. Mol Phylogenet Evol. 2009; 52(2):498–511. doi: 10.1016/j.ympev.2009.02.011 PMID: WOS:000266693400021.

84. Gay L, Neubauer G, Zagalska-Neubauer M, Debain C, Pons JM, David P, et al. Molecular and morphological patterns of introgression between two large white-headed gull species in a zone of recent secondary contact. Mol Ecol. 2007; 16(15):3215–3227. doi: 10.1111/j.1365-294X.2007.03363.x PMID: WOS:000248847600013.

85. Martinsen GD, Whitham TG, Turek RJ, Keim P. Hybrid populations selectively filter gene introgression between species. Evolution. 2001; 55(7):1325–1335. Epub 2001/08/30. PMID: 11525457.

86. Collins RA, Cruickshank RH. The seven deadly sins of DNA barcoding. Mol Ecol Resour. 2013; 13 (6):969–975. doi: 10.1111/1755-0998.12046 PMID: 23280099.

87. DeSalle R, Egan MG, Siddall M. The unholy trinity: taxonomy, species delimitation and DNA barcoding. Philos Trans R Soc Lond B Biol Sci. 2005; 360(1462):1905–1916. doi: 10.1098/rstb.2005.1722 PMID: 16214748; PubMed Central PMCID: PMC1609226.

88. Turney S, Cameron ER, Cloutier CA, Buddle CM. Non-repeatable science: assessing the frequency of voucher specimen deposition reveals that most arthropod research cannot be verified. PeerJ. 2015; 3:e1168. doi: 10.7717/peerj.1168 PMID: 26339546

89. Resch MC, Shrubovych J, Bartel D, Szucsich NU, Timelthaler G, Bu Y, et al. Where taxonomy based on subtle morphological differences is perfectly mirrored by huge genetic distances: DNA barcoding

in Protura (Hexapoda). Plos One. 2014; 9(3). doi: 10.1371/journal.pone.0090653 PMID: WOS:000332485800041.

90. Huemer P, Karsholt O, Mutanen M. DNA barcoding as a screening tool for cryptic diversity: an example from *Caryocolum*, with description of a new species (Lepidoptera, Gelechiidae). ZooKeys. 2014; (404:):91–111. doi: 10.3897/zookeys.404.7234 PMID: WOS:000339974500001.

91. Lukhtanov VA, Sourakov A, Zakharov EV, Hebert PD. DNA barcoding Central Asian butterflies: increasing geographical dimension does not significantly reduce the success of species identification. Mol Ecol Resour. 2009; 9(5):1302–1310. doi: 10.1111/j.1755-0998.2009.02577.x PMID: 21564901.

92. Bergsten J, Bilton DT, Fujisawa T, Elliott M, Monaghan MT, Balke M, et al. The effect of geographical scale of sampling on DNA barcoding. Syst Biol. 2012; 61(5):851–869. doi: 10.1093/sysbio/sys037 PMID: 22398121; PubMed Central PMCID: PMC3417044.

93. Meyer CP, Paulay G. DNA barcoding: error rates based on comprehensive sampling. PLoS Biol. 2005; 3(12):e422. doi: 10.1371/journal.pbio.0030422 PMID: 16336051; PubMed Central PMCID: PMC1287506.

94. Webb JM, Jacobus LM, Funk DH, Zhou X, Kondratieff B, Geraci CJ, et al. A DNA barcode library for North American Ephemeroptera: progress and prospects. Plos One. 2012; 7(5):e38063. doi: 10.1371/journal.pone.0038063 PMID: 22666447; PubMed Central PMCID: PMC3364165.

95. Zhou X, Jacobus LM, DeWalt RE, Adamowicz SJ, Hebert PDN. Ephemeroptera, Plecoptera, and Trichoptera fauna of Churchill (Manitoba, Canada): insights into biodiversity patterns from DNA barcoding. J N Am Benthol Soc. 2010; 29(3):814–837. doi: 10.1899/09-121.1 PMID: WOS:000280692400004.

96. Schmidt S, Schmid-Egger C, Morinière J, Haszprunar G, Hebert PDN. DNA barcoding largely supports 250 years of classical taxonomy: identifications for Central European bees (Hymenoptera, Apoidea *partim*). Mol Ecol Resour. 2015:n/a-n/a.

97. Zahiri R, Lafontaine JD, Schmidt BC, Dewaard JR, Zakharov EV, Hebert PD. A transcontinental challenge—a test of DNA barcode performance for 1,541 species of Canadian Noctuoidea (Lepidoptera). Plos One. 2014; 9(3):e92797. doi: 10.1371/journal.pone.0092797 PMID: 24667847; PubMed Central PMCID: PMC3965468.

98. Hajibabaei M, Janzen DH, Burns JM, Hallwachs W, Hebert PDN. DNA barcodes distinguish species of tropical Lepidoptera. PNAS. 2006; 103(4):968–971. doi: 10.1073/pnas.0510466103 PMID: WOS:000234938300025.

99. Park DS, Foottit R, Maw E, Hebert PDN. Barcoding bugs: DNA-based Identification of the true bugs (Insecta: Hemiptera: Heteroptera). Plos One. 2011; 6(4). doi: 10.1371/journal.pone.0018749 PMID: WOS:000289578600029.

100. Raupach MJ, Hendrich L, Kuchler SM, Deister F, Moriniere J, Gossner MM. Building-up of a DNA barcode library for true bugs (Insecta: Hemiptera: Heteroptera) of Germany reveals taxonomic uncertainties and surprises. Plos One. 2014; 9(9):e106940. doi: 10.1371/journal.pone.0106940 PMID: 25203616; PubMed Central PMCID: PMC4159288.

101. Monaghan MT, Balke M, Gregory TR, Vogler AP. DNA-based species delineation in tropical beetles using mitochondrial and nuclear markers. Philos Trans R Soc Lond B Biol Sci. 2005; 360 (1462):1925–1933. PMID: 16214750

102. Nzelu CO, Caceres AG, Arrunategui-Jimenez MJ, Lanas-Rosas MF, Yanez-Trujillano HH, Luna-Caipo DV, et al. DNA barcoding for identification of sand fly species (Diptera: Psychodidae) from leishmaniasis-endemic areas of Peru. Acta Trop. 2015; 145:45–51. doi: 10.1016/j.actatropica.2015.02.003 PMID: 25697864.

103. Renaud AK, Savage J, Adamowicz SJ. DNA barcoding of Northern Nearctic Muscidae (Diptera) reveals high correspondence between morphological and molecular species limits. BMC ecology. 2012; 12:24. doi: 10.1186/1472-6785-12-24 PMID: 23173946; PubMed Central PMCID: PMC3537539.

104. Sinclair CS, Gresens SE. Discrimination of *Cricotopus* species (Diptera: Chironomidae) by DNA barcoding. B Entomol Res. 2008; 98(6):555–563. doi: 10.1017/S0007485308005865 PMID: WOS:000261616300003.

105. Pentinsaari M, Hebert PDN, Mutanen M. Barcoding Beetles: A regional survey of 1872 species reveals high identification success and unusually deep interspecific divergences. Plos One. 2014; 9 (9). doi: 10.1371/journal.pone.0108651 PMID: WOS:000344862300102.

DNA barcodes and morphology reveal new semi-cryptic species of Chironomidae (Diptera)

Xiao-Long Lin*, Elisabeth Stur & Torbjørn Ekrem

Department of Natural History, NTNU University Museum, Norwegian University of Science and Technology, NO-7491, Trondheim, Norway

*Corresponding author. E-mail: xiaolong.lin@ntnu.no

Abstract

For over a decade, DNA barcoding has proven an effective modern tool in taxonomy, evolutionary biology and biodiversity research. Many new species have been discovered and described with DNA barcodes as part of their diagnostic features. Using DNA barcodes, we uncovered a number of potential species within the *Tanytarsus curticornis* and *Tanytarsus heusdensis* species complexes (Diptera: Chironomidae) and detected morphological differences *a posteriori* that support the description of new species. In total, eight species new to science are described and figured: *T. adustus* sp. n., *T. heberti* sp. n., *T. madeiraensis* sp. n., *T. pseudoheusdensis* sp. n., *T. songi* sp. n., *T. thomasi* sp. n., *T. tongmuensis* sp. n. and *T. wangi* sp. n.. *Tanytarsus reei* and *T. tamaoctavus* are re-described, and *T. tusimatneous* is listed as a new junior synonym of *T. tamaduodecimus*. The diagnostic characters of the remaining species of the complexes are discussed. Keys to males and pupae are given.

Keywords

COI sequences; Tanytarsini; new species; key.

Introduction

Over the past decade, the use of short standardized genetic markers for species identification, so-called DNA barcoding (Hebert et al. 2003a; Hebert et al. 2003b), has proven effective in biodiversity assessments (Hajibabaei et al. 2016; Lee et al. 2016) and taxonomic revisions (Hausmann et al. 2016; Miller et al. 2016). DNA barcoding has aided our understanding of species community compositions, food webs and genetic variation within species (Baker et al. 2016; Littlefair & Clare 2016; Roslin & Majaneva 2016) and is an important and useful asset in biosecurity (Ashfaq & Hebert 2016; Hodgetts et al. 2016) and biomonitoring of freshwater ecosystems (Brodin et al. 2013; Carew et al. 2013). DNA barcodes can uncover cryptic species diversity in many cases (Macher et al. 2016; Witt et al. 2006; Yang et al. 2012), and indicate species boundaries with additional morphological and ecological data. For instance, in a classic example (Hebert et al. 2004) discovered ten different species in the *Astraptes fulgerator* species complex when combining DNA barcodes, host plant records and larval morphology. Recently, several potential cryptic species of Chironomidae are being increasingly detected by DNA barcodes (Anderson et al. 2013; Carew et al. 2011; Lin et al. 2015; Silva & Wiedenbrug 2014; Song et al. 2016; Stur & Ekrem 2015).

The genus *Tanytarsus* van der Wulp, 1874 (Diptera: Chironomidae) is the most species-rich genus of the tribe Tanytarsini in subfamily Chironominae with more than 400 described species worldwide. Larvae of *Tanytarsus* are eurytopic, occurring in all types of freshwater and some even in marine or terrestrial environments (Epler et al. 2013). The genus was erected by van der Wulp (1874) with *Tanytarsus signatus* (van der Wulp, 1859) as the type species, and various species groups and species have been revised over the last few decades (Cranston 2000; Ekrem 2001, 2002, 2004; Ekrem et al. 2003; Giłka & Paasivirta 2009; Glover 1973; Lindeberg 1963, 1967; Reiss & Fittkau 1971; Sanseverino 2006).

In general, morphological identification at species-level in Chironomidae relies strongly on characters of adult males, especially the hypopygium in combination with a range of morphological measurements, counts and ratios. Morphological determination of species in some *Tanytarsus* species groups can be extremely challenging. Additionally, there are many unknown and cryptic species in *Tanytarsus* and it is difficult to associate the immature stages with adults through rearing since it is time-consuming and not always successful.

The *Tanytarsus curticornis* Kieffer, 1911 and *Tanytarsus heusdensis* Goetghebuer, 1923 species complexes have, based on morphology, previously been placed in the *Tanytarsus chinyensis* species group (Giłka & Paasivirta 2009; Reiss & Fittkau 1971). However, this species group is unsupported (polyphyletic) in results from molecular phylogenetic analyses of *Tanytarsus* based on five protein coding and one ribosomal nuclear marker (Lin et al. in prep.). Therein, *Tanytarsus chinyensis*, *T. curticornis* and *T. heusdensis* are found in three different clades that are not each other's closest relatives. As a consequence, we treat species morphologically extremely similar to *T. curticornis* and *T. heusdensis* in the adult male stage as members of these species complexes, respectively. By this characterization, there are eight hitherto known species in the *T. curticornis* species complex. Six of these species are Holarctic: *Tanytarsus brundini*, Lindeberg, 1963, *T. curticornis* Kieffer, 1911, *T. ikicedeus* Sasa & Suzuki, 1999, *T. neotamaoctavus* Ree, Jeong & Nam, 2011, *T. salmelai* Giłka & Paasivirta, 2009, *T. tamaoctavus* Sasa, 1980; and two that are Afrotropical: *Tanytarsus congus* Lehmann, 1981, *T. pseudocongus* Ekrem, 1999 (Edwards 1929; Ekrem 1999, 2001; Giłka & Paasivirta 2009; Kieffer 1911; Lehmann 1981; Lindeberg 1963; Ree et al. 2011; Reiss & Fittkau 1971; Sasa 1980). The *Tanytarsus heusdensis* complex includes four species occurring in the Palaearctic region: *Tanytarsus heusdensis* Goetghebuer, 1923, *T. reei* Na & Bae, 2010, *T. tamaduodecimus* Sasa, 1983, *T. tusimatneous* Sasa & Suzuki, 1999 (Albu 1980; Giłka & Paasivirta 2009; Goetghebuer 1923, 1928; Lindeberg 1970; Na & Bae 2010; Reiss &

Fittkau 1971; Sasa 1983; Sasa & Ichimori 1983; Sasa & Suzuki 1999a; Sasa & Suzuki 1999b; Storå 1939).

The morphological similarity between species in the *T. curticornis* and *T. heusdensis* species complexes likely has led to misidentifications and underestimation of species diversity in the past. Generally, it appears that DNA barcode data give a very good approximation of species diversity in *Tanytarsus* (Lin et al. 2015) and should, together with morphology, be used in description of closely related species. Here we review species in the *T. curticornis* and *T. heusdensis* species complexes, diagnose and describe them based on morphology and DNA barcodes, and provide keys to adult males and pupae.

Materials and methods

We examined the nominal types of *Tanytarsus heusdensis*, *Tanytarsus ikicedeus*, *Tanytarsus manlyensis*, *Tanytarsus neotamaoctavus*, *Tanytarsus reei* and *Tanytarsus tamaduodecimus*. Additional collections were made in Canada, China, Czech Republic, Germany and Norway, using standard insect collecting techniques such as Malaise traps, sweep nets and light traps. Adult specimens were preserved in 85% ethanol, immatures in 96% ethanol, and stored dark at 4°C before morphological and molecular analyses. Genomic DNA of most specimens was extracted from the thorax and head using Qiangen DNA Blood and Tissue Kit at the Department of Natural History, NTNU University Museum following the standard protocol, except that lysis was done overnight and the final elution volume was 100 µl. After DNA extraction, the cleared exoskeleton was mounted in Euparal on microscopy slides together with the corresponding wings, legs and antennae following the procedures outlined by Sæther (1969).

The 658 bp (barcode fragment) of the cytochrome *c* oxidase subunit 1 (COI) region was PCR-amplified using the universal primers LCO1490 and HCO2198 (Folmer et al. 1994). DNA amplification was carried out in 25 µl reactions using 2.5 µl 10x Takara ExTaq pcr buffer (CL), 2 µl 2.5 mM dNTP mix, 2 µl 25 mM $MgCl_2$, 0.2 µl Takara Ex Taq HS, 1 µl 10 µM of each primer, 2 µl template DNA and 14.3 µl ddH_2O. Amplification cycles were performed on a Biorad C1000 Thermal Cycler and followed a program with an initial denaturation step of 95°C for 5 min, then followed by 34 cycles of 94°C for 30 s, 51°C for 30 s, 72°C for 1 min and 1 final extension at 72°C for 3 min. PCR products were purified using Illustra ExoProStar 1-Step and shipped to MWG Eurofins for bidirectional sequencing using BigDye 3.1 termination. Sequences were assembled and edited using the software Sequencher 4.8 (Gene Codes Corporation). Sequence information was uploaded on BOLD

along with an image and collateral information for each voucher specimen. Alignment of the sequences was carried out using the Muscle algorithm (Edgar 2004) on amino acids in MEGA 6 (Tamura et al. 2013). The pairwise distances of *T. curticornis* and *T. heusdensis* species complexes using the Kimura 2-Parameter (K2P) model were calculated in MEGA 6 (Table S1–2). The neighbor joining tree was constructed using the K2P substitution model, 1000 bootstrap replicates and the "pairwise deletion" option for missing data in MEGA 6. List of all species, specimens, their individual images, georeferences, primers, sequences and other relevant laboratory data of all sequenced specimens can be seen online in the publicly accessible datasets "*Tanytarsus curticornis* species complex [DS-TANYSC]", DOI: XXX and "*Tanytarsus heusdensis* complex [DS-HEUSDEN]", DOI: XXX in the Barcode of Life Data Systems (BOLD) (Ratnasingham & Hebert 2007, 2013).

The morphological terminology and abbreviations follow Sæther (1980) except for the vannal fold (here called postcubitus), "lamellate setae" of median volsella (here called "lamellae"), "sensillae basiconicae" on the anal point (here called "spinulae") and "filamentous setae (LS)" in pupal exuviae (here called "taeniae") (Langton 1994). Measurements are given as ranges followed by the mean, when four or more specimens are measured, followed by the number of specimens measured (n) in parentheses. Digital photography were taken with a resolution of 300 dpi using a Leica DFC420 camera mounted on a Leica DM6000 B compound microscope using bright field or Nomarski DIC light settings and the software Leica Application Suite 4.8. The types from China are deposited at the College of Life and Sciences, Nankai University, Tianjin, China, and the remaining types of new species described herein are deposited at the Department of Natural History, NTNU University Museum, Trondheim, Norway or The Canadian National Collection of Insects, Arachnids & Nematodes.

Institute acronyms used in the text include: ANIC, Australian National Insect Collection, Australia; BDN, The Department of Biology, Nankai University, now The College of Life Science, Nankai University, Tianjin, China; BMNH, British Museum (Natural History), London, England; CNC, The Canadian National Collection of Insects, Arachnids & Nematodes, Ottawa, Ontario, Canada; KU, The Entomological Research Institute, Korea University, Seoul, Korea; NSMT, The National Museum of Nature and Science, Tokyo, Japan; NTNU-VM, The Department of Natural History, NTNU University Museum, Trondheim, Norway; RBINS, The Royal Belgian Institute of Natural Sciences, Bruxelles, Belgium; UMSP, The University of Minnesota Insect Collection, Department of Entomology, University of Minnesota, Minnesota, United States of America; YU, College of Medicine, Yonsei University, Seoul, Korea; ZSM, The Zoologische Staatssammlung München, Munich, Germany; ZMBN, The Department of Natural History, Bergen University Museum, Norway.

Results

DNA barcode analyses

The neighbor joining tree (Fig. 1) based on available COI DNA barcodes of species in the *T. curticornis* species complex reveals nine distinct genetic clusters, of which six could not be associated morphologically or genetically to any previously described species. The neighbor joining tree (Fig. 2) based on available COI DNA barcodes of five *T. heusdensis* species complex presents five distinct genetic clusters indicating two species new to science. In the *T. curticornis* species complex, the minimum interspecific genetic distance is 8.3% between *T. tongmuensis* sp. n. and *T. wangi* sp. n., and the maximum intraspecific genetic distance 9.8% in *T. thomasi* sp. n.. In the *T. heusdensis* species complex, the minimum interspecific genetic distance is 19.4% between *T. heusdensis* and *T. adustus* sp. n., and the maximum intraspecific genetic distance is 8.6% in *T. reei* between the Chinese and German populations. Due to the observed deep intraspecific divergence, we extended the dataset with multiple nuclear genes, on a subset of taxa to explore the species boundaries within these two species complexes using different analytical tools. The results are generally consistent with the pattern observed with DNA barcodes and completely in the accordance with the morphological concepts and named species described here (Lin et al. in prep.).

Taxonomy

The *Tanytarsus curticornis* species complex

The species of the *Tanytarsus curticornis* complex are grouped together based on a number of morphological characters in the adult males: the anal tergal bands are of V-type and widely

separated medially; a few or no small median setae are present near the base of anal point; a few spinulae are present between anal crests; superior volsella is generally oval, often with straight or concave median margin, bearing two anteromedian and 4–5 dorsal setae; digitus extends beyond the inner margin of the superior volsella, always with apical pear-shaped lobe (Fig. 16C); small seta present on stem of digitus (except in *T. neotamaoctavus*); stem of median volsella short.

Key to adult males of the *Tanytarsus curticornis* complex

1. Digitus with apical pear-shape lobe (Fig. 16C), extending beyond inner margin of superior volsella; anal tergal bands of V-type, widely separated medially; superior volsella generally oval, often with straight or concave median margin; spinulae present between anal crests; stem of median volsella short … 2

– Not as above … Not keyed

2. Microtrichia present on superior volsella; lamellae of median volsella not extending to tip of the digitus. Afrotropical region. … 3

– Microtrichia absent on superior volsella, stem of median volsella short, lamellae never reaching tip of digitus. Other zoogeographical regions. … 4

3. AR<0.45; LR_1<2.90; seta on digitus placed basally. Ghana, Nigeria. … *T. pseudocongus* Ekrem

– AR>0.60; LR_1>3.30; seta on digitus placed at half-length. Ghana, Senegal, Democratic Republic of the Congo. … *T. congus* Lehmann

4. Median setae on anal tergite absent (Figs. 5C; 16A) … 5

– Median setae on anal tergite present (Fig. 22A) … 6

5. Wing cell m and vein Cu bare (Fig. 15A). Palaearctic China. … *T. songi* sp. n.

– Wing cell m and vein Cu setose (Fig. 5A). Palaearctic. … *T. curticornis* Kieffer

6. Wing membrane with macrotrichia in distal half of cell r_{4+5} and sometimes in apical part of cell m_{1+2}. Finland. ... *T. salmelai* Giłka & Paasivirta

– Wing membrane almost entirely covered with macrotrichia … 7

7. Thorax entirely dark brown (Fig. 10B); tarsomere 1 of mid leg without sensilla chaetica. Madeira. … *T. madeiraensis* sp. n.

– Thorax pale yellow, or with dark brown patches; tarsomere 1 of mid leg with sensilla chaetica … 8

8. Body pale yellow, thorax with pale brown patches (Fig. 24C); AR 0.43–0.53. Oriental China. … *T. wangi* sp. n.

– Body dark yellow, thorax with dark brown patches; AR > 0.60 … 9

9. Anal point with pointed apex …10

– Anal point blunt apex …11

10. Anal point (Fig. 7A) comparatively long, reaching the apex of inferior volsella; median volsella bearing three falciform lamellae (Fig. 7B). Canada. … *T. heberti* sp. n.

– Anal point (Figs. 4A, C) comparatively short, not reaching the apex of inferior volsella; median volsella bearing pectinate lamellae (Fig. 4B). Palaearctic. … *T. brundini* Lindeberg

11. Frontal tubercles (Fig. 19B) present; LR_1 1.85–2.02. Canada. … *T. thomasi* sp. n.

– Frontal tubercles absent; LR_1 2.37–2.84 … 12

12. AR 0.90–1.00; anal point triangular, with nipple-shaped apex (Fig. 9B). Japan. … *T. ikicedeus* Sasa & Suzuki

– AR 0.60–0.80; anal point not as above … 13

13. Wing length > 1.50 mm; anal point robust … 14

– Wing length < 1.30 mm (Fig. 17C); anal point slender. China, Japan, Korea. … *T. tamaoctavus* Sasa

14. Wing length 1.63–1.73 mm; AR 0.66–0.74; digitus bearing seta (Fig. 22B). Oriental China. … *T. tongmuensis* sp. n.

– Wing length 1.50 mm; AR 0.82; digitus without seta (Fig. 14C). Korea. … *T. neotamaoctavus* Ree, Jeong & Nam

Key to known pupae of the *Tanytarsus curticornis* complex

1. Cephalic tubercles shallow mounds; thoracic horn with chaetae shorter than the diameter of thoracic horn; segment VIII with five lateral taeniae; tergites with small anterior spines in patches … 2

– Without the above combination of characters … Not keyed

2. Tergite II with a pair of spine patches surrounded by shagreen … 3

– Only shagreen present on Tergite II … 4

3. Segments V-VII with 2, 2, 3 lateral taeniae. Palaearctic. … *T. curticornis* Kieffer

– Segments V-VII with 0, 1, 3 lateral taeniae. China, Japan. … *T. tamaoctavus* Sasa

4. Thoracic horn c. 600 μm long; segments V-VII with 1, 1, 3 lateral taeniae; chaetae distributed densely on apical half of thoracic horn. Palaearctic. … *T. brundini* Lindeberg

– Thoracic horn c. 540–550 μm long; segments V-VII with 1, 2, 3 lateral taeniae; chaetae distributed on distal 2/3 of thoracic horn. Madeira. … *T. madeiraensis* sp. n.

Descriptions

***Tanytarsus brundini* Lindeberg, 1963**

Figs. 3–4

Tanytarsus brundini Lindeberg, 1963: 127, fig. 7, 10; Reiss & Fittkau 1971: 98, figs. 4–5; Giłka & Paasivirta 2009: 35, figs. 1, 5–9, 19, 22, 25.

Material examined

Belgium: 1♂ (UMSP), Chiny, 17–22.VIII.1933, leg. M. Goetghebuer. Czech Republic: 1♂ (NTNU-VM: 148235, BOLD Sample ID: XL148), Southern Bohemia, České Budějovice, near River Vltava, 48.977°N, 14.470°E, 387 m a.s.l., 17.VIII.2014, Sweep net, leg. X.L. Lin. China: 2♂♂ (BDN: 21476, 21507), Xinjiang Uyghur Autonomous Region, Aketao County, Kalakule Lake, 18.VIII.2002, leg. N. Tang. Norway: 2♂♂ (NTNU-VM: 136337, BOLD Sample ID: Finnmark239; NTNU-VM: 136338, BOLD Sample ID: Finnmark240), Finnmark, Lebesby, Eastorjavri, Lake at outflow, 70.4427°N, 27.3485°E, 260 m a.s.l., 28.VII.2010, leg. T. Ekrem; 1♂ (ZMBN: chi23847, BOLD Sample ID: To137), Hordaland, Dalseid, Vaksdal, Bolstadfjorden, 60.6552°N, 5.8038°E, 100 m a.s.l., 31.V.2003, Sweep net, leg. E. Stur & T. Ekrem; 1♂ (NTNU-VM: 200130, BOLD Sample ID: TRD-CH137), Sør-Trøndelag, Klæbu, Selbusjøen, near Bjørkly, 63.2744°N, 10.5613°E, 157 m a.s.l., 25.IX.2014, leg. E. Stur. Portugal: 1♂ (UMSP), Vita de Ponte River & Reservoir, 17.IV.1984, leg. E.J. Fittkau. Ukraine: 6♂♂ (NTNU-VM: 148236, BOLD Sample ID: XL402; NTNU-VM: 148237, BOLD Sample ID: XL403; NTNU-VM: 148238, BOLD Sample ID: XL404; NTNU-VM: 148239, BOLD Sample ID: XL405; NTNU-VM: 148240, BOLD Sample ID: XL407), Krym, Sevastopol, near Chornaya River, 44.4861°N, 33.8136°E, 253 m a.s.l., 12.X.2013, Sweep net, leg. V. Baranov.

Diagnosis

Tanytarsus brundini can be separated from other *Tanytarsus* species by the following combination of characters: anal tergal bands of male hypopygium of V-type and widely

separated medially; anal point coniform, tapering to rounded apex, with 4–5 spinulae between anal crests; superior volsella oval with concave inner margin; digitus with pear-shaped apical lobe; median volsella very short, lamellae not reaching tip of digitus; gonostylus straight or slightly curved, with more or less parallel margins tapering to widely rounded apex; larval antennal pedestal with a medially curved, acute spur; pupal segment V-VIII with 1, 1, 3, 5 lateral taeniae respectively; chaetae densely distributed on apical half of pupal thoracic organ.

Remarks

Tanytarsus brundini is regarded as widely distributed in the western Palaearctic region. However, most records should be reevaluated considering the results presented in this review.

Distribution

Northwest China, Europe.

***Tanytarsus congus* Lehmann, 1981**

Tanytarsus congus Lehmann, 1981: 48, figs. 88–91; Ekrem 2001, 8, figs. 5–6. Holotype ♂ (ZSM) Zaire, Kinsangani, Simisimi-stream, 24.III.1975. [Not examined]

Diagnosis

Tanytarsus congus can be separated from other *Tanytarsus* species by the following combination of characters in the adult male: AR 0.60–0.80; LR_1>3.30; spinulae in single row between well-developed anal crests; superior volsella oval with dorsolateral, small patch of microtrichia, two apical seta where one is sitting on small ventral projection, digitus with swollen apex reaching beyond superior volsella at its median posterior margin, carrying one

seta placed at c. 1/2 length of digitus; median volsella relatively short with three distal pectinate lamellae and two normal setae; inferior volsella S-shaped [For further description see Ekrem (2001) and Lehmann (1981)].

Distribution

Ghana, Senegal, Democratic Republic of the Congo.

***Tanytarsus curticornis* Kieffer, 1911**

Fig. 5

Tanytarsus curticornis Kieffer, 1911: 52; Lindeberg 1963: 127, figs. 5, 8; Reiss & Fittkau 1971: 100, fig. 7; Giłka & Paasivirta 2009: 38, figs. 10–14, 20, 23, 26.
Tanytarsus (*Tanytarsus*) *curticornis* Kieffer, 1911: Edwards 1929: 415.

Material examined

Norway: 1♂ (ZMBN: chi23826, BOLD Sample ID: To82), Aust-Agder, Valle, Flåni, Sandnes, 59.1457°N, 7.5394°E, 273 m a.s.l., 29.VI.2001, leg. T. Ekrem; 1♂ (NTNU-VM: 148241, BOLD Sample ID: XL99), Sør-Trøndelag, Trondheim, Lian Lake, 63.400°N, 10.317°E, 219m, 31.VIII.2014, Sweep net, leg. X.L. Lin.

Diagnosis

Tanytarsus curticornis can be separated from other *Tanytarsus* species by the following combination of characters: pupal segment V-VIII with 2, 2, 3, 5 lateral taeniae respectively; chaetae distributed scarcely on apical half of thoracic horn; adult male ground colour of thorax, scutellum, halteres (Fig. 5A), legs and abdomen yellowish green; antennal pedicel,

tentorium, scutal stripes, postnotum and sternum yellowish green to pale brown; wing membrane pale, with C, M and radial veins slightly darker; frontal tubercles usually absent; third palpomere shorter than fourth; wing membrane under M_{3+4}, Cu_1 and An partially free of macrotrichia (Fig. 5B); 1/4 proximal section of R_{4+5}, proximal half of Cu and neighboring false vein bare; gonostylus with slight constriction in distal part or regularly tapered to slender apex; anal tergite with single strong basilateral seta on each side; median setae absent or rarely one present (one Norwegian specimen); anal point with 4–10 spinulae, with blunt, widely rounded or slightly abrupt apex; superior volsella oval with straight median margin (Fig. 5C); pear-shaped apical lobe of digitus roundish, broadly conical, stout in comparison with relatively small superior volsella; median volsella very short, inner margin of coxite above median volsella more or less straight; inferior volsella short, with broadly rounded apex.

Remarks

One of the Norwegian specimens (BOLD Sample ID: To82) possesses one median tergite seta in the adult male (Fig. 5D). This is regarded as an aberrant or rare feature for *T. curticornis*.

Distribution

Palaearctic region.

***Tanytarsus heberti* sp. n.**

Figs. 6–8

Type material

Holotype ♂ (NTNU-VM: 148242, BOLD Sample ID: CHIR_CH342), Canada, Manitoba, Churchill, 12 km S Churchill, Goose Creek Marina, 58.6610°N, 94.1650°W, 5 m a.s.l., 17.VII.2007, Malaise trap, leg. T. Ekrem & E. Stur. Paratypes: 1♂ (CNC, BOLD Sample ID: BIOUG18216-G06), 2♀♀ (CNC, BOLD Sample ID: BIOUG18225-G07; CNC, BOLD Sample ID: BIOUG18226-C03), Canada, Manitoba, Wapusk National Park, 58.723°N, 93.46°W, 2 m a.s.l., 27.VII.2014, leg. D. Iles.

Diagnosis

The adult male can be distinguished from known species of *Tanytarsus* by the following combination of characters: body mostly yellow with pale brown patches on scutum, postnotum, preepisternum (Fig. 6B); AR 0.71; wing vein Cu with 0–2 setae, cell m with one seta; anal point bearing six spinulae placed in regular row between anal crests; superior volsella roundish slightly elongated with straight inner margin, bearing two anteromedian and 4–5 dorsomedian setae; digitus stout, including one pear-shaped apical lobe with rounded apex and cylindrical tubercle lobe below it bearing one digitus-seta; stem of median volsella short, 4–5 µm long, located above superior volsella, bearing three falciform lamellae; gonostylus comparatively thin, broadest at middle, tapering to a blunt apex.

Etymology

Named after Paul D. N. Hebert, for his continued support of Chironomidae DNA barcoding; noun in genitive case.

Description

Adult male (n = 2). Total length 2.38–2.47 mm. Wing length 1.60–1.63 mm. Total length/wing length 1.48–1.52.

Coloration. Head, legs and abdomen yellow; antenna brown. Thorax ground color yellow with light brown patches anteriorly on scutum, laterally under parapsidal suture, postnotum and on preepisternum.

Head (Fig. 6A). Antenna with 13 flagellomeres, ultimate flagellomere 350 µm long. AR 0.71. Frontal tubercles absent. Temporal setae 8–9. Clypeus with 10–13 setae. Tentorium 125 µm long, 28 µm wide. Palpomere lengths (in µm): 33–35, 35–43, 93–103, 98–100, 103. Third palpomere shorter than fourth palpomere, bearing 2 sensilla clavata distally.

Thorax (Fig. 6B). Dorsocentrals 6–7; acrostichals 6–7; prealar 1. Scutellum with 4 setae. Halteres with 3–4 setae.

Wing (Fig. 6C). VR 1.29–1.39. Brachiolum with one seta, Sc bare, R with 14–17 setae, R_1 with 16–17 setae, R_{4+5} with 15–26 setae, M_{1+2} with 44–45 setae, M_{3+4} with 19–26 setae, false vein with 33–39 setae, Cu with 0–2 setae, Cu_1 with 16–18 setae, PCu with 4–14 setae, An with 23–27 setae, remaining veins bare. Cell r_{4+5} with c. 115–120 setae, m with one seta, m_{1+2} with c. 90–95 setae, m_{3+4} with 46–53 setae, cu+an with 6–45 setae, remaining cells bare. Anal lobe of wing strongly reduced.

Legs. Fore leg bearing single tibial spur, 20–23 µm long. Combs of mid tibia 21 µm wide with 25 µm long spur, and 23 µm wide with 20 µm long spur; combs of hind tibia 15 µm wide with 28 µm long spur, 11 µm wide with 20 µm long spur. Tarsomere 1 of mid leg with 2 sensilla chaetica distally. Lengths (in µm) and proportions of legs as in Table 1.

Hypopygium (Fig. 7). Tergite IX 88–95 µm long, with two median setae and small microtrichia-free area around base of anal point. Lateral tooth absent. Anal tergal bands of V-type, widely separated, ending at mid-length of tergite. Anal point 48–63 µm long, tapering to narrow, rounded apex, microtrichia absent between anal crests, four lateral setae on each side of anal point; six spinulae in regular row between anal crests. Transverse sternapodeme 45–50 µm long. Phallapodeme 80–85 µm long. Gonocoxite 123–130 µm long. Gonostylus 100–

105 μm long, curved inwards, comparatively thin, broadest at middle, tapering to a narrowly rounded apex. Superior volsella roundish, slightly elongated, with straight inner margin, bearing two anteromedian and 4–5 dorsomedian setae. Digitus stout, with two lobes, one apical, pear-shaped with rounded apex, one cylindrical tubercle below bearing one seta. Stem of median volsella short, 4–5 μm long, located anterior to superior volsella, bearing three apparently falciform lamellae, 10 μm long. Inferior volsella relatively straight, 70–75 μm long, bearing 10–12 strong apical setae. HR 1.17–1.30, HV 2.35–2.38.

Adult female (n = 2). Total length 1.68–1.72 mm. Wing length 1.45–1.63 mm. Total length/wing length 1.03–1.19.

Coloration. As male.

Head (Fig. 8A). Antenna with 4 flagellomeres, flagellomere length (in μm): 70–75, 53–55, 50–65, 98–128. AR 0.57–0.66. Frontal tubercles absent. Temporal setae 5–7. Clypeus with 10–14 setae. Tentorium 100 μm (2) long, 13–15 μm wide. Palpomere lengths (in μm): 25–38, 30–38, 65–88, 100 (1), 168 (1).

Wing (Fig. 8B). VR 1.22–1.27. Brachiolum with 1 seta, Sc bare, R with 15–16 setae, R_1 with 16–18 setae, R_{4+5} with 28–37 setae, M_{1+2} with 34–38 setae, M_{3+4} with 39–43 setae, false vein with 62–70 setae, Cu with 13–20 setae, Cu_1 with 23–55 setae, PCu with 28–54 setae, An with 22–40 setae, remaining veins bare. Cell r_{4+5} with c. 180–200 setae, m with 7–9 setae, m_{1+2} with c. 110–130 setae, m_{3+4} with 50–60 setae, cu+an with 70–80 setae, remaining cells bare. Anal lobe of wing strongly reduced.

Thorax. Dorsocentrals 7–10; acrostichals 6–8; prealar 1. Scutellum with 4 setae. Halteres with 4 setae.

Legs. As male (all tarsomeres broken).

Genitalia (Fig. 8C). Tergite IX slightly triangular; sternite VIII with 14–16 setae; vaginal floor large, covering about half of vaginal opening ventrally; gonapophysis VIII single lobe

with long posteromedially directed microtrichia; gonocoxapodeme strongly curved; coxosternapodeme well-developed with obvious anterior and posterior lobes. Notum including rami 135–158 μm long, notum alone c. 50–88 μm long. Seminal capsules semi-circular, 43–60 μm long, 43–45 μm wide, with 105–130 μm long spermathecal ducts. Postgenital plate triangular. Cercus 53–55 μm long, with 13–18 setae.

Immatures unknown.

Remarks

The new species resembles *T. brundini* in the adult male, but can be separated from this species by having less setae on the wing vein Cu, apparently falciform lamellae of the median volsella, and more than 20% divergence in partial COI sequences (Fig. 1).

***Tanytarsus ikicedeus* Sasa & Suzuki, 1999**

(Fig. 9)

Tanytarsus ikicedeus Sasa & Suzuki, 1999: 149, figs. 4a-m; Yamamoto & Yamamoto 2014: 354. Holotype ♂ (NSMT Type no. 357: 18), Japan, Nagasaki Prefecture, Iki Island, Satofure, 27.III.1998, leg. H. Suzuki. [Examined]

Diagnosis

Tanytarsus ikicedeus can be separated from other *Tanytarsus* species by the following combination of characters: scutal stripes and postnotum yellowish brown, other scutal portions and scutellum pale, abdomen and legs yellow; frontal tubercles absent; AR 0.90–1.00; third palpomere shorter than fourth; wing membrane covered with macrotrichia from ¼ of wing length to tip; LR_1 2.09–2.29; tarsomere 1 of mid leg with 4 sensilla chaetica; anal

tergite with 2 median setae near base of anal point; anal point triangular, with nipple on apex; spinulae in single row between well-developed anal crests; superior volsella oval, bearing 2 anteromedian and 4 dorsal setae; digitus stout with pear-shaped apical lobe, 1 digitus-seta located on cylindrical tubercle at base; median volsella small, with one pectinate lamella; gonostylus with broadly rounded apex.

Distribution

Japan.

***Tanytarsus madeiraensis* sp. n.**

Figs. 10–13

Type material

Holotype ♂, Pe, L (NTNU-VM: 145314, BOLD Sample ID: MA19), Portugal: Madeira, Rabacal, Levada pond, 32.7340°N, 17.0580°W, 1463 m a.s.l., 06.VIII.2006, Rearing, leg. T. Ekrem. Paratype ♂, Pe, L (NTNU-VM: 145313, BOLD Sample ID: MA18) as holotype.

Diagnosis

Tanytarsus madeiraensis sp. n. can be distinguished from known species of *Tanytarsus* by the following combination of characters in the adult male: head, thorax, legs and abdomen of adult male entirely dark brown to black (Fig. 10B); AR 0.47–0.49; frontal tubercles absent; third palpomere shorter than fourth; wing membrane covered with macrotrichia; LR_1 1.91–2.09; tarsomere 1 of mid leg without sensilla chaetica; three median setae placed near the base of anal point; anal tergal bands of V-type, well separated, ending at mid-length of tergite; digitus stout with pear-shaped apical lobe, digitus-seta located on cylindrical tubercle

at base of digitus; stem of median volsella short and cylindrical, located anterior to superior volsella, with one simple lamella. Pupal thoracic horn slender, arising from spherical base, tapered, terminating in fine apical section, chaetae distributed on distal 2/3; spines of tergites III-VI in anterior, small, elongated patches; segments V-VIII with 1, 2, 3, 5 lateral taeniae respectively; anal lobe with two long taeniate dorsal setae; fringe with 22–23 uniserial taeniae; posterolateral comb of segment VIII 20–23 µm wide, with 4–6 large outermost spines and 6–7 small inner spines; male genital sacs extend beyond anal lobe. Larval mental and mandibular teeth brown-black; AHR 0.20–0.30; AAR 0.58; antenna shorter than head length, 5-segmented, only first and second antennal segments well sclerotized, AR 2.23; LOR 3.43; MVR 0.90; labrum with SI pectinate and chaetae plumose; SII with small points, on pedestal; clypeal seta S3 long, simple; premandible with 4 teeth in addition to lateral spine; premandibular brush well-developed.

Etymology

Named after the type locality, Madeira; adjective in nominative case.

Description

Adult male (n = 2). Total length 2.12–2.54 mm. Wing length 1.37–1.38 mm. Total length/wing length 1.54–1.84.

Coloration. Head, thorax, legs and abdomen entirely dark brown to black.

Head (Fig. 10A). Antenna with 13 flagellomeres, ultimate flagellomere 235–240 µm long. AR 0.47–0.49. Frontal tubercles absent. Temporal setae 8–11. Clypeus with 14–16 setae. Tentorium 100–105 µm long, 25–30 µm wide. Palpomere lengths (in µm): 27–28, 33–43, 90–95, 105–115, 175–180. Third palpomere with 2 sensilla clavata distally.

Thorax (Fig. 10B). Dorsocentrals 8–9; acrostichals 8–9; prealar 1. Scutellum with 4 setae. Halteres with 4 setae.

Wing (Fig. 10C). VR 1.25–1.30. Brachiolum with 1 seta, Sc bare, R with 21–27 setae, R_1 with 16–17 setae, R_{4+5} with 34–45 setae, M_{1+2} with 44–60 setae, M_{3+4} with 23 setae, false vein with 60–63 setae, Cu with 18–20 setae, Cu_1 with 14 setae, PCu with 44–52 setae, An with 31–32 setae, remaining veins bare. Cell r_{4+5} with c. 160–180 setae, m with 10–13 setae, m_{1+2} with c. 100–130 setae, m_{3+4} with 50–60 setae, cu+an with 50–60 setae, remaining cells bare. Anal lobe of wing strongly reduced.

Legs. Fore leg bearing single tibial spur, 30–35 μm long. Combs of mid tibia 15–18 μm wide with 19–28 μm long spur, and 16–18 μm wide with 13–15 μm long spur; combs of hind tibia 20–30 μm wide with 30 μm long spur, 18–20 μm wide with 20 μm long spur. Tarsomere 1 of mid leg without sensilla chaetica. Pulvilli absent. Lengths (in μm) and proportions of legs as in Table 2.

Hypopygium (Fig. 11). Tergite IX 75–77 μm long, with three median setae at base of anal point. Lateral tooth absent. Anal tergal bands of V-type, well separated, ending at mid-length of tergite. Anal point 45–53 μm long, with 3–4 lateral setae on each side, with blunt apex; three spinulae placed in regular row between anal crests. Transverse sternapodeme 40 μm long. Phallapodeme 58–70 μm long. Gonocoxite 103–113 μm long. Gonostylus with straight inner margin, 78–85 μm long, comparatively broad, tapering to pointed apex. Superior volsella roundish with straight to concave median margin, bearing 2 anteromedian and 4 dorsal setae. Digitus stout with pear-shaped apical lobe, digitus-seta located on cylindrical tubercle at base of digitus. Stem of median volsella short and cylindrical, located anterior to superior volsella, 12–14 μm long, with one simple lamella. Inferior volsella relatively straight, 60–63 μm long, with 9–10 apical setae. HR 1.31–1.32, HV 2.72–2.99.

Larva (n = 2, head capsules). Head Capsule (Fig. 12). Length 265–565 µm, width 215–470 µm, length/width 1.20–1.23; mental and mandibular teeth dark brown. Antennal pedestal 80–113 µm long, 46–78 µm wide, with a well-developed spur 28–40 µm long, 6–10 µm wide. AHR 0.20–0.30; AAR 0.58. Antenna shorter than head length, 5-segmented, only first and second antennal segments well sclerotized. Antennal segment length (in µm): 138, 32, 17, 10, 3; AR 2.23. Antennal blade 48 µm long. Lauterborn organ (LO) stems + stylus 103 µm long; LOR 3.43. Mandible 95–175 µm long, 37–68 µm wide, 1 ventral apical tooth, 3 ventral inner teeth, 1 dorsal, pale apical tooth present; two outer mandibular setae present; seta subdentalis thick and curved, 32–53 µm long, reaching beyond apex of dorsal tooth; seta interna well-developed with 4 main branches. Mentum 68–115 µm wide, with 11 teeth; median tooth with small lateral notches; ventromental plate 75–128 µm wide, MVR 0.90. Labrum with S I pectinate and chaetae plumose; S II with small points, on pedestal; clypeal seta S3 long, simple. Labral lamella pectinate. Pecten epipharyngis consisting of three plumose lobes. Premandible 46–83 µm long, with 4 teeth in addition to lateral spine; premandibular brush well-developed. Maxilla with two long and one short lacinial chaetae, palp normally developed, postoccipital margin darkly pigmented, postoccipital plate well-developed, pale.

Pupal exuviae (n = 2). Length 2.80–2.81 mm, pale-light yellow, with darker pigmentation on cephalothorax, basal ¼ of thoracic horn and laterally on abdomen.

Cephalothorax (Figs. 13A-B). Length 780–780 µm. Cephalic area with thin frontal setae, 63–88 µm long. Antepronotals comprising one median and one lateral, each weakly developed, taeniate setae, 25–45 µm long; three precorneals similarly shaped, arranged in triangle, one stouter and darker than remaining two, 25–58 µm long. Thoracic horn c. 545–550 µm long, 44–45 µm wide, arising from spherical base, tapered, terminating to fine apical section, chaetae distributed on distal 2/3. Two relatively closely situated pairs of dorsocentrals, 155–

170 μm between pairs. Dorsocentrals 1 and 2 short (10–15 μm), dorsocentrals 3 and 4 longer (18–35 μm), one thick and thin. Nose of wing sheath well-developed.

Abdomen (Figs. 13C-D). Tergite I bare. Shagreen on tergite II as in Fig. 13C; pedes spurii B on tergite II weakly developed; hook row 125–130 μm long. Spines of tergites III–VI 3–13 μm long, in anterior, elongated patches. Segment I with 2 D setae; segment II with 3 D, 3–4 V and 3 L setae; segment III with 5 D, 3–4 V and 3 L setae; segment IV with 5 D, 4 V and 3 L setae; segment V with 5 D, 4 V, 2 L setae and 1, 70–75 μm long lateral taeniae; segment VI with 5 D, 4 V, 2 L setae and 2, 48–52 μm long lateral taeniae; segment VII with 5 D, 3 V, 1 L setae and 3, 53–70 μm long lateral taeniae; segment VIII with 1 D, 1 V and 5, 63–78 μm long lateral taeniae; anal lobe with two 50–60 μm long taeniate dorsal setae; fringe with 22–23 uniserial taeniae. Posterolateral comb (Fig. 13D) of segment VIII 20–23 μm wide, with 4–6 large outermost spines and 6–7 small inner spines. Genital sacs of male extending beyond anal lobe.

Female unknown.

Remarks

The new species resembles *Tanytarsus salmelai* in the adult male, but can be separated from this species by the absence of sensilla chaetica on tarsomere 1 of mid leg, and dense setation on the wing membrane. The new species also resembles *Tanytarsus brundini* in the adult male, but can be separated from this species by the darker body color, lower AR, and more than 13% mean divergence in partial COI sequences (Fig. 1).

***Tanytarsus neotamaoctavus* Ree, Jeong & Nam, 2011**

(Fig. 14)

Tanytarsus neotamaoctavus Ree, Jeong & Nam, 2011: 254, fig. 7. Holotype ♂ (YU no. CH-6758), Korea, Jeollabuk-do, Muju-gun, Muju-eup, Dangsan-ri, 22.V.2009, leg. K.Y. Jeong [Not examined]; Paratypes 2♂♂ (YU no. RCH-6757, RCH-6763) as holotype [Examined].

Diagnosis

Tanytarsus neotamaoctavus can be separated from other *Tanytarsus* species by the following combination of characters in the adult male: body mostly yellow with darker scutal stripes and post notum; AR 0.80–0.82; third palpomere longer than fourth; LR_1 = 2.51–2.61; anal point robust with narrow, rounded apex; digitus twisted, without digitus-seta; median volsella tiny (absent in the original description).

Remarks

Based on the original description (Ree et al. 2011), *Tanytarsus neotamaoctavus* is closely related to *T. tamaoctavus* in the shape of hypopygium, e.g. median volsella absent. The two species can be separated from each other by the slightly higher AR (0.80–0.82) and stout anal point in *T. neotamaoctavus*, opposed to the lower AR (0.65) and slender anal point in *T. tamaoctavus*. After examination of the paratypes of *T. neotamaoctavus*, we discovered the presence of a tiny median volsella hidden by the superior volsella. The median volsella was noted as absent in the original description; digitus seta absent.

Distribution

South Korea.

***Tanytarsus pseudocongus* Ekrem, 1999**

Tanytarsus pseudocongus Ekrem, 1999: 56, fig. 2; Ekrem 2001: 22, figs. 30–31. Holotype ♂ (ZMBN: no.305), Ghana, Western Region, Ankasa Game Production Reserve, Malaise trap, 7.–11.XII.1993. [Not examined]

Diagnosis

Tanytarsus pseudocongus can be separated from other *Tanytarsus* species by the following combination of characters: AR<0.45; LR_1<2.90; spinulae in single row between well-developed anal crests; superior volsella oval with a few microtrichia between 4–5 dorsal setae and 2 median setae where 1 is sitting on a small ventral projection; digitus with a swollen apex reaching beyond superior volsella at its median posterior margin, carrying 1 seta basally; median volsella relatively short with 3 distal, feathery lamellae in addition to 2 simple lamellae (Ekrem 1999).

Distribution

Ghana, Nigeria.

***Tanytarsus salmelai* Giłka & Paasivirta 2009**

Tanytarsus salmelai Giłka & Paasivirta, 2009: 32, figs. 3, 4, 15–18, 21, 24, 27. Holotype ♂ Finland, Arcto-Alpine ecoregion, Aksonjunni, 36 km south of Nuorgam, Utsjoki, 2.VII.2007, leg. J. Salmela. [Not examined].

Diagnosis

Tanytarsus salmelai can be separated from other *Tanytarsus* species by the following combination of characters: colour dark, with wing 1.15–1.50 mm long and AR 0.44–0.51;

frontal tubercles always present; third palpomere longer than fourth; anal lobe of wing strongly reduced; membrane brownish, sparse macrotrichia apically; LR_1 1.52–1.59; tarsomere 1 of mid leg with 3 sensilla chaetica; anal point slender, with narrowed and strongly elongated apex; superior volsella oval with straight median margin, bearing two anteromedian setae; digitus stout, with apical pear-shaped lobe and single seta at base; stem of median volsella short, with group of short pectinate lamellae; inferior volsella parallel-sided, with square apex and darkly pigmented dorsomedian, subapical ridge.

Distribution

Finland.

***Tanytarsus songi* sp. n.**

Figs. 15–16

Type material

Holotype ♂ (BDN & BOLD Sample ID: XL222), China: Hebei, Handan, Shexian, Kuangmenkou, 36.518°N, 113.703°E, 670 m a.s.l., 14.X.2014, Sweep net, leg. C. Song.

Diagnosis

The adult male can be distinguished from known species of *Tanytarsus* by the following combination of characters: body mostly brown with darker vittae, postnotum, epimeron II, median anepisternum II and preepisternum (Fig. 15B); frontal tubercles absent; third palpomere shorter than fourth; wing vein Cu and cell m bare, vein PCu with 1–3 setae; tarsomere 1 of mid leg with four sensilla chaetica distally; anal tergite without median seta; superior volsella almost square with straight median margin, bearing two anteromedian and

four dorsal setae; digitus stout, with apical pear-shaped lobe, digitus-seta located on cylindrical tubercle at base of digitus; stem of median volsella short, located underneath superior volsella, bearing group of short pectinate lamellae; gonostylus comparatively narrow, slightly curved inwards, with rounded apex.

Etymology

Named after C. Song, the collector of the material; noun in genitive case.

Description

Adult male (n = 1). Total length 2.68 mm. Wing length 1.60 mm. Total length/wing length 1.72.

Coloration. Thorax ground color brown with dark brown patches anteriorly on scutum, laterally under parapsidal suture, postnotum and on preepisternum; dark brown median anepisternum II, epimeron II. Head and legs brown. Abdomen yellow.

Head (Fig. 15A). Antenna lost. Frontal tubercles absent. Temporal setae 8. Clypeus with ten setae. Tentorium 115 μm long, 28 μm wide. Palpomere lengths (in μm): 45, 35, 108, 118, 180.

Thorax (Fig. 15B). Dorsocentrals 7; acrostichals 12; prealar 1. Scutellum with four setae. Halteres with three setae.

Wing (Fig. 15C). VR 1.20. Brachiolum with 1 seta, Sc bare, R with 21 setae, R_1 with 22 setae, R_{4+5} with 33 setae, M_{1+2} with 50 setae, M_{3+4} with 26 setae, false vein with 49 setae, Cu_1 with 22 setae, PCu with three setae, An with 23 setae, remaining veins bare. Cell r_{4+5} with c. 140 setae, m_{1+2} with c. 60 setae, m_{3+4} with 48 setae, cu+an with 36 setae, remaining cells bare. Anal lobe of wing strongly reduced.

Legs. Fore leg bearing single tibial spur, 18 µm long. Combs of mid tibia 13 µm wide with 23 µm long spur, and 10 µm wide with 18 µm long spur; combs of hind tibia 25 µm wide with 25 µm long spur, 13 µm wide with 23 µm long spur. Tarsomere 1 of mid leg with four sensilla chaetica distally. Lengths (in µm) and proportions of legs as in Table 3.

Hypopygium (Fig. 16). Tergite IX 65 µm long. Median seta absent. Small microtrichia-free area surrounding base of anal point. Lateral tooth absent. Anal tergite bands of V-type, widely separated medially, ending at half length of tergite. Anal point 50 µm long, triangular, tapering to rounded apex, four lateral setae on each side; six spinulae placed in regular row between anal crests. Transverse sternapodeme 45 µm long, with slightly developed oral projections. Phallapodeme 75 µm long. Gonocoxite 110 µm long. Gonostylus slightly curved, 95 µm long, with rounded apex. Superior volsella almost square, with straight median margin, slightly elongated and medially directed, bearing two anteromedian and four dorsal setae. Digitus (Fig. 16C) stout, with apical pear-shaped lobe, digitus-seta located on cylindrical tubercle at base of digitus. Stem of median volsella short, located underneath superior volsella, bearing group of short pectinate lamellae. Inferior volsella relatively straight, 55 µm long, bearing ten strong apical setae. HR 1.16, HV 2.82.

Female and immatures unknown.

Remarks

The new species resembles *Tanytarsus curticornis* in the adult male, but can be separated from this species by having less setae on the wing veins Cu and PCu and more than 20% K2P-divergence in partial COI sequences. Previous records of *T. curticornis* from the eastern Palaearctic region might be *T. songi* sp. n..

***Tanytarsus tamaoctavus* Sasa, 1980**

Figs. 17–18

Tanytarsus tamaoctavus Sasa, 1980: 23, figs. 23–25; Na 2004: 30, fig. 17; Na *et al*. 2010: 61, 62; Sasa & Kikuchi 1995: 51, 138; Yamamoto & Yamamoto 2014: 359. Holotype ♂ (NSMT Type no. A 43:51), Japan, Tokyo, Minamiasakawa River, 17.VIII.1979, leg. M. Sasa. [Type material lost, not examined]

Material examined

China: 1♂ (BDN & BOLD Sample ID: XL423), Guangdong, Guangzhou, Conghua, Guifeng Mountain, 22.5416°N, 113.0120°E, 68 m a.s.l., 29.V.2015, Light trap, leg. H.Q. Tang; 1♂ (BDN: GSF3), Guangdong, Guangzhou, Conghua, Guifeng Mountain, 22.5416°N, 113.0120°E, 68 m a.s.l., 19.IV.2015, Sweep net, leg. H.Q. Tang; 2♂♂ (BDN & BOLD Sample ID: XL351; BDN: G5A9), Zhejiang, Jinhua, Pan'an, Dapanshan National Nature Reserve, 28.9728°N, 120.5250°E, 700 m a.s.l., 19.VII.2012, leg. X.L. Lin; 2♂♂ (BDN & BOLD Sample ID: XL287; BDN: I4A144), Zhejiang, Quzhou, Kaihua, Suzhuangzheng, 29.1749°N, 118.1340°E, 300 m a.s.l., 15–17.IV.2011, Light trap, leg. X.L. Lin. Korea: 1♂ (YU no.A-354), Gyeonggi-do, Gapyeong, Jeokmok-ri, Garim, Gapyeongcheon, 5.VI.2004, Light trap, leg. Y.J. Bae.

Diagnosis

Tanytarsus tamaoctavus can be separated from other *Tanytarsus* species by the following combination of characters in the adult male: body mostly yellow with brown patches on scutum, postnotum and preepisternum (Fig. 17B); AR 0.62–0.70; frontal tubercles absent; third palpomere equal or slightly longer than fourth; wing membrane covered with macrotrichia; LR_1 2.37–2.75; tarsomere 1 of mid leg with 2–4 sensilla chaetica (16 in

female); two median setae near the base of anal point; anal tergal bands of V-type, well separated, ending at mid-length of tergite; anal point robust compared to size of hypopygium, with blunt apex; superior volsella roundish, bearing 2 anteromedian and 4–5 dorsal setae; digitus stout with pear-shaped apical lobe, digitus-seta located on cylindrical tubercle at base of digitus; median volsella tiny and hyaline (absent in the original description). Pupa can be separated by having a long, narrow thoracic horn, tapered to fine apical section, chaetae distributed on distal 2/3; tergite II with a pair of spine patches surrounded by shagreen; small spines of tergite III-VI in elongated patches anteriorly; segments V-VIII with 0, 1, 3, 5 lateral taeniae; fringe with 30–34 uniserial taeniae; posterolateral comb of segment VIII bearing one large spine and 8–12 small accessory spines; male genital sacs extending beyond anal lobe.

Description

Adult male (n = 4). Total length 2.08–2.50 mm. Wing length 1.13–1.30 mm. Total length/wing length 1.78–1.82.

Coloration. Head, legs and abdomen yellow. Thorax ground color yellow with pale brown patches anteriorly on scutum, laterally under parapsidal suture, basally on scutellum, dorsally on postnotum and on preepisternum.

Head. Antenna usually with 13 flagellomeres, ultimate flagellomere 260–340 μm long (hermaphrodite with female-like antenna with 5 flagellomeres found in Zhejiang, China, Fig. 17A; normally developed *T. tamaoctavus* female antenna has 4 flagellomeres). AR 0.60–0.69. Frontal tubercles 3–5 μm long, 3–4 μm wide. Temporal setae 5–9. Clypeus with 9–20 setae. Tentorium 105–118 μm long, 23–28 μm wide. Palpomere lengths (in μm): 25–30, 25–25, 78–110, 78–108, 138–190. Third palpomere equal or a little longer than fourth palpomere, bearing 2 sensilla clavata distally.

Thorax (Fig. 17B). Dorsocentrals 6–8; acrostichals 4–10; prealar 1. Scutellum with 2–6 setae. Halteres with 3–4 setae.

Wing (Fig. 17C). VR 1.18–1.28. Brachiolum with 1 seta, Sc bare, R with 13–20 setae, R_1 with 15–23 setae, R_{4+5} with 10–30 setae, M_{1+2} with 18–29 setae, M_{3+4} with 16–26 setae, false vein with 29–52 setae, Cu with 2–13 setae, Cu_1 with 13–14 setae, PCu with 10–24 setae, An with 16–22 setae, remaining veins bare. Cell r_{4+5} with c. 81–120 setae, m with 0–7 setae, m_{1+2} with c. 40–82 setae, m_{3+4} with 32–47 setae, cu+an with 21–51 setae, remaining cells bare. Anal lobe of wing strongly reduced.

Legs. Fore leg bearing single tibial spur, 10–20 μm long. Combs of mid tibia 10–16 μm wide with 20–25 μm long spur, and 10–15 μm wide with 13–15 μm long spur; combs of hind tibia 15–18 μm wide with 15–28 μm long spur, 15–20 μm wide with 15–25 μm long spur. Tarsomere 1 of mid leg with 2–4 sensilla chaetica. Pulvilli absent. Lengths (in μm) and proportions of legs as in Table 4.

Hypopygium (Fig. 18). Tergite IX 60–65 μm long, with two median setae near the base of anal point. Lateral tooth absent. Anal tergal bands of V-type, well separated, ending at mid-length of tergite. Anal point robust compared to size of hypopygium, 30–42 μm long, with 3–4 lateral setae on each side, blunt apex; 6–8 spinulae placed irregularly between anal crests. Transverse sternapodeme broad, 40–55 μm long. Phallapodeme 48–75 μm long. Gonocoxite 88–100 μm long. Gonostylus 73–75 μm long. Superior volsella roundish, bearing 2 anteromedian and 4–5 dorsal setae. Digitus stout with pear-shaped apical lobe, digitus-seta located on cylindrical tubercle at base of digitus. Stem of median volsella short, located underneath superior volsella, 4 μm long, with group of subulate lamellae. Inferior volsella relatively straight, 50–60 μm long, with 9–11 apical setae. HR 1.17–1.33, HV 2.77–2.33.

Remarks

According to Sasa's original description, *Tanytarsus tamaoctavus* is closely related to *T. brundini* and *T. curticornis* based on the shape of adult male hypopygium, but can be separated from the latter two species by the absence of median volsella in the adult male, presence of a pair of spine patches surrounding by shagreen on pupal tergite II and presence of 0, 1, 3, 5 lateral taeniae on pupal segments V-VIII respectively. Unfortunately, the type material of *T. tamaoctavus* was lost when Sasa's collection was transferred from Toyama to NIES in September, 2000 (Tadashi Kobayashi pers. comm.). Na (2004) recorded and re-described *T. tamaoctavus* from Korea and based the identification partly on the absence of median volsella in the adult male hypopygium. Here, we re-describe the species based on the available Chinese specimens and find no significant difference in morphology between the Chinese and Korean specimens and the holotype description except for the putative absence of the median volsella. After examination of specimens from China and Korea and observations in a new collection of the species from Japan (Koichiro Kawai pers. comm.), the presences of a tiny median volsella underneath (and hidden by) the superior volsella can be confirmed in all populations. Thus, the apparent absence noted in the original description likely is due to an error. A slight morphological variation between populations is recorded for the pupa where Chinese specimens have 1, 2, 3, 5 lateral taeniae on segments V-VIII respectively (Hongqu Tang pers. comm.). In general, *T. tamaoctavus* is difficult to differentiate morphologically from the presumed sibling species in Asia (see diagnostic characters and key), but the species is well supported as a distinct genetic lineage based on mitochondrial and nuclear markers (Lin et al. in prep.). Through associations of adult life stages with DNA barcodes we found aberrant sexual characters in two adults from Zhejiang Province, China (female type bodies with male hypopygia).

Distribution

China, Japan, Korea.

***Tanytarsus thomasi* sp. n.**

Figs. 19–20

Type material

Holotype: ♂ (NTNU-VM: 148251, BOLD Sample ID: CHIR_CH166), Canada, Manitoba, Churchill, Ramsey Creek, 58.73054°N, 93.78007°W, 13 m a.s.l., 14.VIII.2006, Netting, leg. J. Knopp. Paratypes: 4♂♂, (NTNU-VM: 148248, BOLD Sample ID: CHIR_CH124; NTNU-VM: 148249, BOLD Sample ID: CHIR_CH164; NTNU-VM: 148250, BOLD Sample ID: CHIR_CH165; NTNU-VM: 148252, BOLD Sample ID: CHIR_CH167) as holotype; 1♂, (NTNU-VM: 148253, BOLD Sample ID: CHIR_CH224), Canada, Manitoba, Churchill, Ramsey Creek, 58.73054°N, 93.78007°W, 13 m a.s.l., 15–17.VIII.2006, Malaise trap, leg. T. Ekrem & E. Stur; 1♂, (NTNU-VM: 136760, BOLD Sample ID: Finnmark666), Norway, Finnmark, Sør-Varanger, Tormajavri, 69.26996°N, 29.11843°E, 146 m a.s.l., 20.VI.2010, leg. T. Ekrem & E. Stur.

Diagnosis

The adult male can be distinguished from known species of *Tanytarsus* by the following combination of characters: body mostly brown, darker vittae, postnotum and preepisternum; AR 0.71–0.94; frontal tubercles present; third palpomere longer than fourth; wing membrane covered with macrotrichia; LR_1 1.85–2.02; tarsomere 1 of mid leg with 2–3 sensilla chaetica; 2–4 median tergite setae near base of anal point; anal tergal bands of V-type, well separated, ending at mid-length of tergite; digitus stout with pear-shaped apical lobe, digitus-seta

located on cylindrical tubercle at base of digitus; stem of median volsella short, with 2–3 pectinate lamellae.

Etymology

Named after Thomas Stur Ekrem for good company in the field; noun in genitive case.

Description

Adult male (n = 4). Total length 2.58–3.11, 2.77 mm. Wing length 1.60–1.95, 1.71 mm. Total length/wing length 1.56–1.68, 1.60.

Coloration. Head, legs and abdomen brown. Thorax ground color brown with dark brown patches anteriorly on scutum, laterally under parapsidal suture, on postnotum and on preepisternum; dark brown median anepisternum II, epimeron II.

Head (Figs. 19A-B). Antenna with 13 flagellomeres, ultimate flagellomere 355–470, 398 μm long. AR 0.71–0.94, 0.79. Frontal tubercles cylindrical (Figure 20b), 8–10, 9 μm long, 4–5, 4 μm wide. Temporal setae 8–11, 9. Clypeus with 12 (n = 4) setae. Tentorium 105–140, 123 μm long, 23–39, 27 μm wide. Palpomere lengths (in μm): 26–38, 33; 35–38, 36; 100–130, 114; 100–123, 111; 135–193, 168. Third palpomere always longer than fourth palpomere, bearing 2 sensilla clavata distally.

Thorax (Fig. 19C). Dorsocentrals 8–9, 9; acrostichals 7–9, 8; prealar 1. Scutellum with 4–6, 6 setae. Halteres with 2–5, 4 setae.

Wing (Fig. 19D). VR 1.15–1.20, 1.17. Brachiolum with 1 (n = 4) seta, Sc bare, R with 17–21, 19 setae, R_1 with 15–19, 17 setae, R_{4+5} with 21–38, 27 setae, M_{1+2} with 41–50, 46 setae, M_{3+4} with 22–28, 25 setae, false vein with 53–60, 56 setae, Cu with 4–17, 10 setae, Cu_1 with 14–17, 15 setae, PCu with 19–42, 27 setae, An with 20–28, 24 setae, remaining veins bare. Cell r with 4 setae (only found in the specimen CHIR_CH165), r_{4+5} with c. 145–180, 160 setae, m

with 3–8, 5 setae, m_{1+2} with c. 140–150, 143 setae, m_{3+4} with 43–80, 55 setae, cu+an with 12–96, 63 setae, remaining cells bare. Anal lobe of wing strongly reduced.

Legs. Fore leg bearing single tibial spur, 18–28, 23 μm long. Combs of mid tibia 13–15, 14 μm wide with 20–25, 22 μm long spur, and 12–14, 13 μm wide with 10–18, 14 μm long spur; combs of hind tibia 14–25, 18 μm wide with 25–28, 27 μm long spur, 13–25, 16 μm wide with 16–28, 22 μm long spur. Tarsomere 1 of mid leg with 2–3, 2 sensilla chaetica. Pulvilli absent. Lengths (in μm) and proportions of legs as in Table 5.

Hypopygium (Fig. 20). Tergite IX with 2–4, 3 median setae near the base of anal point. Lateral tooth absent. Anal tergal bands of V-type, well separated, ending at mid-length of tergite. Anal point strong, triangular with blunt apex, a few microtrichia placed near base, 49–65, 57 μm long, with 3–4, 3 lateral setae on each side; 5–7, 6 spinulae in single row between well-developed anal crests. Transverse sternapodeme 38–50, 44 μm long. Phallapodeme 80–108, 97 μm long. Gonocoxite 120–125, 123 μm long. Gonostylus 110–120, 113 μm long, curved, with rounded apex. Superior volsella oval, bearing 2 anteromedian and 5 dorsal setae. Digitus stout with pear-shaped apical lobe, digitus-seta located on cylindrical tubercle at base of digitus. Stem of median volsella very small, with 2–3, 2 pectinate lamellae. Inferior volsella relatively straight, 75–78, 76 μm long, with 11–13, 12 apical setae. HR 1.00–1.12, 1.09, HV 2.34–2.59, 2.44.

Female and immatures unknown.

Remarks

In one specimen (BOLD Sample ID: CHIR_CH165), cell r has four setae which is unusual for *Tanytarsus*. *Tanytarsus thomasi* is similar to *T. ikicedeus* Sasa & Suzuki in the adult male hypopygium, but can be separated from the latter species by having frontal tubercles, third palpomere longer than fourth, a median volsella with 2–3 pectinate lamellae and

comparatively lower AR (0.71–0.94) and LR_1 (1.85–2.02). Future DNA data on *T. ikicedeus* from Japan will reveal if these species also can be separated genetically. *Tanytarsus thomasi* has unusually high intraspecific K2P-divergence in partial COI sequences (up to 9.8%), but can be differentiated from other species within the *T. curticornis* complex by more than 15% mean K2P-divergence (Fig. 1).

***Tanytarsus tongmuensis* sp. n.**

Figs. 21–23

Type material

Holotype: ♂ (BDN & BOLD Sample ID: XL323), China, Fujian, Nanping, Wuyi Mountian, Tongmu, 27.745°N, 117.677°E, 800 m a.s.l., 29.IV.2015, leg. Q. Wang. Paratypes: 5♂♂ (BDN & BOLD Sample ID: XL346–349), 1♀ (BDN & BOLD Sample ID: XL350) as holotype; 16♂♂ (BDN & BOLD Sample ID: XL314–317, XL319, XL324, XL326, XL327, XL329–335, XL337, XL345), 1♀ (BDN & BOLD Sample ID: XL337), China, Fujian, Nanping, Wuyi Mountian, Tongmu, 27.7452°N, 117.6778°E, 720 m a.s.l., 27–28.IV.2015, leg. Q. Wang.

Diagnosis

The adult male can be distinguished from known species of *Tanytarsus* by the following combination of characters: body mostly pale brown with dark vittae, postnotum and preepisternum; AR 0.66–0.74; frontal tubercles absent; third palpomere longer than fourth; wing length 1.63–1.73 mm; wing membrane covered with macrotrichia; LR_1 2.38–2.72; tarsomere 1 of mid leg with 4–5 sensilla chaetica; 1–5 median setae near the base of anal point; anal tergite bands of V-type, well separated, ending at mid-length of tergite; anal point

robust, with rounded apex; digitus stout with pear-shaped apical lobe, one digitus-seta located on cylindrical tubercle at base of digitus; stem of median short, with 2 subulate lamellae.

Etymology

Named after the type locality, Tongmu; noun in genitive case.

Description

Adult male (n = 8). Total length 2.42–2.77, 2.63 mm. Wing length 1.63–1.73, 1.68 mm. Total length/wing length 1.49–1.65, 1.08.

Coloration. Thorax ground color pale brown with dark patches anteriorly on scutum, laterally under parapsidal suture, on postnotum and paler on preepisternum; pale brown median anepisternum II, epimeron II. Head and legs pale brown. Abdomen yellow.

Head (Fig. 21A). Antenna with 13 flagellomeres, ultimate flagellomere 350–360, 355 μm long. AR 0.66–0.74, 0.69. Frontal tubercles absent. Temporal setae 7–9, 8. Clypeus with 10–12, 11 setae. Tentorium 120–125, 123 μm long, 28–45, 30 μm wide. Palpomere lengths (in μm): 28–33, 30; 31–35, 33; 110–125, 116; 105–120, 113; 185–215, 198. Third palpomere always longer than fourth palpomere, bearing 2 sensilla clavata distally.

Thorax (Fig. 21B). Dorsocentrals 6–8, 7; acrostichals 8–10, 9; prealar 1. Scutellum with 2–4, 3 setae. Halteres with 2–3, 3 setae.

*Wing (Fig. 21C)***.** VR 1.13–1.25, 1.18. Brachiolum with 1 seta, Sc bare, R with 16–26, 20 setae, R_1 with 19–25, 22 setae, R_{4+5} with 32–38, 34 setae, M_{1+2} with 38–55, 46 setae, M_{3+4} with 25–34, 29 setae, false vein with 51–80, 70 setae, Cu with 7–12, 10 setae, Cu_1 with 15–17, 16 setae, PCu with 23–28, 25 setae, An with 21–27, 25 setae, remaining veins bare. Cell r_{4+5} with c. 90–160, 130 setae, m with 4–5, 4 setae, m_{1+2} with c. 110–120, 115 setae, m_{3+4}

with 60–65, 63 setae, cu+an with 59–99, 75 setae, remaining cells bare. Anal lobe of wing strongly reduced.

Legs. Fore leg bearing single tibial spur, 20–30, 25 µm long. Combs of mid tibia 20–23, 21 µm wide with 20–28, 26 µm long spur, and 15–20, 18 µm wide with 13–20, 16 µm long spur; combs of hind tibia 20–25, 22 µm wide with 23–30, 26 µm long spur, 16–25, 19 µm wide with 12–25, 17 µm long spur. Tarsomere 1 of mid leg with 4–5, 4 sensilla chaetica. Pulvilli absent. Lengths (in µm) and proportions of legs as in Table 6.

Hypopygium (Fig. 22). Tergite IX with 1–5, 3 median setae near base of anal point. Lateral tooth absent. Anal tergal bands of V-type, well separated, ending at mid-length of tergite. Anal point strong, long, almost parallel-sided, with blunt apex, microtrichia absent in between crests, 43–75, 60 µm long, with 4–5, 4 lateral setae on each side; 4–6, 5 spinulae placed in single row between well-developed anal crests. Transverse sternapodeme narrow, 33–45, 39 µm long. Phallapodeme 58–85, 73 µm long. Gonocoxite 90–100, 95 µm long. Gonostylus 85–100, 93 µm long, comparatively thin, slightly medially curved, with rounded apex. Superior volsella medially directed, oval with short, straight inner margin, bearing 2–3, 2 anteromedian and 4–5, 5 dorsal setae. Digitus stout with pear-shaped apical lobe, digitus-seta located on cylindrical tubercle at base of digitus. Stem of median volsella short, located underneath superior volsella, 4 µm long, with 2 subulate lamellae. Inferior volsella relatively straight, 63–68, 65 µm long, with 9–11, 10 apical setae. HR 1.00–1.06, 1.04, HV 2.71–2.85, 2.79.

Adult female (n = 2). Total length 1.98–2.24 mm. Wing length 1.63–1.75 mm. Total length/wing length 1.13–1.38.

Coloration. As male.

Head (Figs. 23A-B). Antenna with 4 flagellomeres (Fig. 23B), ultimate flagellomere 125–135 µm long, AR 0.72–0.76. Frontal tubercles absent. Temporal setae 5–8. Clypeus with 18 setae.

Tentorium 110 μm long, 15 μm wide. Palpomere lengths (in μm): 38, 28–30, 103–125, 115–118, 195–203.

Thorax. Humerals 5–6; dorsocentrals 8; acrostichals 8–10; prealar 1. Scutellum with 4 setae. Halteres with 3 setae.

Wing (Fig. 23C). VR 1.25–1.40. Brachiolum with 1 seta, Sc bare, R with 14–22 setae, R_1 with 20–24 setae, R_{4+5} with 43–61 setae, M_{1+2} with 59–80 setae, M_{3+4} with 30–40 setae, false vein with 100–114 setae, Cu with 24–27 setae, Cu_1 with 14 setae, PCu with 33–57 setae, An with 28–37 setae, remaining veins bare. Cell r_{4+5} with c. 240–260 setae, m with 7–16 setae, m_{1+2} with c. 190–200 setae, m_{3+4} with 90–100 setae, cu+an with 160–170 setae, remaining cells bare. Anal lobe of wing strongly reduced.

Legs. As male, except 12–13 sensilla chaetica distally on mid tarsomere 1. Lengths (in μm) and proportions of legs as in Table 7.

Genitalia (Fig. 23D). Sternite VIII with 28–30 setae; vaginal floor small, covering c. 1/4 of vaginal opening ventrally; gonapophysis VIII single lobe with long posteromedially directed microtrichia; gonocoxapodeme strongly curved; coxosternapodeme well-developed with obvious anterior and posterior lobes. Notum including rami 128–168 μm long, notum alone c. 60–83 μm long. Seminal capsules ovoid, large, 65–68 μm long, 38–40 μm wide, with 125–130 μm long spermathecal ducts. Postgenital plate subtriangular. Cercus 50–53 μm long, 45–49 μm wide, with 18–30 setae.

Immatures unknown.

Remarks

Tanytarsus tongmuensis sp. n. is similar to *T. tamaoctavus* and *T. neotamaoctavus* in the adult male, but can be separated from the latter two species by having stout, almost parallel-

sided anal point. DNA barcoded *T. tongmuensis* specimens are more than 14% different from specimens of *T. tamaoctavus* in partial COI sequences (Fig. 1).

***Tanytarsus wangi* sp. n.**

Figs. 24–25

Type material

Holotype ♂ (BDN: L7A23), China, Zhejiang, Lishui, Qinyuan, Baishanzu Nature Reserve, 27.756°N, 119.194°E, 1564 m a.s.l., 24–26.VII.2012, Light trap, leg. X.L. Lin; Paratypes: 2♂♂, 1♂ (BDN & BOLD Sample ID: XL1) as Holotype; 1♂ (BDN: 2630), China, Fujian, Nanping, Wuyishan Mountain, Sangang, 117.680°N, 27.748°E, 934 m a.s.l., Light trap, leg. X.H. Wang.

Diagnosis

The adult male can be distinguished from known species of *Tanytarsus* by the following combination of characters: body pale yellow; AR low (0.43–0.49); frontal tubercles absent; third palpomere equal or longer than fourth; wing membrane covered with macrotrichia; tarsomere 1 of mid leg with two sensilla chaetica; anal point almost parallel-sided, evenly tapered distally, with rounded apex, bearing 5–7 spinulae irregularly placed between anal crests and 3–4 lateral setae; 2–4 median setae near the base of anal point; superior volsella roundish with slightly concave inner margin, bearing two anteromedian setae, two dorsal setae and two lateral setae; digitus with pear-shaped apical lobe, bearing one seta at base; stem of median volsella short, bearing three falciform lamellae; gonostylus short, slightly curved inwards, tapered to pointed apex.

Etymology

Named after Xin-Hua Wang, for his outstanding contribution to the knowledge of Chironomidae in China; noun in genitive case.

Description

Adult male (n = 3). Total length 1.95–2.63 mm. Wing length 0.92–1.15 mm. Total length/wing length 1.89–2.28.

Coloration. Head, thorax, legs and abdomen pale yellow.

Head (Fig. 24A). Antenna with 13 flagellomeres, ultimate flagellomere 190–200 μm long. AR 0.43–0.49. Frontal tubercles absent. Temporal setae 6–8. Clypeus with 12–14 setae. Tentorium 88–100 μm long, 20–25 μm wide. Palpomere lengths (in μm): 25–35, 25–30, 88–93, 80–93, 145–160. Third palpomere equal or longer than fourth, bearing 2 sensilla clavata distally.

Thorax (Fig. 24B). Dorsocentrals 3–6; acrostichals 3–7; prealar 1. Scutellum with 2–4 setae. Halteres with 3–4 setae.

Wing (Fig. 24C). VR 1.35–1.37. Brachiolum with 1 seta, Sc bare, R with 14–18 setae, R_1 with 13–18 setae, R_{4+5} with 15–22 setae, M_{1+2} with 22–33 setae, M_{3+4} with 19–23 setae, false vein with 50–80 setae, Cu with 12–12 setae, Cu_1 with 11–14 setae, PCu with 22–24 setae, An with 19–22 setae, remaining veins bare. Cell r_{4+5} with c. 50–60 setae, m with 2–5 setae, m_{1+2} with c. 50–80 setae, m_{3+4} with 41–50 setae, cu+an with 27–36 setae, remaining cells bare. Anal lobe of wing strongly reduced.

Legs. Fore leg bearing single tibial spur, 10–25 μm long. Combs of mid tibia 13–18 μm wide with 18–25 μm long spur, and 18–23 μm wide with 13–18 μm long spur; combs of hind tibia 20–26 μm wide with 20–28 μm long spur, 17–25 μm wide with 13–18 μm long spur.

Tarsomere 1 of mid leg with 2 sensilla chaetica. Lengths (in μm) and proportions of legs as in Table 8.

Hypopygium (Fig. 25). Tergite IX 66–70 μm long, with 2–4 median setae near the base of anal point. Lateral tooth absent. Anal tergite bands of V-type, well separated, ending at mid-length of tergite. Anal point almost parallel-sided, 33–53 μm long, with 3–4 lateral setae on each side, with blunt apex; 6–7 spinulae placed irregularly between anal crests. Transverse sternapodeme 30–40 μm long. Phallapodeme 48–68 μm long. Gonocoxite 85–100 μm long. Gonostylus 58–80 μm long, slightly curved inwards, tapered to pointed apex. Superior volsella roundish with concave median margin, bearing 2 anteromedian and 4 dorsal setae. Digitus stout with pear-shaped apical lobe, one digitus-seta located on cylindrical tubercle at base of digitus. Stem of median volsella short, located underneath superior volsella, 5 μm long, with three falciform lamellae. Inferior volsella 60–68 μm long, with 8–10 apical setae. HR 1.10–1.47, HV 2.44–3.75.

Female and immatures unknown.

Remarks

The new species is most similar to *Tanytarsus tamaoctavus* in the adult male, but can be separated morphologically from this species by having paler body color and a lower AR. They separate by more than 15% K2P-divergence in partial COI sequences (Fig. 1).

The *Tanytarsus heusdensis* species complex

In general, the species of the *T. heusdensis* species complex have the following morphological characters in adult males: the anal tergite bands are of V-type, widely separated; median setae of the anal tergite are comparatively long, placed near the base of anal point; anal point is stout, apically pointed, with several spinulae in between well-

developed crests; superior volsella is sub-circular, with concave inner margin, bearing 1–2 anteromedian and 5–7 dorsal setae; digitus is long, extending well beyond the median margin of the superior volsella; stem of the median volsella is shorter than its lamellae; transverse sternapodeme has oral projections.

Key to adult males of the *Tanytarsus heusdensis* species complex

1. Hind tibia bear one spur only (Figs. 34D-E). China, Japan. … *T. tamaduodecimus* Sasa

– Hind tibia bear two separate spurs, one on each comb … 2

2. Wing vein Cu bare (Fig. 32C). China, Germany, Korea. … *T. reei* Na & Bae

– Wing vein Cu setose … 3

3. Body entirely brown; wing length < 1.5 mm; tarsomere 1 of mid leg without sensilla chaetica (Fig. 26D); anal crests fused posteriorly, reaching the apex of anal point (Fig. 27A). Norway. … *T. adustus* sp. n.

– Body mostly yellow; wing length > 1.8 mm; tarsomere 1 of mid leg with sensilla chaetica; anal crests not as above … 4

4. Gonostylus straight (Fig. 31); AR 0.59–0.67. Germany. … *T. pseudoheusdensis* sp. n.

– Gonostylus curved inward (Fig. 29D); AR 1.02–1.10. Palaearctic region. … *T. heusdensis* Goetghebuer

***Tanytarsus adustus* sp. n.**

Figs. 26–28

Type material

Holotype ♂, (NTNU-VM: 124470, BOLD Sample ID: SOE247), Norway: Sør-Trøndelag, Røros kommune, Sølendet, Springbrook A2, 62.6903°N, 11.8416°E, 763 m a.s.l.,

3.VIII.2006, Malaise trap, leg. O. Frengen. Paratypes: 1♂ (NTNU-VM: 148234, BOLD Sample ID: XL459), Norway, Sør-Trøndelag, Røros kommune, Sølendet, Springbrook C2, 62.69°N, 11.842°E, 763 m a.s.l., 7.VIII.2006, Malaise trap, leg. O. Frengen; 1♂ (ZMBN: chi23817), Luxemburg, Oesling, W Clervaux, Helokrene-E3, Emergency trap, 50.05°N, 5.988°E, 455 m a.s.l., 18.V.1999, leg. I. Schrankel; 2♀♀ (NTNU-VM: 124617, BOLD Sample ID: SOE380; NTNU-VM: 124623, BOLD Sample ID: SOE386; NTNU-VM: 124624, BOLD Sample ID: SOE387): Norway, Sør-Trøndelag, Røros kommune, Sølendet, Springbrook A1–2, 62.6903°N, 11.8416°E, 763 m a.s.l., 22.VI-3.VII.2006, Malaise trap, leg. O. Hanssen.

Diagnosis

The adult male can be distinguished from known species of *Tanytarsus* by the following combination of characters: body entirely brown with darker patches on the thorax; AR 0.56–0.62; wing cell m bare; tarsomere 1 of mid leg without sensilla chaetica; LR_1 1.76–1.84; 6–10 median setae near the base of anal point; anal point triangular, tapered to pointed, attenuate apex; anal crests fused posteriorly at c. half length of anal point; superior volsella sub-circular, with slightly concave inner margin, bearing 2 anteromedian and 5–6 dorsal setae; digitus long, with blunt apex, extending well beyond inner margin of superior volsella; transverse sternapodeme with weak oral projections; gonostylus widest at mid length, slightly curved inwards, with rounded apex.

Etymology

The specific name is from Latin '*adustus*', adjective referring to the brown body coloration.

Description

Adult male (n = 3). Total length 1.95–2.26 mm. Wing length 1.30–1.50 mm. Total length/wing length 1.50–1.57.

Coloration. Thorax ground color brown with dark brown patches anteriorly on scutum, laterally under parasidal suture, postnotum, preepisternum; and median anepisternum II. Head, legs and abdomen brown. Head, legs and abdomen brown. Halteres and wing pale brown.

Head (Fig. 26A). Antenna with 13 flagellomeres, ultimate flagellomere 250–310 μm long. AR 0.56–0.62. Frontal tubercles absent. Temporal setae 9–11. Clypeus with 8–10 setae. Tentorium 105–115 μm long, 20–30 μm wide. Palpomere lengths (in μm): 28–33, 28–40, 100–125, 80–105, 153–185.

Thorax (Fig. 26B). Dorsocentrals 7–8; acrostichals 6–9; prealar 1. Scutellum with 4 setae. Halteres with 4–5 setae.

Wing (Fig. 26C). VR 1.08–1.17. Brachiolum with 1 seta, Sc bare, R with 16–24 setae, R_1 with 13–18 setae, R_{4+5} with 25–33 setae, M_{1+2} with 40–50 setae, M_{3+4} with 25–44 setae, false vein with 36–54 setae, Cu with 7–18 setae, Cu_1 with 12–16 setae, PCu with 16–19 setae, An with 14–22 setae, remaining veins bare. Cell r_{4+5} with c. 80–90 setae, m bare, m_{1+2} with c. 55–110 setae, m_{3+4} with 27–55 setae, cu+an with 31–72 setae, remaining cells bare. Anal lobe of wing strongly reduced.

Legs. Fore leg bearing single tibial spur, 15–20 μm long. Combs of mid tibia 20–25 μm wide with 25–26 μm long spur, and 10–20 μm wide with 18–23 μm long spur; combs of hind tibia 14–23 μm wide with 28–30 μm long spur, 20–36 μm wide with 20–28 μm long spur. Tarsomere 1 of mid leg without sensilla chaetica (Fig. 26D). Lengths (in μm) and proportions of legs as in Table 9.

Hypopygium (Fig. 27). Tergite IX 73–75 μm long, with 6–10 median setae near the base of anal point. Lateral tooth absent. Anal tergite bands of V-type, widely separated, ending at

mid-length of tergite. Anal point triangular, tapering to pointed, attenuate apex, 40–45 μm long, with 4–6 lateral setae on each side; 4–6 spinulae placed regularly between anal crests which fused posteriorly at c. half length of anal point. Transverse sternapodeme 43–48 μm long, with weak oral projections. Phallapodeme 70–95 μm long. Gonocoxite 110–120 μm long. Gonostylus widest in middle, slightly curved inward, 88–108 μm long with rounded apex. Superior volsella sub-circular, with slightly concave inner margin, bearing 2 anteromedian and 5–6 dorsal setae. Digitus long, with blunt apex, extending beyond anterior margin of superior volsella. Stem of median volsella 10–15 μm long, bearing 3 setae and 3–5 subulate lamellae. Inferior volsella relatively straight, 75–88 μm long, bearing 9–11 apical setae. HR 1.07–1.28, HV 2.09–2.22.

Adult female (n = 3). Total length 1.53–1.56 mm. Wing length 1.30–1.50 mm. Total length/wing length 1.02–1.515.

Coloration. Same color pattern as male, but paler.

Head (Figs. 28A-B). Antenna with 4 flagellomeres (Fig. 28B), ultimate flagellomere 105–113 μm long, AR 0.51–0.62. Frontal tubercles absent. Temporal setae 8. Clypeus with 10 setae. Tentorium 113 μm long, 10–13 μm wide. Palpomere lengths (in μm): 28–29, 30–33, 98–100, 83–93, 158–170.

Thorax (Fig. 28C). Humeral 1; dorsocentrals 6–8; acrostichals 6–9; prealar 1. Scutellum with 4 setae. Halteres with 4–5 setae.

Wing (Fig. 28D). VR 1.11–1.20. Brachiolum with 1 seta, Sc bare, R with 14–17 setae, R_1 with 13–14 setae, R_{4+5} with 25–26 setae, M_{1+2} with 33–37 setae, M_{3+4} with 19–29 setae, false vein with 40–53 setae, Cu with 14–17 setae, Cu_1 with 12–14 setae, PCu with 23–28 setae, An with 16–19 setae, remaining veins bare. Cell r_{4+5} with c. 120–145 setae, m with 4–5 setae, m_{1+2} with c. 130–140 setae, m_{3+4} with 50–68 setae, cu+an with 83–88 setae, remaining cells bare. Anal lobe of wing strongly reduced.

Legs. As male, except five sensilla chaetica distally on mid tarsomere 1. Lengths (in μm) and proportions of legs as in Table 10.

Genitalia (Fig. 28E). Tergite IX slightly triangular; sternite VIII with 22 setae; vaginal floor small, covering c. 1/4 of vaginal opening ventrally; gonapophysis VIII single lobe with long posteromedially directed microtrichia; gonocoxapodeme strongly curved; coxosternapodeme well-developed with obvious anterior and posterior lobes. Notum including rami 140–150 μm long, notum alone c. 95–100 μm long. Seminal capsules ovoid, large, 50–63 μm long, 30–40 μm wide, with 155–193 μm long spermathecal ducts. Postgenital plate subtriangular. Cercus 50–58 μm long, 35–45 μm wide, with 21–31 setae.

Immatures unknown.

Remarks

The new species resembles *T. heusdensis* in the adult male hypopygium, but can be separated from the latter species by having an entirely brown body with darker patches on the thorax, a lower AR and by lacking sensilla chaetica on mid ta_1. The new species also separates from *T. heusdensis* by more than 19% divergence in partial COI sequences (Fig. 2).

***Tanytarsus heusdensis* Goetghebuer, 1923**

Fig. 29

Tanytarsus heusdensis Goetghebuer, 1923: 118, fig. 11; Albu 1980: 250, fig. 168; Reiss & Fittkau 1971: 101, figs. 8–9; Lindeberg 1970: 311. Holotype ♂ (RBINS 18.073), leg. M. Goetghebuer [Examined].

Tanytarsus gotchi Goetghebuer, 1928: 143, fig. 11. Holotype ♂ (BMNH 235909), England, Surrey, Richmond-Upon-Thames, 29.VII.1914, leg. D.H. Gotch [Not examined].

Tanytarsus heusdensis var. *kuusamoensis* Storå, 1939: 30, fig. 22. [Not examined].

Additional material examined

Germany: 2♂♂ (NTNU-VM: 148243, BOLD Sample ID: XL183; NTNU-VM: 148244, BOLD Sample ID: XL186), Bavaria, Pfaffenhofen, Scheller-Mühle, Ilm River, 430 m a.s.l., 48.53°N, 11.509°E, 27.IV.2003, Sweep net, leg. E. Stur; Norway: 2♂♂ (NTNU-VM: 143621, BOLD Sample ID: CH-OSF102; NTNU-VM: 143623, BOLD Sample ID: CH-OSF104), Oslo, S Nordstrand, Ljanselva, Liadalen, 59.8481°N, 10.7927°E, 2.VI.2010, leg. G. Søli & M. Steinert.

Diagnosis

Tanytarsus heusdensis can be distinguished from known species of *Tanytarsus* by the following combination of characters: body mostly yellow with light brown patches on anterior scutum, postnotum, median anepisternum II and preepisternum (Fig. 29B); front tubercles absent; AR 1.02–1.10 (n = 3); wing length > 2 mm; wing membrane covered with macrotrichia; LR_1 1.89–1.92 (n = 3); tarsomere 1 of mid leg with 3–4 sensilla chaetica; anal tergite bands of V-type, widely separated, diagonally pointing towards base of anal point; anal point widened basally, tapering to pointed apex, bearing several spinulae placed irregularly between posteriorly fused anal crests; superior volsella circular with concave inner margin bearing 1–2 anteromedian and 5–7 dorsal setae; digitus thumb-like, tapered to blunt apex, extending beyond inner margin of superior volsella, with one digitus-seta; stem of median volsella about two times longer than wide, lamella longer than stem, wide from the base to near the tip, where it splits into several fine points in the form of a crown; transverse sternapodeme with strong oral projections.

Remarks

Tanytarsus heusdensis is widely recorded in the Palearctic Region, but its distribution should be revised considering the new, morphologically similar species described here. *Tanytarsus gotchi* was described by Goetghebuer (1928) using few characters and a simple illustration. Reiss & Fittkau (1971) synonymized *T. gotchi* with *T. heusdensis* after examining both holotypes, arguing that the coloration and remaining diagnostic characters fit within the diagnosis of *T. heusdensis*. Storå (1939) described *Tanytarsus heusdensis* var. *kuusamoensis* having a pale body with dark mesonotal stripes and an AR of about 1.00. The similar species *T. adustus* sp. n. and *T. pseudoheusdensis* sp. n. have an AR of 0.56–0.62 and entirely brown body and an AR of 0.59–0.67 and mostly yellow body, respectively. Thus, we are convinced that neither *T. gotchi* nor *T. heusdensis* are conspecific with the new species we describe and regard them as junior synonyms of *T. heusdensis*.

Distribution

Palaearctic Region.

***Tanytarsus pseudoheusdensis* sp. n.**

Figs. 30–31

Type material

Holotype ♂ (NTNU-VM: 148246, BOLD Sample ID: ES79), Germany: Bavaria, Nationalpark Berchtesgaden, Herrenrointquelle 312c, 47.58°N, 12.975°E, 1230 m a.s.l., 12.VII.2005, Sweep net, leg. F. Eder & A. Schellmoser. Paratypes: 1 ♂ (NTNU-VM: 148245, BOLD Sample ID: ES77) as holotype; 1 ♂ (NTNU-VM: 93565) Germany, Bavaria,

Nationalpark Berchtesgaden, Herrenrointquelle 312c, 47.58°N, 12.975°E, 1230 m a.s.l., 23.VIII-06.IX.2005, leg. F. Eder.

Diagnosis

The adult male can be distinguished from known species of *Tanytarsus* by the following combination of characters: body mostly yellow with pale brown patches anteriorly on scutum, on postnotum, ventrally on preepisternum, median anepisternum II and epimeron II (Fig. 30B); AR 0.59–0.67; wing cell m with 22 setae; LR_1 1.84–2.07; tarsomere 1 of mid leg with 2–3 sensilla chaetica distally; anal tergite with ten median setae near base of anal point; lateral tooth absent; anal tergite bands of V-type, well separated, ending at mid-length of tergite; anal point with digitiform distal end, crests fused posteriorly at half length; 4–6 spinulae placed in irregular row between anal crests; gonostylus with more or less straight inner margin, with rounded apex; superior volsella roundish, slightly elongated and medially directed, with concave inner margin, bearing 2 anteromedian and 5–6 dorsal setae; digitus long, with blunt apex, extending well beyond median margin of superior volsella; median volsella short, barely longer than wide, bearing 3–5 subulate lamellae and a few simple setae; transverse sternapodeme with strong oral projections.

Etymology

The specific name, '*pseudoheusdensis*', reflects the similarities in morphology to *T. heusdensis*.

Description

Adult male (n = 3). Total length 2.85–2.93 mm. Wing length 1.93–1.95 mm. Total length/wing length 1.46–1.52.

Coloration. Thorax ground color yellow with pale brown patches anteriorly on scutum, laterally under parapsidal suture, on postnotum and ventrally on preepisternum; pale brown median anepisternum II, epimeron II. Legs and abdomen pale yellow.

Head (Fig. 30A). Antenna with 13 flagellomeres, ultimate flagellomere 325–375 µm long. AR 0.59–0.67. Frontal tubercles absent. Temporal setae 10–13. Clypeus with 11–12 setae. Tentorium 108–128 µm long, 25–45 µm wide. Palpomere lengths (in µm): 25–35, 33–35, 120–123, 120–123, 200–213.

Thorax (Fig. 30B). Dorsocentrals 7–9; acrostichals 9–10; prealar 1. Scutellum with 4–6 setae. Halteres with 3–4 setae.

Wing (Fig. 30C). VR 1.12–1.13. Brachiolum with 1 seta, Sc bare, R with 28–34 setae, R_1 with 28–29 setae, R_{4+5} with 27–37 setae, M_{1+2} with 40–50 setae, M_{3+4} with 30–36 setae, false vein with 60–70 setae, Cu with 19 setae, Cu_1 with 18–22 setae, PCu with 44–47 setae, An with 30–35 setae, remaining veins bare. Cell r_{4+5} with c. 200–210 setae, m with 22 setae, m_{1+2} with c. 120–140 setae, m_{3+4} with 90–100 setae, cu+an with 110–115 setae, remaining cells bare. Anal lobe of wing strongly reduced.

Legs. Fore leg bearing single tibial spur, 25 µm long. Combs of mid tibia 20–25 µm wide with 25 µm long spur, and 15–25 µm wide with 15–25 µm long spur; combs of hind tibia 35 µm wide with 25 µm long spur, 20–36 µm wide with 30–38 µm long spur. Tarsomere 1 of mid leg with 2–3 sensilla chaetica distally. Lengths (in µm) and proportions of legs as in Table 11.

Hypopygium (Fig. 31). Tergite IX 75–100 µm long, with 10 median setae near the base of anal point. Lateral tooth absent. Anal tergal bands of V-type, well separated, ending at mid-length of tergite. Anal point 48–53 µm long, with 4 lateral setae on each side, digitiform distal end; 4–6 spinulae placed in irregular row between anal crests which are fused posteriorly at half length of anal point. Transverse sternapodeme 50–53 µm long, with strong

oral projections. Phallapodeme 90–105 µm long. Gonocoxite 133–135 µm long. Gonostylus with more or less straight inner margin, 118–128 µm long, with rounded apex. Superior volsella roundish with concave median margin, slightly elongated and medially directed, bearing 2 anteromedian and 5–6 dorsal setae. Digitus long, with blunt apex, extending well beyond median margin of superior volsella. Stem of median volsella stout, barely longer than wide, bearing 3–5 subulate lamellae and a few simple setae. Inferior volsella relatively straight, 65–90 µm long, bearing 8–10 strong apical setae. HR 1.04–1.14, HV 2.23–2.48. *Female and immatures unknown*.

Remarks

The new species is most similar to *Tanytarsus heusdensis* in the adult male, but can be separated morphologically from this species by having a lower AR and a median volsella bearing subulate lamellae. They also separate by more than 26% K2P-divergence in partial COI sequences (Fig. 2).

***Tanytarsus reei* Na & Bae, 2010**

Figs. 32–33

Tanytarsus reei Na & Bae, 2010: 35, fig. 2. Holotype ♂ (KU No. SWU-CHI-A-218), Korea, Gyeonggi-do, Namyangju, Sinwol-ri, Wangsukcheon, Imsonggyo, 14.V.2003, leg. K.B. Na & Y.J. Bae; Paratype ♂ (KU No. SWU-CHI-A-217), same as holotype [Examined].

Additional specimens examined

1♂ (NTNU-VM: 148247, BOLD Sample ID: XL180), Germany, Bavaria, Pfaffenhofen, Scheller-Mühle, Ilm River, 48.53°N, 11.509°E, 430 m a.s.l., 27.IV.2003, Sweep net, leg. E.

Stur. China: 2♂♂ (BDN & BOLD Sample ID: XL12; BDN & BOLD Sample ID: XL13), Henan, Zhengzhou, Gongyi, Yungou Village, 34.564°N, 113.035°E, 760 m a.s.l., Sweep net, leg. S.L. Li; 1♂ (BDN: 21374), Heilongjiang Province, Shangzhi, Maoer Mountain, 25.VII.2003, Light trap, leg. J. Li.

Diagnosis

The adult male can be distinguished from known species of *Tanytarsus* by the following combination of characters: body mostly yellow-green with brown patches on scutum, postnotum, preepisternum and median anepisternum II (Fig. 32B); wing length 1.58–2.18 mm; wing membrane with comparatively few setae: vein Cu bare, vein PCu with 0–4 setae, cell m bare, cu+an with 3–7 setae; frontal tubercles small; AR 0.90–1.00; superior volsella sub-circular with concave inner margin, bearing 2 anteromedian and 5–7 dorsal setae; digitus long, with slightly swollen blunt apex, extending beyond median margin of superior volsella; median volsella short, slightly longer than wide, bearing several simple lamellae; transverse sternapodeme with strong oral projections.

Description

Adult male (n = 3). Total length 2.38–3.2 mm. Wing length 1.58–2.18 mm. Total length/wing length 1.47–1.53.

Coloration. Thorax ground color brown with dark patches anteriorly on scutum, laterally under parapsidal suture, on postnotum and preepisternum; pale brown median anepisternum II, epimeron II. Head, legs and abdomen yellow, slightly darker tarsi.

Head (Fig. 32A). Antenna with 13 flagellomeres, ultimate flagellomere 430–495 μm long. AR 0.96–1.01. Frontal tubercles small, 5–8 μm long, 4–5 μm wide. Temporal setae 9–12.

Clypeus with 12–14 setae. Tentorium 125–138 µm long, 30–43 µm wide. Palpomere lengths (in µm): 28–38, 28–50, 115–125, 105–128, 203–230.

Thorax (Fig. 32B). Dorsocentrals 7–9; acrostichals 6–7; prealar 1. Scutellum with 2–6 setae. Halteres with 2–6 setae.

Wing (Fig. 32C). VR 1.12–1.13. Brachiolum with 1 seta, Sc bare, R with 17–23 setae, R_1 with 14–22 setae, R_{4+5} with 18–21 setae, M_{1+2} with 32–40 setae, M_{3+4} with 17–22 setae, false vein with 12–28 setae, Cu bare, Cu_1 with 14–19 setae, PCu with 0–4 setae, An with 20–35 setae, remaining veins bare. Cell r_{4+5} with c. 110–150 setae, m bare, m_{1+2} with c. 85–130 setae, m_{3+4} with 23–50 setae, cu+an with 3–7 setae, remaining cells bare. Anal lobe of wing strongly reduced.

Legs. Fore leg bearing single tibial spur, 20–25 µm long. Combs of mid tibia 16–28 µm wide with 28–30 µm long spur, and 16–25 µm wide with 18–23 µm long spur; combs of hind tibia 24–40 µm wide with 28–30 µm long spur, 20–25 µm wide with 26–28 µm long spur. Tarsomere 1 of mid leg with 6–8 sensilla chaetica. Lengths (in µm) and proportions of legs as in Table 12.

Hypopygium (Figs. 33A-B). Tergite IX 70–80 µm long, with 5–8 median setae near the base of anal point. Lateral tooth present. Anal tergal bands of V-type, well separated, ending at mid-length of tergite. Anal point with convex margins in basal part, parallel sided distal part, rounded apex, 38–51 µm long, with 3–4 lateral setae on each side; 6–7 spinulae placed between anal crests which are fused posteriorly at 2/3 length of anal point. Transverse sternapodeme 48–65 µm long, with strong oral projections. Phallapodeme 102–105 µm long. Gonocoxite 93–150 µm long. Gonostylus with inner margin more or less straight, slightly curved inward, 120–125 µm long. Superior volsella sub-circular with concave inner margin, bearing 2 anteromedian and 5–7 dorsal setae. Digitus long, with slightly swollen blunt apex, extending beyond median margin of superior volsella. Stem of median volsella 8–13 µm

long, barely longer than wide, bearing several simple lamellae. Inferior volsella relatively straight, 55–93 μm long, bearing 10–11 apical setae. HR 0.74–1.20, HV 1.90–2.56. *Female and immatures unknown*.

Remarks

After re-examination of the holotype, we found a few median setae placed near the base of the anal point that were not mentioned in the original description (Na & Bae 2010). *Tanytarsus reei* is here re-described based on additional material from China and Germany. The species is most similar to *T. heusdensis* in the adult male hypopygium, but can be separated from latter species by having bare wing vein Cu, a sub-circular superior volsella and a median volsella bearing simple lamellae. The two species also separate by more than 22% K2P-divergence in partial COI sequences (Fig. 2).

Distribution

China, Korea, Germany.

***Tanytarsus tamaduodecimus* Sasa, 1983**

Figs. 34–35

Tanytarsus tamaduodecimus Sasa, 1983: 21, fig. 17; Sasa & Kikuchi 1995: 51, fig. 45E; Yamamoto & Yamamoto: 359. Holotype ♂ (NSMT Type no. 069: 061) Japan, Hikawa, Station C, 12.VI.1981, leg. M. Sasa & A. Shirasaka [Examined].

Tanytarsus tusimatneous Sasa & Suzuki, 1999: 33, fig. 40; Yamamoto & Yamamoto: 360. Holotype ♂ (NSMT Type no. 354: 095) Japan, Tsushima, Mitsushima, Sumokawa, 35.III.1998, leg. H. Suzuki [Examined]. syn. n.

Tanytarsus tusimatpequeus Sasa & Suzuki, 1999: 35, fig. 42; Yamamoto & Yamamoto: 360. Holotype ♂ (NSMT Type no. 353: 094) Japan, Tsushima, Izuhara, Uchiyama, 24.III.1998, leg. H. Suzuki [Not examined].

Additional material examined

China: 1♂ (BDN & BOLD Sample ID: LGT01), Shaanxi, Louguantai National Forest Park, Light trap, 34.0629°N, 108.3296°E, 600 m a.s.l., 25.VII.2013, leg. Q. Wang.

Diagnosis

The adult male can be distinguished from known species of *Tanytarsus* by the following combination of characters: body mostly yellow-green with pale brown patches on scutum, postnotum, preepisternum and median anepisternum II (Fig. 34A); AR 0.55–0.71; frontal tubercles minute; wing cell m bare; LR_1 2.24–2.55; only one comb on hind tibia bearing spur; ten median setae placed irregularly near the base of anal point; anal tergite bands of V-type, moderately widely separated medially; anal point triangular, tapering to pointed, attenuate, pigmented apex; several spinulae between anal crests which are fused posteriorly at 2/3 length of anal point; superior volsella sub-circular, with concave inner margin, bearing two anteromedian and 5–7 dorsal setae; digitus curved, with blunt apex, extending beyond median margin of superior volsella, bearing one digitus-seta at base; stem of median volsella short, as long as wide, bearing 4–6 subulate lamellae; transverse sternapodeme with strong oral projections.

Remarks

We examined the holotypes of *T. tamaduodecimus* and *T. tusimatneous* and compared the observed morphology with the original descriptions of *T. tamaduodecimus* and *T.*

tusimatneous (Sasa 1983; Sasa & Suzuki 1999a). The two species are similar in all characters considered diagnostic, e.g. anal point tapering to a pointed, attenuate apex combined with the presence of a single spur on the hind tibia (unusual for *Tanytarsus*) and we therefore treat *T. tusimatneous* as a junior synonym of *T. tamaduodecimus*. The small differences observed in the hypopygia (Fig. 35) are considered to be due to intraspecific variation and/or differences due to the slide mount. DNA barcodes data support *T. tamaduodecimus* as a separate species from other species in the *T. heusdensis* species complex (Fig. 2).

Distribution

China, Japan.

Discussion

DNA barcodes and morphospecies

In general, our results demonstrate that COI is an effective tool for species delimitation and recognition of cryptic species. However, a fixed threshold of COI sequences is not appropriate for all taxonomic groups. In insects for instance, a 2% threshold provides effective identification at the species level of Ephemeroptera (Schmidt et al. 2015; Webb et al. 2012; Zhou et al. 2010), Lepidoptera (Zahiri et al. 2014) and Trichoptera (Zhou et al. 2016), while a 2.2% threshold of Heteroptera (Knebelsberger et al. 2014), a 2.5% threshold of aquatic beetle (Monaghan et al. 2005), and a >3% threshold for several dipteran groups (Nzelu et al. 2015; Renaud et al. 2012). Furthermore, an average threshold of 4–5% appears appropriate for Chironomidae (Lin et al. 2015; Meier et al. 2015).

In this study, unusual deep intraspecific K2P-divergences in DNA barcodes are observed. The 9.8% maximum intraspecific divergence in the *T. curticornis* species complex and 8.6% maximum intraspecific divergence in the *T. heusdensis* species complex are much higher than the average intraspecific divergences (0.9%–2.32%) previously reported in Chironomidae (Ekrem et al. 2007; Lin et al. 2015; Silva & Wiedenbrug 2014; Sinclair & Gresens 2008; Song et al. 2016). We nevertheless refrain from describing the divergent lineages as separate species since their morphology is consistent and regarded as conspecific. Moreover, nuclear markers show little or no divergence (Lin et al. in prep.), indicating that other explanations for the large divergence in COI are likely. *Wolbachia* infections can lead to divergent mitochondrial lineages within insect species (Smith et al. 2012; Whitworth et al. 2007), but this bacterial endoparasite has not yet been found in Chironomidae. Thus, incomplete lineage

sorting (Ballard & Whitlock 2004; Heckman et al. 2007; Willyard et al. 2009) might be a better explanation for the observed differences in DNA barcodes.

Taxonomy

Tanytarsus species have traditionally been subdivided into several species groups to aid in identification, species revisions, and classification. New molecular and morphological data show that the *T. curticornis* and *T. heusdensis* species complexes are distinct from the *T. chinyensis* species group (Lin et al. in prep.) and that characters previously used to define the *chinyensis* group (Giłka & Paasivirta 2009; Reiss & Fittkau 1971) have evolved several times within *Tanytarsus*. Thus, new sets of characters were needed to define the *T. curticornis* and *T. heusdensis* species complexes. This proved to be challenging, but we believe the suggested characters will hold as diagnostic features for species in these two complexes. Two candidate species for the here investigated species groups remain to be sampled for DNA before exclusion can be confirmed, but *T. manlyensis* Glover, 1973 and *T. trifidus* Freeman, 1958 have a S-shaped digitus, without pear-shaped apical lobe. Thus, even if these are superficially similar to species in the *T. curticornis* complex, they do not have the most characteristic feature of this complex.

Traditionally, in taxonomy of the Tanytarsini, some morphological features (e.g. body coloration and wing setation) have been ignored and often treated as intraspecific variation dependent on emergence period and temperature (Lindeberg 1960; Lindeberg 1963). However, there seems to be a constant interspecific variation in pigmentation for several of the *Tanytarsus* species treated here. For instance, *T. madeiraensis* sp. n. and *T. thomasi* sp. n. of the *T. curticornis* species complex have been regarded as *T. brundini* based on the high morphological similarity in the adult male hypopygium. However, these species have quite

different coloration, and also show additional morphological differences when examined more closely (see key and diagnostic characters above). A potential additional species very similar to *T. brundini* was reported by Lindeberg (1963) from Finland. We have not been able to sample fresh material from this population for DNA comparison and are unable to separate it morphologically from *T. brundini*. In the *T. heusdensis* species complex, *T. adustus* sp. n. and *T. pseudoheusdensis* sp. n. have been misidentified as *T. heusdensis* in previous barcode studies due to the similar shape in the adult male hypopygium (Ekrem et al. 2010). Upon re-examination of the barcode voucher specimens, these genetically distinct semi-cryptic species also can be separated from the nominal *T. heusdensis* by differences in body coloration and wing setation.

Immature life stages are important in biodiversity assessments of chironomids and biological monitoring (Anderson et al. 2013; Ekrem et al. 2010; Ferrington et al. 1991; Kranzfelder et al. 2015; Raunio et al. 2007). In particular chironomid pupal exuviae might provide important characters to help resolve taxonomic issues for cryptic species complex. Unfortunately, there are few species with associated and described immature life stages in the *T. curticornis* and *T. heusdensis* complexes, but those known display characters that appear to be species specific. For instance, morphological features of pupa of *T. madeiraensis* sp. n. (Fig. 13) will separate this species from others in the *T. curticornis* complex with known pupae. Since it's time consuming to rear, the immature stages can be associated with adults using DNA barcodes.

Conclusion

Overall, our study has revealed strong concordance between morphological species concepts and DNA barcodes. After reviewing the *T. curticornis* and *T. heusdensis* species complexes using DNA barcodes, we have detected and described seven new species, one new junior synonym, several misidentifications, and provided keys to adult male and known pupae. In the future, a comprehensive sampling of these species, in particular the immature life stages, is required to provide more morphological characters and expand the DNA barcode database for chironomids. With the rapid development and lowered costs of modern molecular techniques, integrative taxonomy combining morphological and molecular data should be more available to Chironomidae taxonomists. This will certainly provide the scientific community more accurate measures of the diversity in one of the most abundant and species rich groups of aquatic insects.

Acknowledgements

This paper is part of the first author's PhD-thesis at the Norwegian University of Science and Technology, Norway, entitled "Systematics and evolutionary history of *Tanytarsus* van der Wulp, 1874 (Diptera: Chironomidae)".

Many thanks to Xin-Hua Wang and Chao Song (College of Life Sciences, Nankai University, Tianjin, China), Wojciech Giłka (Department of Invertebrate Zoology and Parasitology, University of Gdańsk, Poland), Yeon Jae Bae and Hyojeong Kang (College of Life Sciences, Korea University, Korea), Han-Il Ree (College of Medicine, Yonsei University, Seoul, Korea), Viktor Baranov (Leibniz Institute of Freshwater Ecology and Inland Fisheries, Berlin, Germany) for collecting and sending material, also to Dr. Natsuko Kondo (Center for Environmental Biology and Ecosystem Studies National Institute for Environmental Studies, Tsukuba, Japan) and Koichiro Kawai (Graduate School of Biosphere Science, Hiroshima University, Hiroshima, Japan) for sharing DNA barcode data and morphological observations of Japanese specimen. Many thanks to Akihiko Shinohara (National Museum of Nature and Science, Tsukuba, Japan) for the loan of type specimens from the Sasa collection and to Alan Lanford and David Yeates (Australian National Insect Collection, Australia), and Pol Limbourg (The Royal Belgian Institute of Natural Sciences, Bruxelles, Belgium) for the loan of type specimens. Thanks also to Allison Brown (Biodiversity Institute of Ontario, University of Guelph, Canada) for the loan of barcode vouchers from Canada.

References

Albu, P. (1980) Diptera Fam. Chironomidae - Subfam. Chironominae. *Fauna Republicii Socialista România, Insecta* **11:** 1–320.

Anderson, A.M., Stur, E. & Ekrem, T. (2013) Molecular and morphological methods reveal cryptic diversity and three new species of Nearctic *Micropsectra* (Diptera: Chironomidae). *Freshwater Science* **32:** 892–921.

Ashfaq, M. & Hebert, P.D.N. (2016) DNA barcodes for bio-surveillance: regulated and economically important arthropod plant pests. *Genome* **59:** 933–945.

Baker, C.C., Bittleston, L.S., Sanders, J.G. & Pierce, N.E. (2016) Dissecting host-associated communities with DNA barcodes. *Philosophical Transactions of the Royal Society B: Biological Sciences* **371:** 20150328.

Ballard, J.W.O. & Whitlock, M.C. (2004) The incomplete natural history of mitochondria. *Molecular Ecology* **13:** 729–744.

Brodin, Y., Ejdung, G., Strandberg, J. & Lyrholm, T. (2013) Improving environmental and biodiversity monitoring in the Baltic Sea using DNA barcoding of Chironomidae (Diptera). *Molecular Ecology Resources* **13:** 996–1004.

Carew, M.E., Marshall, S.E. & Hoffmann, A.A. (2011) A combination of molecular and morphological approaches resolves species in the taxonomically difficult genus *Procladius* Skuse (Diptera: Chironomidae) despite high intra-specific morphological variation. *Bulletin of Entomological Research* **101:** 505–519.

Carew, M.E., Pettigrove, V.J., Metzeling, L. & Hoffmann, A.A. (2013) Environmental monitoring using next generation sequencing: rapid identification of macroinvertebrate bioindicator species. *Frontiers in Zoology* **10:** 45.

Cranston, P.S. (2000) Monsoonal tropical *Tanytarsus* van der Wulp (Diptera: Chironomidae) reviewed: New species, life histories and significance as aquatic environmental indicators. *Australian Journal of Entomology* **39:** 138–159.

Edgar, R.C. (2004) MUSCLE: multiple sequence alignment with high accuracy and high throughput. *Nucleic Acids Research* **32:** 1792–1797.

Edwards, F.W. (1929) British non-biting midges (Diptera, Chironomidae). *Transactions of the Royal Entomological Society of London* **77:** 279–430.

Ekrem, T. (1999) Six new *Tanytarsus* species from Ghana, West Africa (Insecta, Diptera, Chironomidae). *Spixiana* **22:** 53–68.

Ekrem, T. (2001) A Review of Afrotropical *Tanytarsus* van der Wulp (Diptera: Chironomidae). *Tijdschrift voor Entomologie* **144:** 5–40.

Ekrem, T. (2002) A review of selected South- and East Asian *Tanytarsus* v.d. Wulp (Diptera: Chironomidae). *Hydrobiologia* **474:** 1–39.

Ekrem, T. (2004) Immature stages of European *Tanytarsus* species I. The *eminulus*-, *gregarius*-, *lugens*- and *mendax* species groups (Diptera, Chironomidae). *Deutsche Entomologische Zeitschrift* **51:** 97–146.

Ekrem, T., Stur, E. & Hebert, P.D.N. (2010) Females do count: Documenting Chironomidae (Diptera) species diversity using DNA barcoding. *Org Divers Evol* **10:** 397–408.

Ekrem, T., Sublette, M.F. & Sublette, J.E. (2003) North American *Tanytarsus* I. Descriptions and Keys to Species in the *eminulus*, *gregarius*, *lugens* and *mendax* Species Groups (Diptera : Chironomidae). *Annals of the Entomological Society of America* **96:** 265–328.

Ekrem, T., Willassen, E. & Stur, E. (2007) A comprehensive DNA sequence library is essential for identification with DNA barcodes. *Molecular Phylogenetics and Evolution* **43:** 530–542.

Epler, J.H., Ekrem, T. & Cranston, P.S. (2013) The larvae of Chironominae (Diptera: Chironomidae) of the Holarctic region—keys and diagnoses. In: Cederholm L, ed. Chironomidae of the Holarctic Region: Keys and Diagnoses, Part 1: Larvae. Lund, Sweden: Insect Systematics and Evolution, Supplement **66:** 387–556.

Ferrington, L.C., Blackwood, M.A., Wright, C.A., Crisp, N.H., Kavanaugh, J.L. & Schmidt, F.J. (1991) A protocol for using surface-floating pupal exuviae of Chironomidae for rapid bioassessment of changing water-quality. *Sediment and Stream Water Quality in a Changing Environment : Trends and Explanation* **203:** 181–190.

Folmer, O., Black, M., Hoeh, W., Lutz, R. & Vrijenhoek, R. (1994) DNA primers for amplification of mitochondrial cytochrome c oxidase subunit I from diverse metazoan invertebrates. *Molecular Marine Biology and Biotechnology* **3:** 294–299.

Giłka, W. & Paasivirta, L. (2009) Evaluation of diagnostic characters of the *Tanytarsus chinyensis* group (Diptera: Chironomidae), with description of a new species from Lapland. *Zootaxa* **2197:** 31–42.

Glover, B. (1973) The Tanytarsini (Diptera: Chironomidae) of Australia. *Australian Journal of Zoology Supplementary Series* **21:** 403–478.

Goetghebuer, M. (1923) Nouveaux matériaux pour l'étude de la faune des Chironomides de Belgique. 2e note. *Annales du Biologie Lacustre* **12:** 103–120.

Goetghebuer, M. (1928) Diptères (Nématocères). Chironomidae. III. Chironomariae. *Faune de France* **18:** 1–174.

Hajibabaei, M., Baird, D.J., Fahner, N.A., Beiko, R. & Golding, G.B. (2016) A new way to contemplate Darwin's tangled bank: how DNA barcodes are reconnecting biodiversity science and biomonitoring. *Philosophical Transactions of the Royal Society B: Biological Sciences* **371:** 20150330.

Hausmann, A., Miller, S.E., Holloway, J.D., deWaard, J.R., Pollock, D., Prosser, S.W.J. & Hebert, P.D.N. (2016) Calibrating the taxonomy of a megadiverse insect family: 3000 DNA barcodes from geometrid type specimens (Lepidoptera, Geometridae). *Genome* **59:** 671–684.

Hebert, P.D.N., Cywinska, A. & Ball, S.L. (2003a) Biological identifications through DNA barcodes. *Proceedings of the Royal Society of London B: Biological Sciences* **270:** 313–321.

Hebert, P.D.N., Penton, E.H., Burns, J.M., Janzen, D.H. & Hallwachs, W. (2004) Ten species in one: DNA barcoding reveals cryptic species in the neotropical skipper butterfly Astraptes fulgerator. *Proceedings of the National Academy of Sciences of the United States of America* **101:** 14812–14817.

Hebert, P.D.N., Ratnasingham, S. & de Waard, J.R. (2003b) Barcoding animal life: cytochrome c oxidase subunit 1 divergences among closely related species. *Proceedings of the Royal Society of London B: Biological Sciences* **270:** S96–S99.

Heckman, K.L., Mariani, C.L., Rasoloarison, R. & Yoder, A.D. (2007) Multiple nuclear loci reveal patterns of incomplete lineage sorting and complex species history within western mouse lemurs (*Microcebus*). *Molecular Phylogenetics and Evolution* **43:** 353–367.

Hodgetts, J., Ostojá-Starzewski, J.C., Prior, T., Lawson, R., Hall, J. & Boonham, N. (2016) DNA barcoding for biosecurity: case studies from the UK plant protection program 1. *Genome* **59:** 1033–1048.

Kieffer, J.J. (1911) Nouvelles descriptions de chironomides obtenus d'éclosion. *Bulletin de la Société d'Histoire naturelle de Metz* **27:** 1–60.

Knebelsberger, T., Landi, M., Neumann, H., Kloppmann, M., Sell, A.F., Campbell, P.D., Laakmann, S., Raupach, M.J., Carvalho, G.R. & Costa, F.O. (2014) A reliable DNA barcode reference library for the identification of the North European shelf fish fauna. *Molecular Ecology Resources* **14:** 1060–1071.

Kranzfelder, P., Anderson, A.M., Egan, A.T., Mazack, J.E., Bouchard, R.W., Rufer, M.M. & Ferrington, L.C. (2015) Use of Chironomidae (Diptera) surface-floating pupal exuviae as a rapid bioassessment protocol for water bodies. *JoVE (Journal of Visualized Experiments)***:** e52558.

Langton, P. (1994) If not "filaments" then what? *CHIRONOMUS Journal of Chironomidae Research* **6:** 9.

Lee, P.S., Gan, H.M., Clements, G.R. & Wilson, J.J. (2016) Field calibration of blowfly-derived DNA against traditional methods for assessing mammal diversity in tropical forests. *Genome* **59:** 1008–1022.

Lehmann, J. (1981) Chironomidae (Diptera) aus Fließgewässern Zentralafrikas. Teil II: Die Region um Kisangani, Zentralzaire. *Spixiana. Supplement* **5:** 1–85.

Lin, X.L., Stur, E. & Ekrem, T. (2015) Exploring genetic divergence in a species-rich insect genus using 2790 DNA Barcodes. *PloS One* **10:** e0138993.

Lindeberg, B. (1960) Taxonomy, ecology and voltinism of *Chironomus neglectus* n. sp. (Diptera) and some related species. *Annales Entomologici Fennici* **26:** 69–74.

Lindeberg, B. (1963) Taxonomy, biology and biometry of *Tanytarsus curticornis* Kieff. and *T. brundini* n. sp. (Dipt., Chironomidae). *Annales Entomologici Fennici* **29:** 118–130.

Lindeberg, B. (1967) Sibling species delimitation in the *Tanytarsus lestagei* aggregate Diptera, Chironomidae. *Annales Zoologici Fennici* **4:** 45–86.

Lindeberg, B. (1970) Tanytarsini (Diptera, Chironomidae) from northern Fennoscandia. *Annales Zoologici Fennici* **7:** 303–312.

Littlefair, J.E. & Clare, E.L. (2016) Barcoding the food chain: from Sanger to high-throughput sequencing. *Genome* **59:** 946–958.

Macher, J.N., Salis, R.K., Blakemore, K.S., Tollrian, R., Matthaei, C.D. & Leese, F. (2016) Multiple-stressor effects on stream invertebrates: DNA barcoding reveals contrasting responses of cryptic mayfly species. *Ecological Indicators* **61:** 159–169.

Meier, R., Wong, W., Srivathsan, A. & Foo, M. (2015) $1 DNA barcodes for reconstructing complex phenomes and finding rare species in specimen-rich samples. *Cladistics* **32:** 1–11.

Miller, S.E., Hausmann, A., Hallwachs, W. & Janzen, D.H. (2016) Advancing taxonomy and bioinventories with DNA barcodes. *Philosophical Transactions of the Royal Society B: Biological Sciences* **371:** 20150339.

Monaghan, M.T., Balke, M., Gregory, T.R. & Vogler, A.P. (2005) DNA-based species delineation in tropical beetles using mitochondrial and nuclear markers. *Philosophical Transactions of the Royal Society of London B: Biological Sciences* **360:** 1925–1933.

Na, K.B. & Bae, Y.J. (2010) New Species of *Stictochironomus*, *Tanytarsus* and *Conchapelopia* (Diptera: Chironomidae) from Korea. *Entomological Research Bulletin* **26:** 33–39.

Nzelu, C.O., Caceres, A.G., Arrunategui-Jimenez, M.J., Lanas-Rosas, M.F., Yanez-Trujillano, H.H., Luna-Caipo, D.V., Holguin-Mauricci, C.E., Katakura, K., Hashiguchi, Y. & Kato, H. (2015) DNA barcoding for identification of sand fly species (Diptera: Psychodidae) from leishmaniasis-endemic areas of Peru. *Acta Tropica* **145:** 45–51.

Ratnasingham, S. & Hebert, P.D.N. (2007) BOLD: The Barcode of Life Data System (www.barcodinglife.org). *Molecular Ecology Notes* **7:** 355–364.

Ratnasingham, S. & Hebert, P.D.N. (2013) A DNA-based registry for all animal species: the barcode index number (BIN) system. *PloS One* **8:** e66213.

Raunio, J., Paavola, R. & Muotka, T. (2007) Effects of emergence phenology, taxa tolerances and taxonomic resolution on the use of the chironomid pupal exuvial technique in river biomonitoring. *Freshwater Biology* **52:** 165–176.

Ree, H.I., Jeong, K.Y. & Nam, S.H. (2011) Six New and Four Unrecorded Species of Tanytarsini (Diptera, Chironomidae, Chironominae) Found in Korea. *Animal Systematics, Evolution and Diversity* **27:** 246–261.

Reiss, F. & Fittkau, E.J. (1971) Taxonomie und Ökologie europäisch verbreiteter *Tanytarsus*-Arten (Chironomidae, Diptera). *Archiv für Hydrobiologie, Supplement* **40:** 75–200.

Renaud, A.K., Savage, J. & Adamowicz, S.J. (2012) DNA barcoding of Northern Nearctic Muscidae (Diptera) reveals high correspondence between morphological and molecular species limits. *BMC Ecology* **12:** 24.

Roslin, T. & Majaneva, S. (2016) The use of DNA barcodes in food web construction—terrestrial and aquatic ecologists unite! 1. *Genome* **59:** 603–628.

Sæther, O.A. (1969) Some Nearctic Pondonominae, Diamesinae, and Orthocladiinae (Diptera: Chironomidae). *Bulletin of the Fisheries Research Board of Canada* **170:** 1–154.

Sæther, O.A. (1980) Glossary of chironomid morphology terminology (Diptera: Chironomidae). *Entomologica scandinavica, Supplements* **14:** 1–51.

Sanseverino, A.M. (2006) A review of the genus *Tanytarsus* van der Wulp, 1874 (Insecta, Diptera, Chironomidae) from the Neotropical region. *Dissertation zur Erlangung des Doktorgrades der Fakultät für Biologie der Ludwig-Maximilians-Universität, München***:** pp. 306.

Sasa, M. (1980) Studies on chironomid midges of the Tama River. Part 2. Description of 20 species of Chironominae recovered from a tributary. *Research Report from the National Institute for Environmental Studies, Japan* **13:** 9–107.

Sasa, M. (1983) Studies on chironomid midges of the Tama River. Part 5. An observation on the distribution of Chironominae along the main stream in June, with description of 15 new species. *Research Report from the National Institute for Environmental Studies, Japan* **43:** 1–67.

Sasa, M. & Ichimori, K. (1983) Studies on chironomid midges of the Tama River. Part 7. Additional species collected in winter from the main stream. *Research Report from the National Institute for Environmental Studies, Japan* **43:** 101–122.

Sasa, M. & Suzuki, H. (1999a) Studies on the Chironomid Midges of Tsushima and Iki Islands, Western Japan: Part 1. Species of Chironominae Collected on Tsushima. *Tropical Medicine* **41:** 1–53.

Sasa, M. & Suzuki, H. (1999b) Studies on the Chironomid Midges of Tsushima and Iki Islands, Western Japan: Part 3. The Chironomid Species Collected on Iki Island. *Tropical Medicine* **41:** 143–179.

Schmidt, S., Schmid-Egger, C., Morinière, J., Haszprunar, G. & Hebert, P.D. (2015) DNA barcoding largely supports 250 years of classical taxonomy: identifications for Central European bees (Hymenoptera, Apoidea *partim*). *Molecular Ecology Resources* **15:** 985–1000.

Silva, F.L. & Wiedenbrug, S. (2014) Integrating DNA barcodes and morphology for species delimitation in the *Corynoneura* group (Diptera: Chironomidae: Orthocladiinae). *B Entomol Res* **104:** 65–78.

Sinclair, C.S. & Gresens, S.E. (2008) Discrimination of *Cricotopus* species (Diptera: Chironomidae) by DNA barcoding. *B Entomol Res* **98:** 555–563.

Smith, M.A., Bertrand, C., Crosby, K., Eveleigh, E.S., Fernandez-Triana, J., Fisher, B.L., Gibbs, J., Hajibabaei, M., Hallwachs, W. & Hind, K. (2012) *Wolbachia* and DNA barcoding insects: patterns, potential, and problems. *PloS One* **7:** e36514.

Song, C., Wang, Q., Zhang, R.L., Sun, B.J. & Wang, X.H. (2016) Exploring the utility of DNA barcoding in species delimitation of *Polypedilum* (*Tripodura*) non-biting midges (Diptera: Chironomidae). *Zootaxa* **4079:** 534–550.

Storå, R. (1939) Mitteilungen über die Nematoceren Finnlands II. *Notulae entomologicae* **19:** 16–30.

Stur, E. & Ekrem, T. (2015) A review of Norwegian *Gymnometriocnemus* (Diptera, Chironomidae) including the description of two new species and a new name for *Gymnometriocnemus volitans* (Goetghebuer) sensu Brundin. *ZooKeys* **508:** 127–142.

Tamura, K., Stecher, G., Peterson, D., Filipski, A. & Kumar, S. (2013) MEGA6: molecular evolutionary genetics analysis version 6.0. *Molecular Biology and Evolution* **30:** 2725–2729.

Webb, J.M., Jacobus, L.M., Funk, D.H., Zhou, X., Kondratieff, B., Geraci, C.J., DeWalt, R.E., Baird, D.J., Richard, B., Phillips, I. & Hebert, P.D. (2012) A DNA barcode library for North American Ephemeroptera: progress and prospects. *PloS One* **7:** e38063.

Whitworth, T., Dawson, R., Magalon, H. & Baudry, E. (2007) DNA barcoding cannot reliably identify species of the blowfly genus *Protocalliphora* (Diptera: Calliphoridae). *Proceedings of the Royal Society of London B: Biological Sciences* **274:** 1731–1739.

Willyard, A., Cronn, R. & Liston, A. (2009) Reticulate evolution and incomplete lineage sorting among the ponderosa pines. *Molecular Phylogenetics and Evolution* **52:** 498–511.

Witt, J.D., Threloff, D.L. & Hebert, P.D. (2006) DNA barcoding reveals extraordinary cryptic diversity in an amphipod genus: implications for desert spring conservation. *Molecular Ecology* **15:** 3073–3082.

Wulp, F.M. (1874) Dipterologische aanteekeningen. *Tijdschrift voor Entomologie* **17:** 109–148.

Yang, Z.F., Landry, J.F., Handfield, L., Zhang, Y.L., Alma Solis, M., Handfield, D., Scholtens, B.G., Mutanen, M., Nuss, M. & Hebert, P.D.N. (2012) DNA barcoding and morphology reveal three cryptic species of *Anania* (Lepidoptera: Crambidae: Pyraustinae) in North America, all distinct from their European counterpart. *Systematic Entomology* **37:** 686–705.

Zahiri, R., Lafontaine, J.D., Schmidt, B.C., Dewaard, J.R., Zakharov, E.V. & Hebert, P.D. (2014) A transcontinental challenge–a test of DNA barcode performance for 1,541 species of Canadian Noctuoidea (Lepidoptera). *PloS One* **9:** e92797.

Zhou, X., Frandsen, P.B., Holzenthal, R.W., Beet, C.R., Bennett, K.R., Blahnik, R.J., Bonada, N., Cartwright, D., Chuluunbat, S. & Cocks, G.V. (2016) The Trichoptera barcode initiative: a strategy for generating a species-level Tree of Life. *Philosophical Transactions of the Royal Society B: Biological Sciences* **371:** 20160025.

Zhou, X., Jacobus, L.M., DeWalt, R.E., Adamowicz, S.J. & Hebert, P.D.N. (2010) Ephemeroptera, Plecoptera, and Trichoptera fauna of Churchill (Manitoba, Canada): insights into biodiversity patterns from DNA barcoding. *Journal of the North American Benthological Society* **29:** 814–837.

Figure captions

Figure 1. Neighbor joining tree for nine morphospecies of the *Tanytarsus curticornis* species complex based on K2P distances in DNA barcodes. Numbers on branches represent bootstrap support (>70%) based on 1000 replicates; scale equals K2P genetic distance; figures show the full body or thorax of adult males of each corresponding morphospecies.

Figure 2. Neighbor joining tree for five species of the *Tanytarsus heusdensis* species complex based on K2P distances in DNA barcodes. Numbers on branches represent bootstrap support (>70%) based on 1000 replicates; scale equals K2P genetic distance; figures show the full body or thorax of adult males of each corresponding morphospecies.

Figure 3. *Tanytarsus brundini*, male: A) head; B) thorax; C) wing. Scale bar = 200 µm.

Figure 4. *Tanytarsus brundini*, male: A) hypopygium dorsal view (Chiny, Belgium); B) hypopygium ventral view (Chiny, Belgium); C) hypopygium dorsal view (Portugal); D) hypopygium ventral view (Portugal). Scale bar = 50 µm.

Figure 5. *Tanytarsus curticornis*, male: A) thorax, scale bar = 100 µm; B) wing, scale bar = 100 µm; C) hypopygium (Trondheim, Norway); D). partial anal tergite showing one median seta present (Aust-Agder, Norway).

Figure 6. *Tanytarsus heberti* sp. n., holotype male: A) head; B) thorax; C) wing. Scale bar = 100 µm.

Figure 7. *Tanytarsus heberti* sp. n., holotype male: A) hypopygium dorsal view; B) hypopygium ventral view. Scale bar = 50 µm.

Figure 8. *Tanytarsus heberti* sp. n., paratype female: A) head; B) wing; C) genitalia. Scale bar = 100 µm.

Figure 9. *Tanytarsus ikicedeus*, holotype male: A) microscope slide; B) wing, scale bar = 50 µm; C) hypopygium, scale bar = 50 µm.

Figure 10. *Tanytarsus madeiraensis* sp. n., A) holotype male head; B) paratype male thorax; C) holotype male wing. Scale bar = 100 µm.

Figure 11. *Tanytarsus madeiraensis* sp. n., male: A) hypopygium dorsal view; B) hypopygium ventral view showing median volsella and digitus. Scale bar = 50 µm.

Figure 12. *Tanytarsus madeiraensis* sp. n., paratype larval head capsule, scale bar = 100 µm.

Figure 13. *Tanytarsus madeiraensis* sp. n., holotype pupal exuviae: A) cephalothorax; B) thoracic horn; C) abdomen; D) segment VIII showing posterolateral comb. Scale bar = 100 µm.

Figure 14. *Tanytarsus neotamaoctavus*, paratype male: A) wing; B) thorax; C) hypopygium. Scale bar = 100 µm.

Figure 15. *Tanytarsus songi* sp. n., holotype male: A) head; B) thorax; C) wing. Scale bar = 100 µm.

Figure 16. *Tanytarsus songi* sp. n., holotype male: A) hypopygium dorsal view, scale bar = 50 µm; B) hypopygium ventral view, scale bar = 50 µm; C) superior volsella with digitus.

Figure 17. *Tanytarsus tamaoctavus*, male from China: A) hermaphrodite female antenna; B) thorax; C) wing. Scale bar = 100 µm.

Figure 18. *Tanytarsus tamaoctavus*, male from Guangdong, China: A) hypopygium dorsal view; B) hypopygium ventral view showing median volsella and digitus-seta. Scale bar = 50 µm.

Figure 19. *Tanytarsus thomasi* sp. n., male: A) holotype head, scale bar = 100 µm; B) holotype partial head shwoing frontal tubercles, scale bar = 20 µm; C) paratype thorax, scale bar = 100 µm; D) paratype wing showing four unusual setae presenting in the cell r, scale bar = 100 µm.

Figure 20. *Tanytarsus thomasi* sp. n., male: A) holotype hypopygium dorsal view; B) holotype hypopygium ventral view; C) paratype hypopygium dorsal view; D) paratype hypopygium ventral view. Scale bar = 50 µm.

Figure 21. *Tanytarsus tongmuensis* sp. n., holotype male: A) head; B) thorax; C) wing. Scale bar = 100 µm.

Figure 22. *Tanytarsus tongmuensis* sp. n., holotype male: A) hypopygium dorsal view; B) hypopygium ventral view. Scale bar = 50 µm.

Figure 23. *Tanytarsus tongmuensis* sp. n., paratype female: A) head; B) antenna; C) wing; D) genitalia. Scale bar = 100 µm.

Figure 24. *Tanytarsus wangi* sp. n., male: A) paratype head; B) holotype antenna; C) paratype thorax; D) paratype wing. Scale bar = 100 µm.

Figure 25. *Tanytarsus wangi* sp. n., male: A) holotype hypopygium dorsal view; B) holotype hypopygium ventral view. Scale bar = 50 µm.

Figure 26. *Tanytarsus adustus* sp. n., male: A) holotype head; B) paratype thorax; C) paratype wing; D) paratype tarsomere 1 of mid leg showing the absence of sensilla chaetica. Scale bar = 100 µm.

Figure 27. *Tanytarsus adustus* sp. n., holotype male: A) hypopygium dorsal view; B) hypopygium ventral view. Scale bar = 50 µm.

Figure 28. *Tanytarsus adustus* sp. n., paratype female: A) head; B) antenna; C) thorax; D) wing; E) genitalia. Scale bar = 200 µm.

Figure 29. *Tanytarsus heusdensis*. A) holotype microscope slide; B) male thorax of Norwegian specimen; C) holotype male wing; D) holotype male hypopygium. Scale bar = 100 µm.

Figure 30. *Tanytarsus pseudoheusdensis* sp. n., holotype male: A) antenna and head; B) thorax; C) wing. Scale bar = 200 µm.

Figure 31. *Tanytarsus pseudoheusdensis* sp. n., holotype male: A) hypopygium dorsal view; B) hypopygium ventral view. Scale bar = 50 µm.

Figure 32. *Tanytarsus reei*, male: A) head; B) thorax; C) wing. Scale bar = 200 µm.

Figure 33. *Tanytarsus reei*, male: A) hypopygium dorsal view; B) hypopygium ventral view. Scale bar = 100 µm.

Figure 34. *Tanytarsus tamaduodecimus*, male: A) thorax of Chinese specimen, scale bar = 100 µm; B) holotype wing, dry mounted, scale bar = 200 µm; C) wing of *Tanytarsus tusimatneous* syn. n., holotype, dry mounted, scale bar = 200 µm; D) hind spur of Chinese specimen, scale bar = 50 µm; E) hind spur of *Tanytarsus tusimatneous* syn. n., holotype, scale bar = 50 µm.

Figure 35. *Tanytarsus tamaduodecimus*, male: A) holotype hypopygium; B) hypopygium of *Tanytarsus tusimatneous* syn. n.; C) dorsal view of hypopygium of Chinese specimen; D) ventral view of hypopygium of Chinese specimen. Scale bar = 50 µm.

Figure 1

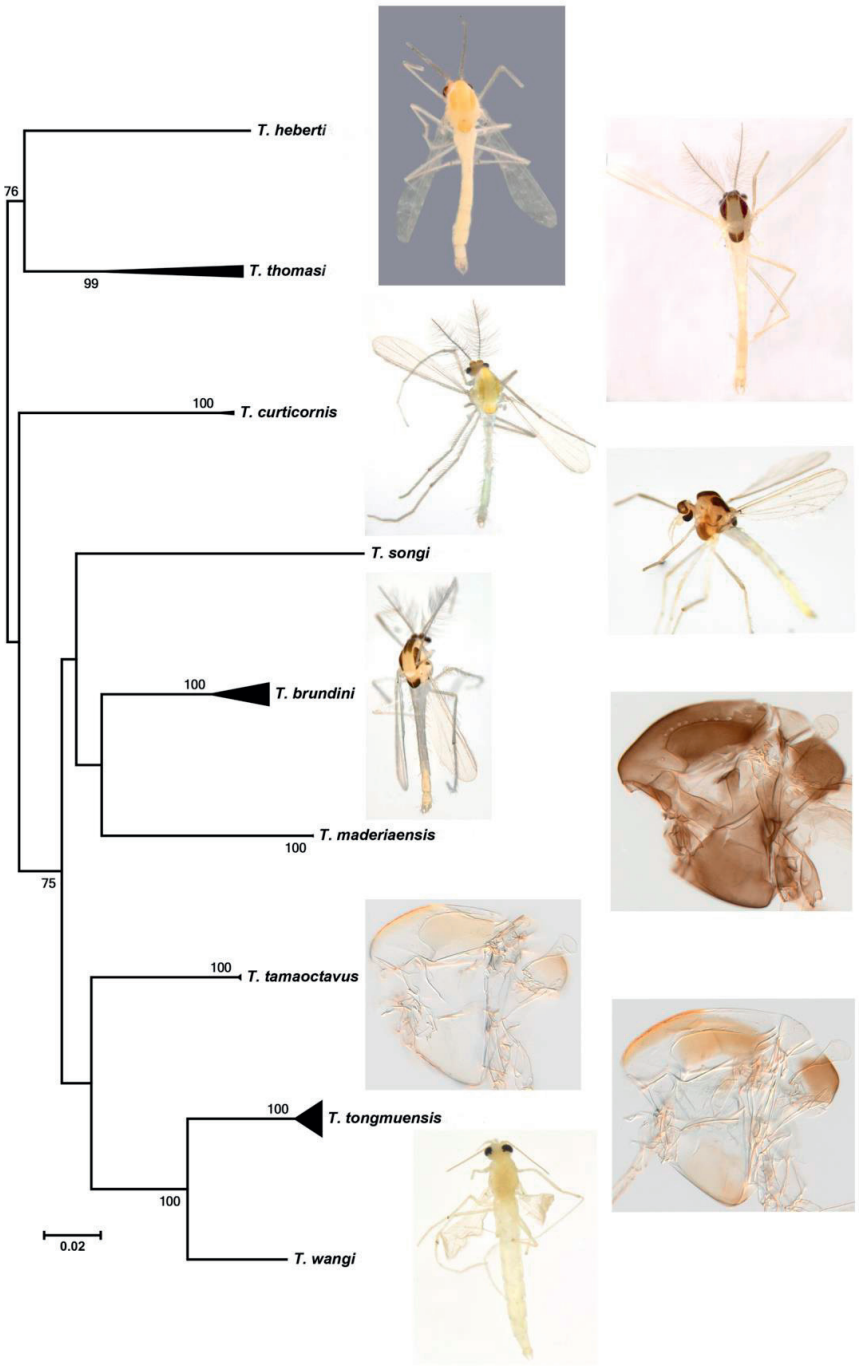
T. heberti
T. thomasi
T. curticornis
T. songi
T. brundini
T. maderiaensis
T. tamaoctavus
T. tongmuensis
T. wangi
76
99
100
100
100
75
100
100
100
0.02

Figure 2

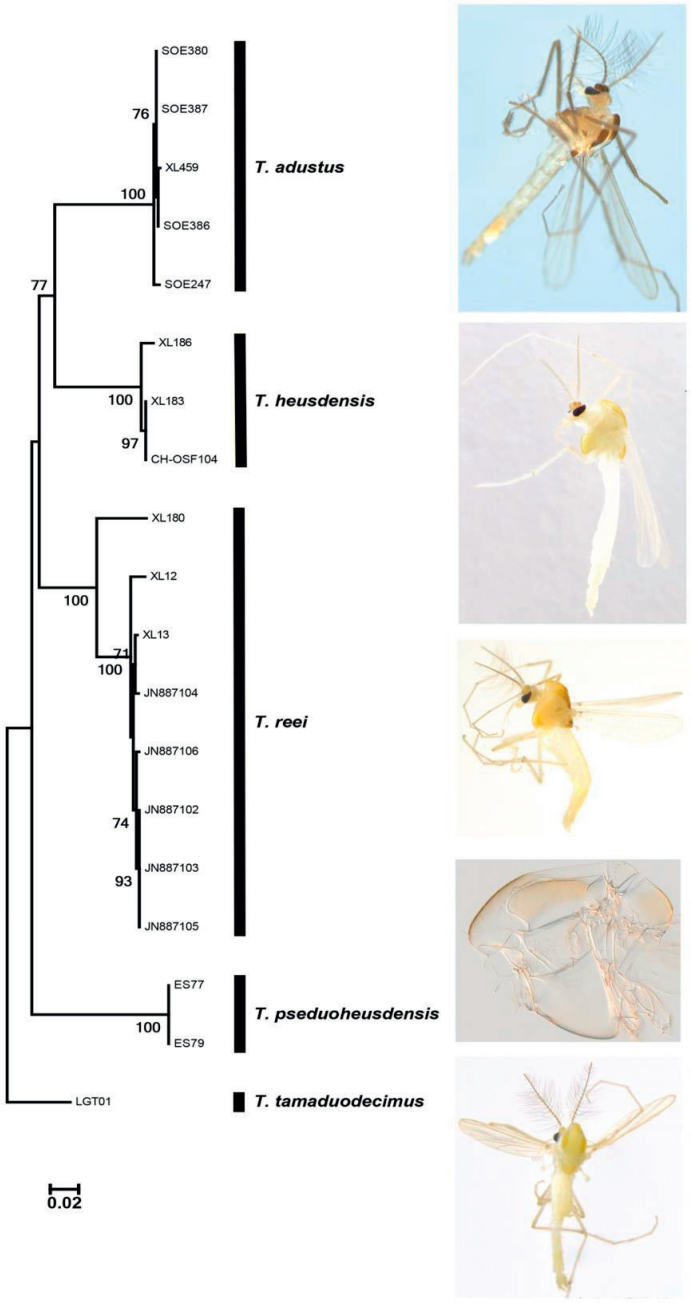
SOE380
SOE387
XL459
SOE386
SOE247
76
100
77
T. adustus
XL186
XL183
CH-OSF104
100
97
T. heusdensis
XL180
XL12
XL13
JN887104
JN887106
JN887102
JN887103
JN887105
100
71
100
74
93
T. reei
ES77
ES79
100
T. pseduoheusdensis
LGT01
T. tamaduodecimus
0.02

Figure 3

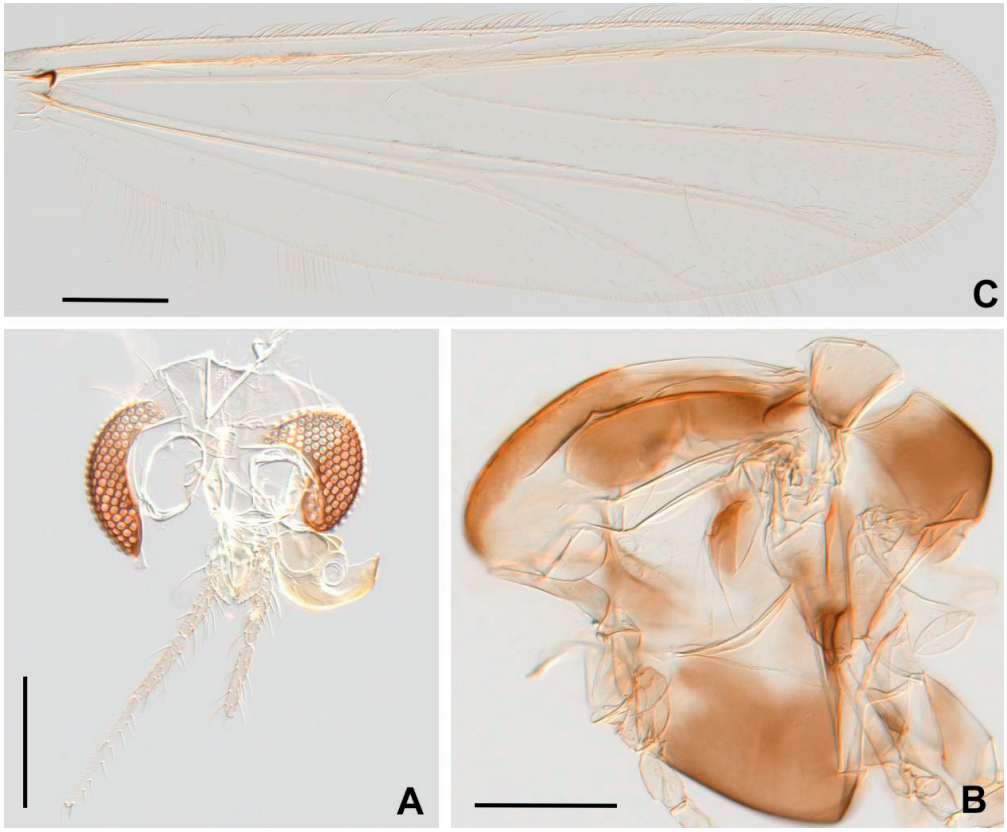

Figure 4

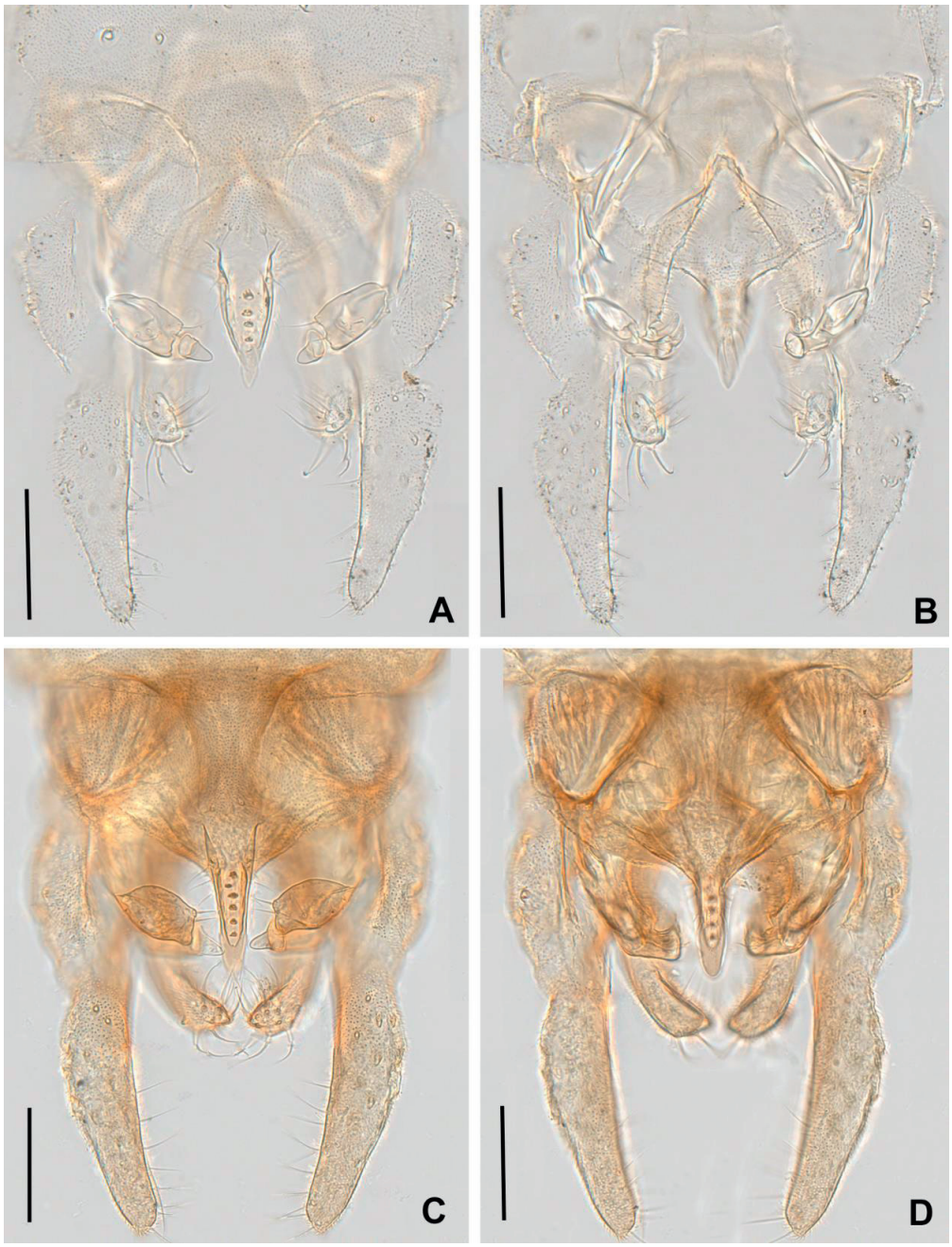

Figure 5

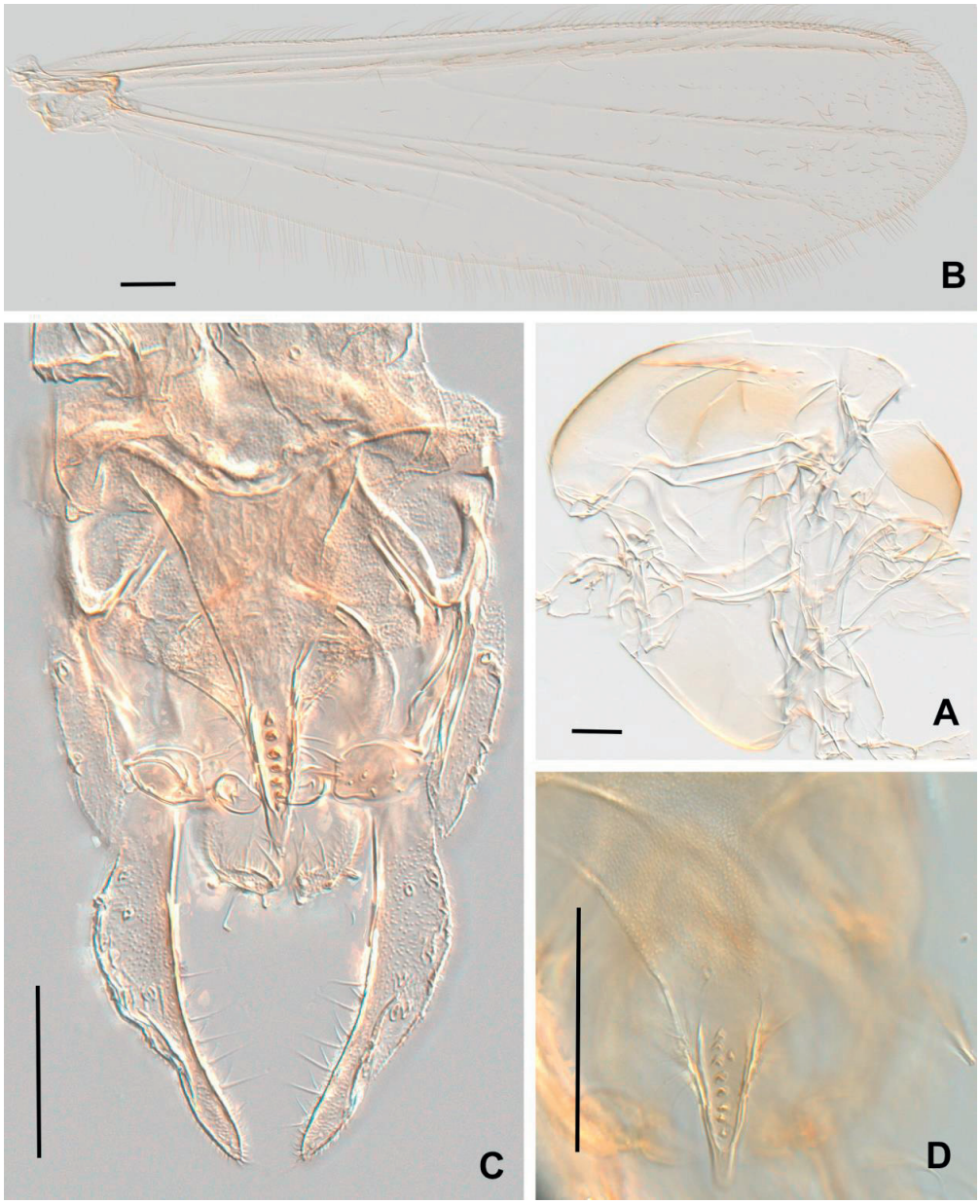

Figure 6

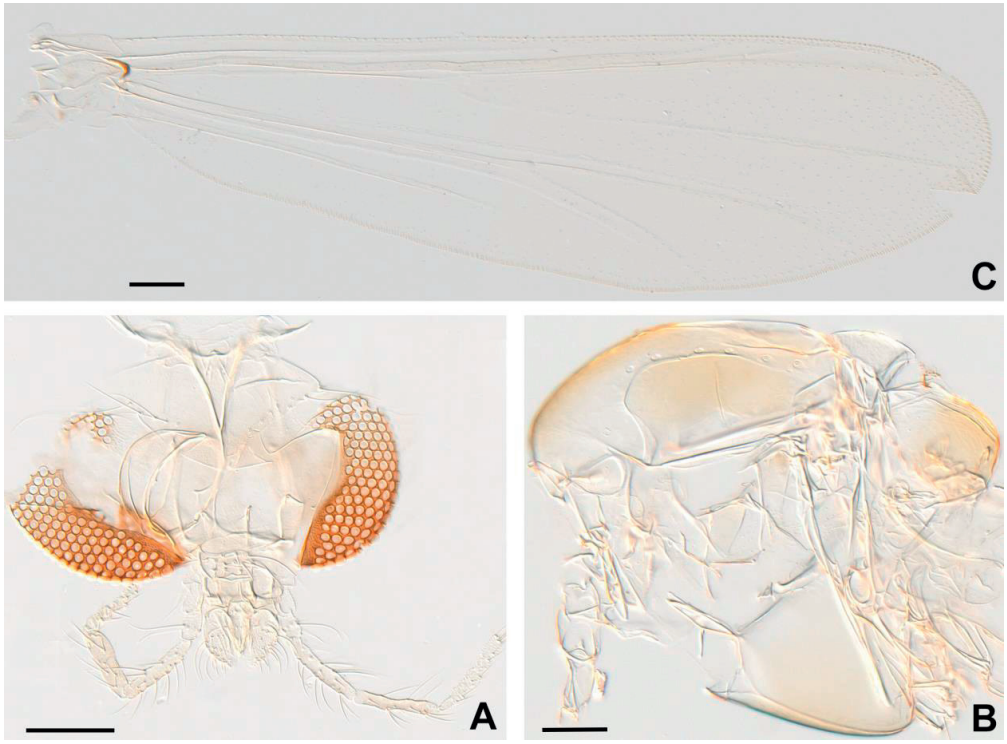

Figure 7

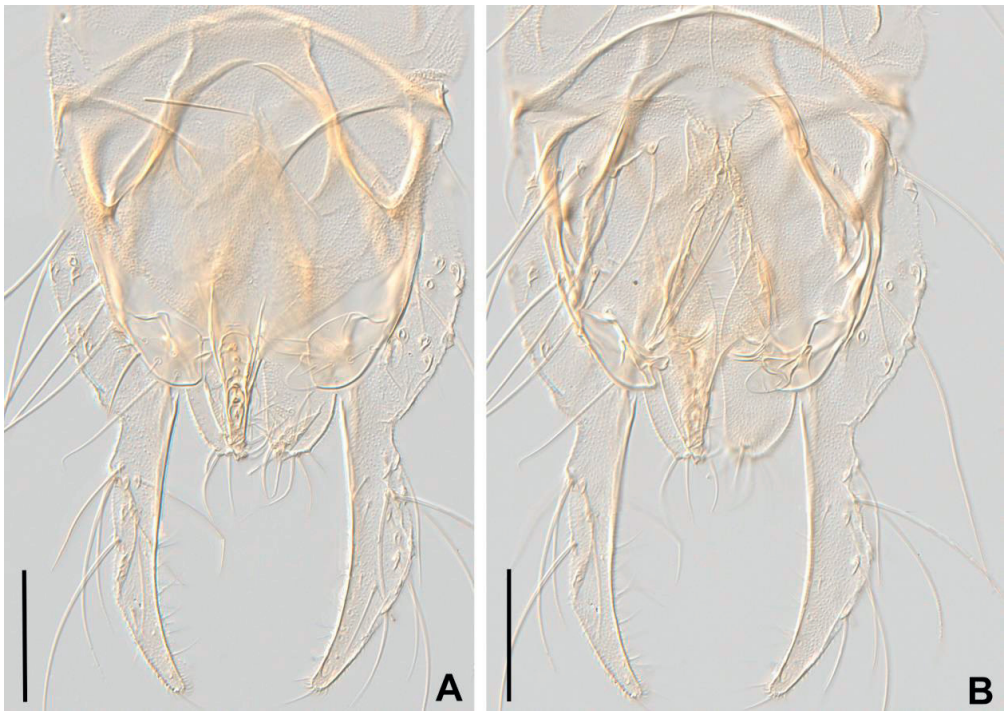

Figure 8

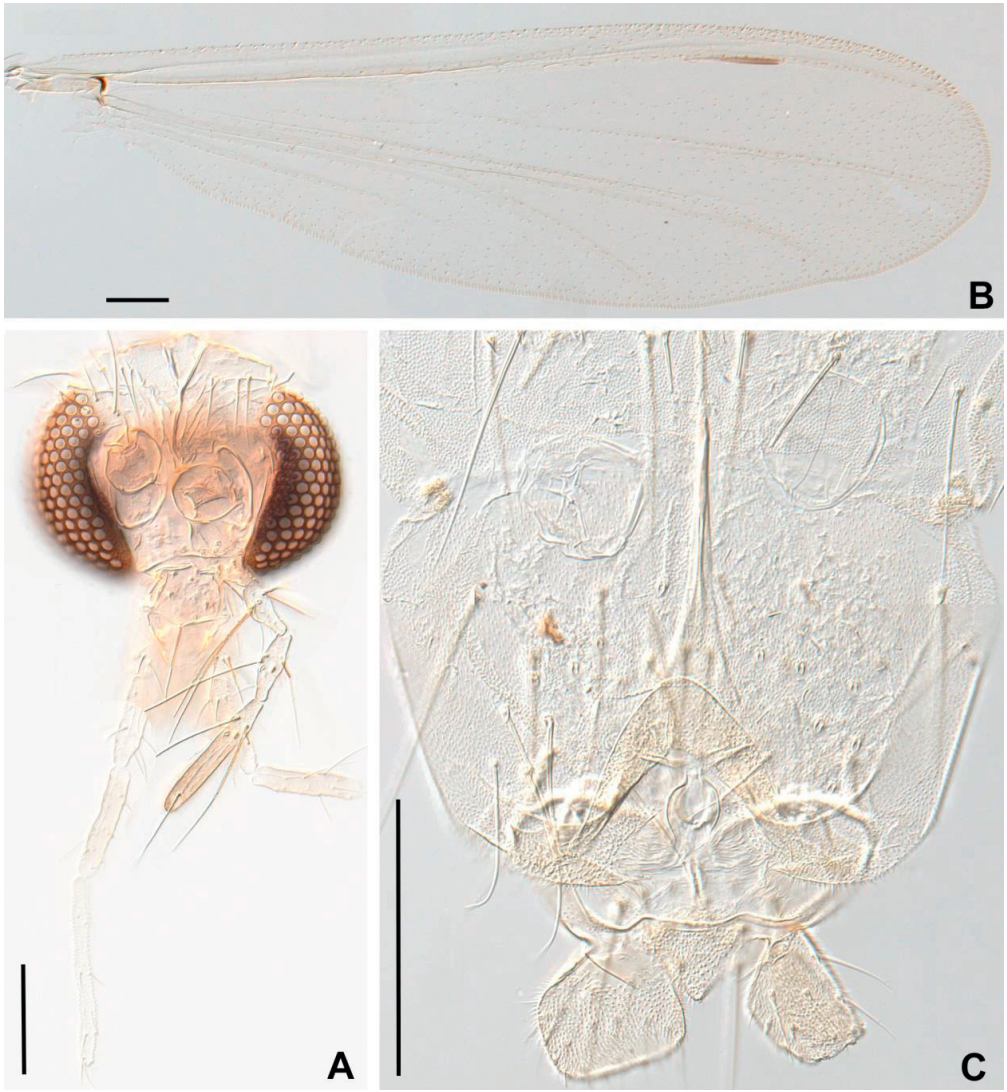

Figure 9

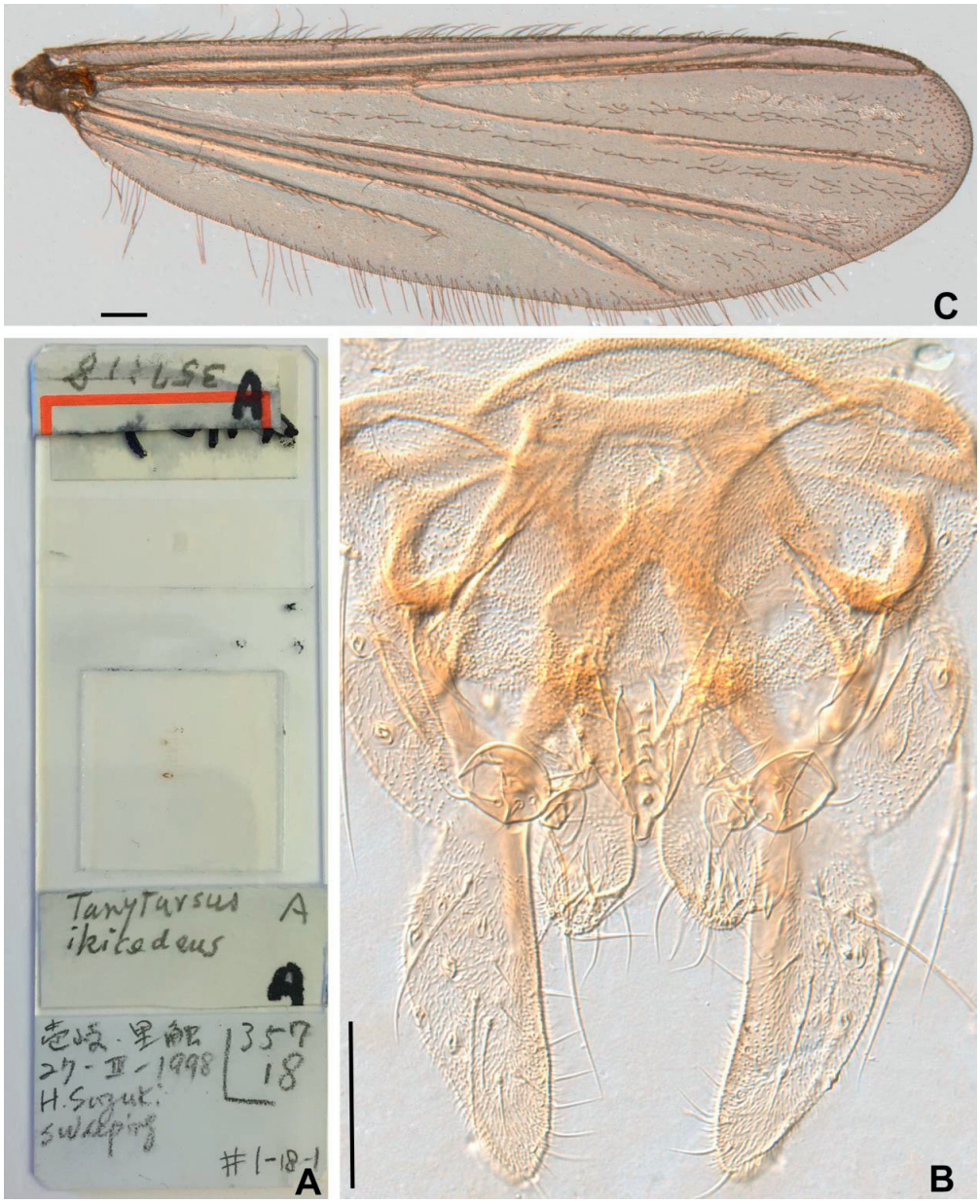

Figure 10

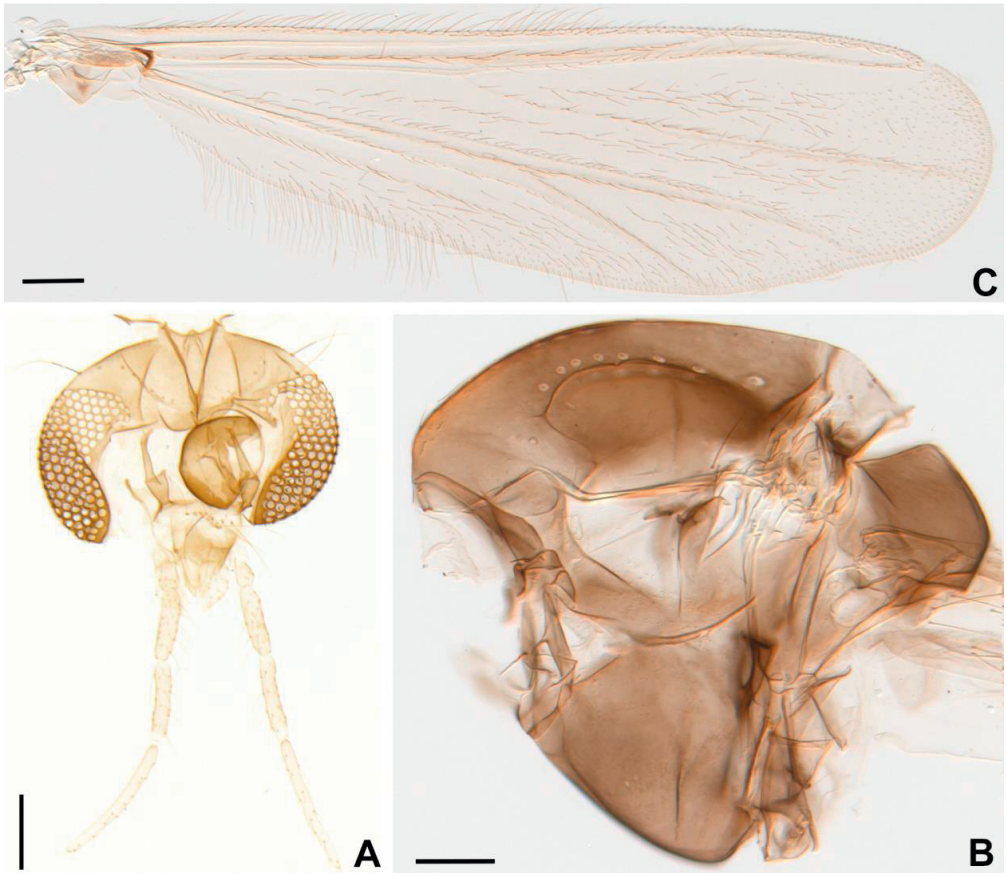

Figure 11

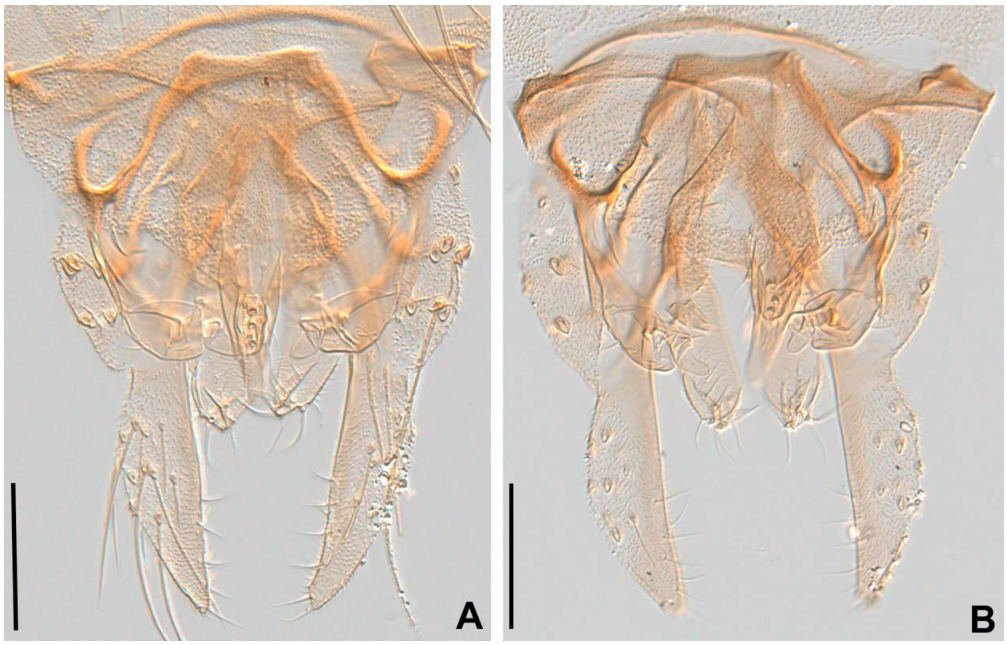

Figure 12

Figure 13

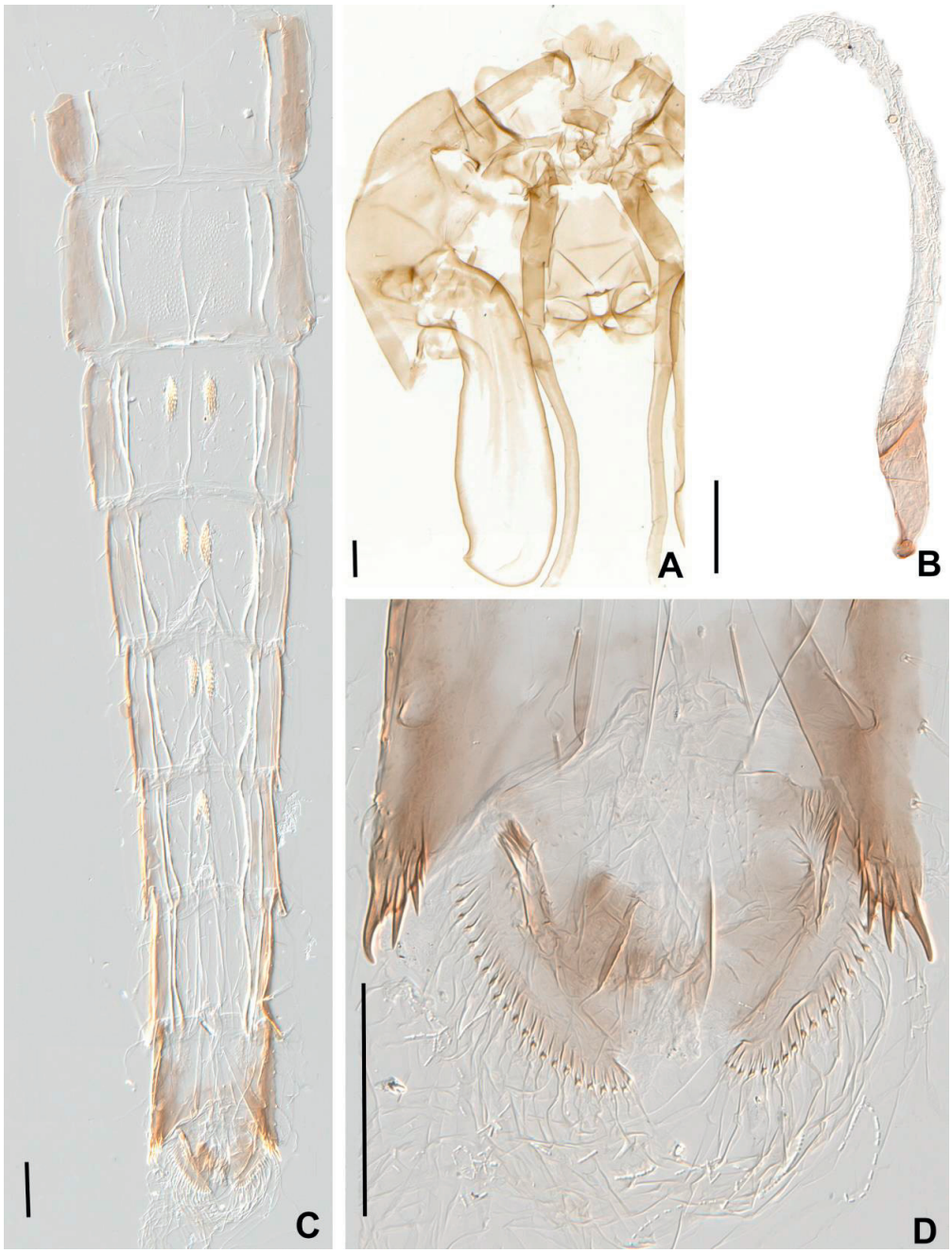

Figure 14

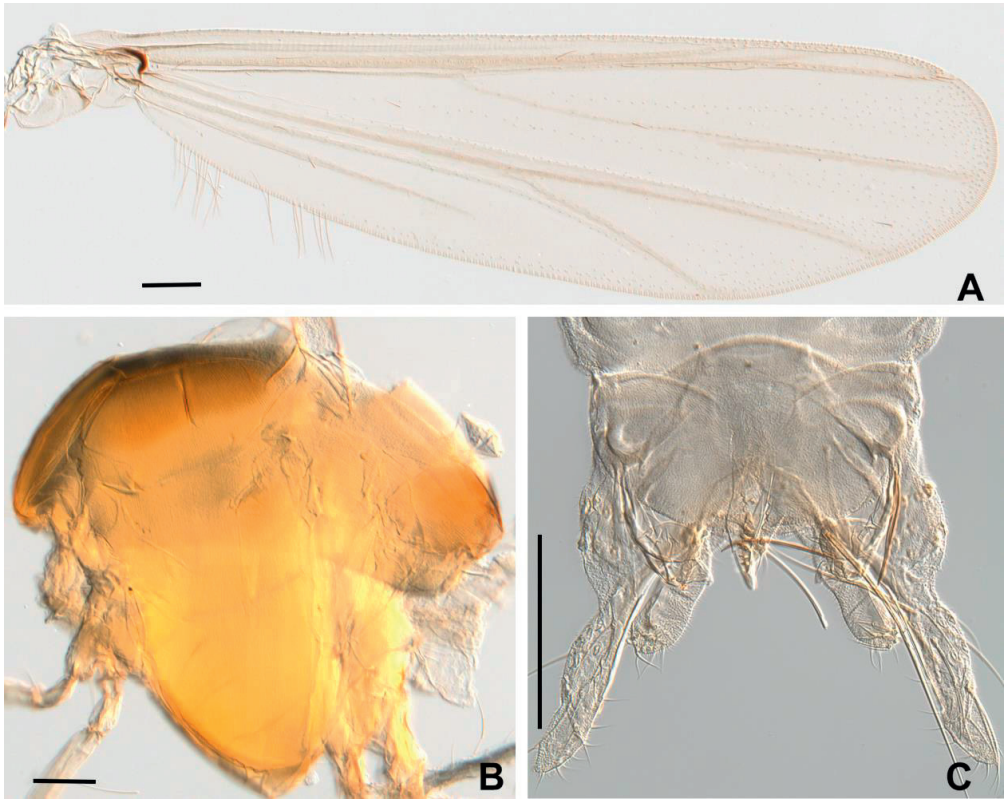

Figure 15

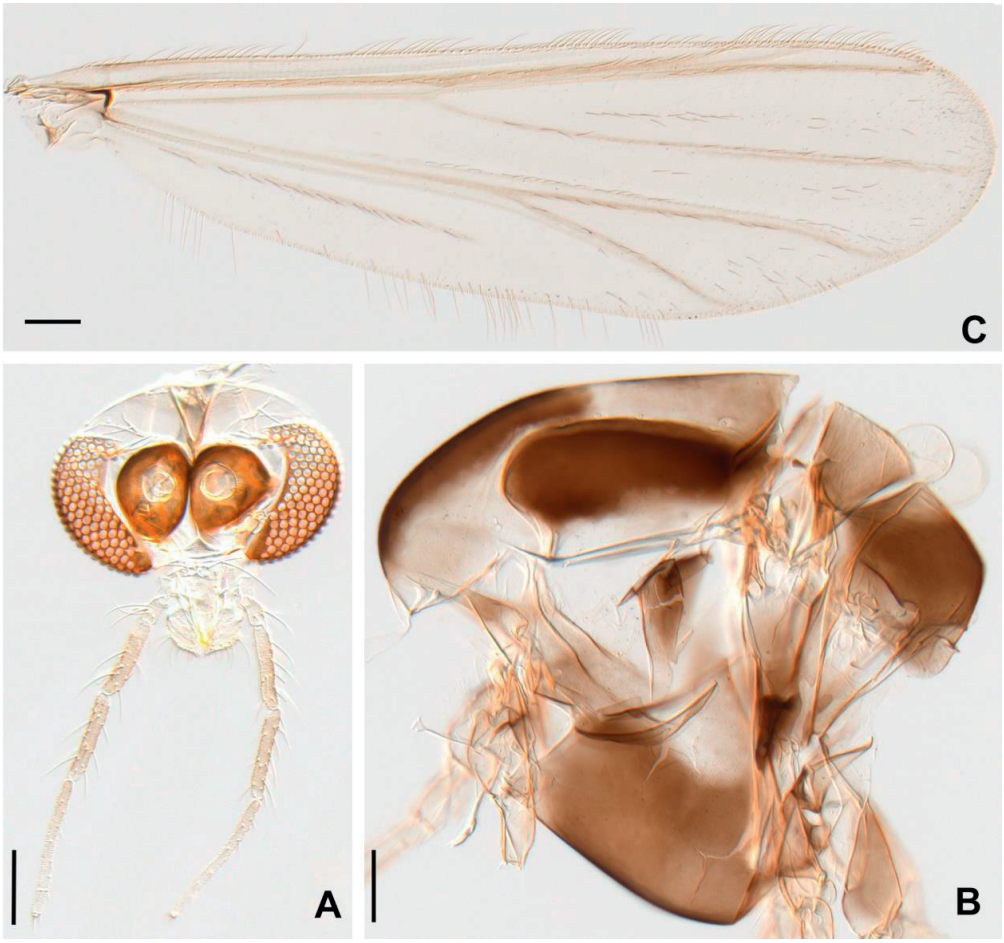

Figure 16

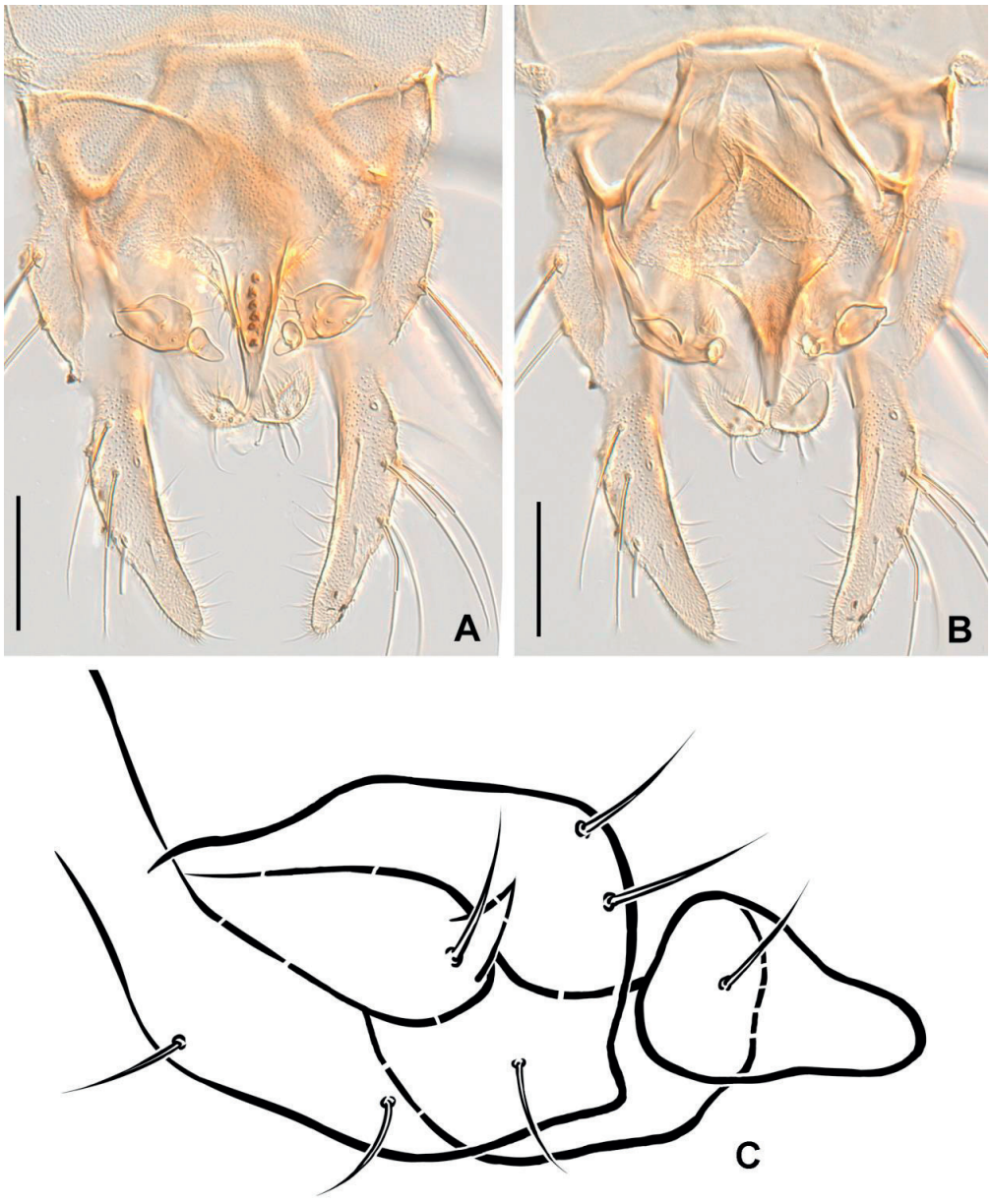

Figure 17

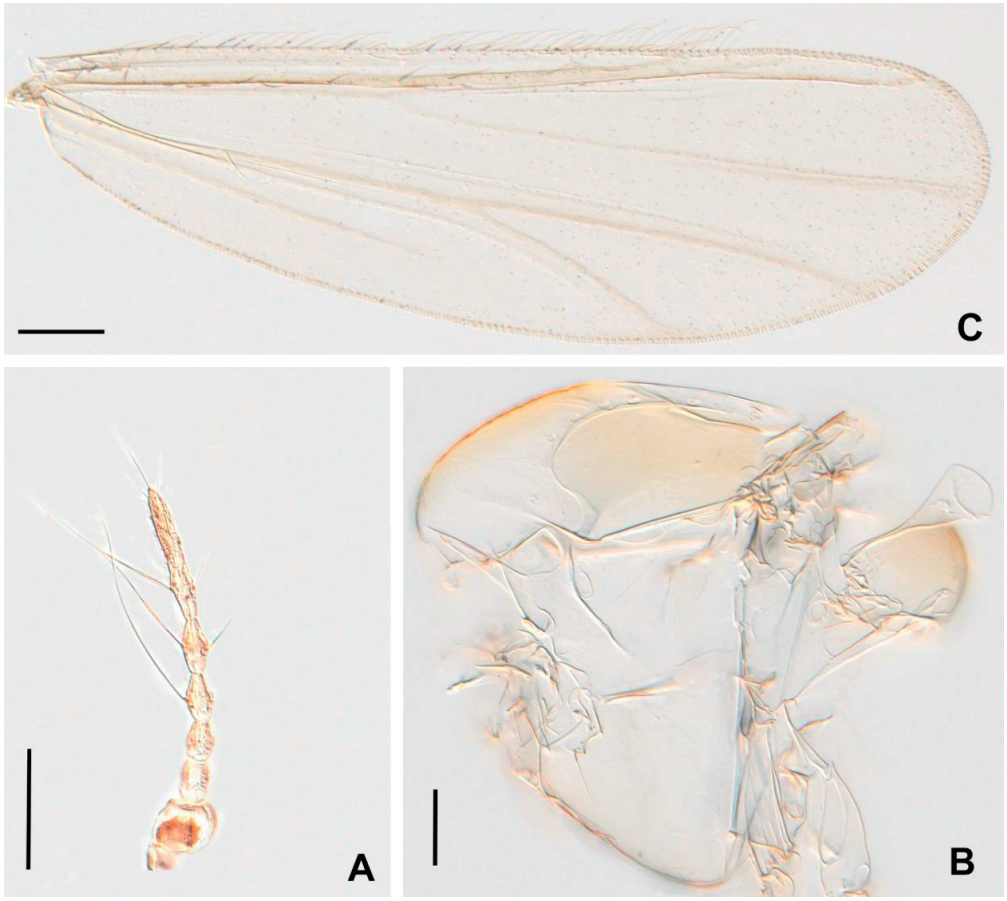

Figure 18

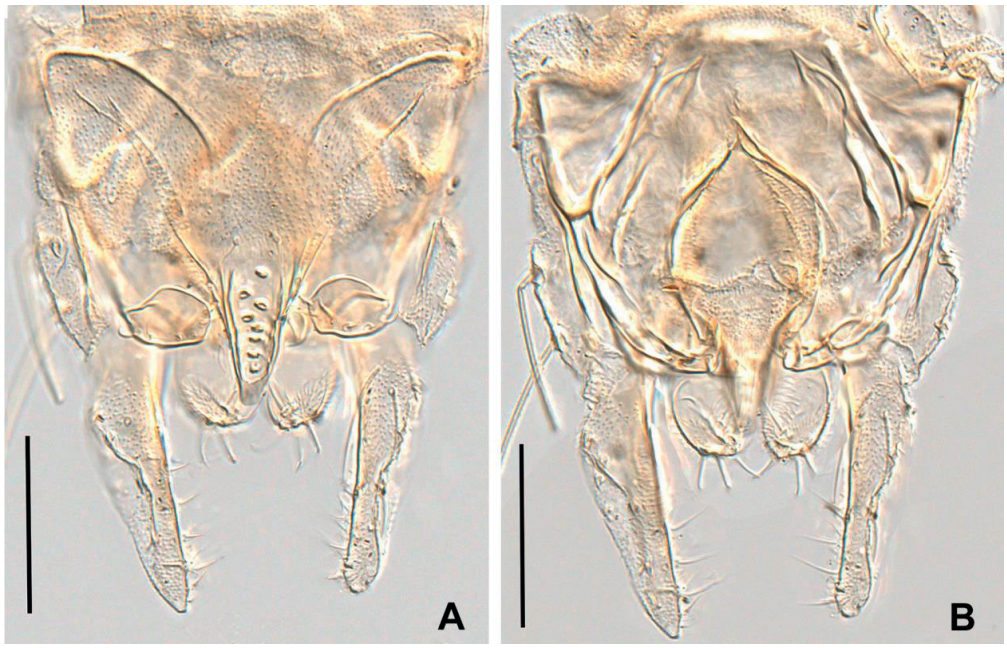

Figure 19

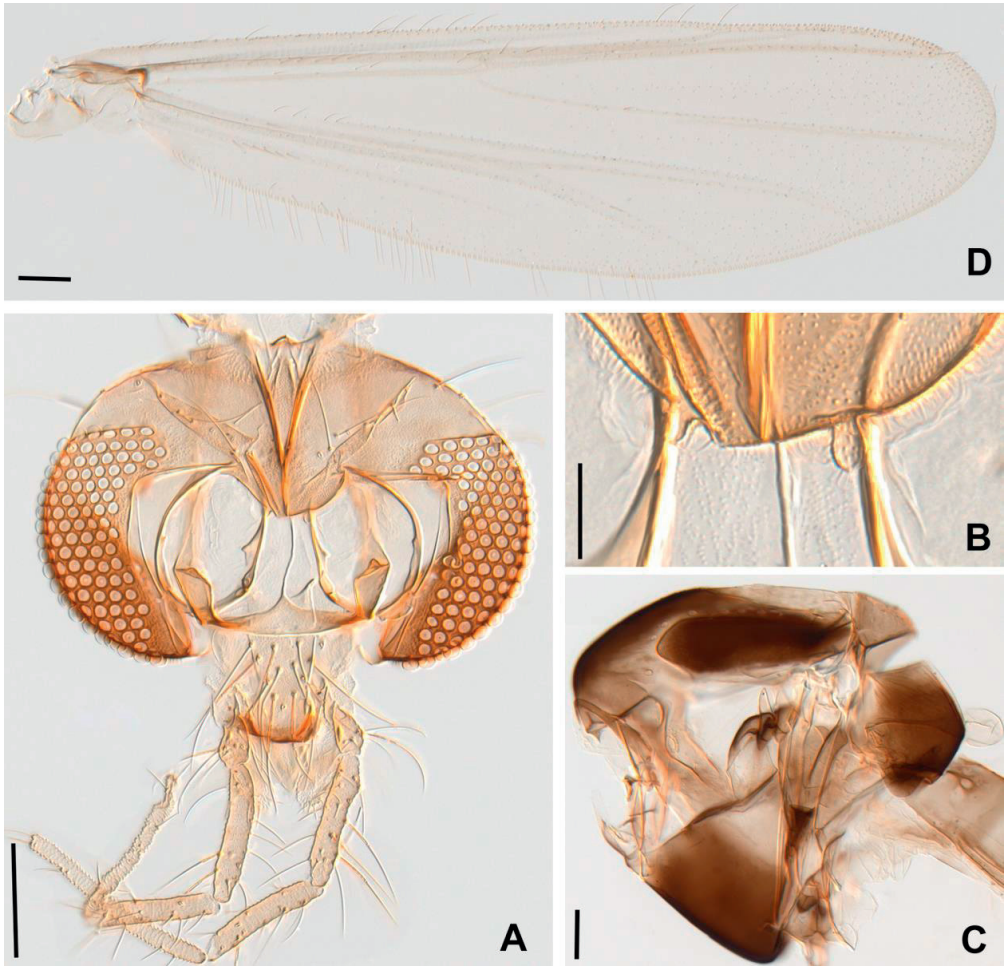

Figure 20

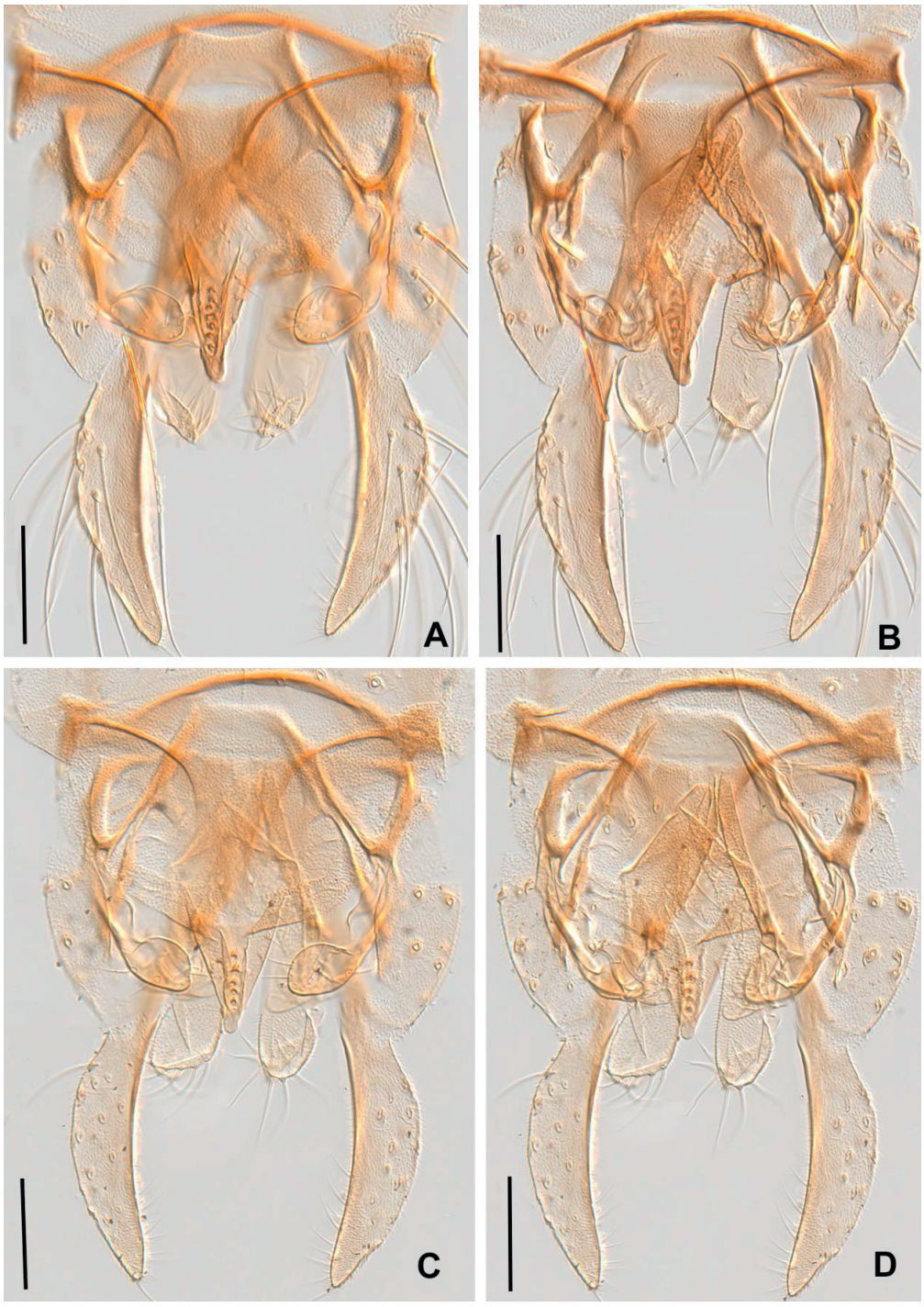

Figure 21

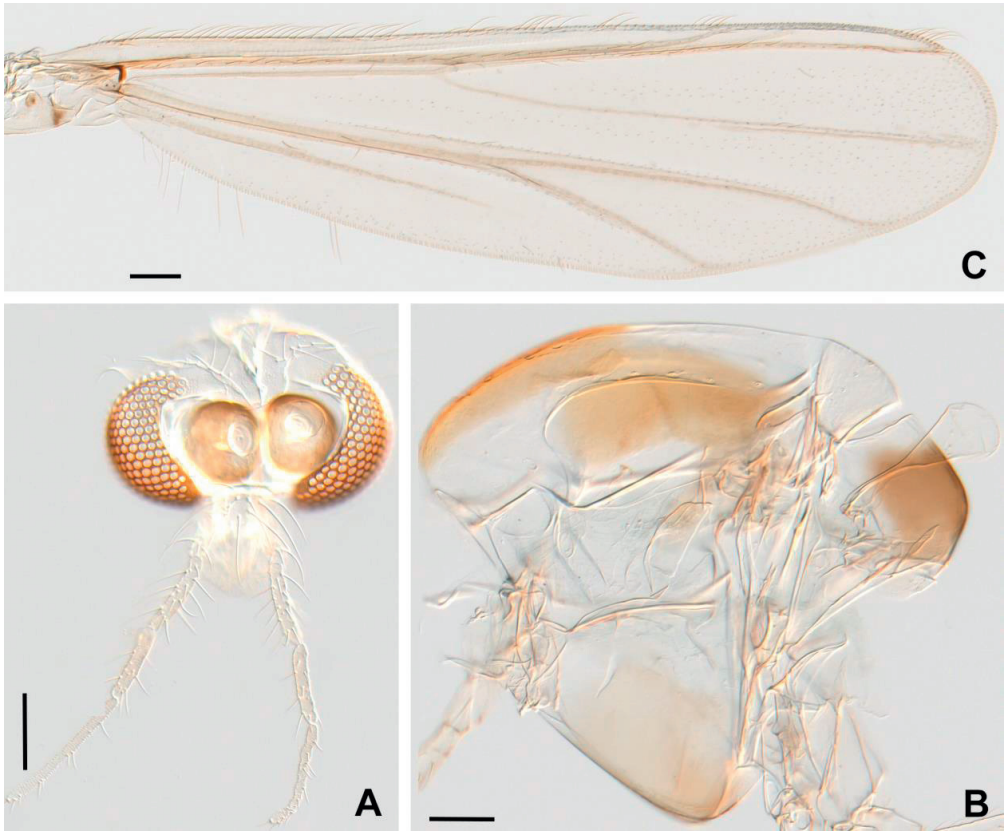

Figure 22

Figure 23

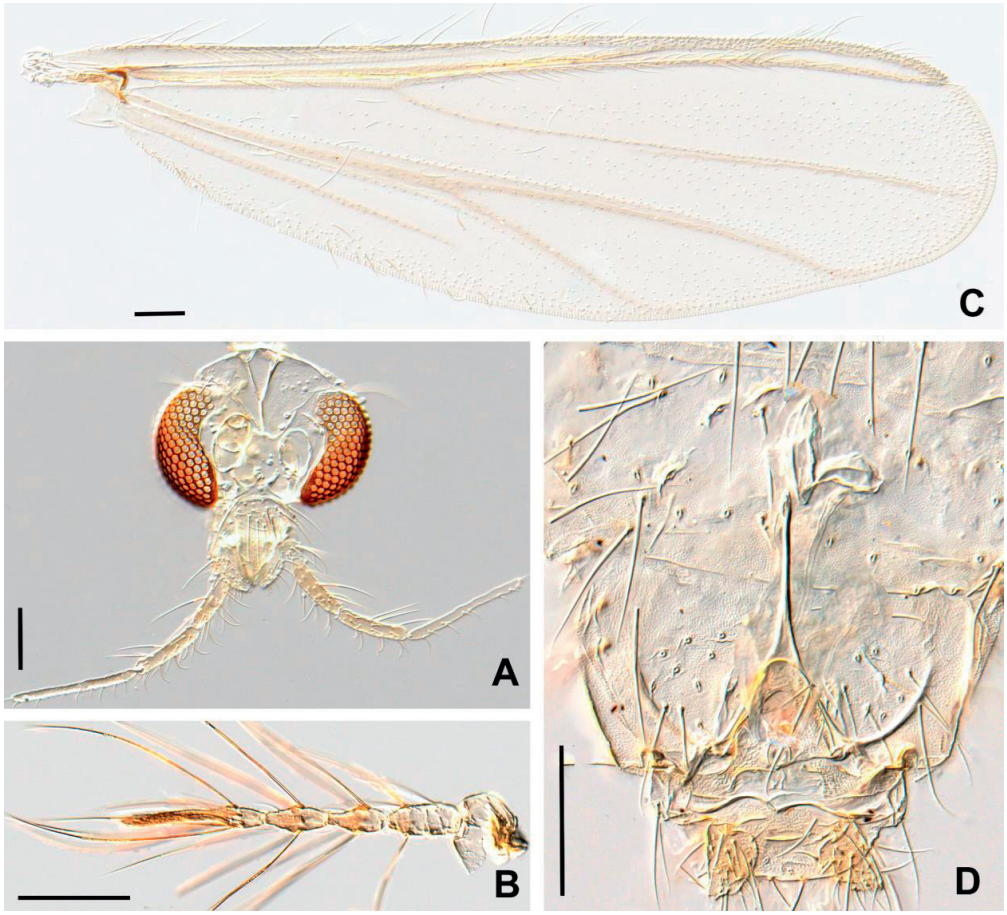

Figure 24

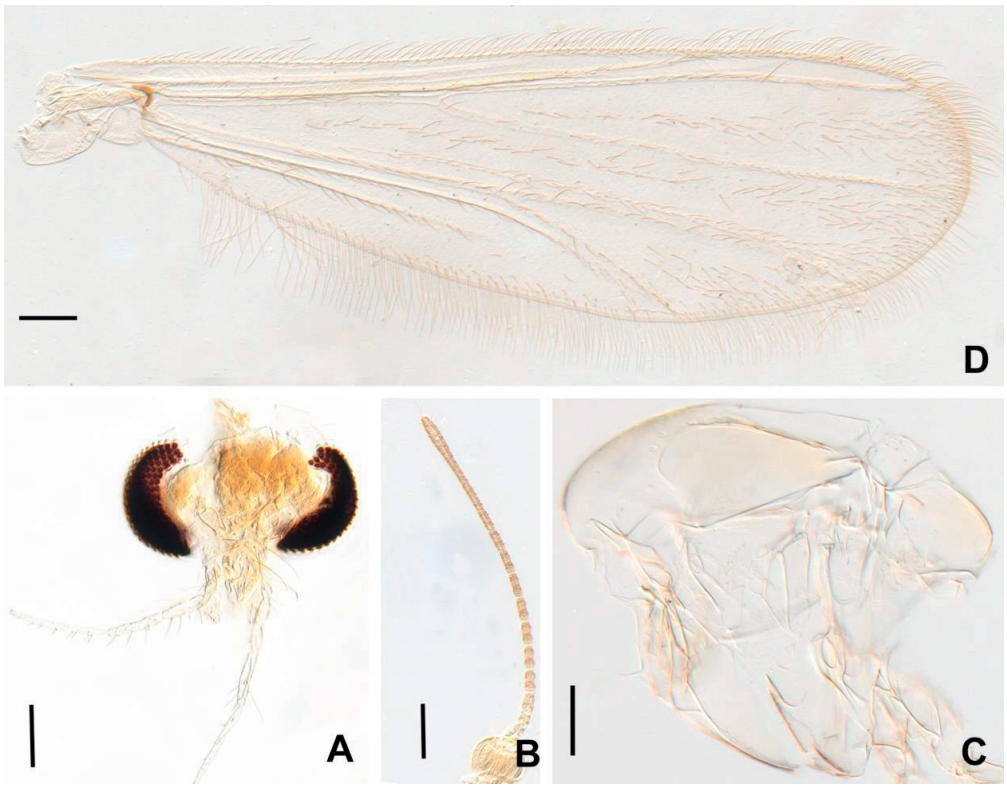

Figure 25

Figure 26

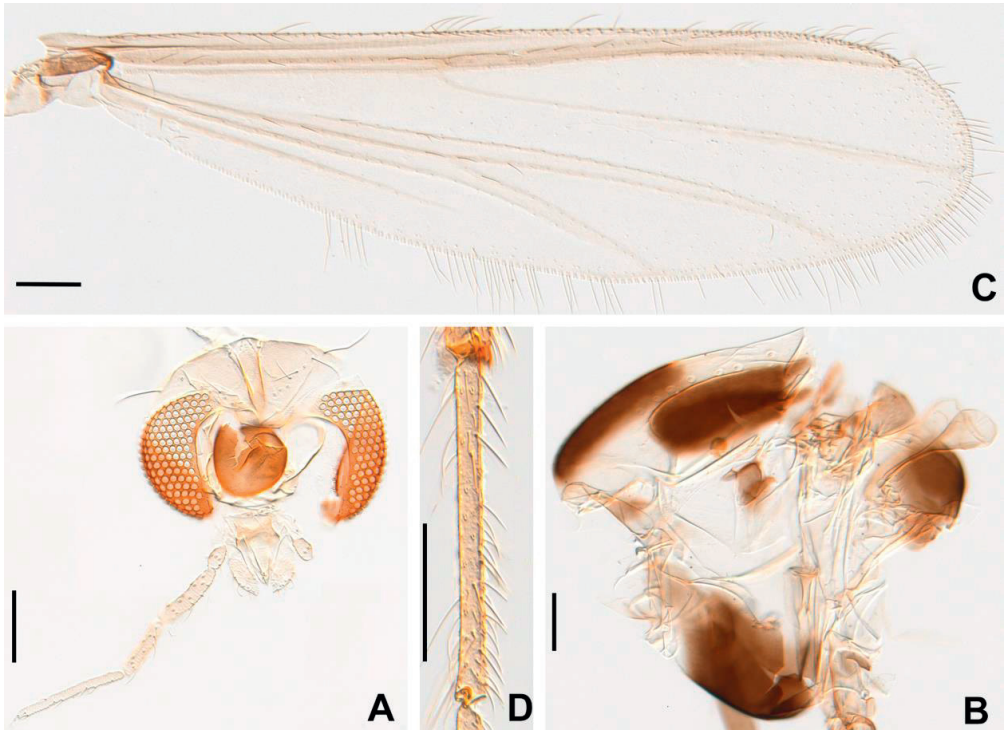

Figure 27

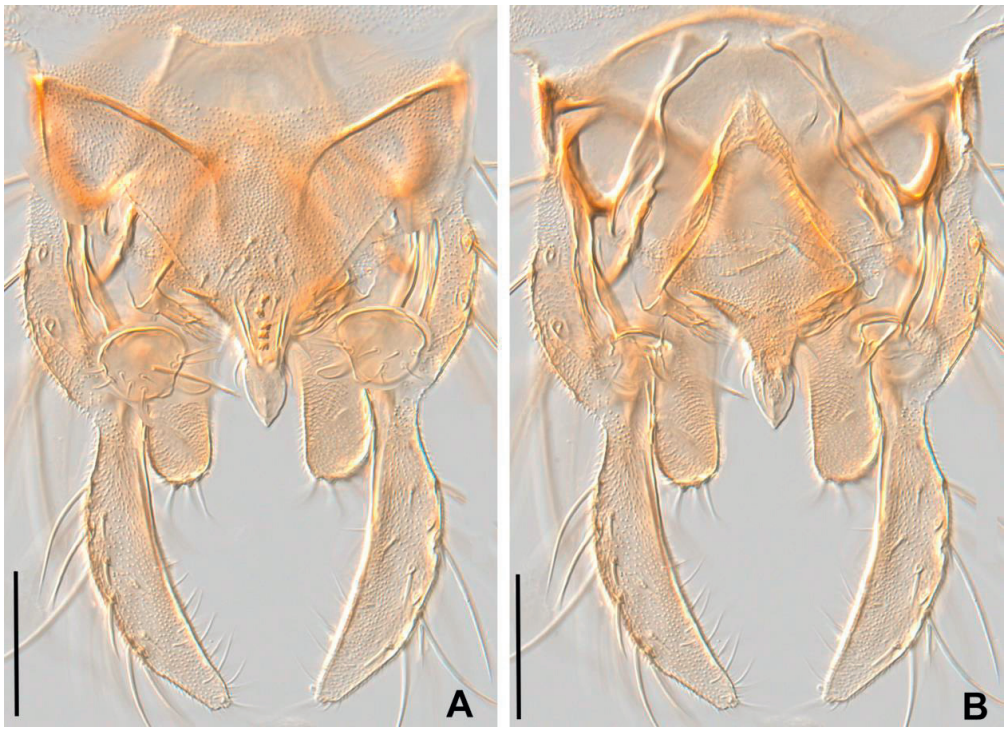

Figure 28

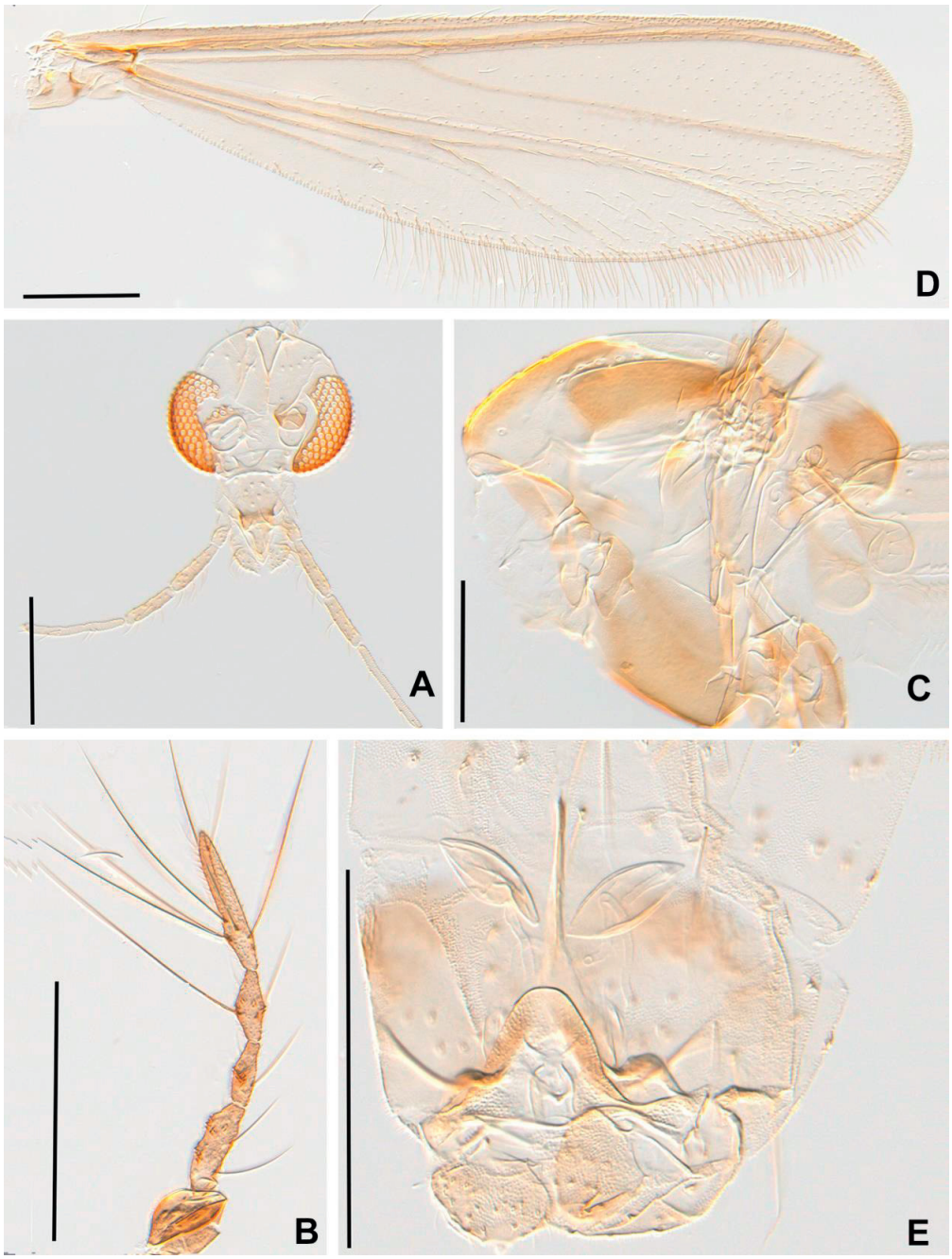

Figure 29

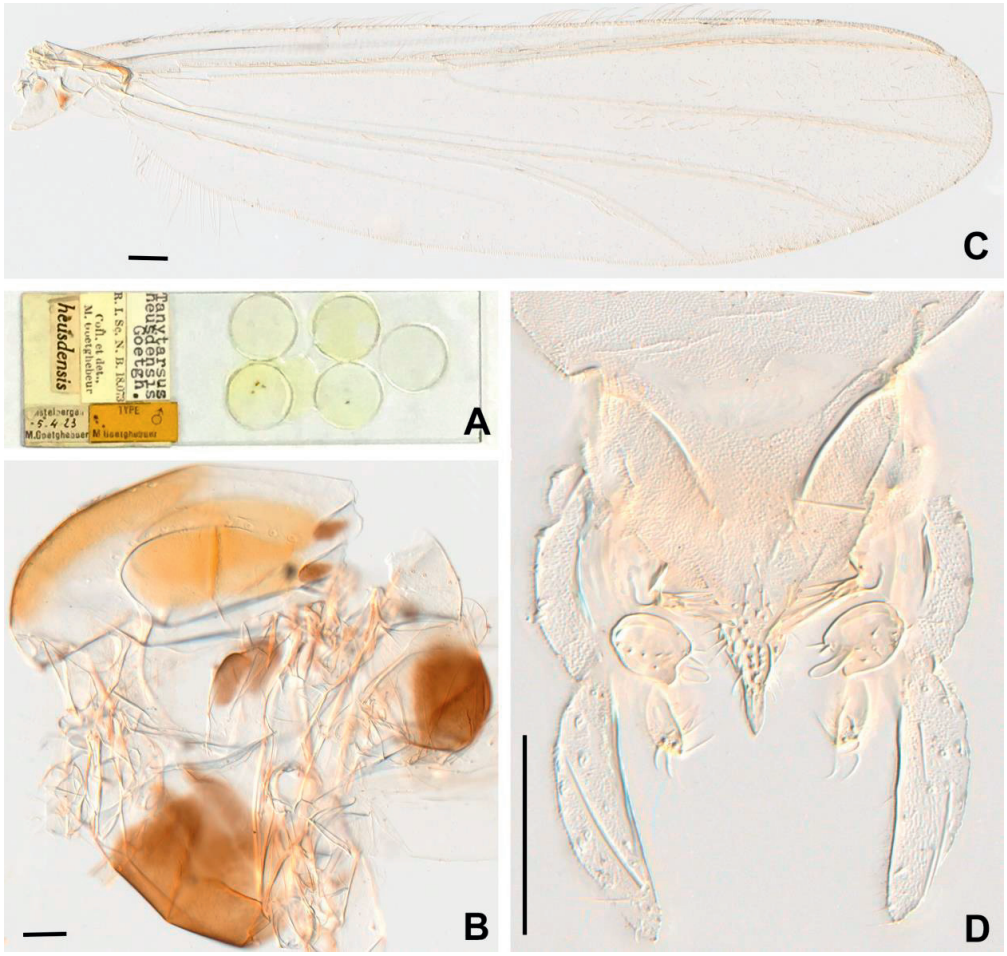

Figure 30

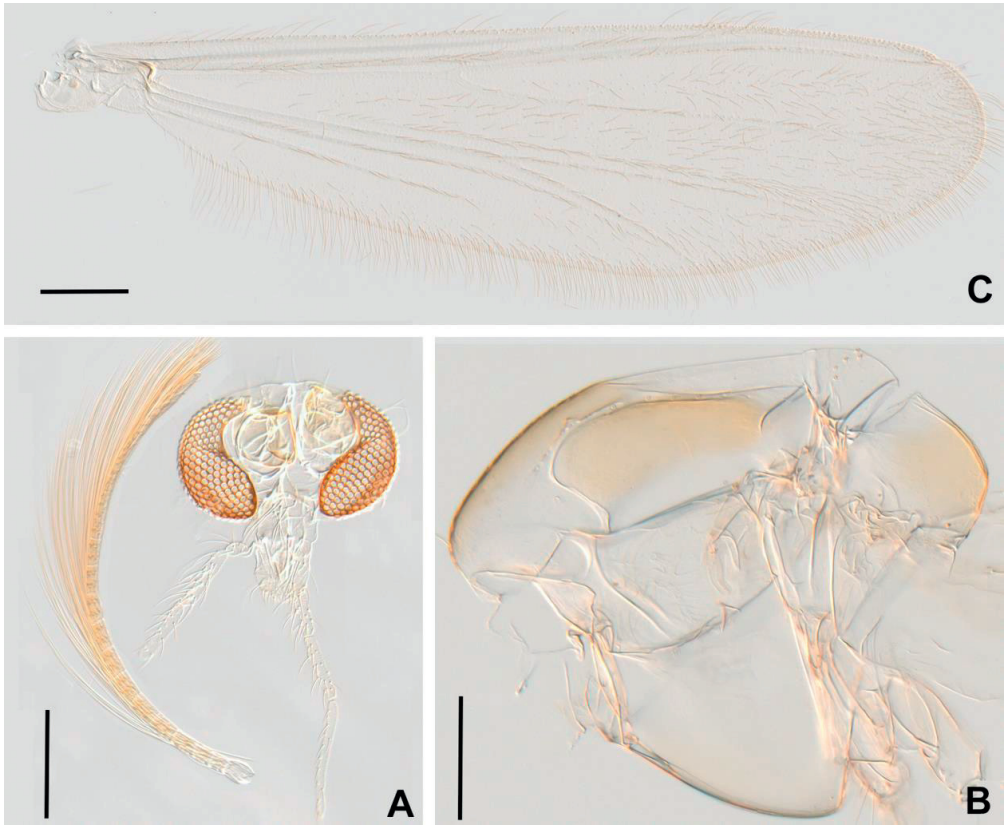

Figure 31

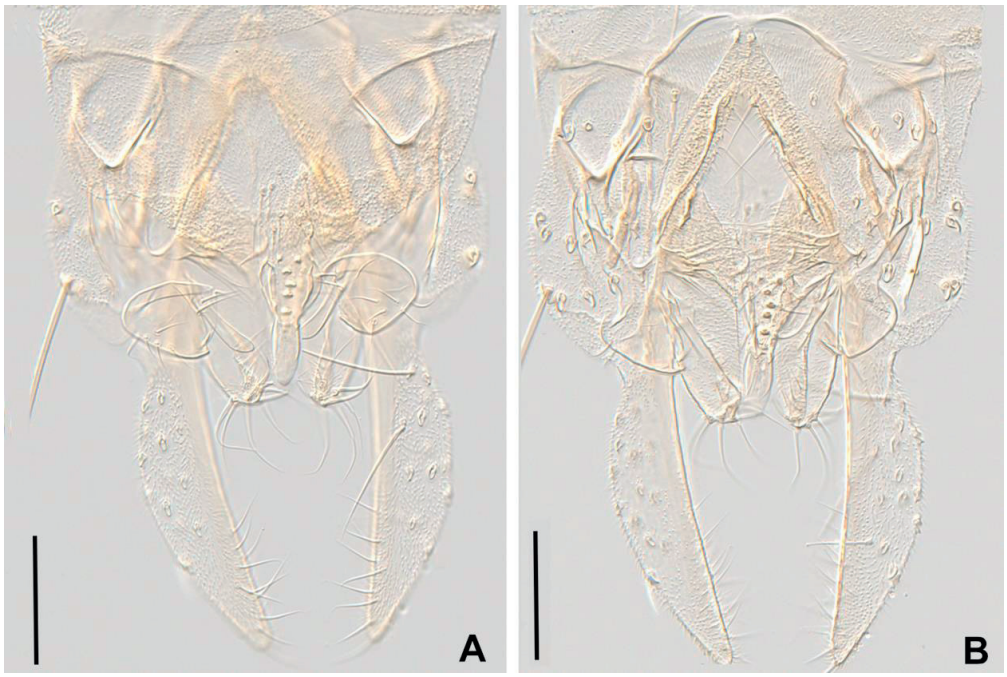

Figure 32

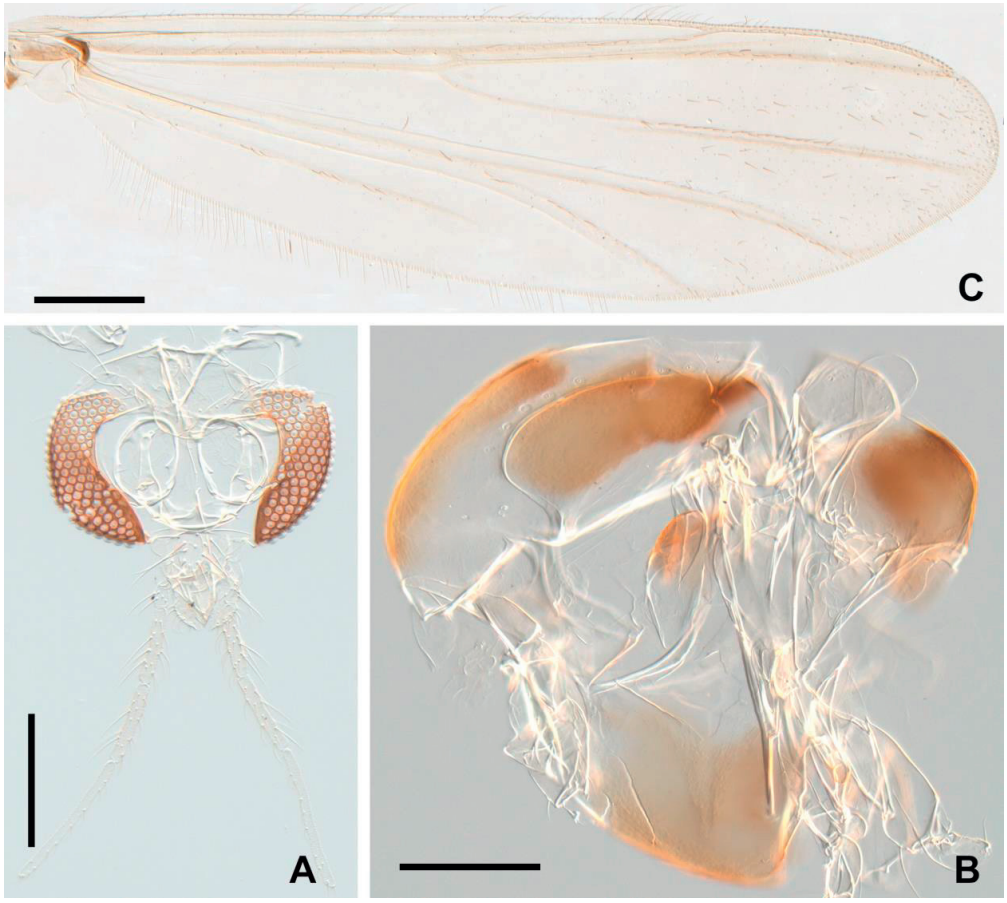

Figure 33

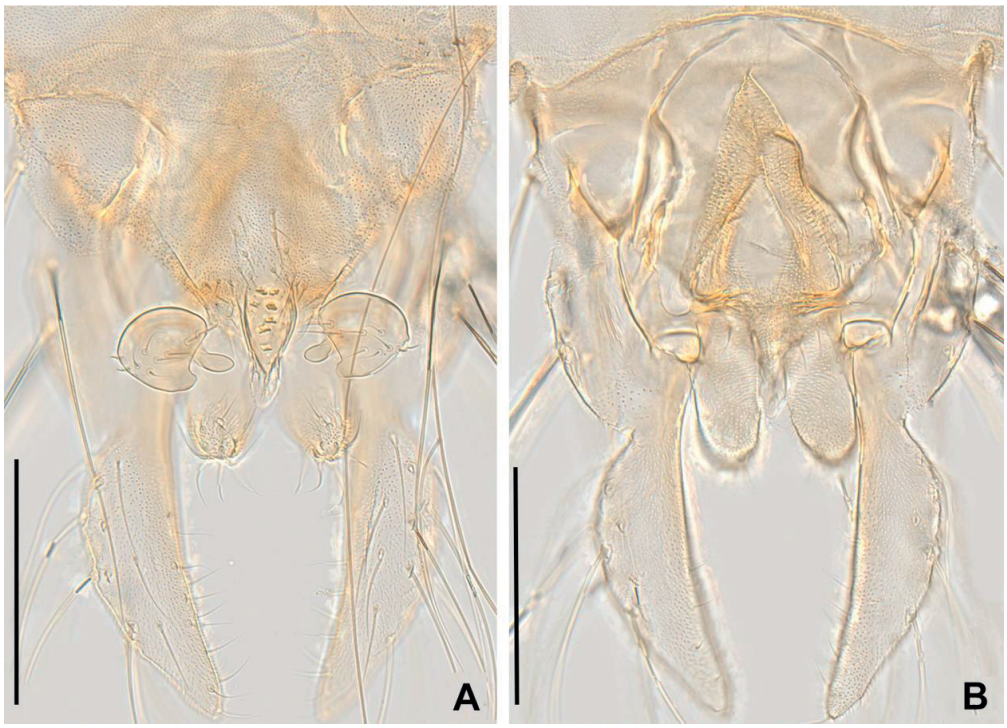

Figure 34

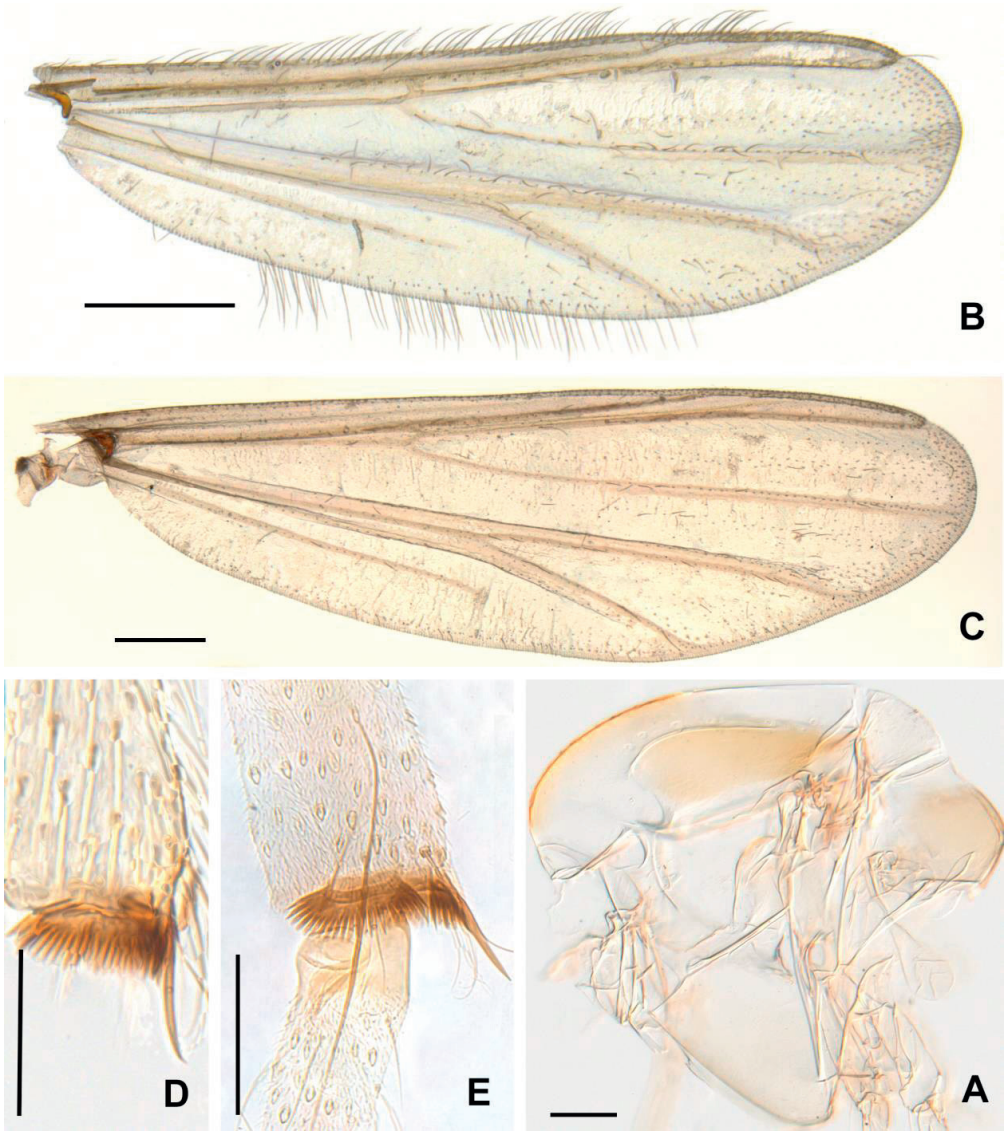

Figure 35

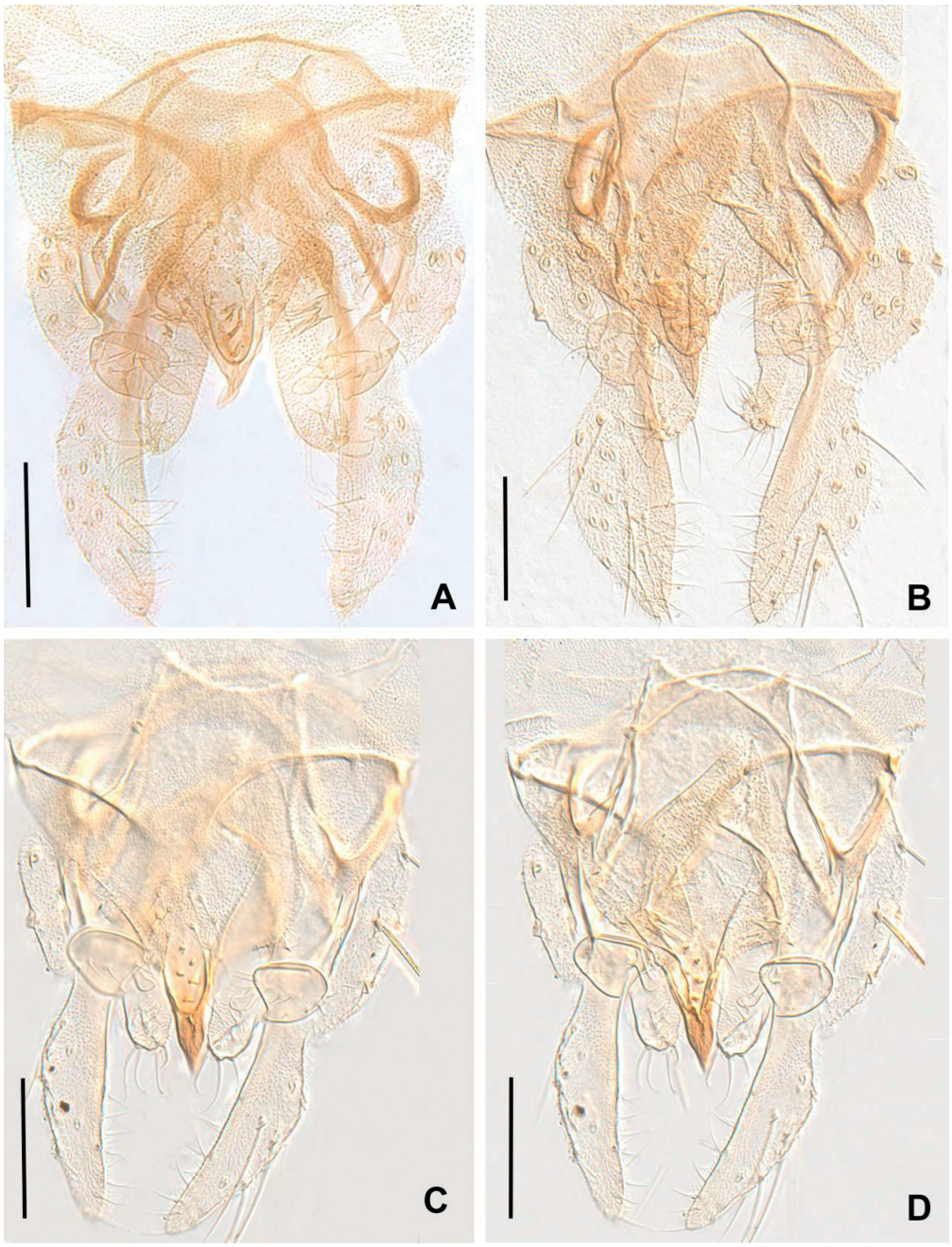

Tables

Table 1. Lengths (in µm) and proportions of legs for *Tanytarsus heberti* sp. n., adult male

	fe	ti	ta_1	ta_2	ta_3	ta_4	ta_5	LR	BV	SV	BR
p_1	660	380	-	-	-	-	-	-	-	-	-
p_2	770	710	-	-	-	-	-	-	-	-	-
p_3	670	530	290	170	110	85	65	0.55	3.47	4.14	3.50

Table 2. Lengths (in µm) and proportions of legs for *Tanytarsus madeiraensis* sp. n., adult male

	fe	ti	ta_1	ta_2	ta_3	ta_4
p_1	650–670	340–350	670–710	340–350	270–280	230
p_2	650	460–500	300	140–150	100	60
p_3	680	600–650	410–430	250	210–220	130–140

	ta_5	LR	BV	SV	BR
p_1	100	1.91–2.09	1.79	1.39–1.52	2.50–2.72
p_2	50–60	0.60–0.65	3.81–4.14	3.70–3.83	3.57–3.82
p_3	70–80	0.63–0.72	2.55–2.56	2.98–3.24	2.70–2.81

Table 3. Lengths (in µm) and proportions of legs for *Tanytarsus songi* sp. n., adult male

	fe	ti	ta_1	ta_2	ta_3	ta_4	ta_5	LR	BV	SV	BR
p_1	690	340	-	-	-	-	-	-	-	-	-
p_2	700	500	290	140	100	70	50	0.58	4.13	4.14	5.71
p_3	770	650	-	-	-	-	-	-	-	-	-

Table 4. Lengths (in µm) and proportions of legs for *Tanytarsus tamaoctavus*, adult male

	fe	ti	ta_1	ta_2	ta_3	ta_4
p_1	540–640	255–300	620–780	300–390	250–300	180–250
p_2	485–620	405–440	235–250	100–120	60–90	35–50
p_3	505–650	505–570	360–410	195–240	180–230	105–140

	ta_5	LR	BV	SV	BR
p_1	90–110	2.43–2.75	1.64–1.73	1.14–1.28	2.88–3.13
p_2	35–40	0.57–0.59	4.44–4.89	3.79–4.24	3.57–5.45
p_3	60–70	0.72–0.88	2.38–2.55	2.73–3.14	3.63–6.38

Table 5. Lengths (in μm) and proportions of legs for *Tanytarsus thomasi* sp. n., adult male

	fe	ti	ta_1	ta_2	ta_3	ta_4
p_1	700–790, 740	390–420, 405	720–850, 778	390–450, 413	310–340, 325	250–270, 262
p_2	690–800, 723	550–600, 565	290–350, 315	170–190, 178	130–140, 135	90–100, 94
p_3	780–910, 817	740–760, 750	450–480, 467	280–290, 283	250–280, 262	170–180, 175

	ta_5	LR	BV	SV	BR
p_1	110–130, 113	1.85–2.02, 1.90	1.65–1.84, 1.74	1.42–1.53, 1.48	1.67–3.33, 2.65
p_2	70–80, 74	0.53–0.58, 0.55	3.14–3.65, 3.36	3.94–4.31, 4.13	3.75–5.25, 4.62
p_3	90–100, 94	0.61–0.65, 0.63	2.32–2.54, 2.45	3.21–3.38, 3.26	5.00–5.35, 5.30

Table 6. Lengths (in μm) and proportions of legs for *Tanytarsus tongmuensis* sp. n., adult male

	fe	ti	ta_1	ta_2	ta_3	ta_4
p_1	690–790, 745	290–370, 343	790–930, 830	410–450, 428	340–370, 356	280–300, 285
p_2	700–760, 733	540–550, 545	280–350, 313	100–160, 136	100–110, 106	60–70, 65
p_3	750–820, 780	710–730, 718	470–520, 496	270–300, 288	250–270, 259	160–190, 182

	ta_5	LR	BV	SV	BR
p_1	110–130, 119	2.38–2.72, 2.47	1.65–1.76, 1.70	1.26–1.30, 1.28	2.50–3.25, 2.86
p_2	40–50, 45	0.56–0.65, 0.60	4.18–4.67, 4.35	3.68–4.13, 3.89	2.70–4.38, 3.60
p_3	85–95, 89	0.68–0.71, 0.69	2.36–2.37, 2.36	3.04–3.06, 3.05	3.75–5.33, 4.56

Table 7. Lengths (in μm) and proportions of legs for *Tanytarsus tongmuensis* sp. n., adult female

	fe	ti	ta_1	ta_2	ta_3	ta_4
p_1	700–730	360–380	910	410–420	340–350	280–281
p_2	660–690	500–520	280–300	140–142	100–103	60–70
p_3	720–760	660–700	420	240–250	220–230	130–150

	ta_5	LR	BV	SV	BR
p_1	120–121	2.39–2.53	1.68–1.76	1.16–1.22	3.38–4.29
p_2	50–60	0.56–0.58	4.00–4.19	4.03–4.14	3.70–4.00
p_3	80–100	0.60–0.64	2.61–2.65	3.29–3.48	4.40–5.00

Table 8. Lengths (in μm) and proportions of legs for *Tanytarsus wangi* sp. n., adult male

	fe	ti	ta_1	ta_2	ta_3	ta_4
p_1	370–500	225–265	610–705	285–330	200–260	170–220
p_2	410–500	350–400	225–240	105–110	60–73	35–50
p_3	410–540	350–395	320–350	180–210	140–200	85–120

	ta_5	LR	BV	SV	BR
p_1	100–105	2.65–2.84	1.56–1.68	0.93–1.09	2.25–3.43
p_2	35–40	0.60–0.64	4.15–4.30	3.49–3.78	3.57–4.71
p_3	65–75	0.73–0.85	2.14–2.36	2.47–2.91	2.00–6.25

Table 9. Lengths (in μm) and proportions of legs for *Tanytarsus adustus* sp. n., adult male

	fe	ti	ta_1	ta_2	ta_3	ta_4
p_1	610–720	320–390	590–690	320–390	270–310	190–240
p_2	590–680	460–530	240–300	130–160	90–110	60–80
p_3	640–740	600–670	350–420	210–250	200–240	110–150

	ta_5	LR	BV	SV	BR
p_1	90–120	1.76–1.84	1.73–1.75	1.58–1.61	2.01–2.11
p_2	50–70	0.52–0.57	3.61–3.91	4.00–4.38	3.11–3.22
p_3	60–90	0.58–0.62	2.51–2.74	3.36–3.54	3.11–4.00

Table 10. Lengths (in μm) and proportions of legs for *Tanytarsus adustus* sp. n., adult female

	fe	ti	ta_1	ta_2	ta_3	ta_4
p_1	570–620	320–370	610–640	310–340	250–290	200–210
p_2	560–600	440–510	240–250	120–140	90–100	50–70
p_3	600–630	600–670	330–370	190–220	180–200	120–120

	ta_5	LR	BV	SV	BR
p_1	90–100	1.73–1.91	1.73–1.76	1.46–1.55	1.44–2.86
p_2	40–60	0.49–0.55	3.68–4.13	4.17–4.44	2.00–2.38
p_3	70–80	0.57–0.59	2.66–2.70	3.46–3.58	1.44–1.88

Table 11. Lengths (in μm) and proportions of legs for *Tanytarsus pseudoheusdensis* sp. n.

	fe	ti	ta_1	ta_2	ta_3	ta_4
p_1	800–860	460–490	900–990	460–480	380–400	180–310
p_2	800–820	610	380–390	200	130–140	80–90
p_3	900–930	810–840	590	345–360	280–300	190–200

	ta_5	LR	BV	SV	BR
p_1	140–150	1.84–2.07	1.67–1.76	1.36–1.44	2.00–2.21
p_2	70–75	0.60–0.63	3.64–3.73	3.67–3.71	3.88–4.01
p_3	90–100	0.70–0.73	2.40–2.58	2.90–3.00	6.88–6.91

Table 12. Lengths (in μm) and proportions of legs for *Tanytarsus reei* Na & Bae

	fe	ti	ta_1	ta_2	ta_3	ta_4
p_1	690–880	350–480	810–1010	410–540	340–420	280–350
p_2	680–870	530–670	310–420	180–220	100–160	70–110
p_3	750–950	700–900	490–650	290–380	250–300	180–200

	ta_5	LR	BV	SV	BR
p_1	120–150	2.10–2.31	1.61–1.65	1.28–1.35	2.36–4.00
p_2	60–100	0.57–0.63	3.32–3.71	3.67–4.00	4.31–5.78
p_3	90–130	0.58–0.70	2.40–2.48	2.85–3.00	3.88–4.02

Supporting information

Table S1. Estimates of evolutionary divergences between sequences of the *Tanytarsus curticornis* species complex. Kimura 2-parameter genetic distances.

XL1_{*Tanytarsus wangi*}
XL323_{*Tanytarsus tongmuensis*}	0.083
XL344_{*Tanytarsus tongmuensis*}	0.084	0.018
XL319_{*Tanytarsus tongmuensis*}	0.083	0.000	0.018
XL331_{*Tanytarsus tongmuensis*}	0.084	0.018	0.000	0.018
XL334_{*Tanytarsus tongmuensis*}	0.083	0.000	0.018	0.000	0.018
XL330_{*Tanytarsus tongmuensis*}	0.083	0.000	0.018	0.000	0.018	0.000
XL314_{*Tanytarsus tongmuensis*}	0.083	0.000	0.018	0.000	0.018	0.000	0.000
XL329_{*Tanytarsus tongmuensis*}	0.083	0.000	0.018	0.000	0.018	0.000	0.000	0.000
XL324_{Tanytarsus tongmuensis}	0.084	0.002	0.020	0.002	0.020	0.002	0.002	0.002	0.002
XL333_{*Tanytarsus tongmuensis*}	0.083	0.000	0.018	0.000	0.018	0.000	0.000	0.000	0.000	0.002
XL317_{Tanytarsus tongmuensis}	0.084	0.018	0.000	0.018	0.000	0.018	0.018	0.018	0.018	0.020	0.018
XL347_{*Tanytarsus tongmuensis*}	0.083	0.000	0.017	0.000	0.017	0.000	0.000	0.000	0.000	0.002	0.000	0.017
XL349_{*Tanytarsus tongmuensis*}	0.083	0.000	0.018	0.000	0.018	0.000	0.000	0.000	0.000	0.002	0.000	0.018	0.000
XL335_{*Tanytarsus tongmuensis*}	0.083	0.000	0.018	0.000	0.018	0.000	0.000	0.000	0.000	0.002	0.000	0.018	0.000	0.000
XL316_{*Tanytarsus tongmuensis*}	0.083	0.000	0.018	0.000	0.018	0.000	0.000	0.000	0.000	0.002	0.000	0.018	0.000	0.000	0.000
XL327_{*Tanytarsus tongmuensis*}	0.083	0.000	0.018	0.000	0.018	0.000	0.000	0.000	0.000	0.002	0.000	0.018	0.000	0.000	0.000	0.000
XL332_{*Tanytarsus tongmuensis*}	0.083	0.000	0.018	0.000	0.018	0.000	0.000	0.000	0.000	0.002	0.000	0.018	0.000	0.000	0.000	0.000	0.000
XL326_{*Tanytarsus tongmuensis*}	0.083	0.000	0.018	0.000	0.018	0.000	0.000	0.000	0.000	0.002	0.000	0.018	0.000	0.000	0.000	0.000	0.000	0.000
XL346_{*Tanytarsus tongmuensis*}	0.083	0.000	0.018	0.000	0.018	0.000	0.000	0.000	0.000	0.002	0.000	0.018	0.000	0.000	0.000	0.000	0.000	0.000	0.000
XL345_{*Tanytarsus tongmuensis*}	0.085	0.002	0.020	0.002	0.020	0.002	0.002	0.002	0.002	0.003	0.002	0.020	0.002	0.002	0.002	0.002	0.002	0.002	0.002	0.002
XL348_{*Tanytarsus tongmuensis*}	0.083	0.000	0.018	0.000	0.018	0.000	0.000	0.000	0.000	0.002	0.000	0.018	0.000	0.000	0.000	0.000	0.000	0.000	0.000	0.000	0.002
XL315_{*Tanytarsus tongmuensis*}	0.083	0.000	0.018	0.000	0.018	0.000	0.000	0.000	0.000	0.002	0.000	0.018	0.000	0.000	0.000	0.000	0.000	0.000	0.000	0.000	0.002	0.000
CHIR_CH167_{*Tanytarsus thomasi*}	0.170	0.190	0.184	0.190	0.184	0.190	0.190	0.190	0.190	0.190	0.190	0.184	0.188	0.190	0.190	0.190	0.190	0.190	0.190	0.190	0.191	0.190	0.190
CHIR_CH124_{*Tanytarsus thomasi*}	0.178	0.195	0.188	0.195	0.188	0.195	0.195	0.195	0.195	0.195	0.195	0.188	0.195	0.195	0.195	0.195	0.195	0.195	0.195	0.195	0.195	0.195	0.195	0.000
CHIR_CH166_{*Tanytarsus thomasi*}	0.185	0.211	0.209	0.211	0.209	0.211	0.211	0.211	0.211	0.211	0.211	0.209	0.209	0.211	0.211	0.211	0.211	0.211	0.211	0.211	0.212	0.211	0.211	0.031	0.031
CHIR_CH164_{*Tanytarsus thomasi*}	0.182	0.205	0.205	0.205	0.205	0.205	0.205	0.205	0.205	0.205	0.205	0.205	0.201	0.205	0.205	0.205	0.205	0.205	0.205	0.205	0.208	0.205	0.205	0.095	0.093	0.093
CHIR_CH165_{*Tanytarsus thomasi*}	0.185	0.211	0.209	0.211	0.209	0.211	0.211	0.211	0.211	0.211	0.211	0.209	0.209	0.211	0.211	0.211	0.211	0.211	0.211	0.211	0.212	0.211	0.211	0.031	0.031	0.000	0.093
CHIR_CH224_{*Tanytarsus thomasi*}	0.170	0.198	0.201	0.198	0.201	0.198	0.198	0.198	0.198	0.198	0.198	0.201	0.199	0.198	0.198	0.198	0.198	0.198	0.198	0.198	0.199	0.198	0.198	0.030	0.031	0.015	0.098	0.015
Finnmark666_{*Tanytarsus thomasi*}	0.172	0.207	0.205	0.207	0.205	0.207	0.207	0.207	0.207	0.207	0.207	0.205	0.205	0.207	0.207	0.207	0.207	0.207	0.207	0.207	0.207	0.207	0.207	0.034	0.036	0.018	0.096	0.018	0.015
XL423_{*Tanytarsus tamaoctavus*}	0.126	0.142	0.135	0.142	0.135	0.142	0.142	0.142	0.142	0.142	0.142	0.135	0.139	0.142	0.142	0.142	0.142	0.142	0.142	0.142	0.143	0.142	0.142	0.163	0.170	0.175	0.191	0.175	0.175	0.177
XL351_{*Tanytarsus tamaoctavus*}	0.126	0.142	0.135	0.142	0.135	0.142	0.142	0.142	0.142	0.142	0.142	0.135	0.139	0.142	0.142	0.142	0.142	0.142	0.142	0.142	0.143	0.142	0.142	0.163	0.170	0.175	0.191	0.175	0.175	0.177	0.000
XL287_{*Tanytarsus tamaoctavus*}	0.125	0.140	0.133	0.140	0.133	0.140	0.140	0.140	0.140	0.140	0.140	0.133	0.137	0.140	0.140	0.140	0.140	0.140	0.140	0.140	0.141	0.140	0.140	0.161	0.168	0.173	0.189	0.173	0.173	0.175	0.002	0.002
XL222_{*Tanytarsus songi*}	0.183	0.210	0.208	0.210	0.208	0.210	0.210	0.210	0.210	0.210	0.210	0.208	0.209	0.210	0.210	0.210	0.210	0.210	0.210	0.210	0.209	0.210	0.210	0.200	0.199	0.200	0.213	0.200	0.204	0.200	0.157	0.157	0.159
MA18_{*Tanytarsus madeiraensis*}	0.170	0.189	0.191	0.189	0.191	0.189	0.189	0.189	0.189	0.189	0.189	0.191	0.187	0.189	0.189	0.189	0.189	0.189	0.189	0.189	0.190	0.189	0.189	0.212	0.212	0.207	0.220	0.207	0.212	0.212	0.164	0.164	0.162	0.201
MA19_{*Tanytarsus madeiraensis*}	0.171	0.190	0.192	0.190	0.192	0.190	0.190	0.190	0.190	0.190	0.190	0.192	0.188	0.190	0.190	0.190	0.190	0.190	0.190	0.190	0.190	0.190	0.190	0.212	0.212	0.208	0.220	0.208	0.213	0.212	0.165	0.165	0.163	0.201	0.000
CHIR_CH342_{*Tanytarsus heberti*}	0.203	0.202	0.202	0.202	0.202	0.202	0.202	0.202	0.202	0.202	0.202	0.202	0.200	0.202	0.202	0.202	0.202	0.202	0.202	0.202	0.204	0.202	0.202	0.154	0.162	0.153	0.158	0.153	0.153	0.157	0.201	0.201	0.198	0.239	0.212	0.213
To82_{*Tanytarsus curticornis*}	0.192	0.191	0.189	0.191	0.189	0.191	0.191	0.191	0.191	0.191	0.191	0.189	0.190	0.191	0.191	0.191	0.191	0.191	0.191	0.191	0.192	0.191	0.191	0.158	0.159	0.160	0.158	0.160	0.160	0.164	0.158	0.158	0.160	0.200	0.169	0.169	0.176
XL99_{*Tanytarsus curticornis*}	0.199	0.196	0.194	0.196	0.194	0.196	0.196	0.196	0.196	0.196	0.196	0.194	0.194	0.196	0.196	0.196	0.196	0.196	0.196	0.196	0.196	0.196	0.196	0.157	0.154	0.159	0.161	0.159	0.159	0.163	0.163	0.163	0.165	0.207	0.168	0.168	0.181	0.009
XL148_{*Tanytarsus brundini*}	0.181	0.192	0.198	0.192	0.198	0.192	0.192	0.192	0.192	0.192	0.192	0.198	0.192	0.192	0.192	0.192	0.192	0.192	0.192	0.192	0.190	0.192	0.192	0.175	0.182	0.174	0.189	0.174	0.172	0.180	0.160	0.160	0.158	0.174	0.143	0.143	0.221	0.175	0.182
TRD-CH137_{*Tanytarsus brundini*}	0.174	0.187	0.191	0.187	0.191	0.187	0.187	0.187	0.187	0.187	0.187	0.191	0.187	0.187	0.187	0.187	0.187	0.187	0.187	0.187	0.185	0.187	0.187	0.177	0.185	0.178	0.191	0.178	0.177	0.185	0.164	0.164	0.162	0.173	0.138	0.138	0.214	0.177	0.184	0.022
To137_{Tanytarsus brundini}	0.184	0.190	0.192	0.190	0.192	0.190	0.190	0.190	0.190	0.190	0.190	0.192	0.190	0.190	0.190	0.190	0.190	0.190	0.190	0.190	0.188	0.190	0.190	0.165	0.172	0.172	0.179	0.172	0.171	0.179	0.164	0.164	0.162	0.175	0.141	0.142	0.219	0.173	0.180	0.017	0.020
Finnmark239_{*Tanytarsus brundini*}	0.178	0.190	0.192	0.190	0.192	0.190	0.190	0.190	0.190	0.190	0.190	0.192	0.190	0.190	0.190	0.190	0.190	0.190	0.190	0.190	0.190	0.190	0.190	0.173	0.178	0.176	0.187	0.176	0.175	0.183	0.166	0.166	0.164	0.179	0.143	0.144	0.219	0.175	0.182	0.015	0.015	0.017
SOE239_{*Tanytarsus brundini*}	0.167	0.168	0.174	0.168	0.174	0.168	0.168	0.168	0.168	0.168	0.168	0.174	0.170	0.168	0.168	0.168	0.168	0.168	0.168	0.168	0.167	0.168	0.168	0.171	0.176	0.169	0.187	0.169	0.169	0.171	0.142	0.142	0.140	0.171	0.140	0.140	0.209	0.166	0.167	0.047	0.044	0.046	0.047
Finnmark240_{*Tanytarsus brundini*}	0.166	0.187	0.189	0.187	0.189	0.187	0.187	0.187	0.187	0.187	0.187	0.189	0.187	0.187	0.187	0.187	0.187	0.187	0.187	0.187	0.186	0.187	0.187	0.167	0.174	0.168	0.185	0.168	0.167	0.174	0.152	0.152	0.150	0.167	0.134	0.134	0.208	0.171	0.178	0.026	0.011	0.022	0.017	0.042
XL402_{*Tanytarsus brundini*}	0.169	0.171	0.177	0.171	0.177	0.171	0.171	0.171	0.171	0.171	0.171	0.177	0.171	0.171	0.171	0.171	0.171	0.171	0.171	0.171	0.170	0.171	0.171	0.169	0.174	0.170	0.173	0.170	0.169	0.177	0.148	0.148	0.146	0.177	0.136	0.136	0.212	0.169	0.172	0.031	0.022	0.031	0.026	0.044	0.023
XL404_{*Tanytarsus brundini*}	0.171	0.173	0.179	0.173	0.179	0.173	0.173	0.173	0.173	0.173	0.173	0.179	0.173	0.173	0.173	0.173	0.173	0.173	0.173	0.173	0.172	0.173	0.173	0.167	0.172	0.165	0.177	0.165	0.167	0.171	0.146	0.146	0.144	0.167	0.141	0.142	0.212	0.171	0.178	0.030	0.023	0.029	0.028	0.042	0.025	0.008
SOE05_{*Tanytarsus brundini*}	0.166	0.167	0.173	0.167	0.173	0.167	0.167	0.167	0.167	0.167	0.167	0.173	0.168	0.167	0.167	0.167	0.167	0.167	0.167	0.167	0.165	0.167	0.167	0.168	0.176	0.165	0.187	0.165	0.166	0.168	0.141	0.141	0.139	0.170	0.137	0.137	0.205	0.164	0.164	0.046	0.043	0.044	0.046	0.002	0.041	0.043	0.041
XL407_{*Tanytarsus brundini*}	0.173	0.175	0.181	0.175	0.181	0.175	0.175	0.175	0.175	0.175	0.175	0.181	0.175	0.175	0.175	0.175	0.175	0.175	0.175	0.175	0.174	0.175	0.175	0.169	0.174	0.170	0.177	0.170	0.169	0.177	0.152	0.152	0.150	0.173	0.139	0.140	0.212	0.167	0.174	0.030	0.020	0.029	0.022	0.046	0.018	0.005	0.006	0.044
SOE13_{*Tanytarsus brundini*}	0.168	0.169	0.175	0.169	0.175	0.169	0.169	0.169	0.169	0.169	0.169	0.175	0.170	0.169	0.169	0.169	0.169	0.169	0.169	0.169	0.167	0.169	0.169	0.170	0.176	0.167	0.185	0.167	0.168	0.170	0.141	0.141	0.139	0.170	0.138	0.139	0.207	0.166	0.166	0.047	0.044	0.046	0.047	0.000	0.043	0.044	0.043	0.002	0.046
XL405_{*Tanytarsus brundini*}	0.180	0.177	0.184	0.177	0.184	0.177	0.177	0.177	0.177	0.177	0.177	0.184	0.177	0.177	0.177	0.177	0.177	0.177	0.177	0.177	0.176	0.177	0.177	0.174	0.179	0.179	0.177	0.179	0.177	0.185	0.156	0.156	0.154	0.177	0.145	0.145	0.210	0.171	0.178	0.039	0.030	0.036	0.031	0.052	0.028	0.011	0.015	0.051	0.009	0.052
SOE248_{*Tanytarsus brundini*}	0.169	0.174	0.180	0.174	0.180	0.174	0.174	0.174	0.174	0.174	0.174	0.180	0.174	0.174	0.174	0.174	0.174	0.174	0.174	0.174	0.173	0.174	0.174	0.172	0.180	0.174	0.180	0.174	0.174	0.176	0.151	0.151	0.149	0.171	0.130	0.130	0.208	0.165	0.169	0.043	0.030	0.035	0.035	0.030	0.030	0.038	0.043	0.028	0.038	0.030	0.044
XL403_{*Tanytarsus brundini*}	0.169	0.175	0.181	0.175	0.181	0.175	0.175	0.175	0.175	0.175	0.175	0.181	0.175	0.175	0.175	0.175	0.175	0.175	0.175	0.175	0.174	0.175	0.175	0.169	0.174	0.170	0.177	0.170	0.169	0.177	0.152	0.152	0.150	0.175	0.141	0.142	0.214	0.169	0.176	0.023	0.017	0.026	0.019	0.046	0.018	0.008	0.009	0.044	0.006	0.046	0.015	0.040

Table S2. Estimates of evolutionary divergences between sequences of the *Tanytarsus heusdensis* species complex. Kimura 2-parameter genetic distances.

XL186_{*T. heusdensis*}																		
XL183_{*T. heusdensis*}	0.014																	
CH-OSF104_{*T. heusdensis*}	0.014	0.000																
ES79_{*T. pseudoheusdensis*}	0.265	0.260	0.260															
ES77_{*T. pseudoheusdensis*}	0.265	0.260	0.260	0.000														
XL12_{ *T. reei* }	0.239	0.226	0.226	0.286	0.286													
XL180_{ *T. reei*}	0.222	0.217	0.217	0.291	0.291	0.086												
XL13_{*T. reei*}	0.234	0.221	0.221	0.273	0.273	0.015	0.084											
SOE380_{ *T. adustus* }	0.196	0.194	0.194	0.272	0.272	0.225	0.240	0.228										
SOE387_{ *T. adustus* }	0.196	0.194	0.194	0.272	0.272	0.225	0.240	0.228	0.000									
SOE247_{ *T. adustus* }	0.196	0.194	0.194	0.273	0.273	0.231	0.247	0.233	0.006	0.006								
XL459_{ *T. adustus* }	0.199	0.197	0.197	0.272	0.272	0.231	0.245	0.233	0.003	0.003	0.010							
SOE386_{*T. adustus*}	0.196	0.194	0.194	0.272	0.272	0.228	0.243	0.230	0.002	0.002	0.008	0.002						
JN887103_{ *T. reei* }	0.236	0.223	0.223	0.267	0.267	0.020	0.080	0.008	0.222	0.222	0.227	0.227	0.225					
JN887105_{ *T. reei* }	0.236	0.223	0.223	0.267	0.267	0.020	0.080	0.008	0.222	0.222	0.227	0.227	0.225	0.000				
JN887104_{ *T. reei* }	0.228	0.215	0.215	0.267	0.267	0.017	0.079	0.005	0.230	0.230	0.235	0.235	0.232	0.009	0.009			
JN887102_{ *T. reei* }	0.236	0.223	0.223	0.267	0.267	0.020	0.080	0.008	0.222	0.222	0.227	0.227	0.225	0.000	0.000	0.009		
JN887106_{*T. reei*}	0.230	0.218	0.218	0.266	0.266	0.019	0.079	0.009	0.216	0.216	0.221	0.221	0.219	0.005	0.005	0.011	0.005	
LGT01_{*T. tamaduodecimus*}	0.233	0.226	0.226	0.232	0.232	0.204	0.211	0.207	0.221	0.221	0.230	0.224	0.221	0.201	0.201	0.201	0.201	0.196

Exploring species boundaries with multiple genetic loci using empirical data from non-biting midges

Xiao-Long Lin*, Elisabeth Stur, Torbjørn Ekrem

Department of Natural History, NTNU University Museum, Norwegian University of Science and Technology, NO-7049, Trondheim, Norway

* Corresponding author, E-mail: xiaolong.lin@ntnu.no

Abstract

Over the past decade, molecular approaches to species delimitation have seen rapid development. However, species delimitation based on a single locus, e.g. DNA barcodes, can lead to inaccurate results in cases of recent speciation and incomplete lineage sorting. Here we compare the performance of Automatic Barcode Gap Discovery (ABGD), Bayesian Poisson tree processes (PTP), networks, Generalized Mixed Yule Coalescent (GMYC) and Bayesian Phylogenetics and Phylogeography (BPP) models to delineate cryptic species previously detected by DNA barcodes within *Tanytarsus* non-biting midges. We compare the results from analyses of one mitochondrial (COI) and three nuclear (AATS1, CAD1 and PGD) protein-coding genes. Our results show that species delimitation based on multiple nuclear DNA markers is a more reliable predictor of morphological variation than delimitations using a single locus, e.g. the COI barcode. Moreover, ABGD, GMYC, PTP and network models arrive at conflicting results based on a single locus and delineate species differently than morphology. Results from BPP analyses on multiple loci correspond best with current morphological species concept. In total, nine lineages of the *Tanytarsus curticornis* species complex were uncovered, excluding the Sølendet population of *Tanytarsus brundini* which might have undergone recent hybridization, suggesting six semi-cryptic species new to science. Five distinct species are well supported in the *Tanytarsus heusdensis* species complex, including two semi-cryptic species new to science.

Keywords

ABGD; BPP; cryptic species; GMYC; networks; species delimitation; Chironomidae; *Tanytarsus*.

1. Introduction

Accurate assessment of species boundaries is critical for our understanding of patterns of diversity and speciation (Pimm et al. 2014). However, limited understanding of the evolutionary potential of species makes global estimates of diversity constrained (Appeltans et al. 2012; Costello et al. 2013; Moritz 2002). Documentation of genetic variation between species, particular through large DNA barcoding initiatives (Hebert et al. 2003a; Hebert et al. 2003b), has proven very informative for the detection and resolution of species complexes, and has provided insights into the evolutionary history of species (Kress et al. 2015). Potentially cryptic species are detected now more frequently than ever. However, the presence of introgression (Gay et al. 2007; Martinsen et al. 2001) and incomplete lineage sorting (Ballard & Whitlock 2004; Heckman et al. 2007; Willyard et al. 2009) can present obstacles in species delimitation using a single genetic marker. Moreover, deep mitochondrial genetic divergence is not always accompanied by correspondingly deep nuclear differentiation. Due to genealogical concordance among samples, multiple loci can provide convincing evidence for genetic boundaries, and validate the presence of genetically distinctive but morphologically cryptic lineages. For instance, Fossen et al. (2016) explored the species boundaries in northern European water scavenger beetles using multiple loci and a few morphological characters. Low et al. (2016) delineated taxonomic boundaries in the largest species complex of black files using multiple genes, morphological and chromosomal data. Also within the Chironomidae, several potential cryptic species were detected by DNA barcodes and new species boundaries confirmed by additional nuclear DNA markers and analyses of morphological characters (Anderson et al. 2013).

Several tools to investigate species boundaries are available and frequently used in analyses of species diversity using DNA sequence data. For instance, species delimitation methods based on single loci include the Automatic Barcode Gap Discovery (ABGD) (Puillandre et al. 2012),

the Generalized Mixed Yule Coalescent model (GMYC) (Pons et al. 2006; Zhang et al. 2013) and the Poisson tree processes (PTP). While for multiple loci, the Bayesian Phylogenetics and Phylogeography (BPP) method (Zhang et al. 2013) has been found to perform more accurately than alternative approaches (Yang 2015; Yang & Rannala 2010, 2017).

ABGD recursively detects for barcode gaps in the distribution of pairwise sequence divergences, and assign input sequences into hypothetical species based on pairwise distance. It is recognized that ABGD performs well on large barcode datasets with an appropriate prior of maximum intraspecific divergence (Lin et al. 2015; Pentinsaari et al. 2016; Puillandre et al. 2012), however, it is sensitive to singleton sequences and requires knowledge of threshold values (Pentinsaari et al. 2016; Puillandre et al. 2012).

The GMYC model, combines a Yule species birth model with a neutral coalescent model of intraspecific branching (Fujisawa & Barraclough 2013; Pons et al. 2006) and has been widely accepted for species delimitation based on single-locus data under many circumstances, including high singleton presence, taxon richness and the presence of gaps in intraspecific sampling coverage (Talavera et al. 2013). However, relative to other methods, GMYC has a tendency of over-splitting lineages resulting from errors in the reconstruction of ultrametric input trees (Paz & Crawford 2012; Pentinsaari et al. 2016; Tänzler et al. 2012). The method also shows a tendency of over-lumping in cases where different lineages are results of rapid and recent divergences (Esselstyn et al. 2012).

The recently proposed PTP model requires an rooted input tree and assumes that intra- and interspecific substitutions follow distinct Poisson processes, and that intraspecific substitutions are discernibly fewer than interspecific substitution (Tang et al. 2014; Zhang et al. 2013). The bPTP model, an updated version of the original PTP with Bayesian support values, provides more accurate results for species delimitation (Zhang et al. 2013).

Statistical parsimony network analysis implemented in the TCS software provides a rapid and useful tool for species delimitation (Hart & Sunday 2007), when applied to non-recombinate loci. TCS calculates the maximum number of mutational steps constituting a 95% parsimonious connection between two haplotypes or genotypes, and then joins these into networks following specific algorithms (Templeton et al. 1992).

The BPP method (Yang & Rannala 2010) adopts the biological species concept and implements a reversible jump Markov chain Monte Carlo (rjMCMC) search to estimate the posterior probability of species delimitation hypotheses. The method estimates ancestral population sizes and species population divergence times through estimated distributions of gene trees from multiple loci. The method requires sequence data and a guide species tree with defined topology as input. However, BPP can lead to false species delimitation when the guide tree is inaccurately specified (Rannala & Yang 2013).

The genus *Tanytarsus* van der Wulp, 1874 (Diptera: Chironomidae) is the most species-rich genus of the tribe Tanytarsini in subfamily Chironominae with more than 400 described species worldwide. Larvae of *Tanytarsus* are eurytopic, occur in all types of freshwater, sometimes even in marine or terrestrial environments, and play an important role in freshwater biomonitoring. However, morphological determination of species in some *Tanytarsus* species groups can be notoriously difficult. Additionally, there are many unknown and cryptic *Tanytarsus* species where the boundaries remain uncertain. In a previous study, DNA barcodes uncovered several potential cryptic species within *Tanytarsus curticornis* Kieffer, 1911 and *Tanytarsus heusdensis* Goetghebuer, 1923 species complexes (Lin et al. 2015).

Based on morphologically similar characteristics in the adult male, the *T. curticornis* species complex currently includes *T. brundini*, Lindeberg, 1963, *T. congus* Lehmann, 1981, *T.*

curticornis Kieffer, 1911, *T. ikicedeus* Sasa & Suzuki, 1999, *T. neotamaoctavus* Ree, Jeong & Nam, 2011, *T. pseudocongus* Ekrem, 1999, *T. salmelai* Giłka & Paasivirta, 2009, *T. tamaoctavus* Sasa, 1980. The *T. heusdensis* species complex includes four described species: *T. heusdensis* Goetghebuer, 1923, *T. reei* Na & Bae, 2010, *T. tamaduodecimus* Sasa, 1983, *T. tusimatneous* Sasa & Suzuki, 1999. The similar phenotypes within the *T. curticornis* and *T. heusdensis* species complexes likely have led to misidentifications and an underestimation of species biodiversity in *Tanytarsus*. Thus, these two species complexes are well suited to explore the suitability of different molecular markers and analytical methods in the analyses of species boundaries within non-biting midges.

The goal of this study was to investigate if different molecular markers and analytical tools give similar results when applied to a set of morphologically similar species of Chironomidae, and if the results are comparable to those achieved from DNA barcodes or morphological analysis alone.

2. Material and methods

2.1. Taxon sampling

We obtained 63 specimens of the *T. curticornis* and *T. heusdensis* species complexes from Canada, China, Czech Republic, Germany, Norway and Ukraine and included additional five public COI sequences of *Tanytarsus reei* from South Korea. List of all species, specimens, their individual images, georeferences, primers, sequences and other relevant laboratory data of all sequenced specimens can be seen online in the publicly accessible datasets "*Tanytarsus curticornis* species complex [DS-TANYSC]", DOI: XXX and "*Tanytarsus heusdensis* species complex [DS-HEUSDEN]", DOI: XXX in the Barcode of Life Data Systems (BOLD) (Ratnasingham & Hebert 2007, 2013). Specimens were identified morphologically by re-examination of available type material and use of taxonomic revisions and species

descriptions (Giłka & Paasivirta 2009; Kieffer 1911; Lindeberg 1963; Na & Bae 2010; Reiss & Fittkau 1971; Sasa 1980).

2.2. Molecular methods and analyses

Adult specimens were preserved in 85% ethanol, immatures in 96% ethanol, and stored dark at 4°C before morphological and molecular analyses. Genomic DNA of most specimens was extracted from the thorax and head using QIAGEN® DNeasy Blood & Tissue Kit and GeneMole DNA Tissue Kit on a GeneMole® instrument (Mole Genetics, Lysaker, Norway) at the Department of Natural History, NTNU University Museum. The standard protocol of the using QIAGEN® DNeasy Blood & Tissue Kit was used, except that the final elution volume was 100 µl due to small specimen size. When using GeneMole DNA Tissue Kit, the standard protocol was followed, except that 4 µl Proteinase K was mixed with 100 µl buffer for overnight lysis at 56 °C and the final elution volume was 100 µl. After DNA extraction, the cleared exoskeleton was washed with 96% ethanol and mounted in Euparal on the same microscope slide as its corresponding antennae, wings, legs and abdomen following the procedure outlined by Sæther (1969). Vouchers are deposited at the Department of Natural History, NTNU University Museum, Trondheim, Norway, University Museum of Bergen, Bergen, Norway or the College of Life Sciences, Nankai University, Tianjin, China.

Fragments of one mitochondrial protein-coding gene cytochrome *c* oxidase subunit I (COI) and three nuclear protein-coding genes [alanyl-tRNA synthetase 1 (AATS1), carbamoyl phosphate synthetase (CAD) and 6-phosphogluconate dehydrogenase (PGD)] were amplified. The primers used to amplify the four regions are shown in Table 1. DNA amplification of COI was carried out in 25 µl reactions using 2.5 µl 10x Takara ExTaq pcr buffer (CL), 2 µl 2.5 mM dNTP mix, 2 µl 25 mM $MgCl_2$, 0.2 µl Takara Ex Taq HS, 1 µl 10 µM of each primer, 2 µl template DNA and 14.3 µl ddH2O. Amplification cycles were performed on a Biorad

C1000 Thermal Cycler (Bio-Rad, California, USA) and followed a program with an initial denaturation step of 95 °C for 5 min, then followed by 34 cycles of 94 °C for 30 s, 51 °C for 30 s, 72 °C for 1 min and 1 final extension at 72 °C for 3 min. DNA amplifications of selected three nuclear genes were carried out using 2.5 µL 10x Ex Taq Buffer, 2 µL 2.5 mM dNTP Mix, 0.1 µL Ex Taq HS (all TaKaRa Bio INC, Japan), 0.5 µL 25 mM $MgCl_2$ and 1 µl of each 10 µM primer. The amount of template DNA was adjusted according to the DNA concentration and varied between 2–5 µL. ddH2O was added to make a total of 25 µL for each reaction. Amplification cycles were performed on a Biorad C1000 Thermal Cycler and followed a program with an initial denaturation step of 98°C for 10 s, then 94°C for 1 min followed by 5 cycles of 94°C for 30 s, 52°C for 30 s, 72°C for 2 min and 7 cycles of 94°C for 30 s, 51°C for 1 min, 72°C for 2 min and 37 cycles of 94°C for 30 s, 45°C for 20 s, 72 °C for 2 min 30 s and 1 final extension at 72°C for 3 min. PCR products were visualized on a 1% agarose gel, purified using Illustra ExoProStar 1-Step (GE Healthcare Life Sciences, Buckinghamshire, UK) and shipped to MWG Eurofins (Ebersberg, Germany) for bidirectional sequencing using BigDye 3.1 (Applied Biosystems, Foster City, CA, USA) termination. Not all individuals were successfully sequenced for all three nuclear loci. Sequences were assembled and edited using Sequencher 4.8 (Gene Codes Corp., Ann Arbor, Michigan, USA). The forward and reverse sequences were automatically assembled by the software and the contig was inspected and edited manually. The appropriate International Union of Pure and Applied Chemistry (IUPAC) code was applied when the ambiguous base calls existed. Sequence information was uploaded on BOLD (www.boldsystems.org) along with an image and collateral information for each voucher specimen. The sequences names were edited using MESQUITE 2.7.5 (Maddison & Maddison 2010). Alignment of the sequences was carried out using the Muscle algorithm (Edgar 2004) on nucleotides in MEGA 7 (Kumar et al. 2016). Introns were detected with a reference sequence (*Chironomus tepperi*,

GenBank: FJ040616) and removed from the alignment using GT-AT rule (Rogers & Wall 1980). After removing introns, the codons were aligned. No evidence of paralogue copies was observed in any sequences.

Table 1. Overview of gene segments and primer combinations.

Gene segment	Oligo name	Oligo sequence (5'-3')	Reference
COI	LCO1490	GGTCAACAAATCATAAAGATATTGG	Folmer et al. (1994)
	HCO2198	TAAACTTCAGGGTGACCAAAAAATCA	Folmer et al. (1994)
CAD1	54F	GTNGTNTTYCARACNGGNATGGT	Moulton and Wiegmann (2004)
	405R	GCNGTRTGYTCNGGRTGRAAYTG	Moulton and Wiegmann (2004)
AATS1	A1-92F	TAYCAYCAYACNTTYTTYGARATG	Regier et al. (2008)
	A1-244R	ATNCCRCARTCNATRTGYTT	Su et al. (2008)
PGD	PGD-2F	GATATHGARTAYGGNGAYATGCA	Regier et al. (2008)
	PGD-3R	TRTGIGCNCCRAARTARTC	Brian Cassel unpublished

2.2.1. Automatic Barcode Gap Discovery (ABGD)

Although several species had fewer than three specimens, the aligned COI barcodes of *T. curticornis* and *T. heusdensis* species complexes were sorted into hypothetical species using the ABGD method to discover the existence of the DNA barcode gaps and estimate the number of molecular OTUs. The analyses were conducted on the website with a prior *P* that ranges from 0.005 to 0.1, and the K2P model, following default settings.

2.2.2. Phylogenetic reconstructions

All nuclear genetic markers were concatenated using SequenceMatrix v1.7.8 (Vaidya et al. 2011). Phylogenetic analyses used the partition strategies and models of sequence evolution selected based on the Bayesian Information Criterion (BIC) in the jModelTest 2.1.7 (Darriba et al. 2012). We used a maximum likelihood (ML) phylogenetic analysis on each loci, and on the concatenated nuclear gene dataset with RAxML8.1.2 (Stamatakis 2006, 2014) using raxmlGUI v1.5b1 (Silvestro & Michalak 2012), with unlinked partitions as selected by

PartitionFinder (Lanfear et al. 2012). We used 1000 bootstrap replicates in a rapid bootstrap analysis, and a thorough search for the best scoring ML tree. Results indicated no conflict between nuclear gene trees, but incongruence between mitochondrial and nuclear trees. As a result, we used a concatenated nuclear dataset and mitochondrial COI dataset separately to reconstruct phylogenetic relationships of all specimens sequenced. We also implemented Bayesian inference in MrBayes v3.2.6 (Ronquist et al. 2012). In the Bayesian analyses, data sets were partitioned by gene, 4 chains on 2 runs for 20 million generations, sampled every 1000 generations with a burn in of 0.25. Convergence of posterior probabilities in each run was monitored using Tracer v1.6 (Rambaut et al. 2014); the first 10% of the sampled trees were discarded as burn-in.

2.2.3. Network analyses

A genotype (or haplotype) network for each gene segment was reconstructed with PopART (Leigh & Bryant 2015) using the TCS method (Clement et al. 2000; Clement et al. 2002) with gaps and missing data excluded.

2.2.4. GMYC

The single-threshold GMYC analyses were conducted in R v3.2.3 (R Core Team 2016) in a Linux environment, with the use of the *splits* package. The ultrametric single locus gene tree required for the GMYC method was obtained using BEAST 1.8.2 (Drummond et al. 2012) on the reduced dataset (identical sequences were excluded in RAxML), with 10 million MCMC generations under the Yule speciation model. A strict molecular clock was shown to be appropriate to infer the ultrametric trees through the model comparison using a Bayes factor test in Tracer 1.6 (Rambaut et al. 2014). For the *T. curticornis* species complex, the GTR + G substitution model (Tavaré 1986) was selected for the AATS1, CAD1 and PGD genes, the HKY + G substitution model (Hasegawa et al. 1985) was selected for COI. For the *T.*

heusdensis species complex, the GTR + G substitution model was selected for PGD, the HKY+G substitution model was selected for AATS1, CAD1 and COI. Effective sample sizes (ESS) and trace plots estimated with Tracer 1.6 were used as convergence diagnostics, and a burn-in of one million generations was used to avoid suboptimal trees in the final consensus tree. Ultrametric maximum clade credibility (MCC) trees were computed using the mean node heights with TreeAnnotator v1.8.2 for each locus gene.

2.2.5. PTP

A rooted input tree for each gene was generated with RAxML using rapid Bootstrap with 1000 replicates and the GTR + G +I substitution model. The PTP and bPTP analyses for each gene were run on a web server (http://species.h-its.org/ptp/) with 500,000 MCMC generations, excluding outgroup, following the remaining default settings.

2.2.6. BPP

We combined the datasets of the *T. curticornis* and *T. heusdensis* species complexes for the BPP analyses because the statistical power of BPP can be increased when closely related outgroups are included (Rannala & Yang 2013). The multi-locus Bayesian species delimitation method in BPP X1.2.2 (Yang 2015; Yang & Rannala 2010) was used with two concatenated datasets [three nuclear loci (AATS1, CAD1 and PGD) and all loci (AATS1, COI, CAD1 and PGD)].

Two start guide species trees were estimated in *BEAST v1.8.2 (Drummond et al. 2012) on the above concatenated datasets and run with 40 million MCMC generations under the Yule Process speciation model. The HKY + G substitution model was selected for AATS1, COI, CAD1 and PGD genes for the *T. curticornis* and *T. heusdensis* species complexes. Effective sample sizes (ESS) and trace plots were examined in Tracer 1.6 and used as convergence diagnostics. A burn-in of one million generations was used to avoid suboptimal trees in the

final consensus tree. Ultrametric maximum clade credibility (MCC) trees were computed using the mean node heights with TreeAnnotator v1.8.2. Trees were visualized using FigTree 1.4.3 (available at http://tree.bio.ed.ac.uk/software/figtree).

We used algorithm 0 with a default fine-tuning parameter ε = 2, and species model prior with 1 as uniform rooted trees. The estimation of the marginal posterior probability of speciation associated with each node in the guide tree is performed by summarizing the probabilities for all models that support a particular speciation event with probability values of ⩾95% (Leaché & Fujita 2010). The posterior probabilities for models can be mainly affected by the prior distributions on the ancestral population size (θ) and root age (τ), with large values for θ and small values for τ favouring conservative models containing fewer species (Yang & Rannala 2010). Since no empirical data were available for the studied species, we ran the species delimitation analyses by the following combinations of gamma distributions: 1. Θ: G (2: 1000), τ: G (2: 200); 2. Θ: G (2: 1000), τ: G (2: 2000); 3. Θ: G (2: 100), τ: G (2: 200); 4. Θ: G (2: 100), τ: G (2: 2000); 5. Θ: G (2: 100), τ: G (2: 500). All BPP analyses were run for 500,000 generations with sampling every five generations, after discarding an initial burn-in of 20,000 generations. Heredity scalars were set to 1.0 for AATS1, COI, CAD1 and PGD, while algorithm was set to "0". Every analysis was run twice to check for convergence between runs and agreement on the posterior probability of the species delimitation models.

3. Result and discussion

3.1 Sequencing results

The aligned length for the four loci used in the full analysis were: AATS1 (408), CAD1 (909), COI (658), PGD (747). The number of variable and parsimony informative sites as well as the average nucleotide composition in each genetic marker are shown in Tables S3–4. The COI

sequences were heavily AT-biased, especially in third position (>82%), in both two species complexes.

3.2 ABGD

In the *T. curticornis* species complex, the COI sequences were sorted into ten molecular OTUs, but no clear "barcode gap" was observed in the pairwise K2P distances due to deep intraspecific divergences in some morphospecies (Fig. S1A). For the *T. heusdensis* species complex, two gaps were detected (Fig. S1B), and the COI sequences were sorted into five molecular OTUs when the threshold was placed at 9% based on the gap in the distribution of pairwise nucleotide distances (Fig. S1B).

3.3 Phylogenetic analyses

The phylogenetic analyses under ML and Bayesian inference produced identical trees in the *T. curticornis* and *T. heusdensis* species complexes for the concatenated nuclear genes data. In the *T. curticornis* species complex, the concatenated nuclear genes data yielded ten well-supported monophyletic groups (Fig. 1). A population of *T. brundini* from Sølendet, Norway was separated from other populations of *T. brundini* in all three nuclear markers (Fig. 1) and in the trees resulting from analyses of a concatenated mitochondrial and nuclear dataset (Fig. 2). All *T. brundini* sequences clustered together in the trees based on COI barcodes (Fig. 3). In the *T. heusdensis* species complex, the dataset based on concatenated nuclear genes as well as the dataset based on COI barcodes yielded five well supported monophyletic groups (Fig. 4A, B).

3.4 Patterns of genotype diversity

For the *T. curticornis* species complex, generally the networks based on mitochondrial and nuclear genes showed ten genetic groups (Figs. 5–6). However, sequences of *T.* sp.23XL were

sorted into one genetic group in AATS1 gene network, two haplotype groups in COI and two genotype group in CAD1. The PGD marker gave three genotype groups. Furthermore, sequences of *T. brundini* were arranged into one haplotype in the COI network, and two genetic groups in all networks based on nuclear markers (Figs. 5B, 6).

For the *T. heusdensis* species complex, the TCS network of mitochondrial haplotypes showed six genetic groups where the sequences of *T. reei* split into two haplotype groups (Fig. 7A) resulting from the high intraspecific divergence in COI sequences for this species. As expected, the TCS networks based on all three nuclear alleles confirmed the results obtained in the phylogenetic trees and retrieved five genetic groups (Fig. 7B-D).

3.5 *Species delimitation*

3.5.1 Species delimitation with GMYC

In the *T. curticornis* species complex, the GMYC model resulted in a slight over-splitting in COI- (Fig. S2), CAD1- (Fig. S3) and PGD-data (Fig. S4) varying between 10–14 OTUs (Table 2). Surprisingly, the GMYC analysis of AATS1 using an ultrametric tree with 44 terminals returned a result where only three OTUs were distinguished (Fig. 8). This might be a result of insufficient sampling, low intraspecific divergences and recent speciation of the *T. curticornis* species complex (Timothy Barraclough pers. comm.). We excluded a few sequences with little divergence and generated a new ultrametric tree with 33 individuals under the same settings in BEAST. This AATS1 dataset yielded seven OTUs (Fig. 9). We also ran the smaller dataset for AATS1 using different ultrametric input trees, but still got a lower number of distinguished clusters (3–7 OTUs) compared to the other markers. However, recent and rapid divergences can result in uncertainty in the GMYC model and lead to a certain tendency of over-lumping (Esselstyn et al. 2012; Reid & Carstens 2012). Given the observed variation in AATS1 and the results of the other analyses presented here, it is

difficult to explain how recent and divergence should influence the results of the AATS1 dataset and we speculate that the observed pattern might be caused by systematic errors with the GMYC model.

In the *T. heusdensis* species complex, the GMYC analyses delimited five species with a single threshold. The most likely solution showed concordant results between all nuclear markers and corresponded well to defined morphospecies. The analyses of CAD1 (Fig. S5) and PGD (Fig. S6) both distinguished five molecular OTUs, but since we failed to amplify the AATS1 segment for *T.* sp.7XL, this marker resulted in four distinct molecular OTUs for the *T. heusdensis* species complex (Fig. S7). For COI, GMYC analysis resulted in six distinguished clusters as geographically divergent populations of *T. reei* from Germany and Eastern Asia formed two separate OTUs (Fig. S8). The lack of similar pattern in the nuclear sequence datasets is difficult to explain, but could be due to higher evolutionary rate of the COI barcodes. Thus, in the *T. heusdensis* species complex, species delimitations based on the AATS1, CAD1 and PGD nuclear markers appear more reliable than those using the mitochondrial COI gene.

Table 2. Results of species delimitation with GMYC model

Gene	OTUs	Likelihood of null model	Maximum likelihood of GMYC model	Likelihood ratio
T. curticornis species complex				
COI	10	196.7564	203.6784	13.84397
AATS1	3–7	210.2633–299.4416	211.2459–300.2484	1.613635–1.965244
CAD1	12	365.6418	367.1871	3.090735
PGD	14	326.1291	328.7436	5.229101
T. heusdensis species complex				
COI	6	62.55684	69.92735	14.74101
AATS1	4	30.13732	34.00053	7.726431
CAD1	5	40.20682	42.42386	4.434082
PGD	5	33.71124	37.10057	6.778666

3.5.2 Species delimitation with PTP and bPTP

The bPTP analysis of COI for the *T. curticornis* species complex failed to reach convergence by 500,000 MCMC generations which is the upper limit of the web server. Disregarding this, the PTP and bPTP analyses yielded similar result with the GMYC analysis of the COI-, CAD1- and PGD datasets delineating 10–14 OTUs (Table 3). For the marker AATS1, the PTP and bPTP analyses resulted in 14 and 16 OTUs respectively, considerably higher than the results of the GMYC analyses as well as more than the expected nine morphospecies. The PTP and bPTP analyses of the *T. heusdensis* species complex yielded same results as the GMYC model, delineating 4–6 OTUs for each marker (Table 3).

Table 3. Results of species delimitation with PTP and bPTP models

	T. curticornis species complex			*T. heusdensis* species complex		
	PTP	bPTP	Accptance rate	PTP	bPTP	Accptance rate
COI	10 OTUs	-	0.52	6 OTUs	6 OTUs	0.39
AATS1	14 OTUs	16 OTUs	0.67	4 OTUs	4 OTUs	0.34
CAD1	11 OTUs	11 OTUs	0.38	5 OTUs	5 OTUs	0.37
PGD	13 OTUs	14 OTUs	0.56	5 OTUs	5 OTUs	0.39

3.5.3 Species delimitation with BPP

Initial runs showed errors in the RJ fine-tune variable (<= 0) when the parameters were set as follow: Θ: G (2: 100), τ0: G (2: 2000) and Θ: G (2: 100), τ0: G (2: 1000). Thus, we used the parameters as Θ: G (2: 100), τ0: G (2: 500) in the final runs. The results from BPP analyses on the concatenated datasets of both nuclear genes and all genes (including COI), showed that 15 candidate species were well supported (posterior probabilities 0.99–1.00) (Table 4). The *T. curticornis* species complex was divided into ten species where the Sølendet population of *Tanytarsus brundini* was isolated as a separate species. For the *T. heusdensis* species complex, both datasets isolated five species in the BPP analyses.

Table 4. Posterior probabilities for the number of delimited species using different priors for model parameters in BPP on concatenated datasets of nuclear markers and all genetic markers.

Prior	Posterior probability for the number of delimited species (all nuclear genes)	Posterior probability for the number of delimited species (all genes)
Θ: G (2: 1000), τ: G (2: 200)	P_{15} = 1.000	P_{13} =1.000
Θ: G (2: 1000), τ: G (2: 2000)	P_{15} = 1.000	P_{15} =1.000
Θ: G (2: 100), τ: G (2: 200)	P_{15} = 0.995, P_{14} = 0.005	P_{15} = 0.999, P_{14} = 0.001
Θ: G (2: 100), τ: G (2: 500)	P_{15} = 0.995, P_{14} = 0.005	P_{15} = 0.999, P_{14} = 0.001

3.6 Discussion

Several previous studies have evaluated the performance of the species delimitation approaches used here on single-locus data. GMYC appears to have a tendency to over-splitting and sometimes over-lumping lineages by the sampling bias, differences in population size and speciation rates (Dellicour & Flot 2015; Esselstyn et al. 2012; Fujisawa & Barraclough 2013; Pentinsaari et al. 2016; Reid & Carstens 2012; Talavera et al. 2013). PTP generates more robust results or results that are highly congruent with GMYC (Pentinsaari et al. 2016; Tang et al. 2014). While ABGD and parsimony networks appear to perform well when speciation rates are low and interspecific divergence is high (Dellicour & Flot 2015). When sampling is comprehensive within species and effective population sizes are small, these species delimitation methods using single locus datasets generally yield the same results.

However, when intraspecific divergence is high and interspecific divergence is low, species delimitation models using single locus dataset often are unable to separate species properly. Moreover, non-monophyletic species caused by infrequent horizontal gene flow and incomplete lineage sorting may also lead to inaccurate species delimitation results when using single-locus dataset (Camargo et al. 2012; Fontaneto et al. 2015; Fujita et al. 2012). To overcome these problems, species delimitation using multiple loci can be used. The BPP

species delimitation method is perhaps the most popular method using multiple loci and has been proven efficient in species separation (Fehlauer-Ale et al. 2014; Leaché et al. 2017; Yang & Rannala 2010). Using various species delimitation approaches with different criteria and searching a consensus from different outcomes may increase our confidence regarding species boundaries of target groups.

In this study, species delimitation analyses based on single loci using ABGD, parsimony networks, GMYC and PTP give the same results for the *T. heusdensis* species complex, but different results for the *T. curticornis* species complex. The BPP species delimitation model is based on multiple loci and provides a result that better reflects the observations on morphological divergence.

The above results show that while the COI marker divides the *T. curticornis* species complex into nine lineages, the three nuclear genes identify ten lineages. The conflicting result between mitochondrial and nuclear genes is caused by a Norwegian population of *Tanytarsus brundini* which has COI sequences similar to other populations of *T. brundini*, while all nuclear markers show deep divergence. We are not able to detect morphological differences between the specimens of this particular population and other populations of *T. brundini*. It is widely recognized that the discordance among gene trees can be caused by the stochastic process of lineage sorting (Maddison 1997; Pamilo & Nei 1988) and numerous examples exist in literature. For instance, the phylogenetic incongruence in the *Drosophlia melanogaster* species complex is caused by incomplete lineage sorting (Pollard et al. 2006). Thus, incomplete lineage sorting in the nuclear markers is a possible explanation for the discordance between mitochondrial and nuclear gene trees. Another explanation can be horizontal gene transfer by infrequent hybridization between two cryptic species, resulting in equal mitochondrial genotypes while keeping divergent nuclear genomes. This pattern is previously

documented for crickets (Shaw 2002) and water fleas (Taylor et al. 2005) and would fit well with our observations.

Based on the observed genetic divergence, we searched and found fine but consistent morphological differences that separates six of the distinct clusters of the *T. curticornis* species complex from previously described species (*T.* sp.TE01, *T.* sp.4XL, *T.* sp.5XL, *T.* sp.13XL, *T.* sp.14XL, *T.* sp.23XL). These taxa are diagnosed and described elsewhere (Lin et al. submitted).

The five mitochondrial DNA lineages we previously identified in the *T. heusdensis* species complex (Lin et al. 2015) are also recognized in the analyses based on nuclear markers. The divergence among the *T. heusdensis* sensu lato lineages is on par with that between other recognized *Tanytarsus* species, suggesting that the complex as of now comprises five distinct species. Two are recognized as new to science based on morphology (*T.* sp.7XL and *T.* sp.20XL) and are described by Lin et al. (submitted).

Overall, DNA barcodes are effective in distinguishing chironomid species, and provide novel insight into the taxonomy of some groups. However, DNA barcodes sometimes fail to separate genetically distinct species, and can give inaccurate results due to deep intraspecific divergence (Meier et al. 2006; Zhou et al. 2009). Multiple reasons why gene trees and species trees are often not the same exist (Maddison 1997; Nichols 2001; Rosenberg 2002) and incomplete lineage sorting, insufficient taxon sampling, horizontal gene flow or recent speciation can be difficult to distinguish regardless of analytic method implemented. Thus, species delimitation analyses based on multiple loci with coalescent models is widely accepted as it improves the discovery, resolution, consistency, and stability of our understanding of species (Fujita et al. 2012; Leaché & Fujita 2010). Our findings are consistent with those of Dupuis et al. (2012) who found that one marker is not enough for

species delimitation in closely related animals and fungi. Also in insects, a multi-loci based species delimitation has proved to be more successful and favorable (Boykin et al. 2014; Dincă et al. 2011; Hsieh et al. 2014; Malausa et al. 2011; Song & Ahn 2014) as it is not equally susceptible to introgression. Our results are in agreement with this and demonstrate that species delimitation analyses based on multiple loci give a more convincing result than a single locus.

4. Conclusion

In our study, species delimitations based on the AATS1, CAD1 and PGD nuclear DNA markers proved a more reliable predictor of morphological variation than delimitations using the mitochondrial COI gene. Moreover, Bayesian species delimitation based on multiple loci gives a more reliable result than single locus based species delimitation methods. In total, 15 species of the *T. curticornis* and *T. heusdensis* species complexes were differentiated genetically except the Sølendet population of *Tanytarsus brundini*. The additional detection of morphological characters supported the species boundaries and led to the discovery of seven semi-cryptic species new to science.

5. Acknowledgments

This paper is part of the first author's thesis for the partial fulfilment of a PhD degree of the Norwegian University of Science and Technology, Norway, entitled "Systematics and evolutionary history of *Tanytarsus* van der Wulp, 1874 (Diptera: Chironomidae)".

Many thanks to Xin-Hua Wang and Chao Song (College of Life Sciences, Nankai University, China), Viktor Baranov (Leibniz Institute of Freshwater Ecology and Inland Fisheries, Berlin, Germany) for collecting and sending material, and Koichiro Kawai (Graduate School of Biosphere Science, Hiroshima University, Hiroshima, Japan) for sharing DNA barcode data and morphological observations of Japanese specimen.

6. References

Anderson, A.M., Stur, E. & Ekrem, T. (2013) Molecular and morphological methods reveal cryptic diversity and three new species of Nearctic *Micropsectra* (Diptera: Chironomidae). *Freshwater Science* **32:** 892–921.

Appeltans, W., Ahyong, S.T., Anderson, G., Angel, M.V., Artois, T., Bailly, N., Bamber, R., Barber, A., Bartsch, I., Berta, A., Blazewicz-Paszkowycz, M., Bock, P., Boxshall, G., Boyko, C.B., Brandao, S.N., Bray, R.A., Bruce, N.L., Cairns, S.D., Chan, T.Y., Cheng, L., Collins, A.G., Cribb, T., Curini-Galletti, M., Dahdouh-Guebas, F., Davie, P.J., Dawson, M.N., De Clerck, O., Decock, W., De Grave, S., de Voogd, N.J., Domning, D.P., Emig, C.C., Erseus, C., Eschmeyer, W., Fauchald, K., Fautin, D.G., Feist, S.W., Fransen, C.H., Furuya, H., Garcia-Alvarez, O., Gerken, S., Gibson, D., Gittenberger, A., Gofas, S., Gomez-Daglio, L., Gordon, D.P., Guiry, M.D., Hernandez, F., Hoeksema, B.W., Hopcroft, R.R., Jaume, D., Kirk, P., Koedam, N., Koenemann, S., Kolb, J.B., Kristensen, R.M., Kroh, A., Lambert, G., Lazarus, D.B., Lemaitre, R., Longshaw, M., Lowry, J., Macpherson, E., Madin, L.P., Mah, C., Mapstone, G., McLaughlin, P.A., Mees, J., Meland, K., Messing, C.G., Mills, C.E., Molodtsova, T.N., Mooi, R., Neuhaus, B., Ng, P.K., Nielsen, C., Norenburg, J., Opresko, D.M., Osawa, M., Paulay, G., Perrin, W., Pilger, J.F., Poore, G.C., Pugh, P., Read, G.B., Reimer, J.D., Rius, M., Rocha, R.M., Saiz-Salinas, J.I., Scarabino, V., Schierwater, B., Schmidt-Rhaesa, A., Schnabel, K.E., Schotte, M., Schuchert, P., Schwabe, E., Segers, H., Self-Sullivan, C., Shenkar, N., Siegel, V., Sterrer, W., Stohr, S., Swalla, B., Tasker, M.L., Thuesen, E.V., Timm, T., Todaro, M.A., Turon, X., Tyler, S., Uetz, P., van der Land, J., Vanhoorne, B., van Ofwegen, L.P., van Soest, R.W., Vanaverbeke, J., Walker-Smith, G., Walter, T.C., Warren, A., Williams, G.C., Wilson, S.P. & Costello, M.J. (2012) The magnitude of global marine species diversity. *Current Biology* **22:** 2189–2202.

Ballard, J.W.O. & Whitlock, M.C. (2004) The incomplete natural history of mitochondria. *Molecular Ecology* **13:** 729–744.

Boykin, L., Schutze, M., Krosch, M., Chomič, A., Chapman, T., Englezou, A., Armstrong, K., Clarke, A., Hailstones, D. & Cameron, S. (2014) Multi-gene phylogenetic analysis of south-east Asian pest members of the *Bactrocera dorsalis* species complex (Diptera: Tephritidae) does not support current taxonomy. *Journal of Applied Entomology* **138:** 235–253.

Camargo, A., Morando, M., Avila, L. & Sites Jr, J. (2012) Species delimitation with ABC and other coalescent-based methods in lizards of the *Liolaemus darwinii* complex (Squamata: Liolaemidae). *Evolution* **66:** 2834–2849.

Clement, M., Posada, D. & Crandall, K.A. (2000) TCS: a computer program to estimate gene genealogies. *Molecular Ecology* **9:** 1657–1659.

Clement, M., Snell, Q., Walker, P., Posada, D. & Crandall, K. (2002). TCS: estimating gene genealogies. Proceeding 16th International Parallel Distributed Processing Symposium, p. 184.

Costello, M.J., May, R.M. & Stork, N.E. (2013) Can we name Earth's species before they go extinct? *Science* **339:** 413–416.

Darriba, D., Taboada, G.L., Doallo, R. & Posada, D. (2012) jModelTest 2: more models, new heuristics and parallel computing. *Nature Methods* **9:** 772–772.

Dellicour, S. & Flot, J.F. (2015) Delimiting species-poor datasets using single molecular markers: a study of barcode gaps, haplowebs and GMYC. *Systematic Biology* **64:** 900–908.

Dincă, V., Lukhtanov, V.A., Talavera, G. & Vila, R. (2011) Unexpected layers of cryptic diversity in wood white *Leptidea* butterflies. *Nature Communications* **2:** 324.
Drummond, A.J., Suchard, M.A., Xie, D. & Rambaut, A. (2012) Bayesian phylogenetics with BEAUti and the BEAST 1.7. *Molecular Biology and Evolution* **29:** 1969–1973.
Dupuis, J.R., Roe, A.D. & Sperling, F.A. (2012) Multi-locus species delimitation in closely related animals and fungi: one marker is not enough. *Molecular Ecology* **21:** 4422–4436.
Edgar, R.C. (2004) MUSCLE: multiple sequence alignment with high accuracy and high throughput. *Nucleic Acids Research* **32:** 1792–1797.
Esselstyn, J.A., Evans, B.J., Sedlock, J.L., Khan, F.A.A. & Heaney, L.R. (2012) Single-locus species delimitation: a test of the mixed Yule–coalescent model, with an empirical application to Philippine round-leaf bats. *Proceedings of the Royal Society of London B: Biological Sciences* **279:** 3678–3686.
Fehlauer-Ale, K.H., Mackie, J.A., Lim-Fong, G.E., Ale, E., Pie, M.R. & Waeschenbach, A. (2014) Cryptic species in the cosmopolitan *Bugula neritina* complex (Bryozoa, Cheilostomata). *Zoologica Scripta* **43:** 193–205.
Folmer, O., Black, M., Hoeh, W., Lutz, R. & Vrijenhoek, R. (1994) DNA primers for amplification of mitochondrial cytochrome c oxidase subunit I from diverse metazoan invertebrates. *Molecular Marine Biology and Biotechnology* **3:** 294–299.
Fontaneto, D., Flot, J.F. & Tang, C.Q. (2015) Guidelines for DNA taxonomy, with a focus on the meiofauna. *Marine Biodiversity* **45:** 433–451.
Fossen, E.I., Ekrem, T., Nilsson, A.N. & Bergsten, J. (2016) Species delimitation in northern European water scavenger beetles of the genus *Hydrobius* (Coleoptera, Hydrophilidae). *ZooKeys* **564:** 71–120.
Fujisawa, T. & Barraclough, T.G. (2013) Delimiting species using single-locus data and the generalized mixed yule coalescent approach: a revised method and evaluation on simulated data sets. *Systematic Biology* **62:** 707–724.
Fujita, M.K., Leaché, A.D., Burbrink, F.T., McGuire, J.A. & Moritz, C. (2012) Coalescent-based species delimitation in an integrative taxonomy. *Trends in Ecology & Evolution* **27:** 480–488.
Gay, L., Neubauer, G., Zagalska-Neubauer, M., Debain, C., Pons, J.M., David, P. & Crochet, P.A. (2007) Molecular and morphological patterns of introgression between two large white-headed gull species in a zone of recent secondary contact. *Molecular Ecology* **16:** 3215–3227.
Giłka, W. & Paasivirta, L. (2009) Evaluation of diagnostic characters of the *Tanytarsus chinyensis* group (Diptera: Chironomidae), with description of a new species from Lapland. *Zootaxa* **2197:** 31–42.
Hart, M.W. & Sunday, J. (2007) Things fall apart: biological species form unconnected parsimony networks. *Biology Letters* **3:** 509–512.
Hasegawa, M., Kishino, H. & Yano, T. (1985) Dating of the human-ape splitting by a molecular clock of mitochondrial DNA. *Journal of Molecular Evolution* **22:** 160–174.
Hebert, P.D.N., Cywinska, A. & Ball, S.L. (2003a) Biological identifications through DNA barcodes. *Proceedings of the Royal Society of London B: Biological Sciences* **270:** 313–321.
Hebert, P.D.N., Ratnasingham, S. & de Waard, J.R. (2003b) Barcoding animal life: cytochrome c oxidase subunit 1 divergences among closely related species. *Proceedings of the Royal Society of London B: Biological Sciences* **270:** S96–S99.
Heckman, K.L., Mariani, C.L., Rasoloarison, R. & Yoder, A.D. (2007) Multiple nuclear loci reveal patterns of incomplete lineage sorting and complex species history within

western mouse lemurs (*Microcebus*). *Molecular Phylogenetics and Evolution* **43:** 353–367.
Hsieh, C.H., Ko, C.C., Chung, C.H. & Wang, H.Y. (2014) Multilocus approach to clarify species status and the divergence history of the *Bemisia tabaci* (Hemiptera: Aleyrodidae) species complex. *Molecular Phylogenetics and Evolution* **76:** 172–180.
Kieffer, J.J. (1911) Nouvelles descriptions de chironomides obtenus d'éclosion. *Bulletin de la Société d'Histoire naturelle de Metz* **27:** 1–60.
Kress, W.J., García-Robledo, C., Uriarte, M. & Erickson, D.L. (2015) DNA barcodes for ecology, evolution, and conservation. *Trends in Ecology & Evolution* **30:** 25–35.
Kumar, S., Stecher, G. & Tamura, K. (2016) MEGA7: Molecular Evolutionary Genetics Analysis version 7.0 for bigger datasets. *Molecular Biology and Evolution* **33:** 1870–1874.
Lanfear, R., Calcott, B., Ho, S.Y.W. & Guindon, S. (2012) PartitionFinder: Combined Selection of Partitioning Schemes and Substitution Models for Phylogenetic Analyses. *Molecular Biology and Evolution* **29:** 1695–1701.
Leaché, A.D. & Fujita, M.K. (2010) Bayesian species delimitation in West African forest geckos (Hemidactylus fasciatus). *Proceedings of the Royal Society of London B: Biological Sciences* **277:** 3071–3077.
Leaché, A.D., Grummer, J.A., Miller, M., Krishnan, S., Fujita, M.K., Böhme, W., Schmitz, A., Lebreton, M., Ineich, I. & Chirio, L. (2017) Bayesian inference of species diffusion in the West African *Agama agama* species group (Reptilia, Agamidae). *Systematics and Biodiversity* **15:** 192–203.
Leigh, J.W. & Bryant, D. (2015) popart: full-feature software for haplotype network construction. *Methods in Ecology and Evolution* **6:** 1110–1116.
Lin, X.L., Stur, E. & Ekrem, T. (2015) Exploring genetic divergence in a species-rich insect genus using 2790 DNA Barcodes. *PloS One* **10:** e0138993.
Lin, X.L., Stur, E. & Ekrem, T. (submitted) DNA barcodes and morphology reveal new semi-cryptic species of Chironomidae (Diptera). *Insect Systematics & Evolution*.
Lindeberg, B. (1963) Taxonomy, biology and biometry of *Tanytarsus curticornis* Kieff. and *T. brundini* n. sp. (Dipt., Chironomidae). *Annales Entomologici Fennici* **29:** 118–130.
Low, V.L., Takaoka, H., Pramual, P., Adler, P.H., Ya'cob, Z., Huang, Y.T., Da Pham, X., Ramli, R., Chen, C.D. & Wannaket, A. (2016) Delineating taxonomic boundaries in the largest species complex of black flies (Simuliidae) in the Oriental Region. *Scientific Reports* **6:** 20346.
Maddison, W. & Maddison, D. (2010) Mesquite: a modular system for evolutionary analysis. 2011; Version 2.75. *Available at: mesquiteproject. org/mesquite/download/download. html*.
Maddison, W.P. (1997) Gene trees in species trees. *Systematic Biology* **46:** 523–536.
Malausa, T., Fenis, A., Warot, S., Germain, J.F., Ris, N., Prado, E., Botton, M., Vanlerberghe-Masutti, F., Sforza, R. & Cruaud, C. (2011) DNA markers to disentangle complexes of cryptic taxa in mealybugs (Hemiptera: Pseudococcidae). *Journal of Applied Entomology* **135:** 142–155.
Martinsen, G.D., Whitham, T.G., Turek, R.J. & Keim, P. (2001) Hybrid populations selectively filter gene introgression between species. *Evolution* **55:** 1325–1335.
Meier, R., Shiyang, K., Vaidya, G. & Ng, P.K. (2006) DNA barcoding and taxonomy in Diptera: a tale of high intraspecific variability and low identification success. *Systematic Biology* **55:** 715–728.
Moritz, C. (2002) Strategies to protect biological diversity and the evolutionary processes that sustain it. *Systematic Biology* **51:** 238–254.

Moulton, J.K. & Wiegmann, B.M. (2004) Evolution and phylogenetic utility of CAD (rudimentary) among Mesozoic-aged Eremoneuran Diptera (Insecta). *Molecular Phylogenetics and Evolution* **31:** 363–378.
Na, K.B. & Bae, Y.J. (2010) New Species of *Stictochironomus*, *Tanytarsus* and *Conchapelopia* (Diptera: Chironomidae) from Korea. *Entomological Research Bulletin* **26:** 33–39.
Nichols, R. (2001) Gene trees and species trees are not the same. *Trends in Ecology & Evolution* **16:** 358–364.
Pamilo, P. & Nei, M. (1988) Relationships between gene trees and species trees. *Molecular Biology and Evolution* **5:** 568–583.
Paz, A. & Crawford, A.J. (2012) Molecular-based rapid inventories of sympatric diversity: a comparison of DNA barcode clustering methods applied to geography-based vs clade-based sampling of amphibians. *Journal of Biosciences* **37:** 887–896.
Pentinsaari, M., Vos, R. & Mutanen, M. (2016) Algorithmic single-locus species delimitation: effects of sampling effort, variation and nonmonophyly in four methods and 1870 species of beetles. *Molecular Ecology Resources***:** http://dx.doi.org/10.1111/1755-0998.12557.
Pimm, S.L., Jenkins, C.N., Abell, R., Brooks, T.M., Gittleman, J.L., Joppa, L.N., Raven, P.H., Roberts, C.M. & Sexton, J.O. (2014) The biodiversity of species and their rates of extinction, distribution, and protection. *Science* **344:** 1246752.
Pollard, D.A., Iyer, V.N., Moses, A.M. & Eisen, M.B. (2006) Widespread discordance of gene trees with species tree in *Drosophila*: evidence for incomplete lineage sorting. *PLOS Genetics* **2:** e173.
Pons, J., Barraclough, T.G., Gomez-Zurita, J., Cardoso, A., Duran, D.P., Hazell, S., Kamoun, S., Sumlin, W.D. & Vogler, A.P. (2006) Sequence-based species delimitation for the DNA taxonomy of undescribed insects. *Systematic Biology* **55:** 595–609.
Puillandre, N., Lambert, A., Brouillet, S. & Achaz, G. (2012) ABGD, Automatic Barcode Gap Discovery for primary species delimitation. *Molecular Ecology* **21:** 1864–1877.
Rambaut, A., Suchard, M.A., Xie, D. & Drummond, A.J. (2014) Tracer v1.6, Available from http://beast.bio.ed.ac.uk/Tracer.
Rannala, B. & Yang, Z. (2013) Improved reversible jump algorithms for Bayesian species delimitation. *Genetics* **194:** 245–253.
Ratnasingham, S. & Hebert, P.D.N. (2007) BOLD: The Barcode of Life Data System (www.barcodinglife.org). *Molecular Ecology Notes* **7:** 355–364.
Ratnasingham, S. & Hebert, P.D.N. (2013) A DNA-based registry for all animal species: the barcode index number (BIN) system. *PloS One* **8:** e66213.
Regier, J.C., Shultz, J.W., Ganley, A.R., Hussey, A., Shi, D., Ball, B., Zwick, A., Stajich, J.E., Cummings, M.P. & Martin, J.W. (2008) Resolving arthropod phylogeny: exploring phylogenetic signal within 41 kb of protein-coding nuclear gene sequence. *Systematic Biology* **57:** 920–938.
Reid, N.M. & Carstens, B.C. (2012) Phylogenetic estimation error can decrease the accuracy of species delimitation: a Bayesian implementation of the General Mixed Yule-Coalescent model. *BMC Evolutionary Biology* **12:** 196.
Reiss, F. & Fittkau, E.J. (1971) Taxonomie und Ökologie europäisch verbreiteter *Tanytarsus*-Arten (Chironomidae, Diptera). *Archiv für Hydrobiologie, Supplement* **40:** 75–200.
Rogers, J. & Wall, R. (1980) A mechanism for RNA splicing. *Proceedings of the National Academy of Sciences* **77:** 1877–1879.
Ronquist, F., Teslenko, M., van der Mark, P., Ayres, D.L., Darling, A., Höhna, S., Larget, B., Liu, L., Suchard, M.A. & Huelsenbeck, J.P. (2012) MrBayes 3.2: efficient bayesian

phylogenetic inference and model choice across a large model space. *Systematic Biology* **61:** 539–542.
Rosenberg, N.A. (2002) The probability of topological concordance of gene trees and species trees. *Theoretical Population Biology* **61:** 225–247.
Sæther, O.A. (1969) Some Nearctic Pondonominae, Diamesinae, and Orthocladiinae (Diptera: Chironomidae). *Bulletin of the Fisheries Research Board of Canada* **170:** 1–154.
Sasa, M. (1980) Studies on chironomid midges of the Tama River. Part 2. Description of 20 species of Chironominae recovered from a tributary. *Research Report from the National Institute for Environmental Studies, Japan* **13:** 9–107.
Shaw, K.L. (2002) Conflict between nuclear and mitochondrial DNA phylogenies of a recent species radiation: what mtDNA reveals and conceals about modes of speciation in Hawaiian crickets. *Proceedings of the National Academy of Sciences* **99:** 16122–16127.
Silvestro, D. & Michalak, I. (2012) raxmlGUI: a graphical front-end for RAxML. *Organisms Diversity & Evolution* **12:** 335–337.
Song, J.H. & Ahn, K.J. (2014) Species delimitation in the *Aleochara fucicola* species complex (Coleoptera: Staphylinidae: Aleocharinae) and its phylogenetic relationships. *Zoologica Scripta* **43:** 629–640.
Stamatakis, A. (2006) RAxML-VI-HPC: maximum likelihood-based phylogenetic analyses with thousands of taxa and mixed models. *Bioinformatics* **22:** 2688–2690.
Stamatakis, A. (2014) RAxML version 8: a tool for phylogenetic analysis and post-analysis of large phylogenies. *Bioinformatics* **30:** 1312–1313.
Su, K.F.Y., Narayanan Kutty, S. & Meier, R. (2008) Morphology versus molecules: the phylogenetic relationships of Sepsidae (Diptera: Cyclorrhapha) based on morphology and DNA sequence data from ten genes. *Cladistics* **24:** 902–916.
Talavera, G., Dincă, V. & Vila, R. (2013) Factors affecting species delimitations with the GMYC model: insights from a butterfly survey. *Methods in Ecology and Evolution* **4:** 1101–1110.
Tang, C.Q., Humphreys, A.M., Fontaneto, D. & Barraclough, T.G. (2014) Effects of phylogenetic reconstruction method on the robustness of species delimitation using single-locus data. *Methods in Ecology and Evolution* **5:** 1086–1094.
Tänzler, R., Sagata, K., Surbakti, S., Balke, M. & Riedel, A. (2012) DNA barcoding for community ecology-how to tackle a hyperdiverse, mostly undescribed Melanesian fauna. *PloS One* **7:** e28832.
Tavaré, S. (1986) Some probabilistic and statistical problems in the analysis of DNA sequences. *Lectures on mathematics in the life sciences* **17:** 57–86.
Taylor, D.J., Sprenger, H.L. & Ishida, S. (2005) Geographic and phylogenetic evidence for dispersed nuclear introgression in a daphniid with sexual propagules. *Molecular Ecology* **14:** 525–537.
Templeton, A.R., Crandall, K.A. & Sing, C.F. (1992) A cladistic analysis of phenotypic associations with haplotypes inferred from restriction endonuclease mapping and DNA sequence data. III. Cladogram estimation. *Genetics* **132:** 619–633.
Vaidya, G., Lohman, D.J. & Meier, R. (2011) SequenceMatrix: concatenation software for the fast assembly of multi-gene datasets with character set and codon information. *Cladistics* **27:** 171–180.
Willyard, A., Cronn, R. & Liston, A. (2009) Reticulate evolution and incomplete lineage sorting among the ponderosa pines. *Molecular Phylogenetics and Evolution* **52:** 498–511.
Yang, Z. (2015) The BPP program for species tree estimation and species delimitation. *Current Zoology* **61:** 854–865.

Yang, Z. & Rannala, B. (2010) Bayesian species delimitation using multilocus sequence data. *Proceedings of the National Academy of Sciences* **107:** 9264–9269.
Yang, Z. & Rannala, B. (2017) Bayesian species identification under the multispecies coalescent provides significant improvements to DNA barcoding analyses. *Molecular Ecology***:** http://dx.doi.org/10.1111/mec.14093.
Zhang, J., Kapli, P., Pavlidis, P. & Stamatakis, A. (2013) A general species delimitation method with applications to phylogenetic placements. *Bioinformatics* **29:** 2869–2876.
Zhou, X., Adamowicz, S.J., Jacobus, L.M., DeWalt, R.E. & Hebert, P.D.N. (2009) Towards a comprehensive barcode library for arctic life-Ephemeroptera, Plecoptera, and Trichoptera of Churchill, Manitoba, Canada. *Frontiers in Zoology* **6:** 30.

Figure captions

Figure 1. Maximum likelihood tree based on the concatenated nuclear dataset of the *Tanytarsus curticornis* species complex. Bootstrap support (1000 replicates) and posterior probabilities of nodes are indicated above and below the branches, respectively. Only nodes with BS>70% and/or BP>0.95 are labelled.

Figure 2. Maximum likelihood tree based on the concatenated mitochondrial and nuclear dataset of the *Tanytarsus curticornis* species complex. Bootstrap support (1000 replicates) and posterior probabilities of nodes are indicated above and below the branches, respectively. Only nodes with BS>70% and/or BP>0.95 are labelled.

Figure 3. Maximum likelihood tree based on the COI barcodes of the *Tanytarsus curticornis* species complex. Bootstrap support (1000 replicates) and posterior probabilities of nodes are indicated above and below the branches, respectively. Only nodes with BS>70% and/or BP>0.95 are labelled.

Figure 4. Maximum likelihood tree based on the COI (A) and the concatenated nuclear (B) datasets of the *Tanytarsus heusdensis* species complex. Bootstrap support (1000 replicates) and posterior probabilities of nodes are indicated above and below the branches, respectively. Only nodes with BS>70% and/or BP>0.95 are labelled.

Figure 5. TCS haplotype/genotype networks based on the mitochondrial COI (A) and the nuclear CAD1 (B) datasets of the *Tanytarsus curticornis* species complex. Different colours correspond to the different putative species. Mutations are shown as lines on the branches.

Figure 6. TCS genotype networks based on the nuclear AATS1 (A) and PGD (B) datasets of the *Tanytarsus curticornis* species complex. Different colours correspond to the different putative species. Mutations are shown as lines on the branches.

Figure 7. TCS haplotype/genotype networks based on the mitochondrial COI (A) and the nuclear AATS1 (B), CAD (C), PGD (D) datasets of the *Tanytarsus heusdensis* species complex. Different colours correspond to the different putative species. Mutations are shown as lines on the branches.

Figure 8. Results of the species delimitation analysis for the *Tanytarsus curticornis* species complex according to the GMYC single-threshold model on the AATS1 dataset with 44 individuals. (A) Lineage-through-time plot based on the ultrametric tree obtained from AATS1 sequences. The sharp increase in branching rate, corresponding to the transition from interspecific to intraspecific branching events, is indicated by a red vertical line. The x-axes (both in panels A and B) show substitutions per nucleotide site; (B) likelihood function produced by GMYC to estimate the peak of transition between cladogenesis (interspecific diversification) and allele intraspecific coalescence along the branches; (C) ultrametric tree with 44 individuals obtained in BEAST setting coalescent prior and strict clock model. Red clusters and black lines (singletons) indicate putative species calculated by the model.

Figure 9. Results of the species delimitation analysis for the *Tanytarsus curticornis* species complex according to the GMYC single-threshold model on the AATS1 dataset with 33 individuals. (A) Lineage-through-time plot based on the ultrametric tree obtained

from AATS1 sequences. The sharp increase in branching rate, corresponding to the transition from interspecific to intraspecific branching events, is indicated by a red vertical line. The x-axes (both in panels A and B) show substitutions per nucleotide site; (B) likelihood function produced by GMYC to estimate the peak of transition between cladogenesis (interspecific diversification) and allele intraspecific coalescence along the branches; (C) ultrametric tree with 33 individuals obtained in BEAST setting coalescent prior and strict clock model. Red clusters and black lines (singletons) indicate putative species calculated by the model.

Figure 1

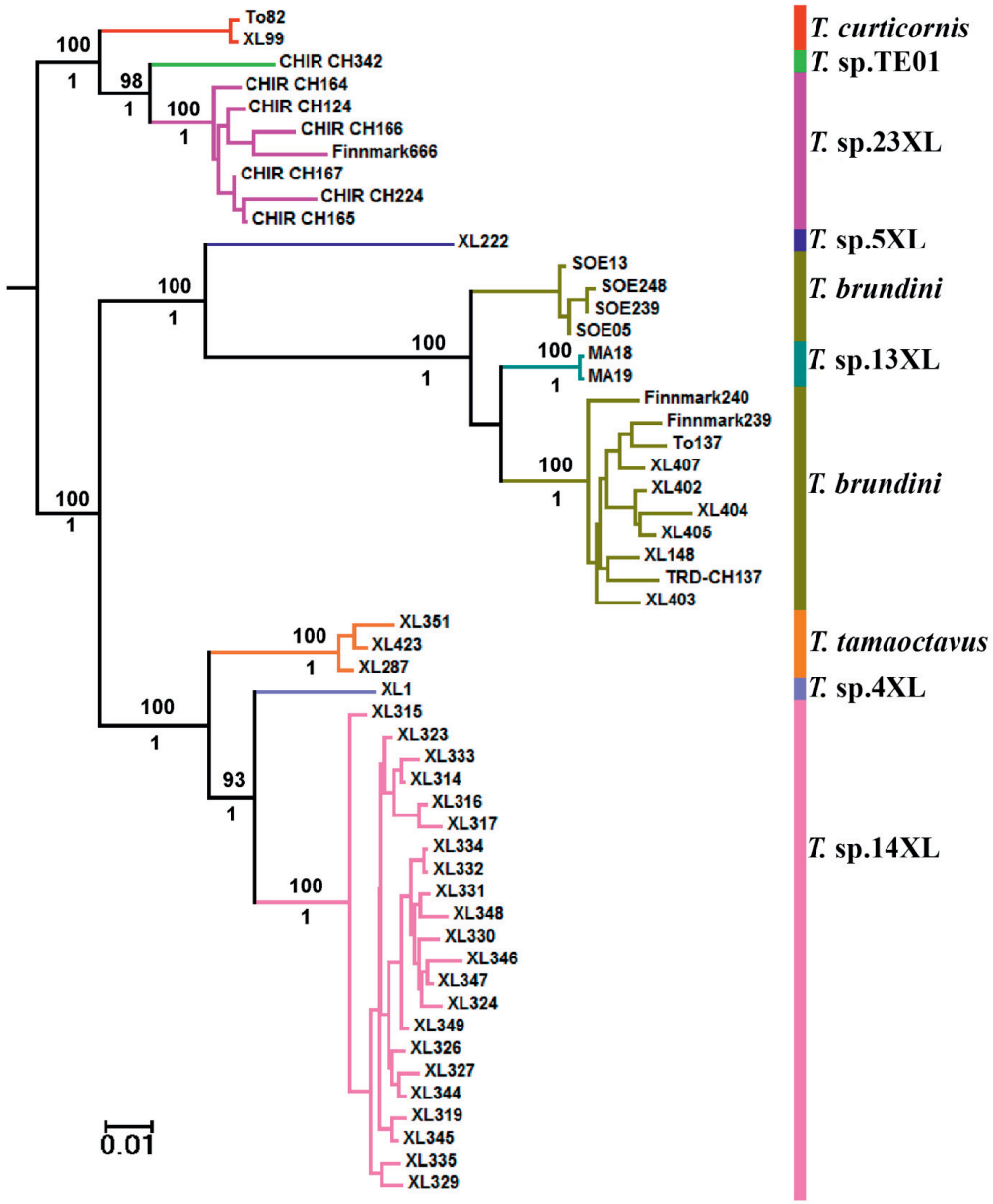
To82
XL99
CHIR CH342
CHIR CH164
CHIR CH124
CHIR CH166
Finnmark666
CHIR CH167
CHIR CH224
CHIR CH165
XL222
SOE13
SOE248
SOE239
SOE05
MA18
MA19
Finnmark240
Finnmark239
To137
XL407
XL402
XL404
XL405
XL148
TRD-CH137
XL403
XL351
XL423
XL287
XL1
XL315
XL323
XL333
XL314
XL316
XL317
XL334
XL332
XL331
XL348
XL330
XL346
XL347
XL324
XL349
XL326
XL327
XL344
XL319
XL345
XL335
XL329
0.01
T. curticornis
T. sp.TE01
T. sp.23XL
T. sp.5XL
T. brundini
T. sp.13XL
T. brundini
T. tamaoctavus
T. sp.4XL
T. sp.14XL

Figure 2

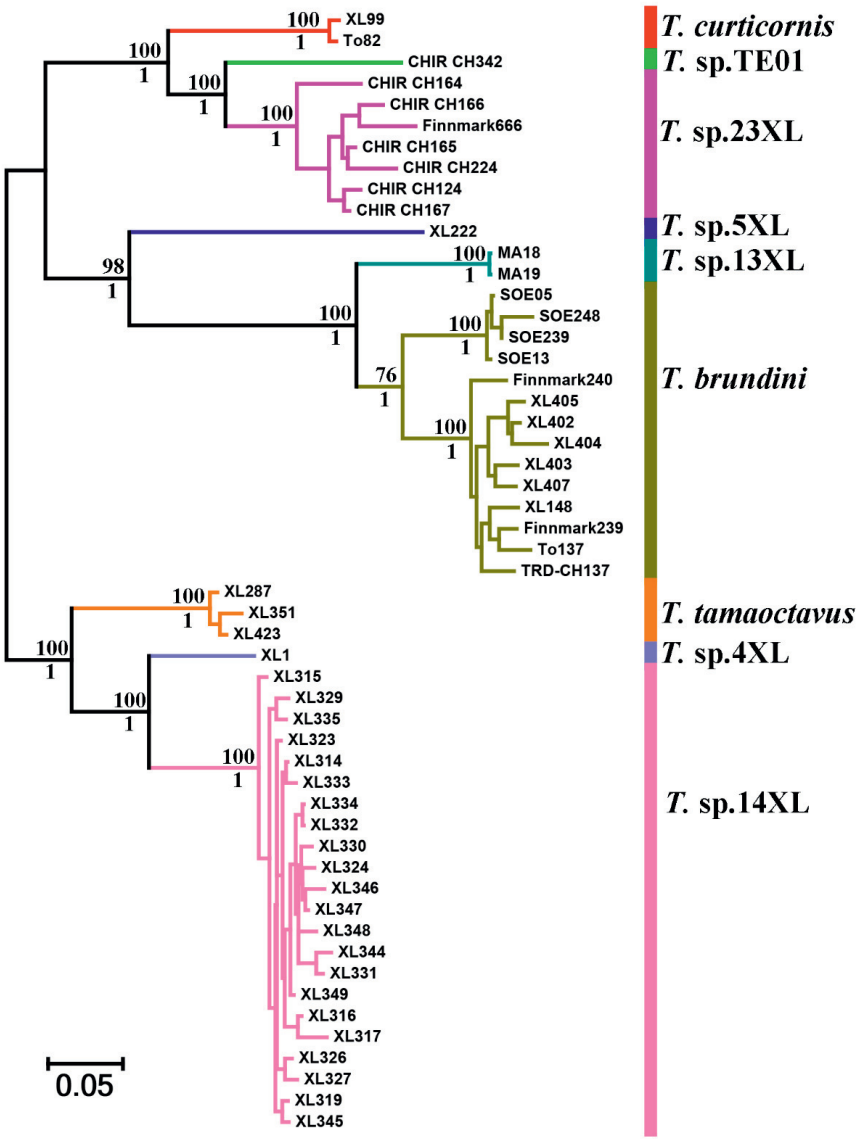
XL99
To82
CHIR CH342
CHIR CH164
CHIR CH166
Finnmark666
CHIR CH165
CHIR CH224
CHIR CH124
CHIR CH167
XL222
MA18
MA19
SOE05
SOE248
SOE239
SOE13
Finnmark240
XL405
XL402
XL404
XL403
XL407
XL148
Finnmark239
To137
TRD-CH137
XL287
XL351
XL423
XL1
XL315
XL329
XL335
XL323
XL314
XL333
XL334
XL332
XL330
XL324
XL346
XL347
XL348
XL344
XL331
XL349
XL316
XL317
XL326
XL327
XL319
XL345
0.05
T. curticornis
T. sp.TE01
T. sp.23XL
T. sp.5XL
T. sp.13XL
T. brundini
T. tamaoctavus
T. sp.4XL
T. sp.14XL

Figure 3

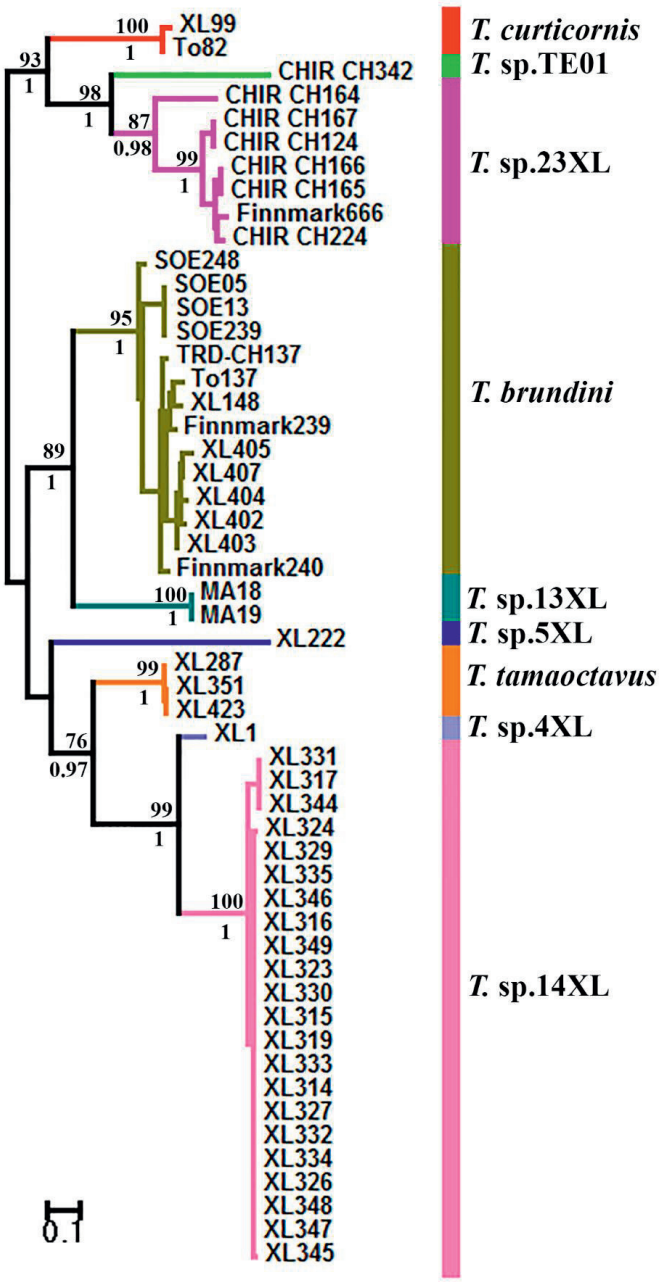
XL99
To82
CHIR CH342
CHIR CH164
CHIR CH167
CHIR CH124
CHIR CH166
CHIR CH165
Finnmark666
CHIR CH224
SOE248
SOE05
SOE13
SOE239
TRD-CH137
To137
XL148
Finnmark239
XL405
XL407
XL404
XL402
XL403
Finnmark240
MA18
MA19
XL222
XL287
XL351
XL423
XL1
XL331
XL317
XL344
XL324
XL329
XL335
XL346
XL316
XL349
XL323
XL330
XL315
XL319
XL333
XL314
XL327
XL332
XL334
XL326
XL348
XL347
XL345
0.1
T. curticornis
T. sp.TE01
T. sp.23XL
T. brundini
T. sp.13XL
T. sp.5XL
T. tamaoctavus
T. sp.4XL
T. sp.14XL

Figure 4

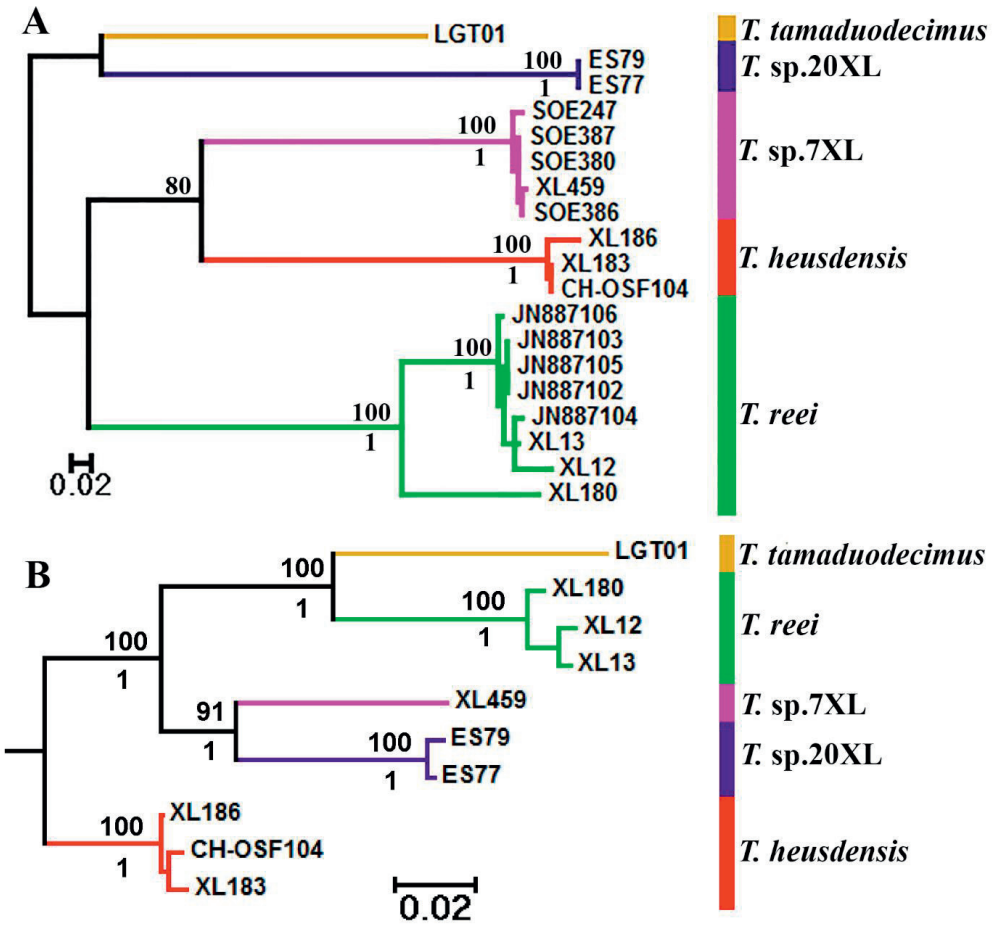
A
LGT01
100
1
ES79
ES77
100
1
SOE247
SOE387
SOE380
XL459
SOE386
80
100
1
XL186
XL183
CH-OSF104
JN887106
100
1
JN887103
JN887105
JN887102
100
1
JN887104
XL13
XL12
XL180
0.02
T. tamaduodecimus
T. sp.20XL
T. sp.7XL
T. heusdensis
T. reei
B
100
1
LGT01
100
1
XL180
XL12
XL13
100
1
91
1
XL459
100
1
ES79
ES77
100
1
XL186
CH-OSF104
XL183
0.02
T. tamaduodecimus
T. reei
T. sp.7XL
T. sp.20XL
T. heusdensis

Figure 5

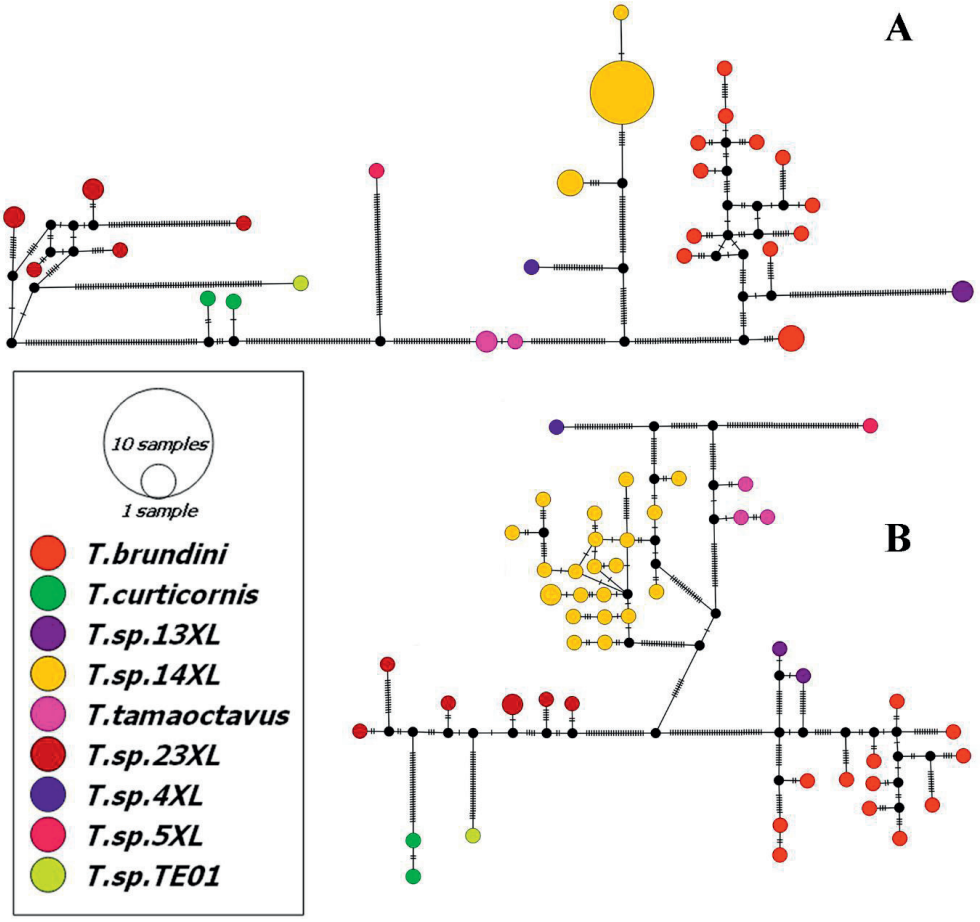
A
B
10 samples
1 sample
T.brundini
T.curticornis
T.sp.13XL
T.sp.14XL
T.tamaoctavus
T.sp.23XL
T.sp.4XL
T.sp.5XL
T.sp.TE01

Figure 6

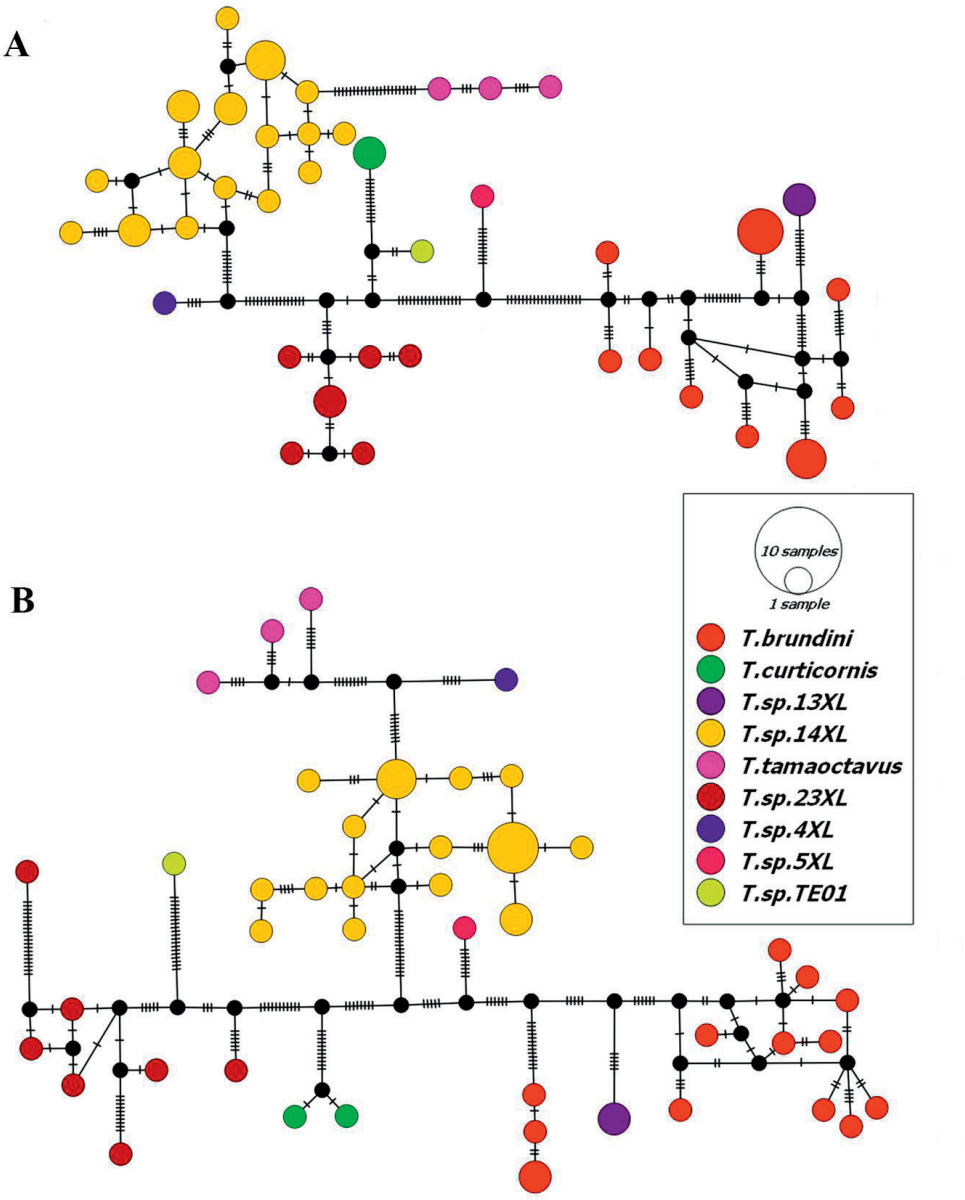
A
B
10 samples
1 sample
T.brundini
T.curticornis
T.sp.13XL
T.sp.14XL
T.tamaoctavus
T.sp.23XL
T.sp.4XL
T.sp.5XL
T.sp.TE01

Figure 7

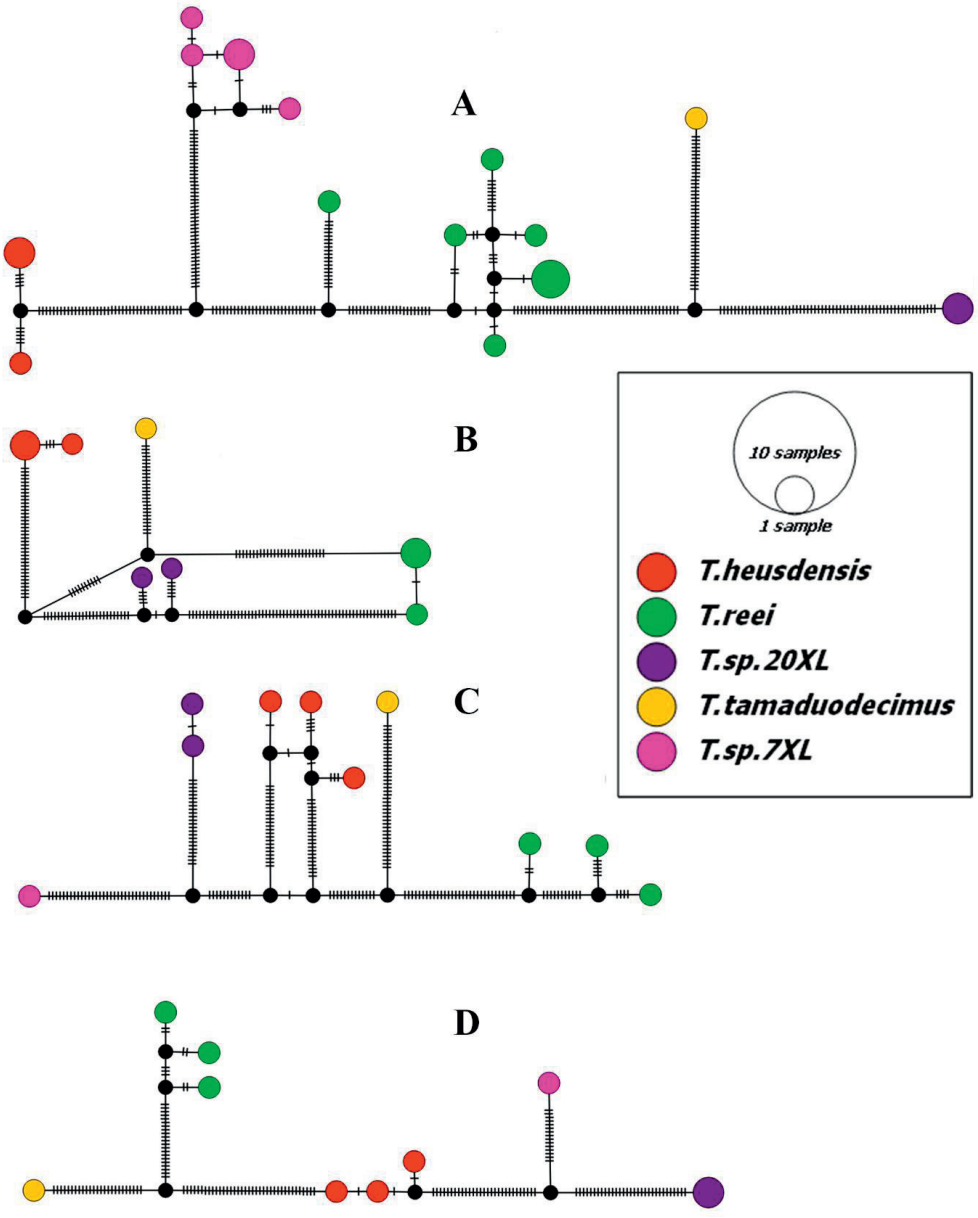
A
B
C
D
10 samples
1 sample
T.heusdensis
T.reei
T.sp.20XL
T.tamaduodecimus
T.sp.7XL

Figure 8

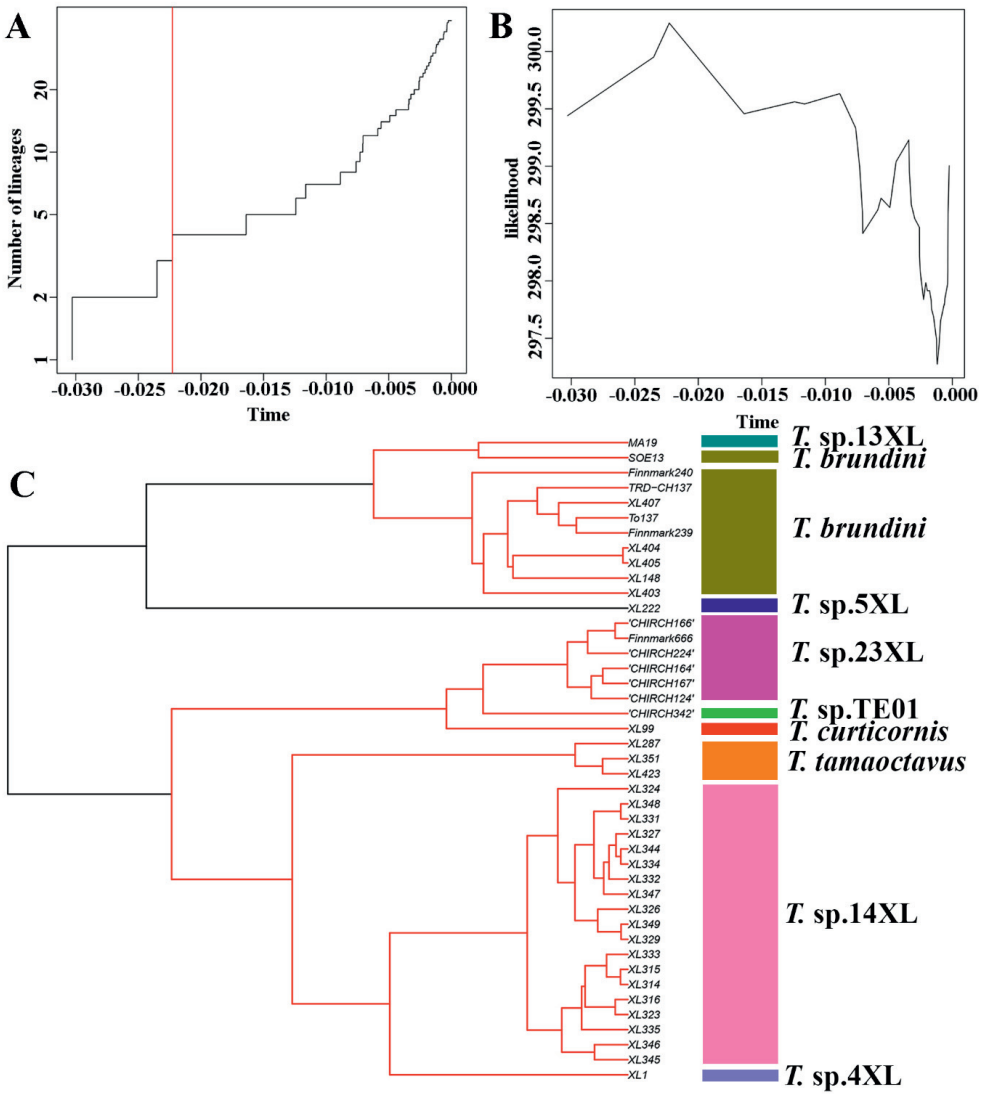
A
Number of lineages
1
2
5
10
20
-0.030 -0.025 -0.020 -0.015 -0.010 -0.005 0.000
Time
B
likelihood
297.5 298.0 298.5 299.0 299.5 300.0
-0.030 -0.025 -0.020 -0.015 -0.010 -0.005 0.000
Time
C
MA19
SOE13
Finnmark240
TRD-CH137
XL407
To137
Finnmark239
XL404
XL405
XL148
XL403
XL222
'CHIRCH166'
Finnmark666
'CHIRCH224'
'CHIRCH164'
'CHIRCH167'
'CHIRCH124'
'CHIRCH342'
XL99
XL287
XL351
XL423
XL324
XL348
XL331
XL327
XL344
XL334
XL332
XL347
XL326
XL349
XL329
XL333
XL315
XL314
XL316
XL323
XL335
XL346
XL345
XL1
T. sp.13XL
T. brundini
T. brundini
T. sp.5XL
T. sp.23XL
T. sp.TE01
T. curticornis
T. tamaoctavus
T. sp.14XL
T. sp.4XL

Figure 9

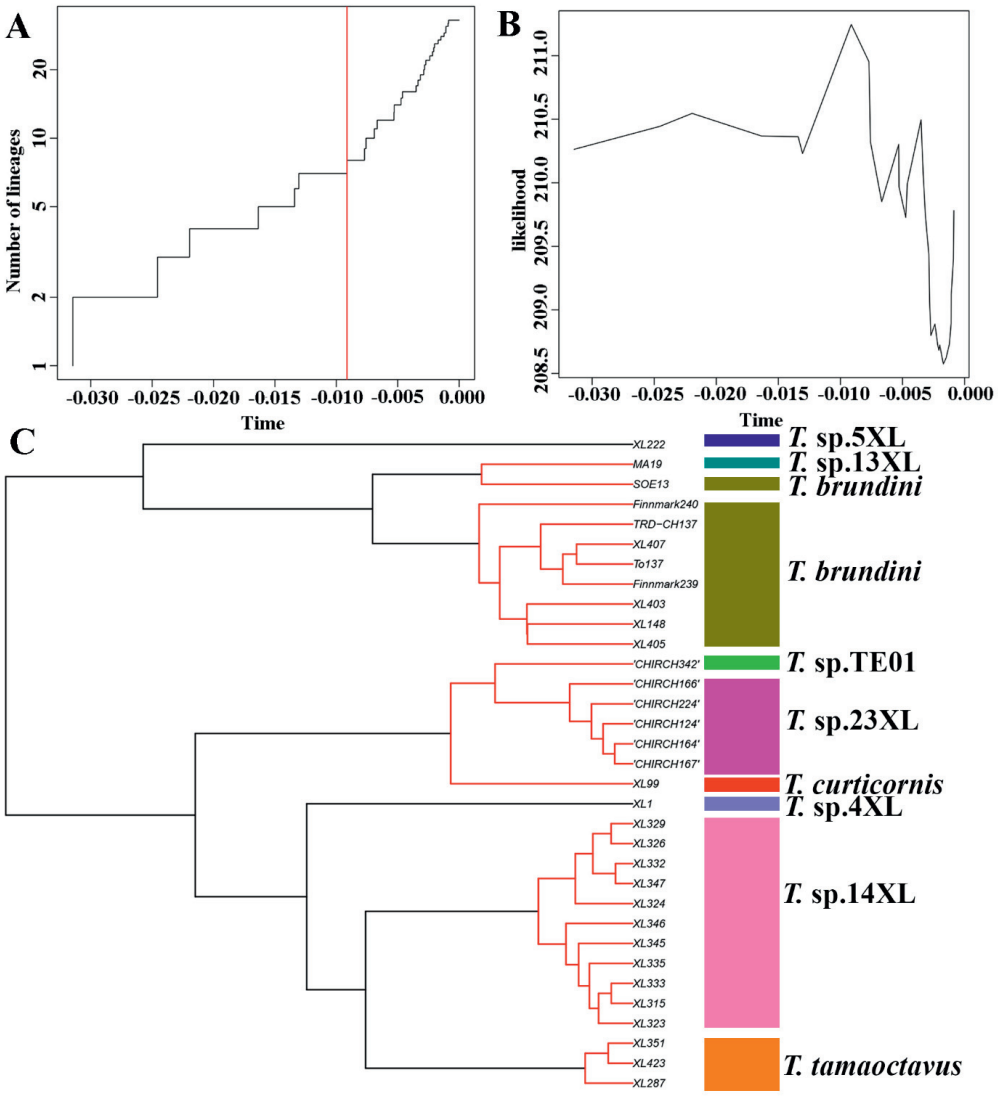
A
Number of lineages
1
2
5
10
20
-0.030 -0.025 -0.020 -0.015 -0.010 -0.005 0.000
Time
B
likelihood
208.5
209.0
209.5
210.0
210.5
211.0
-0.030 -0.025 -0.020 -0.015 -0.010 -0.005 0.000
Time
C
XL222
MA19
SOE13
Finnmark240
TRD−CH137
XL407
To137
Finnmark239
XL403
XL148
XL405
'CHIRCH342'
'CHIRCH166'
'CHIRCH224'
'CHIRCH124'
'CHIRCH164'
'CHIRCH167'
XL99
XL1
XL329
XL326
XL332
XL347
XL324
XL346
XL345
XL335
XL333
XL315
XL323
XL351
XL423
XL287
T. sp.5XL
T. sp.13XL
T. brundini
T. brundini
T. sp.TE01
T. sp.23XL
T. curticornis
T. sp.4XL
T. sp.14XL
T. tamaoctavus

8. Supplementary material

Figure S1. Histogram of pairwise K2P distance of COI barcodes for the *Tanytarsus curticornis* (A) and *T. heusdensis* (B) species complexes using ABGD. The x-axes show the pairwise K2P-distance, and the y-axis shows the number of pairwise sequence comparisons.

Figure S2. Results of the species delimitation analysis for the *Tanytarsus curticornis* species complex according to the GMYC single-threshold model on the COI dataset. (A) Lineage-through-time plot based on the ultrametric tree obtained from COI sequences. The sharp increase in branching rate, corresponding to the transition from interspecific to intraspecific branching events, is indicated by a red vertical line. The x-axes (both in panels A and B) show substitutions per nucleotide site; (B) likelihood function produced by GMYC to estimate the peak of transition between cladogenesis (interspecific diversification) and allele intraspecific coalescence along the branches; (C) ultrametric tree obtained in BEAST setting coalescent prior and strict clock model. Red clusters and black lines (singletons) indicate putative species calculated by the model.

Figure S3. Results of the species delimitation analysis for the *Tanytarsus curticornis* species complex according to the GMYC single-threshold model on the CAD1 dataset. (A) Lineage-through-time plot based on the ultrametric tree obtained from CAD1 sequences. The sharp increase in branching rate, corresponding to the transition from interspecific to intraspecific branching events, is indicated by a red vertical line. The x-axes (both in panels A and B) show substitutions per nucleotide site; (B) likelihood function produced by GMYC to estimate the peak of transition between cladogenesis (interspecific diversification) and allele intraspecific coalescence along the branches; (C) ultrametric tree obtained in BEAST setting coalescent prior and strict clock model. Red clusters and black lines (singletons) indicate putative species calculated by the model.

Figure S4. Results of the species delimitation analysis for the *Tanytarsus curticornis* species complex according to the GMYC single-threshold model on the PGD dataset. (A) Lineage-through-time plot based on the ultrametric tree obtained from PGD sequences. The sharp increase in branching rate, corresponding to the transition from interspecific to intraspecific branching events, is indicated by a red vertical line. The x-axes (both in panels A and B) show substitutions per nucleotide site; (B) likelihood function produced by GMYC to estimate the peak of transition between cladogenesis (interspecific diversification) and allele intraspecific coalescence along the branches; (C) ultrametric tree obtained in BEAST setting coalescent prior and strict clock model. Red clusters and black lines (singletons) indicate putative species calculated by the model.

Figure S5. Results of the species delimitation analysis for the *Tanytarsus heusdensis* species complex according to the GMYC single-threshold model on the CAD1 dataset. (A) Lineage-through-time plot based on the ultrametric tree obtained from CAD1 sequences. The sharp increase in branching rate, corresponding to the transition from interspecific to intraspecific branching events, is indicated by a red vertical line. The x-axes (both in panels A and B) show substitutions per nucleotide site; (B) likelihood function produced by GMYC to estimate the peak of transition between cladogenesis (interspecific diversification) and allele intraspecific coalescence along the branches; (C) ultrametric tree obtained in BEAST setting coalescent prior and strict clock model. Red clusters and black lines (singletons) indicate putative species calculated by the model.

Figure S6. Results of the species delimitation analysis for the *Tanytarsus heusdensis* species complex according to the GMYC single-threshold model on the PGD dataset. (A) Lineage-through-time plot based on the ultrametric tree obtained from PGD sequences. The sharp increase in branching rate, corresponding to the transition from interspecific to intraspecific branching events, is indicated by a red vertical line. The x-axes (both in panels A

and B) show substitutions per nucleotide site; (B) likelihood function produced by GMYC to estimate the peak of transition between cladogenesis (interspecific diversification) and allele intraspecific coalescence along the branches; (C) ultrametric tree obtained in BEAST setting coalescent prior and strict clock model. Red clusters and black lines (singletons) indicate putative species calculated by the model.

Figure S7. Results of the species delimitation analysis for the *Tanytarsus heusdensis* species complex according to the GMYC single-threshold model on the AATS1 dataset. (A) Lineage-through-time plot based on the ultrametric tree obtained from AATS1 sequences. The sharp increase in branching rate, corresponding to the transition from interspecific to intraspecific branching events, is indicated by a red vertical line. The x-axes (both in panels A and B) show substitutions per nucleotide site; (B) likelihood function produced by GMYC to estimate the peak of transition between cladogenesis (interspecific diversification) and allele intraspecific coalescence along the branches; (C) ultrametric tree obtained in BEAST setting coalescent prior and strict clock model. Red clusters and black lines (singletons) indicate putative species calculated by the model.

Figure S8. Results of the species delimitation analysis for the *Tanytarsus heusdensis* species complex according to the GMYC single-threshold model on the COI dataset. (A) Lineage-through-time plot based on the ultrametric tree obtained from COI sequences. The sharp increase in branching rate, corresponding to the transition from interspecific to intraspecific branching events, is indicated by a red vertical line. The x-axes (both in panels A and B) show substitutions per nucleotide site; (B) likelihood function produced by GMYC to estimate the peak of transition between cladogenesis (interspecific diversification) and allele intraspecific coalescence along the branches; (C) ultrametric tree obtained in BEAST setting coalescent prior and strict clock model. Red clusters and black lines (singletons) indicate putative species calculated by the model.

Figure S1

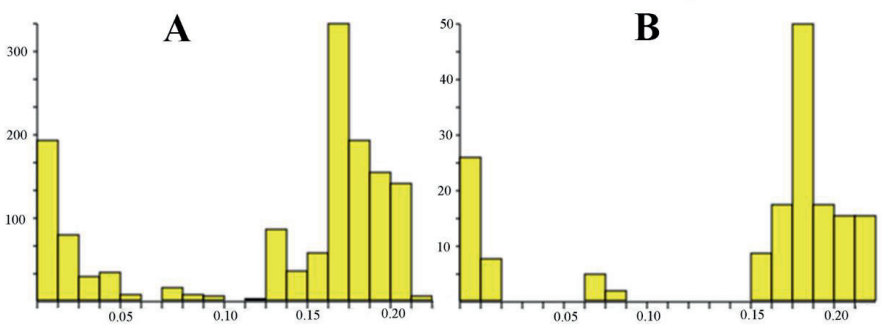

Figure S2

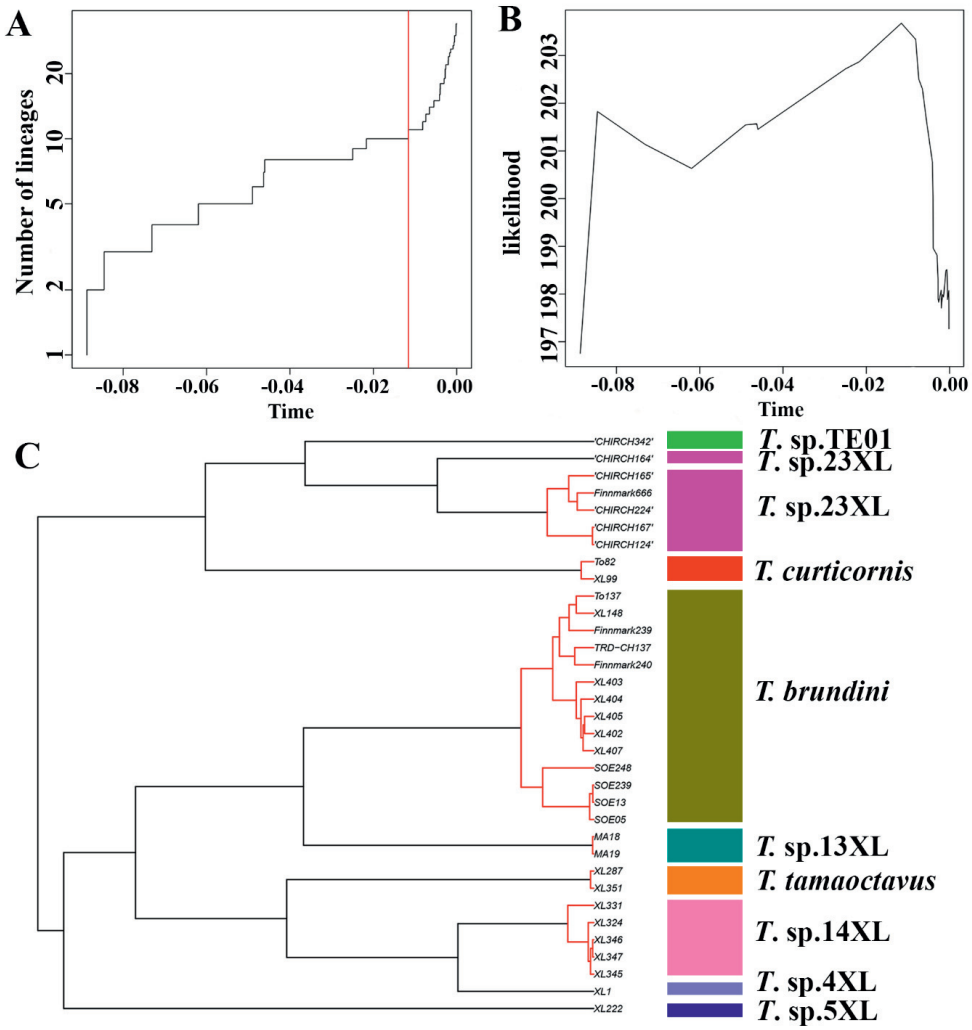
A
Number of lineages
1
2
5
10
20
-0.08
-0.06
-0.04
-0.02
0.00
Time
B
likelihood
197
198
199
200
201
202
203
-0.08
-0.06
-0.04
-0.02
0.00
Time
C
'CHIRCH342'
'CHIRCH164'
'CHIRCH165'
Finnmark666
'CHIRCH224'
'CHIRCH167'
'CHIRCH124'
To82
XL99
To137
XL148
Finnmark239
TRD-CH137
Finnmark240
XL403
XL404
XL405
XL402
XL407
SOE248
SOE239
SOE13
SOE05
MA18
MA19
XL287
XL351
XL331
XL324
XL346
XL347
XL345
XL1
XL222
T. sp.TE01
T. sp.23XL
T. sp.23XL
T. curticornis
T. brundini
T. sp.13XL
T. tamaoctavus
T. sp.14XL
T. sp.4XL
T. sp.5XL

Figure S3

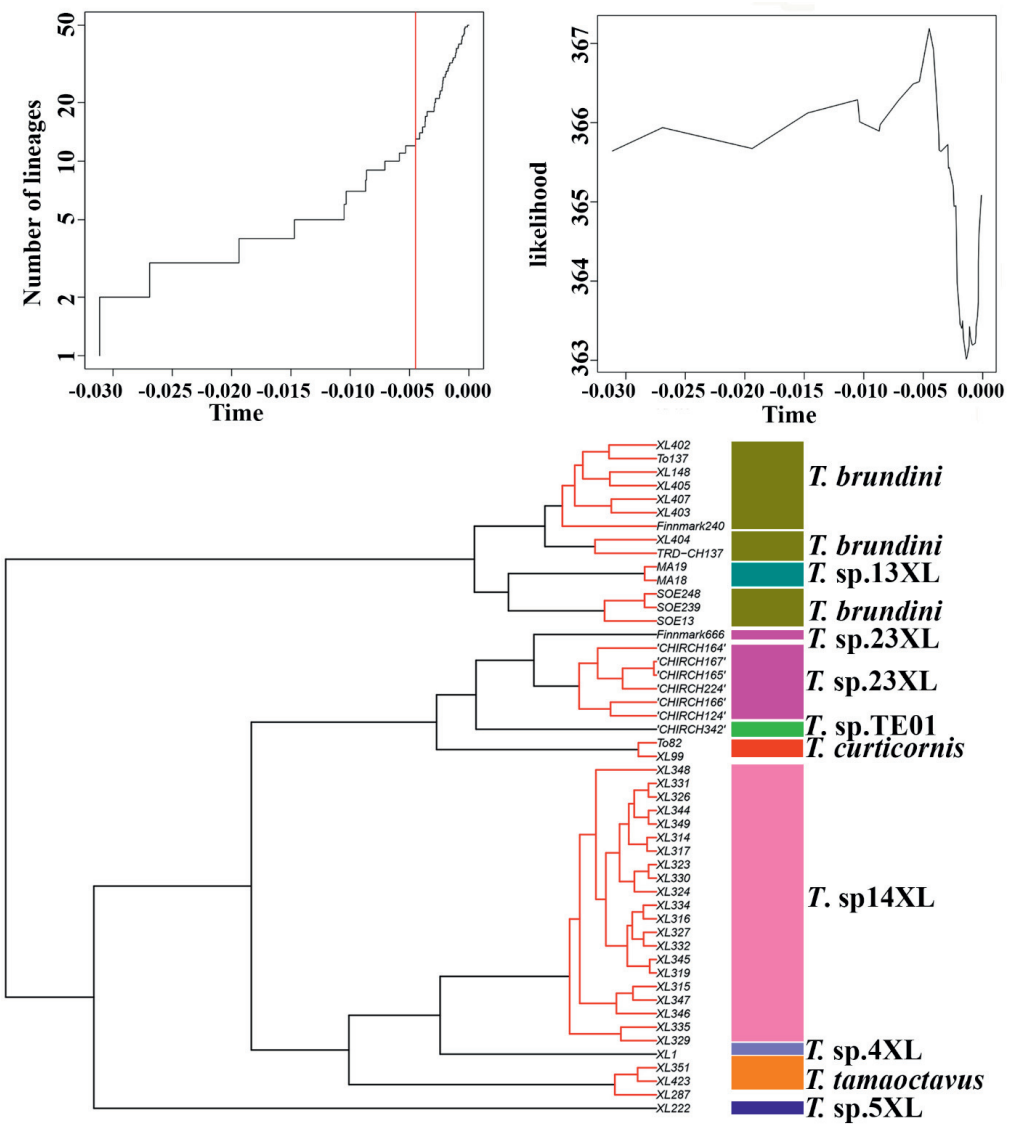
Number of lineages
1
2
5
10
20
50
-0.030 -0.025 -0.020 -0.015 -0.010 -0.005 0.000
Time
likelihood
363
364
365
366
367
-0.030 -0.025 -0.020 -0.015 -0.010 -0.005 0.000
Time
XL402
To137
XL148
XL405
XL407
XL403
Finnmark240
XL404
TRD-CH137
MA19
MA18
SOE248
SOE239
SOE13
Finnmark666
'CHIRCH164'
'CHIRCH167'
'CHIRCH165'
'CHIRCH224'
'CHIRCH166'
'CHIRCH124'
'CHIRCH342'
To82
XL99
XL348
XL331
XL326
XL344
XL349
XL314
XL317
XL323
XL330
XL324
XL334
XL316
XL327
XL332
XL345
XL319
XL315
XL347
XL346
XL335
XL329
XL1
XL351
XL423
XL287
XL222
T. brundini
T. brundini
T. sp.13XL
T. brundini
T. sp.23XL
T. sp.23XL
T. sp.TE01
T. curticornis
T. sp14XL
T. sp.4XL
T. tamaoctavus
T. sp.5XL

Figure S4

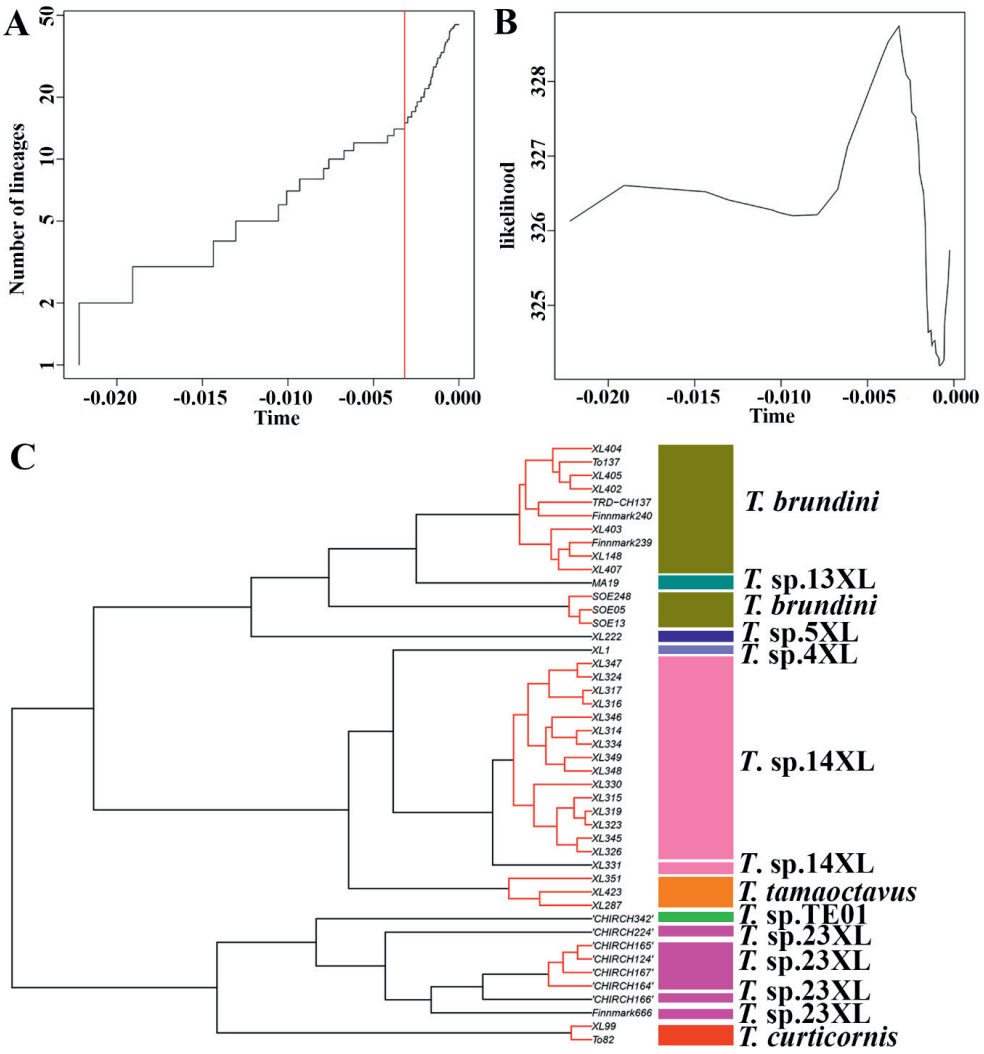
A
Number of lineages
50
20
10
5
2
1
-0.020
-0.015
-0.010
-0.005
0.000
Time
B
likelihood
328
327
326
325
-0.020
-0.015
-0.010
-0.005
0.000
Time
C
XL404
To137
XL405
XL402
TRD-CH137
Finnmark240
XL403
Finnmark239
XL148
XL407
MA19
SOE248
SOE05
SOE13
XL222
XL1
XL347
XL324
XL317
XL316
XL346
XL314
XL334
XL349
XL348
XL330
XL315
XL319
XL323
XL345
XL326
XL331
XL351
XL423
XL287
'CHIRCH342'
'CHIRCH224'
'CHIRCH165'
'CHIRCH124'
'CHIRCH167'
'CHIRCH164'
'CHIRCH166'
Finnmark666
XL99
To82
T. brundini
T. sp.13XL
T. brundini
T. sp.5XL
T. sp.4XL
T. sp.14XL
T. sp.14XL
T. tamaoctavus
T. sp.TE01
T. sp.23XL
T. sp.23XL
T. sp.23XL
T. sp.23XL
T. curticornis

Figure S5

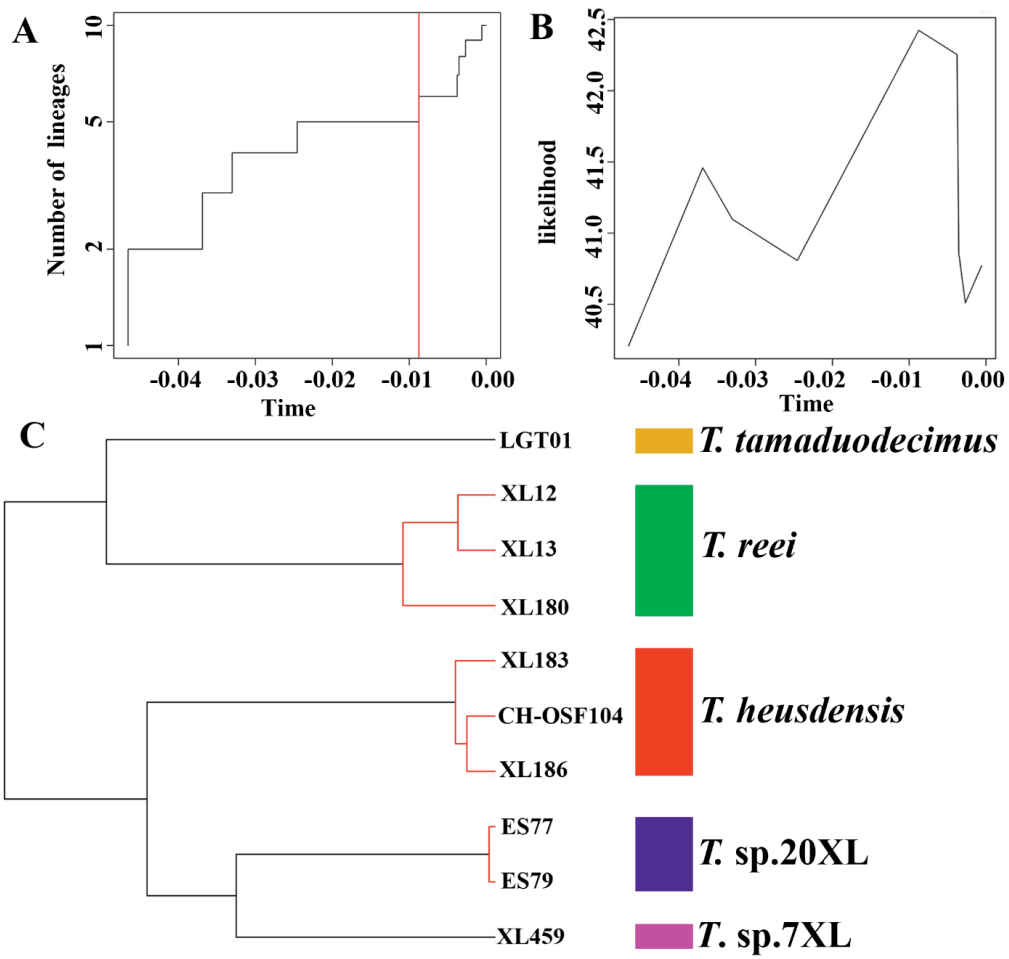
A
Number of lineages
10
5
2
1
-0.04
-0.03
-0.02
-0.01
0.00
Time
B
likelihood
42.5
42.0
41.5
41.0
40.5
-0.04
-0.03
-0.02
-0.01
0.00
Time
C
LGT01
XL12
XL13
XL180
XL183
CH-OSF104
XL186
ES77
ES79
XL459
T. tamaduodecimus
T. reei
T. heusdensis
T. sp.20XL
T. sp.7XL

Figure S6

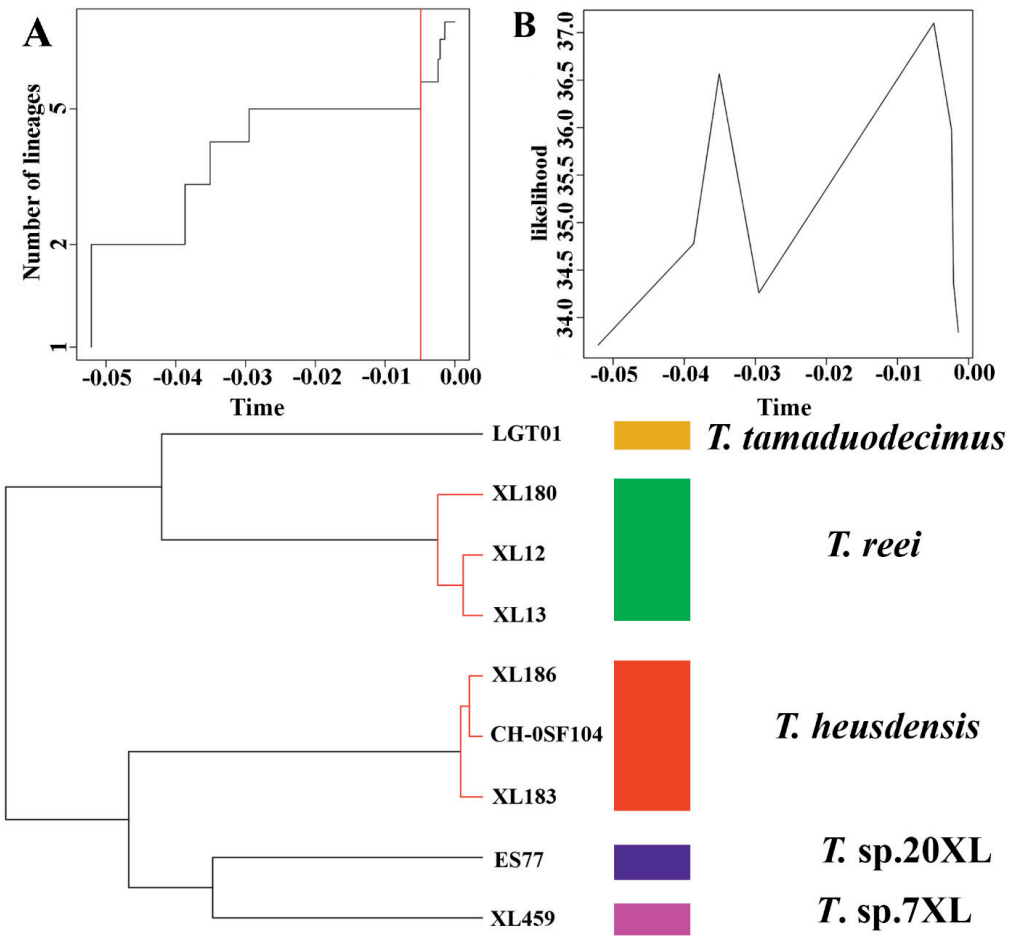
A
Number of lineages
1
2
5
-0.05 -0.04 -0.03 -0.02 -0.01 0.00
Time
B
likelihood
34.0 34.5 35.0 35.5 36.0 36.5 37.0
-0.05 -0.04 -0.03 -0.02 -0.01 0.00
Time
LGT01
XL180
XL12
XL13
XL186
CH-0SF104
XL183
ES77
XL459
T. tamaduodecimus
T. reei
T. heusdensis
T. sp.20XL
T. sp.7XL

Figure S7

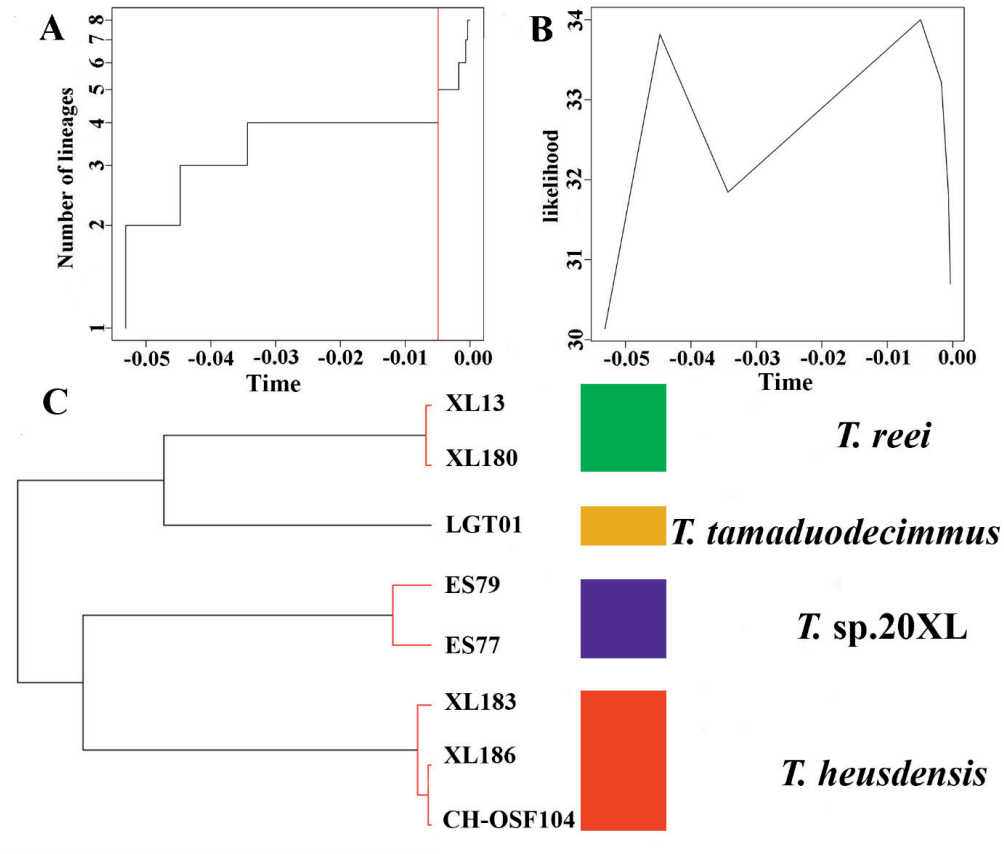
A
Number of lineages
1
2
3
4
5
6
7
8
-0.05
-0.04
-0.03
-0.02
-0.01
0.00
Time
B
likelihood
30
31
32
33
34
-0.05
-0.04
-0.03
-0.02
-0.01
0.00
Time
C
XL13
XL180
LGT01
ES79
ES77
XL183
XL186
CH-OSF104
T. reei
T. tamaduodecimmus
T. sp.20XL
T. heusdensis

Figure S8

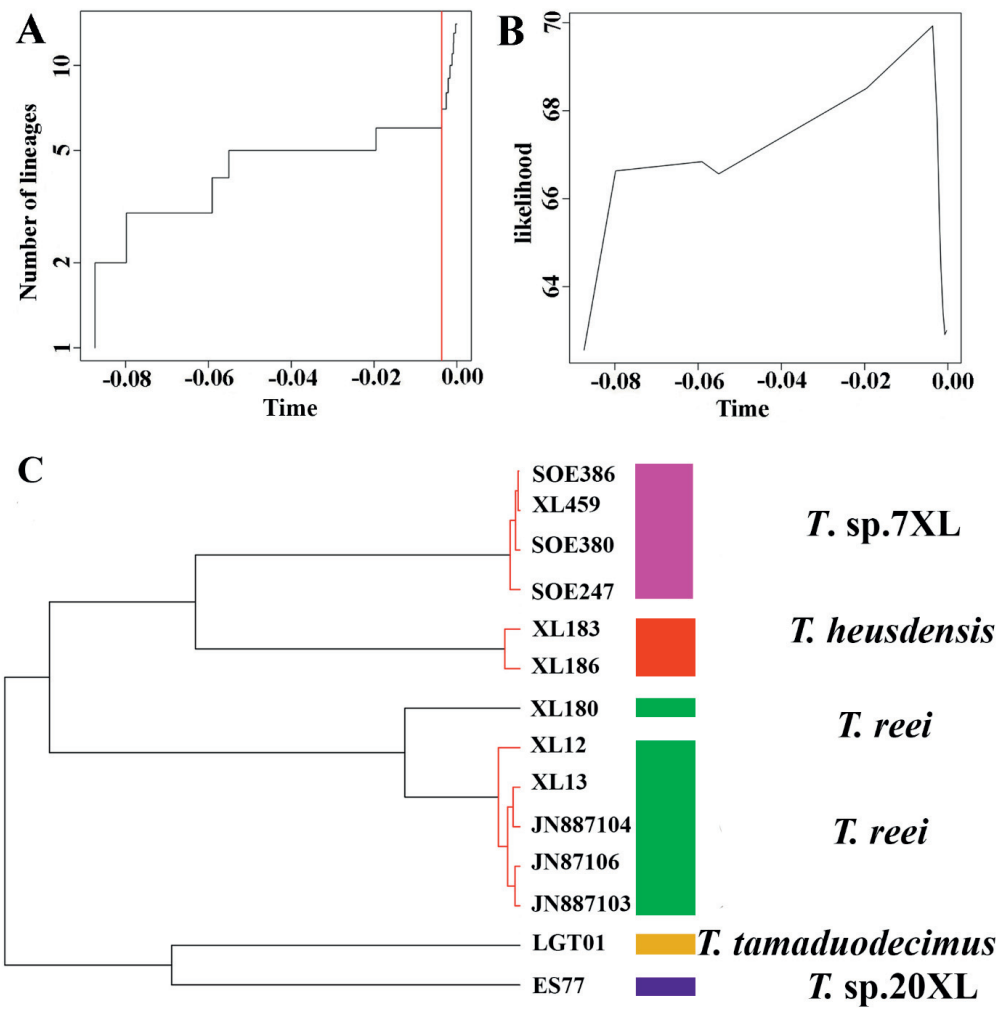
A
Number of lineages
10
5
2
1
-0.08
-0.06
-0.04
-0.02
0.00
Time
B
likelihood
70
68
66
64
-0.08
-0.06
-0.04
-0.02
0.00
Time
C
SOE386
XL459
SOE380
SOE247
XL183
XL186
XL180
XL12
XL13
JN887104
JN87106
JN887103
LGT01
ES77
T. sp.7XL
T. heusdensis
T. reei
T. reei
T. tamaduodecimus
T. sp.20XL

Table S1. BOLD sample ID, genes, localities and collectors of specimens in the *Tanytarsus curticornis* species complex used in the study.

Species	Sample ID	COI	CAD1	AATS1	PGD	Country	Collector
T. brundini	SOE13	654	909	408	745	Norway	K. Aagaard et al.
T. brundini	SOE239	657	909	408	748	Norway	O. Hanssen
T. brundini	XL403	658	909	408	748	Ukraine	V. Baranov
T. brundini	SOE248	651	890	408	748	Norway	O. Frengen
T. brundini	XL404	658	791	408	748	Ukraine	V. Baranov
T. brundini	XL407	658	909	407	748	Ukraine	V. Baranov
T. brundini	XL148	658	909	408	744	Czech Rep.	X.L. Lin
T. brundini	XL405	658	909	407	748	Ukraine	V. Baranov
T. brundini	XL402	658	860	408	748	Ukraine	V. Baranov
T. brundini	Finnmark240	658	894	408	745	Norway	T. Ekrem
T. brundini	SOE05	654	0	408	745	Norway	K. Aagaard et al.
T. brundini	Finnmark239	658	0	408	746	Norway	T. Ekrem
T. brundini	To137	658	909	407	743	Norway	E. Stur, T. Ekrem
T. brundini	TRD-CH137	658	785	402	745	Norway	E. Stur
T. curticornis	XL99	658	908	404	748	Norway	X.L. Lin
T. curticornis	To82	654	890	404	746	Norway	T. Ekrem
T. sp. 13XL	MA19	657	908	408	747	Portugal	T. Ekrem
T. sp. 13XL	MA18	658	907	408	747	Portugal	T. Ekrem
T. sp. 14XL	XL346	658	909	405	748	China	Q. Wang
T. sp. 14XL	XL331	658	909	404	748	China	Q. Wang
T. sp. 14XL	XL345	657	909	405	748	China	Q. Wang
T. sp. 14XL	XL326	658	909	405	747	China	Q. Wang
T. sp. 14XL	XL323	658	884	405	741	China	Q. Wang
T. sp. 14XL	XL344	658	909	405	748	China	Q.Wang
T. sp. 14XL	XL334	658	909	405	748	China	Q. Wang
T. sp. 14XL	XL319	658	909	405	747	China	Q. Wang
T. sp. 14XL	XL347	645	909	405	748	China	Q. Wang
T. sp. 14XL	XL335	658	909	405	748	China	Q.Wang
T. sp. 14XL	XL316	658	909	405	748	China	Q. Wang
T. sp. 14XL	XL327	658	902	405	747	China	Q. Wang
T. sp. 14XL	XL348	658	905	405	746	China	Q.Wang
T. sp. 14XL	XL315	658	898	405	745	China	Q. Wang
T. sp. 14XL	XL349	658	884	405	746	China	Q. Wang
T. sp. 14XL	XL332	658	909	405	748	China	Q. Wang
T. sp. 14XL	XL330	658	909	404	748	China	Q.Wang
T. sp. 14XL	XL314	658	909	405	745	China	Q.Wang
T. sp. 14XL	XL329	658	909	404	748	China	Q. Wang
T. sp. 14XL	XL324	658	909	405	747	China	Q. Wang
T. sp. 14XL	XL333	658	909	405	748	China	Q. Wang
T. sp. 14XL	XL317	658	892	405	748	China	Q. Wang
T. sp. 23XL	CHIR_CH165	658	909	405	748	Canada	J.Knopp
T. sp. 23XL	CHIR_CH224	658	908	405	747	Canada	T. Ekrem, E. Stur
T. sp. 23XL	CHIR_CH164	658	909	405	747	Canada	J. Knopp
T. sp. 23XL	Finnmark666	658	893	405	748	Norway	T. Ekrem, E. Stur
T. sp. 23XL	CHIR_CH124	602	908	405	747	Canada	T. Ekrem, E. Stur
T. sp. 23XL	CHIR_CH166	658	909	405	748	Canada	J. Knopp

T. sp. 23XL	CHIR_CH167	658	908	405	747	Canada	J. Knopp
T. sp. 4XL	XL1	658	892	398	743	China	X.L. Lin
T. sp. 5XL	XL222	658	909	403	744	China	C. Song
T. sp. TE01	CHIR_CH342	658	874	405	745	Canada	T. Ekrem, E. Stur
T. tamaoctavus	XL423	658	892	405	748	China	H.Q. Tang
T. tamaoctavus	XL287	658	909	405	746	China	X.L. Lin
T. tamaoctavus	XL351	658	909	405	746	China	X.L. Lin

Table S2. BOLD sample ID, genes, localities and collectors of specimens in the *Tanytarsus heusdensis* species complex used in the study.

Species	Sample ID	COI	CAD1	AATS1	PGD	Country	Collector
T. heusdensis	XL186	658	909	405	748	Germany	E. Stur
T. heusdensis	XL183	658	886	387	748	Germany	E. Stur
T. heusdensis	CH-OSF104	658	909	403	747	Norway	G. Soli, M.Steinert
T. reei	XL13	658	867	405	748	China	Shuli Li
T. reei	XL180	658	897	405	748	Germany	E. Stur
T. reei	XL12	658	876	405	748	China	S.L. Li
T. sp. 20XL	ES77	658	909	408	748	Germany	F. Eder & A. Schellmoser
T. sp. 20XL	ES79	658	909	408	748	Germany	F. Eder & A. Schellmoser
T. sp. 7XL	SOE380	657	0	0	0	Norway	O. Hanssen
T. sp. 7XL	SOE387	657	0	0	0	Norway	O. Hanssen
T. sp. 7XL	SOE247	629	0	0	0	Norway	O. Frengen
T. sp. 7XL	XL459	658	899	0	731	Norway	O. Frengen
T. sp. 7XL	SOE386	657	0	0	0	Norway	O. Hanssen
T. reei	JN887103	658	0	0	0	South Korea	
T. reei	JN887105	658	0	0	0	South Korea	
T. reei	JN887104	658	0	0	0	South Korea	
T. reei	JN887102	658	0	0	0	South Korea	
T. reei	JN887106	658	0	0	0	South Korea	
T. tamaduodecimus	LGT01	658	893	388	748	China	Q. Wang

Table S3. Variable sites, informative sites, and average nucleotide composition in the aligned sequences of the *Tanytarsus curticornis* species complex.

Gene	Nucleotide position	Variable sites	Informative sites	T(%)	C(%)	A(%)	G(%)	AT(%)	GC(%)
COI	1st	2	0	42.5	26.9	14.1	16.5	56.6	43.4
	2nd	37	35	26.5	18.0	28.0	27.5	54.5	45.5
	3nd	186	167	44.1	12.6	38.0	5.3	82.1	18.9
	All	225	202	37.7	19.2	26.7	16.4	64.4	35.6
AATS1	1st	17	16	24.1	20.5	22.6	32.8	46.7	53.3
	2nd	2	2	28.1	16.6	33.2	22.1	61.3	38.7
	3nd	96	87	27.8	32.5	14.1	25.6	41.9	58.1
	All	115	105	26.7	23.2	23.3	26.8	50.0	50.0
CAD1	1st	43	33	21.3	19.5	29.7	29.5	51.0	49.0
	2nd	16	9	28.4	18.9	34.9	17.8	63.3	36.7
	3nd	206	163	28.1	29.6	19.7	22.6	47.8	52.2
	All	265	205	25.9	22.7	28.1	23.3	50.0	50.0
PGD	1st	18	14	20.0	17.2	29.4	33.4	49.4	50.6
	2nd	2	1	29.9	19.9	31.7	18.5	51.6	48.4
	3nd	150	119	19.1	41.3	14.2	25.5	33.3	66.7
	All	170	134	23.0	26.1	25.1	25.8	48.1	51.9

Table S4. Variable sites, informative sites, and average nucleotide composition in the aligned sequences of the *Tanytarsus heusdensis* species complex.

Gene	Nucleotide position	Variable sites	Informative sites	T(%)	C(%)	A(%)	G(%)	AT(%)	GC(%)
COI	1st	1	1	42.5	27.0	14.5	16.0	57.0	43.0
	2nd	33	30	27.2	17.7	28.4	26.7	55.6	44.4
	3nd	170	150	42.9	11.7	40.7	4.7	83.6	16.4
	All	204	181	37.5	18.8	27.9	15.8	65.4	34.6
AATS1	1st	17	14	23.1	20.3	22.6	34.0	45.7	54.3
	2nd	16	12	29.3	14.9	33.1	22.8	62.4	37.6
	3nd	96	83	37.1	17.6	25.4	19.9	62.5	37.5
	All	129	109	29.8	17.6	27.0	25.6	56.8	43.2
CAD1	1st	29	17	21.9	17.2	31.7	29.2	53.6	46.4
	2nd	12	6	28.1	18.9	35.2	17.8	53.3	46.7
	3nd	147	110	40.7	15.7	27.7	15.9	68.4	31.6
	All	188	133	30.2	17.3	31.5	21.0	61.7	38.3
PGD	1st	8	5	20.6	16.7	29.5	33.2	50.5	49.5
	2nd	3	1	29.8	20.8	30.2	19.2	60.0	40.0
	3nd	114	89	38.0	20.5	19.8	21.7	57.8	42.2
	All	125	95	29.5	19.3	26.5	24.7	56.0	44.0

Molecular phylogeny and temporal diversification of *Tanytarsus* (Diptera: Chironomidae) suggest generic synonyms, new classifications, and place of origin

Xiao-Long Lin*, Elisabeth Stur, Torbjørn Ekrem

Department of Natural History, NTNU University Museum, Norwegian University of Science and Technology, NO-7491, Trondheim, Norway

*Corresponding author. E-mail: xiaolong.lin@ntnu.no

Abstract

Genus *Tanytarsus* is, with approximately 400 described species, a comparatively big genus of non-biting midges (Diptera: Chironomidae). Relationships among *Tanytarsus* and related genera and between species within the genus have been exceptionally difficult to resolve based on morphology or single gene genealogies. Here, the phylogeny of *Tanytarsus* sensu lato is reconstructed based on the combined analysis of five nuclear markers, including both ribosomal (18S) and protein-coding (AATS1, CAD, PGD and TPI) genes. Our results indicate that *Tanytarsus* is paraphyletic with *Caladomyia* placed among South American *Tanytarsus*, *Virgatanytarsus* as part of a Gondwanan clade, and *Corynocera* within the *Tanytarsus norvegicus* species group, suggesting three generic synonyms. As expected, the previously synonymized *Nimbocera* is confirmed to be a junior synonym of *Tanytarsus*, and *Sublettea* remain valid. Moreover, the monophyly of some established species groups is well supported, while other groups remain uncertain. Based on calibrated molecular divergence time analysis, *Tanytarsus* diverged from its sister group *Cladotanytarsus* during the late Cretaceous and early Paleogene (61.28–78.54 Mya). The genus most likely originated in the Old World (Oriental- and Palearctic regions).

Keywords

Diptera; Chironomidae; Bayesian; maximum likelihood; maximum parsimony; nuclear DNA; S-DIVA; biogeography.

Introduction

Over the last decade, advancements in DNA sequencing technologies, bioinformatics and computational biology have provided large amount of molecular data and improved the tools used to analyze them (e.g. Cristescu 2014; Garber et al. 2011; Goodwin et al. 2016; Mardis

2008; Metzker 2010; Scholz et al. 2012; van Dijk et al. 2014; Wagner et al. 2013). Uncertain evolutionary relationships in insects have been resolved by phylogenomics using large amount of genes (Cameron 2014; Misof et al. 2014) and within the Diptera, many molecular phylogenies have been carried out to explore the relationships among families, subfamilies, tribes, genera and species levels (e.g. Buenaventura & Pape 2017; Cranston et al. 2012; Hash et al. 2017; Kjer et al. 2006; Kutty et al. 2010; Ståhls et al. 2003; Tachi & Shima 2010; Virgilio et al. 2015; Winterton et al. 2016). Within the Chironomidae, several molecular phylogenies on various groups have been produced, but only one study has attempted to reconstruct the evolutionary history of critical genera in all subfamilies (Cranston et al. 2012). Cranston et al. (2012) confirm that all sampled subfamilies of Chironomidae, except Prodiamesinae, are monophyletic, while the tempo of diversification of the family shows a Permian origin with subfamily stem-group origin from the mid-late Triassic to the early Cretaceous.

The genus *Tanytarsus* van der Wulp, 1874 has more than 400 described species worldwide and is one of the most diverse genera in Chironomidae. The taxonomy and systematics of *Tanytarsus* have received an amount of attention. Reiss and Fittkau (1971) revised the western Palaearctic *Tanytarsus* and erected eleven species groups based on the morphological characters of adult males. Likewise, Glover (1973) revised the Australian Tanytarsini, and separated *Tanytarsus* into five species groups also based on adult male morphology. The Afrotropical fauna was reviewed as part of Freeman's monumental work on African Chironomidae south of the Sahara (Freeman 1958). The Australian monsoonal tropical *Tanytarsus* were reviewed by Cranston (2000), while species mostly belonging to the *eminulus*, *gregarius*, *lugens* and *mendax* species groups from Africa, Australia, North America and South- and East Asia were revised by Ekrem (2001a, 2001b, 2002, 2004) and Ekrem et al. (2003). The Neotropical fauna also has been described quite extensively (Cranston 2007; Ekrem & Reiss 1999; Giłka & Zakrzewska 2013; Sanseverino 2006; Sanseverino & Fittkau

2006; Sanseverino & Trivinho-Strixino 2010; Sanseverino & Wiedenbrug 2000; Sanseverino et al. 2002; Sublette & Sasa 1994; Trivinho-Strixino & Strixino 2007; Trivinho-Strixino et al. 2015; Vinogradova et al. 2009), and Sanseverino et al. (2010) suggested the synonymy of the American genus *Nimbocera* with *Tanytarsus*. Despite these past efforts, many *Tanytarsus* species remain to be discovered and described. Even in regions considered well investigated, species new to science are found on a regular basis (Ekrem & Halvorsen 2007; Ekrem & Stur 2007; Ghonaim et al. 2004; Giłka & Paasivirta 2007, 2008, 2009; Lin et al. 2015; Lin et al. submitted). The increased use of molecular tools in taxonomy has aided the discovery of new cryptic and semi-cryptic species in *Tanytarsus* (Lin et al. 2015; Lin et al. submitted) and more is to be expected as less investigated regions, such as the East Palearctic and the Oriental regions, are comprehensively explored.

The generic concept of *Tanytarsus* includes species with adults, larvae and pupae similar to those of *Caladomyia* Säwedal, 1981, *Corynocera* Zetterstedt, 1838, *Sublettea* Roback, 1975 and *Virgatanytarsus* Pinder, 1982. The morphological diagnostic features of these genera have not been tested in a phylogenetic framework and it is uncertain if the genera are compatible with a monophyletic *Tanytarsus* as currently defined.

The genus *Caladomyia* is largely Neotropical with a few species reaching the southern and south-western USA (Säwedal 1981; Trivinho-Strixino 2012). One extinct species is recorded from Eocene Baltic amber (Zakrzewska & Giłka 2013). Adult males of *Caladomyia* can be separated from other genera by the posteriorly directed bars on the hypopygial anal point (Säwedal 1981). However, the pupae and larvae of *Caladomyia* cannot be separated from *Tanytarsus*. Hence, we suspect the phylogenetic position of *Caladomyia* within the tribe Tanytarsini.

The genus *Corynocera* is Holarctic with a questionable record from New Zealand (Hirvenoja 1961) based on a larval subfossil head capsules. The genus includes two described

and at least one undescribed species (Epler et al. 2013). The adults are water skaters having comparatively long legs and oar-shaped wings apparently adapted for water surface swarming. These characters are considered diagnostic for adult male *Corynocera*, while wing sheaths without a nose in the pupae (Langton 1991; Pinder 1986) and the central three teeth of the larval mentum are regarded as diagnostic in the immatures. However, the former character is also found in an undescribed species of *Tanytarsus* from Tibet (Lin et al., unpublished) while the latter is observed in the parthenogenetic *Tanytarsus heliomesonyctios* Langton (Stur & Ekrem 2011). Disregarding the special adaptive characters in the adult male, *Corynocera* currently cannot be separated from *Tanytarsus* based on morphology.

The genus *Sublettea* was previously regarded as a subgenus of *Tanytarsus*, and is recorded from the Oriental and Holarctic regions, including two described and at least two undescribed species (Ashe & O'Connor 1995; Epler et al. 2013; Roback 1975). While the genus was shown as separate from *Tanytarsus* in the results of Cranston et al. (2012), their sampling of species within *Tanytarsus* was too sparse to be confident of this placement.

The genus *Virgatanytarsus* was previously described as the *triangularis* group within *Tanytarsus* and species have been recorded from the Afrotropical, Oriental and Palearctic regions (Epler et al. 2013; Pinder 1982). The generic diagnosis separates adult males of *Virgatanytarsus* from *Tanytarsus* by the presence of anteriorly directed bars on the hypopygial anal point (Pinder 1982), separate pupae by the broad lateral comb on the pupal abdominal segment VIII (Pinder 1986), and separate larvae by posterior parapod claws having numerous small hooklets arranged in multiple rows (Epler et al. 2013; Pinder 1982). However, these characters are also found in other *Tanytarsus* species (Cranston 2000; Sanseverino 2006). Hence, there are currently no morphological features that exclusively define and separate *Virgatanytarsus* from *Tanytarsus*, suggesting a potential synonym of these genera.

Morphology alone may be insufficient to generate stable phylogenetic hypotheses on the species-level in chironomids because recent species radiation and parallel selection has caused a high level of homoplasy in available characters (Sæther 1979). Moreover, the lack of larval and pupal data for many species frequently result in high amount of missing data in taxon-character matrices. For instance, Ekrem (2003) concluded that morphological characters did not support the postulated monophyly of the *Tanytarsus eminulus*, *gregarius*, *lugens* and *mendax* groups in unweighted parsimony analyses, and that a constraint based on unique synapomorphies and evidence from molecular data had to be used in order to produce cladograms with reasonable topologies.

Molecular phylogenetic work on *Tanytarsus* has been extremely limited. Ekrem and Willassen (2004) explored Tanytarsini relationships using a single mitochondrial gene (COII), but did not aim to resolve the relationship between *Tanytarsus* and all the morphologically most similar genera, nor was their taxonomic sampling sufficient to address the evolutionary relationships within the genus. Thus, the phylogeny of *Tanytarsus* and related genera remain uncertain.

In this study, we aim to infer the evolutionary history of *Tanytarsus* sensu lato using multiple nuclear genetic markers from over 130 taxa. Specifically, we want to address the following three questions: 1) Is *Tanytarsus* a monophyletic group within the tribe Tanytarsini? 2) What is the phylogenetic relationship among species of *Tanytarsus*, *Caladomyia*, *Corynocera*, *Sublettea* and *Virgatanytarsus*? 3) What is the biogeographical history of the genus *Tanytarsus*, its origin and tempo of diversification?

Material and Methods

Taxon sampling

In order to detect and avoid lab contamination and misidentifications, we selected two individuals of each species, except for some species where only one specimen was available.

For the phylogenetic analyses, we used a reduced dataset where each species was represented by one specimen to reduce computing time. After initial phylogenetic analysis, the position of two taxa of *Tanytarsus*, *Tanytarsus* cf. *riopreto*, *Tanytarsus shouautumnalis* Sasa, 1989, were highly unstable in analyses, and were excluded as rogue taxa to improve phylogenetic accuracy (Aberer et al. 2013). Moreover, two initially selected outgroups, *Pontomyia natans* Edwards, 1926 and *Thienemanniola ploenensis* Kieffer, 1921, were excluded from the dataset after initial analyses as they were placed well outside of *Tanytarsus* sensu lato, displaying very long branches in the initial phylogenetic trees. Hence, our final dataset comprised 130 morphospecies, 111 of which were *Tanytarsus*, while the remaining 19 species from six genera were considered outgroups or potential members of *Tanytarsus* sensu lato: Five species belong to the genus *Caladomyia*, four to *Cladotanytarsus*, one to *Corynocera*, one to *Paratanytarsus*, one to *Rheotanytarsus*, one to *Sublettea* and six belong to *Virgatanytarsus*. In addition, *Tanytarsus rhabdomantis*, which originally was placed in *Nimbocera* Reiss, 1972 (now a junior synonym of *Tanytarsus*) was included in the phylogenetic analysis to confirm the synonymy of *Nimbocera* and *Tanytarsus*. Approximately 99% of all DNA sequences were generated in this study and not used previously in other publications.

List of all species, specimens, their individual images, georeferences, primers, sequences and other relevant laboratory data of all sequences specimens can be seen online in the publicly accessible full dataset “Molecular phylogeny of *Tanytarsus* sensu lato [DS-PHTAN]”, DOI: XXX and the reduced dataset “Reduced dataset for molecular phylogeny of *Tanytarus* sensu lato [DS-REDMTAN]”, DOI: XXX in the Barcode of Life Data Systems (BOLD) (Ratnasingham & Hebert 2007, 2013). Voucher specimens are deposited at the Department of Natural History, NTNU University Museum, Trondheim, Norway, the Department of Natural History, Bergen University Museum, Bergen, Norway and the College of Life Sciences, Nankai University, Tianjin, China. Specimens were identified morphologically using relevant

taxonomic revisions and species descriptions, (e.g. (Cranston 2000, 2007; Ekrem 2001b, 2002; Ekrem et al. 2003; Glover 1973; Lindeberg 1963, 1967; Reiss & Fittkau 1971; Sanseverino 2006; Sasa 1980; Sasa & Kawai 1987; Sublette & Sasa 1994; Trivinho-Strixino 2012; Trivinho-Strixino et al. 2015; Vinogradova et al. 2009).

Gene selection

Here we selected one ribosomal gene marker (18S) and four protein-coding gene markers, including alanyl-tRNA-synthetase (AATS1), two sections of the CPSase region of carbamoyl-phosphate synthase-aspartate transcarbamoylase-dihydroorotase (CAD1 and CAD4), triose phosphate isomerase (TPI) and 6-phosphogluconate dehydrogenase (PGD). These genes have been used previously to reconstruct phylogenetic relationships among Diptera (Bertone et al. 2008; Ekrem et al. 2010; Gibson et al. 2010; Kutty et al. 2010; Moulton & Wiegmann 2004; Petersen et al. 2007; Su et al. 2008; Tachi 2013; Winterton & Ware 2015). Due to the high rate mutation of the mitochondrial cytochrome c oxidase I (COI) and the documented poor performance in phylogenetic analyses on the genus level in Chironomidae (Ekrem et al. 2010). COI sequences were not included in the analyses.

Molecular methods and analyses

DNA extraction, PCR amplification, sequencing and alignment

Adult specimens were preserved in 85% ethanol, immatures in 96% ethanol, and stored dark at 4°C before molecular analyses. Total genomic DNA of specimens was extracted from the thorax and head using QIAGEN® DNA Blood & Tissue Kit and GeneMole DNA Tissue Kit on a GeneMole® instrument (Mole Genetics, Lysaker, Norway) at the Department of Natural History, NTNU University Museum. The standard protocol of the QIAGEN® DNeasy Blood & Tissue Kit was used, except that the final elution volume was 100 µl due to small specimen

size. When using GeneMole DNA Tissue Kit, the standard protocol was followed, except that 4 µl Proteinase K was mixed with 100 µl buffer for overnight lysis at 56°C. The final elution volume was 100 µl. After DNA extraction, the clear exoskeleton was washed with 96% ethanol and mounted in Euparal on microscope slides together with the corresponding antennae, wings and legs following the procedure outlined by Sæther (1969).

DNA amplifications of selected nuclear genes with primers (Table 1) were carried out using 2.5 µL 10x Ex Taq Buffer, 2 µL 2.5 mM dNTP Mix, 0.1 µL Ex Taq HS, 0.5 µL 25 mM $MgCl_2$ and 1 µl of each 10 µM primer. The amount of template DNA was adjusted according to the DNA concentration and varied between 2-5 µL. ddH_2O was added to make a total of 25 µL for each reaction. Fragments of AATS1, CAD1, CAD4, PGD and TPI were amplified with a touchdown program: initial denaturation step of 98°C for 10 s, then 94°C for 1 min followed by 5 cycles of 94°C for 30 s, 52°C for 30 s, 72°C for 2 min and 7 cycles of 94°C for 30 s, 51°C for 1 min, 72°C for 2 min and 37 cycles of 94°C for 30 s, 45°C for 20 s, 72°C for 2 min 30 s and 1 final extension at 72°C for 3 min. A fragment of 18S was amplified with an initial denaturation step of 98°C for 10 s, then 95°C for 3 min followed with subsequent cycling as follows: in each cycle denaturation was performed at 72°C for 1 min; the annealing temperature of the reaction was decreased by 2°C every sixth cycle from 57°C to a touchdown at 47°C, a final additional elongation step at 72°C for 10 min. PCR products were visualized on a 1% agarose gel, purified using Illustra ExoProStar 1-Step and shipped to MWG Eurofins for bidirectional sequencing using BigDye 3.1 termination. Not all individuals were successfully sequenced for all genes (Table S1).

Sequences were assembled and edited using Sequencher 4.8 (Gene Codes Corp., Ann Arbor, Michigan, USA). The forward and reverse sequences were automatically assembled by the software and the contig was inspected and edited manually. In cases of ambiguity of base calls, we used the appropriate IUPAC code, but replaced the ambiguity symbol ‘N’ with ‘?’ in the

data matrices. The sequences names were edited using Mesquite 2.7.5 (Maddison & Maddison 2010). Protein-coding genes were aligned the Muscle algorithm (Edgar 2004) on amino acids in MEGA 6 (Tamura et al. 2013). Introns were detected with reference sequences and removed from the alignment using GT-AT rule (Rogers & Wall 1980). After removing introns, the codons were aligned. No evidence of paralogues was observed in any sequences. Ambiguous regions were excluded in GBlocks v0.91b (Castresana 2000) for 18S. The aligned sequences are shown in File S1.

Table 1. Overview of gene segments and primer combinations

Gene segment	Oligo name	Oligo sequence (5'-3')	Reference
18S	18S_ai	CCTGAGAAACGGCTACCACATC	(Whiting et al. 1997)
	18S_bi	GAGTCTCGTTCGTTATCGGA	(Whiting et al. 1997)
AATS1	A1-92F	TAYCAYCAYACNTTYTTYGARATG	(Regier et al. 2008)
	A1-244R	ATNCCRCARTCNATRTGYTT	(Su et al. 2008)
CAD1	54F	GTNGTNTTYCARACNGGNATGGT	(Moulton & Wiegmann 2004)
	405R	GCNGTRTGYTCNGGRTGRAAYTG	(Moulton & Wiegmann 2004)
	122F	CCACTYATYGGNAAYTATGGNGT	Ekrem unpublished
	909R	AAYYTMAATGAYAAYTCNAAYGARGGA	Ekrem unpublished
CAD4	787F	GGDGTNACNACNGCNTGYTTYGARCC	(Moulton & Wiegmann 2004)
	1098R	TTNGGNAGYTGNCCNCCCAT	(Moulton & Wiegmann 2004)
PGD	PGD-2F	GATATHGARTAYGGNGAYATGCA	(Regier et al. 2008)
	PGD-3R	TRTGIGCNCCRAARTARTC	Brian Cassel unpublished
	PGD-4R	CNGTCCARTTNGTRTG	Brian Cassel unpublished
TPI	TPI-111Fb	GGNAAYTGGAARATGAAYGG	(Bertone et al. 2008)
	TPI-275R	CCCANACNGGYTCRTANGC	Brian Cassel unpublished
	TPI-277R	CDATNGCCCANACNGGYTC	Brian Cassel unpublished
	TPI-281R	TRNCCNGTNCCDATNGCCCA	Brian Cassel unpublished

Molecular phylogenetic reconstructions

The level of base substitution saturation for each gene and each position of the protein-coding genes was assessed by using the substitution saturation test of the program DAMBE v.5.5.25 (Xia 2013; Xia & Lemey 2009; Xia et al. 2003). We calculated the index of substitution saturation (ISS) of each data and compared it with a critical index of substitution saturation (ISSc) defining a threshold for significant saturation in the data. Saturation is postulated when the ISS value is higher than the ISSc value or not significantly different (Xia 2013).

All nuclear genetic markers were concatenated using SequenceMatrix v1.7.8 (Vaidya et al. 2011). In order to determine the best fitting nucleotide model for each gene and the

concatenated dataset, we used the software PartitionFinder v1.1.1 (Lanfear et al. 2012) under the greedy search algorithm based on the Bayesian Information Criterion (BIC) model metric. During analyses, branch lengths were unlinked to allow the program to estimate them independently for each subset. The best fitting models were GTR + G + I for the 18S and first two codons for all nuclear protein-coding genes, and TVM + G + I models for the 3rd codon for all genes based on BIC scores for each partition. We used the partitioning scheme and among-site rate variation suggested by PartitionFinder.

Maximum parsimony (MP) analyses

Maximum parsimony (MP) phylogenetic trees were reconstructed using PAUP 4.0b10 (Swofford 2002) for the concatenated nuclear dataset. All sites were used and 1000 bootstrap-replicates were used to show support for the branches. Gaps were coded as a fifth character state resulting from that gaps may be parsimoniously informative. A Heuristic search and the Tree-Bisection-Regrafting (TBR) branch swapping algorithm (Nei & Kumar 2000) were used to obtain the best MP trees with bootstrapping with 1000 replicates and setting Maxtrees to auto-increase by 100.

Maximum likelihood (ML) analyses

Maximum likelihood (ML) phylogenetic analyses for the concatenated nuclear gene dataset was conducted with the software RAxML v8.2.X (Stamatakis 2006, 2014) using raxmlGUI v1.5b1, with unlinked partitions as selected by PartitionFinder. We used 1000 bootstrap replicates in a rapid bootstrap analyses, the GTR + G + I substitution model and a thorough optimization search for the best scoring ML tree.

Bayesian inference (BI)

Bayesian tree search was carried out in MrBayes 3.2.6 (Ronquist et al. 2012). In the Bayesian analyses, data sets were partitioned by gene and codon for the protein-coding genes and by gene for the non-coding gene, 4 chains on 2 runs for 10 million generations, sampled every 100 generations with a burnin of 0.25 with the model selected by PartitionFinder: GTR + G + I for the 18S and first two codons for all nuclear protein-coding genes, and TVM + G + I models for the 3rd codon for all genes. Markov Chain Monte Carlo using convergence among the runs was monitored using Tracer v1.6 (Rambaut et al. 2014), where we ascertained that the first 25% trees could to be discarded as burn-in.

Divergence time estimates

Phylogenetic divergence times were estimated using BEAST v1.8.2 (Drummond et al. 2012). The DNA sequence dataset was partitioned by gene and codon position (except 18S by gene), and a separate HKY + G model selected by PartitionFinder was applied to each partition. The uncorrelated Lognormal relaxed clock model for among-lineage rate variation was used in conjunction with a Yule speciation model. A Lognormal [initial value = 1.0, Log(mean) = 0.0, Log(Stdev) = 1.0, offset = 0] prior was applied to the ucld.mean parameter (the arithmetic mean of the branch rates). Based on previous dating analyses by Cranston et al. (2012), the outgroup node (including *Paratanytarsus*, *Rheotanytarsus* and *Sublettea*) was calibrated with a normal prior (initial = 68 Ma, mean = 81.46 Ma, stdev = 8.0 Ma). In addition, an amber fossil of *Caladomyia* was dated to 37.2–33.9 Mya (http://fossilworks.org/?a=taxonInfo&taxon_no=262087). Thus, the inter node (including all sampled *Caladomyia* species) was calibrated with a normal prior (initial = 34 Ma, mean = 35.55 Ma, stdev = 2.0 Ma). The Markov Chain Monte Carlo analyses was run for 40 million generations, sampling trees every 10,000 generations after discarding samples from the first 4 million generations. Tracer v1.6 was used to examine the BEAST log file and estimate effective

sample sizes (ESSs) for each parameter which were all greater than 300. The maximum clade credibility tree with median heights was generated using TreeAnnotator v1.8.2 (within the BEAST packages) with 4 million states as burn-in.

Biogeographic analyses

To account for phylogenetic uncertainty and uncertainty in area optimization, the event-based method S-DIVA (statistical dispersal-vicariance analyses) (Yu et al. 2010) was implemented in RASP V3.2 (Reconstruct Ancestral State in Phylogenies) (Yu et al. 2015). Since distributions of outgroups may pose limitations to historical biogeographic analyses (Yu et al. 2015), the outgroup taxa (*Paratanytarsus*, *Rheotanytarsus*, *Sublettea* and *Cladotanytarsus*) were removed before biogeographic analyses. The geographical distribution of the ancestors was inferred by integrating over all 4001 tree topologies in the sample drawn from the Bayesian MCMC under BEAST. The maximum number of ancestral areas at each node was set to two with extinction (slow); maximum reconstruction (slow) was set to 100 with four steps, and maximum reconstruction for the final tree was set to 1000.

Three different division schemes for zoogeographical regions were compared. Based on the traditional Wallace's zoogeographical regions (Wallace 1876), six species distribution areas were included in analyses one: (A) Afrotropical region, (B) Neotropical region, (C) Australian region, (D) Oriental region, (E) Palearctic region, (F) Nearctic region. We then used the updated of Wallace's zoogeographical regions (Holt et al. 2013) and used nine species distribution areas in analyses two: (A) Afrotropical region, (B) Neotropical region, (C) Australian region, (D) Oriental region, (E) Palearctic region, (F) Nearctic region, (G) Sino-Japanese region, (H) Panamanian region, (I) Saharo-Arabian region. Finally, Bănărescu's Zoogeographical regions (Bănărescu 1991) for freshwater fauna was used in analyses three. Since none of the sampled species are found in the Indo-West Pacific, Malagasy and New

Zealand regions, only five species distribution areas remained: (A) Ethiopian region, (B) Neotropical region, (C) Australian region, (D) Sino-Indian region, (E) Holarctic region.

Results and Discussion

Dataset properties

Exclusion of introns and hyper-variable regions resulted in a final multigene dataset of 4281 bp, of which 1717 were parsimony informative. Lengths by locus are: 18S, 933; AATS1, 408; CAD1, 909; CAD4, 846; PGD, 747; TPI, 438. A set of 130 species-level taxa remained, of which 98 were represented by all loci; five lacked 18S data; two lacked AATS1 data; four lacked CAD1 data; 17 lacked CAD4 data; two lacked PGD data; 13 lacked TPI data; 95% of all sequences were obtained successfully (Table S1). It is demonstrated using simulations (Xi et al. 2016) that species tree estimation under separate models are not impacted when the amount of missing data is low or even high as long as it is randomly distributed. Base composition (A + T) ranges from 50.7% (TPI) to 60.4% (CAD4). Most parsimony informative characters (>63%) occurred in the third position of the protein-coding genes (Table S2). The complete results of the substitution saturation tests for all genes and codons indicated that for each partition, ISS values were lower than the ISSc values, suggesting little saturation in base substitution. Hence, we kept all sites in the analyses despite the high variability in third positions of protein coding markers.

For the Bayesian analyses, the standard deviation of split frequencies was in all cases <0.01. The log likelihood values for the best tree of the molecular dataset were -116480.3372. Both the model based methods (ML and BI) yielded mostly congruent nodes. The non-model based method (MP) yielded mostly congruent inter topology with high support value, but basal node (with low support value) were incongruent with other methods, perhaps as a result of the missing data. The results are summarized in Figs 1–4 [ML bootstrap (MLB) and posterior probability (PP) above the nodes; MP bootstrap below the nodes (MPB)]. Concerning the

differences between the outputs of different analytical methods, the BI and ML trees were more robust compared to the MP tree.

Phylogenetic analyses, classification and biology

Relationships of genera inTanytarsus sensu lato

Our study confirms the paraphyly of *Tanytarsus* in both model-based analyses. *Tanytarsus* is paraphyletic as *Virgatanytarsus* is placed within the basal *Tanytarsus* clade (Fig. 1), *Corynocera* within the *Tanytarsus norvegicus* species group (Fig. 2), and *Caladomyia* placed among South American *Tanytarsus* (Fig. 4).

Based on our result, a monophyletic *Virgatanytarsus* is well-supported (Fig. 1; MLB = 74%; PP = 1) as sister to *T. bispinosus*, which as *Virgatanytarsus* has broad lateral combs on pupal abdominal segment VIII but as opposed to *Virgatanytarsus* lacks bars on the adult male anal point. The anteriorly directed bars on hypopygial anal point in the adult male also is not unique to *Virgatanytarsus* and cannot be used to separate these species from *Tanytarsus*. Similar features are found in *Tanytarsus signatus* from the Palearctic region, in *T.* sp.26XL (unpublished) from the Oriental region, in *Tanytarsus bifurcus* Freeman from the Afrotropical and Oriental regions and in the Neotropical species *Tanytarsus curvicristatus*, *T. giovannii* Sanseverino & Trivinho-Strixino and *T. pseudocurvicristatus* Trivinho-Strixino, Wiedenbrug & da Silva (Sanseverino & Trivinho-Strixino 2010; Trivinho-Strixino et al. 2015), and also in the Australian species *Tanytarsus liepae* Glover (Glover 1973). The broad lateral comb on the pupal abdominal segment VIII, a character also found in *Tanytarsus edwardi* Glover and *T. hardwicki* Cranston from Australia (Cranston 2000), and also in the Neotropical *Tanytarsus riopreto* group (Sanseverino 2006) in addition to *T. bispinosus* Freeman mentioned above. Thus, considering both morphological and genetic data we conclude that there are no diagnostic

differences to confidently separate *Virgatanytarsus* from *Tanytarsus* and that these genera should be treated as synonyms.

The genus *Corynocera* is clustered within the *Tanytarsus norvegicus* species group (Fig. 2; MLB = 100%; PP = 1; MPB = 100%). We therefore postulate that the peculiar adult male morphology seen in *Corynocera* species must be an adaptive character evolved within *Tanytarsus* and that it is not appropriate as diagnostic on generic level. Treating the two genera as synonyms poses a nomenclatorial challenge, however, since the publication of *Corynocera* (Zetterstedt 1838) predates that of *Tanytarsus* (Wulp 1874). According to the rules of the International Code of Zoological Nomenclature (ICZN), *Tanytarsus* should then be listed as a junior synonym of the older genus *Corynocera*. However, *Corynocera* only holds four described species that are comparatively rarely encountered, whereas *Tanytarsus* holds more than 400 of which many are widely referred to by taxonomists and ecologists. Hence, following the principle of precedence would not be favoring nomenclatorial stability and an application to the International Code of Zoological Nomenclature to keep the name of *Tanytarsus* for the group is warranted. Moreover, as the type species of *Corynocera* was not included in our analyses, we are not completely certain that the type species will fall within the *T. norvegicus* species group. Thus, a thorough morphological analyses of all life stages of *Corynocera* and *T. norvegicus* group species should be performed before formal synonymy.

The monophyletic *Caladomyia* (MLB = 100%; PP = 1; MPB = 99%) cannot be separated from Neotropical and Holarctic *Tanytarsus* genetically (Fig. 4; MLB = 80%; PP = 1), but also morphological diagnostic characters are absent in the immatures. We therefore regard *Caladomyia* as a junior synonym of *Tanytarsus* and recognize a monophyletic species group in *Tanytarsus*. Larvae of this species group have been found to favour standing water in lakes, reservoirs and ponds.

The species *T. rhabdomantis* groups together with other Neotropical *Tanytarsus* (Fig. 4) and supports the synonymy of *Nimbocera* within *Tanytarsus*. *Sublettea* remain valid, and *Cladotanytarsus* is recovered as a monophyletic sister group to *Tanytarsus*. This is consistent with the results of Cranston et al. (2012).

Relationships among and within species groups

Based on the results from the phylogenetic analyses, we propose eight new monophyletic species groups: the *aterrimus*-, *curticornis*-, *giovannii*-, *heusdensis*-, *kiche*-, *motosuensis*-, *tamakutibasi*- and *thaicus* species groups (Figs 1–4). These groups are consistent with observed morphological characters, which will be discussed elsewhere.

Among previously postulated *Tanytarsus* species groups, the following are confirmed to be monophyletic with high support values: *aculeatus*-, *excavatus*-, *norvegicus*-, *pallidicornis*-, *signatus*- and *verralli*- species groups (Figs 1–4). The relationships between the *aculeatus*-, *signatus*-, (*heusdensis* + *pallidicornis*) species groups and clades A-C (Fig. 1) remain ambiguous with low support values, possibly due to incomplete taxon sampling and/or low number of genetic markers.

The *Tanytarsus signatus* species group was proposed by Reiss and Fittkau (1971) as a monotypic group in Europe with the type species *T. signatus*. Sanseverino (2006) suggested that the South American *Tanytarsus curvicristatus* and Australian *T. liepae* should be included in that group since they also have bars on anal point in adult male. In our molecular analyses, we included *T. signatus*, *T. curvicristatus* and an undescribed species morphologically similar to *T. signatus* to explore the relationship among these species. Our result confirms that *T. signatus* groups with the similar undescribed species (MLB = 100%; MPB = 100%; PP = 1), but *T. curvicristatus* is genetically very divergent to *T. signatus* and groups with more distally placed neotropical taxa. Thus, we believe that *T. curvicristatus* and its morphologically closely

related species (e.g. *T. pseudocurvicristatus* also from Neotropical region) belong to a different species group.

Our results confirm that the *aculeatus* species group is monophyletic (Fig. 1; MLB = 97%; PP = 1; MPB = 80%) when including *T. palettaris* Verneaux previously placed in the paraphyletic *chinyensis* species group. Re-examination of voucher specimens and comparison of previous descriptions revealed that *T. aculeatus* and *T. palettaris* are morphological similar in several key characters in adult males, e.g. both have a long digitus that extends beyond the inner margin of a heart-shaped superior volsella.

The *heusdensis* species complex, previously belonging to the paraphyletic *chinyensis* species group, is proposed as a new species group in *Tanytarsus*. The *pallidicornis* group erected by Reiss and Fittkau (1971) is confirmed as monophyletic and sister to the *heusdensis* group (Fig. 1; MLB = 100%; PP = 1; MPB = 100%).

The species previously placed in the *eminulus*-, *gregarius*-, *lugens*-, *mcmillani*- and *mendax* species groups (Fig. 1, clade A) are well supported and sister to the *motosuensis* + *norvegicus* species groups (Fig. 2; MLB = 96%; PP = 1). However, the phylogenetic relationships between the internal groups remain uncertain with low support value (Fig. 2), suggesting that these perhaps can be lumped into one group. For instance, the postulated *eminulus* species group is divided into different clades, indicating some members should be excluded and transferred to other species groups. Based on our morphological knowledge, species of the *lestagei* species complex (previously placed in the *eminulus* group) have well-defined diagnostic characters in adult males such as a comparatively long median volsella with a broad fan of lamellae; while no unique synapomorphies can be found in what would be the *oscillans* species group. Moreover, the species potentially belonging to the *gregarius* group are clustered within the *lugens* species group, suggesting that there is no evolutionary argument to keep these groups separate. Thus, we suggest that species previously placed in the *gregarius* group should be

transferred to an enlarged *lugens* group to make it monophyletic. The *mcmillani* group from Afrotropical and Oriental regions, postulated by Ekrem (2003), came out paraphyletic with *T. spadiceonotatus* separated from the other key taxa, indicating a different evolutionary history. Additionally, *T. ovatus*, previously placed in the *mendax* group, and an undescribed species similar to *T. mcmillani* are grouped together in the *mcmillani* group. The *mendax* group also came out paraphyletic since three species (*T. formosanus* Kieffer, *T. fuscithorax* Skuse and *T. pallidulus* Freeman) show other sister group relationships.

The herein postulated *motosuensis* group includes the morphologically similar *T. motosuensis* Kawai and *T.* sp.26XL both from oligotrophic lakes in the Oriental region. Species of the *norvegicus* group have been found in oligotrophic lakes in/near Arctic and on the Qinghai-Tibet Plateau.

Within subtree B (Fig. 3), the *aterrimus* species group from the Afrotropical and Oriental regions is sister to the *tamakutibasi* group from the Oriental and Palearctic regions (MLB = 98%; PP = 1; MPB = 87%). The *chinyensis* species group erected by Reiss and Fittkau (1971) is paraphyletic as *T. palettaris* and species within the *T. curticornis* and *T. heusdensis* complexes are not monophyletic. Based on our molecular phylogeny and agreement in morphological characters, we transfer *T. palettaris* to the *aculeatus* species group, erect the *curticornis* and *heusdensis* species groups, and keep a reduced *chinyensis* group with fewer members. The *curticornis* group is sister to the *chinyensis* group (Fig. 3; MLB = 98%; PP = 1), while the *aterrimus* + *tamakutibasi* groups are sister to the *chinyensis* + *curticornis* groups (Fig. 3; MLB = 69%; PP = 1).

This *aterrimus* + *chinyensis* + *curticornis* + *tamakutibasi* species clade is sister to clade C (Fig. 1; MLB = 62%; PP = 1), which includes Neotropical *Tanytarsus* + *Caladomyia* + Holarctic *excavatus*-, *verralli*- and *recurvatus*- species groups (Fig. 4). The monophyly of the ((*excavatus* + *verralli*) + *kiche*) clade is well-supported (Fig. 4; MLB = 100%; PP = 1; MPB =

95%). The newly erected *giovannii* group, containing three species, is sister to *T. curvicrstatus* (MLB = 76%; PP = 1). The Neotropical *riopreto* species group came out paraphyletic as *T. rhabdomantis* and *T. obirciae*, neither fitting the *riopreto* group morphologically, grouped within the clade with defined members of this group (Fig. 4).

Divergence time estimation and biogeographic patterns

Tempo of diversification

Divergence time estimates for the phylogeny of *Tanytarsus* are presented in Figs S2–3. Arrangements of outgroup genera and most species groups were recovered with high support values. The results indicate that the genus *Tanytarsus* diverged from *Cladotanytarsus* during the late Cretaceous and early Paleogene (61.28–78.54 Mya).

Ancestral area reconstruction

The S-DIVA analyses based on three different geographical division schemes yielded similar results (Figs 5–7), and proposed 35–61 dispersal and 24–33 vicariance events, but no extinction events to account for the present distribution of *Tanytarsus*. According to our results, the likely place of origin for *Tanytarsus* lies in the Old World (Oriental- and Palearctic regions) with subsequent dispersal and vicariance events leading to the separation of three major clades (Figs 5–7). An early dispersal event during the Paleocene of Paleogene (64.67 Mya) led to the separation of a Palearctic *signatus* species group from the remaining *Tanytarsus*, suggesting a Laurasian origin. Then the ancestral taxon of Clade 3 (Figs 5–7) originated in the Oriental region and was isolated from Clade 1 + 2 (Figs 5–7) via a vicariance event in the Paleocene (62.32 Mya). This is earlier than the collision of the Indian Subcontinent with Asia (55 Mya), but the presence of Australian and South-East African species in this clade, indicate a possible

Gondwana origin for the Asian species in Clade 3. The center of origin of Clade 1 lies in Palearctic region, while that of Clade 2 lies in Palearctic- and Neotropical regions.

Within the Clade 1, several species groups (*eminulus* + *gregarious* + *lugens* + *mcmillani* + *mendax* + *motosuensis* + *norvegicus*) are not recorded in the Neotropical region, and presence outside the Palaearctic probably was caused by dispersal events during the Eocene (55.63 Mya). Worth mentioning is that the monophyletic *norvegicus* species group only is distributed in/near the Arctic and on Qinghai-Tibet Plateau of the northern hemisphere. The group probably originated in Laurasia and kept a northern/high latitude distribution by adaption to a cold environment. An observation that support this are subfossil larval head capsules of *Corynocera ambigua* (a likely member of the *norvegicus* group) found from Greenland and dated to 1.806–2.588 Mya (Böcher 1995). This is a bit earlier than the cold Dryas, suggesting that *Corynocera* is a survivor from this extremely cold period in this region. Our results also indicate that *Corynocera* originated during the mid-Miocene of Neogene (11.42 Mya) via a vicariance event (e.g. Orogeny in northern hemisphere). The hypothesized place of origin of the *eminulus*-, *gregarius*-, *lugens*-, *mcmillani*- and *mendax*- species groups in Gondwanaland (Afrotropical region) (Ekrem 2003) was supported by our S-DIVA analyses, and subsequent dispersal and vicariance events among these species groups are likely to explain the observed distribution pattern.

Within Clade 2 (Figs 5–7), S-DIVA analyses indicate that a vicariance event took place round 54.79 Mya separating a predominantly Neotropical clade from a predominantly Holarctic clade.

Surprisingly, within the Neotropical clade, there is a group of cold-adapted *Tanytarsus* from the Palaearctic (the *excavatus*, *recurvatus* and *verralli* species groups) that originated about 45 Mya. The result of the S-DIVA analyses indicate that some unknown vicariance events during

the Eocene of Paleogene led to the diversification of the above *excavatus*-, *recurvatus*- and *verralli*- groups.

However, it is difficult to imagine how chironomids could migrate from the neotropics to the northern Holarctic (weak fliers). The observed pattern might also be a result of sampling bias and extinction. For instance, *Caladomyia* is present in Baltic amber, indicating a geographically wider distribution of this now core Neotropical group. Perhaps a colder climate in the Oligcene reduced the distribution of warm-adapted *Tanytarsus*, leaving mostly the Neotropical taxa of this group, except for the cold-adapted clade (the *excavatus*, *recurvatus* and *verralli* species groups). For sampling bias, we have not extensively sampled in the Nearctic region and might lack North American species in the group. The presence of species with Nearctic distribution in the group could support both a broader ancient range and possible ancient dispersion from South to North America over the Central American Seaway. In a recent study, the isthmus of Panama was found to formed 10 My earlier than the previous 3 Mya (Montes et al. 2015). This can explain the more recent recolonization of southern South America indicated by *T. kiche* in our trees (12–13 Mya). The two, undescribed, closest relatives of *T. kiche* are both from Costa Rica (north of the Panama Isthmus).

Our sampling is biased towards the Palaearctic region. Thus, low representation of African, southern North American and Australian species might hide the true evolutionary and biogeographical history of *Tanytarsus*.

Conclusion

The genus *Tanytarsus* as currently understood was not resolved as monophyletic in our analyses, indicating that the genera *Caladomyia*, *Corynocera* and *Virgatanytarsus* should be synonymized with *Tanytarsus*. The monophyly of some species groups (*aculeatus*, *aterrimus*, *curticornis*, *excavatus*, *giovannii*, *heusdensis*, *kiche*, *motosuensis*, *norvegicus*, *pallidicornis*,

signatus, *tamakutibasi*, *thaicus* and *verralli*) is recovered with high support values, but some of the previously postulated groups remain uncertain, possibly due to incomplete sampling. We find that some monophyletic groups can be associated with certain geographical distributions and/or ecology, but details in the biogeographical history likely are masked by sampling bias and possibly extinction in some groups. *Tanytarsus* probably diverged from its sister group *Cladotanytarsus* during the late Cretaceous and early Paleogene (61.28–78.54 Mya) in the Oriental- and Palearctic- regions. More taxon sampling and more genetic data are required to recover the natural history of the diverse genus in future.

Acknowledgments

We would like to thank the following people who have kindly collected and sent us specimens for our study: Viktor Baranov, Richard Cornette, Wojciech Giłka, Xin Qi, Fabio da Silva, Chao Song, Bing-Jiao Sun, Hong-Qu Tang and Xin-Hua Wang. We also acknowledge Erik Boström for assistance in parts of the molecular lab work.

References

Aberer, A.J., Krompass, D. & Stamatakis, A. (2013) Pruning rogue taxa improves phylogenetic accuracy: an efficient algorithm and webservice. *Systematic Biology* **62:** 162–166.

Ashe, P. & O'Connor, J. (1995) A new species of *Sublettea* Roback from Sulawesi. In: Cranston PS, ed. Chironomids, from gene to ecosystem: CSIRO, Australia. 431–436.

Bănărescu, P. (1991) Zoogeography of Fresh Waters. Volume 2: Distribution and Dispersal of Freshwater Animals in North America and Eurasia. *AULA-Verlag GmbH, Wiesbaden***:** 519–1091.

Bertone, M.A., Courtney, G.W. & Wiegmann, B.M. (2008) Phylogenetics and temporal diversification of the earliest true flies (Insecta: Diptera) based on multiple nuclear genes. *Systematic Entomology* **33:** 668–687.

Böcher, J. (1995) Palaeoentomology of the Kap København Formation. *Meddelelser om Grønland, Geoscience* **33:** 1–82.

Buenaventura, E. & Pape, T. (2017) Multilocus and multiregional phylogeny reconstruction of the genus Sarcophaga (Diptera, Sarcophagidae). *Molecular Phylogenetics and Evolution* **107:** 619–629.
Cameron, S.L. (2014) Insect mitochondrial genomics: implications for evolution and phylogeny. *Annual Review of Entomology* **59:** 95–117.
Castresana, J. (2000) Selection of conserved blocks from multiple alignments for their use in phylogenetic analysis. *Molecular Biology and Evolution* **17:** 540–552.
Cranston, P.S. (2000) Monsoonal tropical *Tanytarsus* van der Wulp (Diptera: Chironomidae) reviewed: New species, life histories and significance as aquatic environmental indicators. *Australian Journal of Entomology* **39:** 138–159.
Cranston, P.S. (2007) A new species for a bromeliad phytotelm-dwelling *Tanytarsus* (Diptera: Chironomidae). *Annals of the Entomological Society of America* **100:** 617–622.
Cranston, P.S., Hardy, N.B. & Morse, G.E. (2012) A dated molecular phylogeny for the Chironomidae (Diptera). *Systematic Entomology* **37:** 172–188.
Cristescu, M.E. (2014) From barcoding single individuals to metabarcoding biological communities: towards an integrative approach to the study of global biodiversity. *Trends in Ecology & Evolution* **29:** 566–571.
Drummond, A.J., Suchard, M.A., Xie, D. & Rambaut, A. (2012) Bayesian phylogenetics with BEAUti and the BEAST 1.7. *Molecular Biology and Evolution* **29:** 1969–1973.
Edgar, R.C. (2004) MUSCLE: multiple sequence alignment with high accuracy and high throughput. *Nucleic Acids Research* **32:** 1792–1797.
Ekrem, T. (2001a) Diagnoses and immature stages of some Australian *Tanytarsus* van der Wulp (Diptera : Chironomidae). *Australian Journal of Entomology* **40:** 312–325.
Ekrem, T. (2001b) A Review of Afrotropical *Tanytarsus* van der Wulp (Diptera: Chironomidae). *Tijdschrift voor Entomologie* **144:** 5–40.
Ekrem, T. (2002) A review of selected South- and East Asian *Tanytarsus* v.d. Wulp (Diptera: Chironomidae). *Hydrobiologia* **474:** 1–39.
Ekrem, T. (2003) Towards a phylogeny of *Tanytarsus* van der Wulp (Diptera: Chironomidae). Is morphology alone sufficient to reconstruct the genealogical relationship? *Insect Systematics & Evolution* **34:** 199–219.
Ekrem, T. (2004) Immature stages of European *Tanytarsus* species I. The *eminulus*-, *gregarius*-, *lugens*- and *mendax* species groups (Diptera, Chironomidae). *Deutsche Entomologische Zeitschrift* **51:** 97–146.
Ekrem, T. & Halvorsen, G.A. (2007) Taxonomy of *Tanytarsus lapponicus* Lindeberg, 1970, a species with larval mandible of '*lugens*-type' (Diptera: Chironomidae) Contributions to the systematics and ecology of aquatic Diptera. A tribute to Ole A. Sæther. Columbus, Ohio: Caddis Press. 81–86.
Ekrem, T. & Reiss, F. (1999) Two new *Tanytarsus* species (Diptera : Chironomidae) from Brazil, with reduced median volsella. *Aquatic Insects* **21:** 205–213.
Ekrem, T. & Stur, E. (2007) Description of *Tanytarsus hjulorum*, new species, with notes and DNA barcodes of some South African *Tanytarsus* (Diptera: Chironomidae). In: Andersen T, ed. Contributions to the systematics and ecology of aquatic Diptera. A tribute to Ole A. Sæther. Columbus, Ohio: Caddis Press. 87–92.
Ekrem, T., Sublette, M.F. & Sublette, J.E. (2003) North American *Tanytarsus* I. Descriptions and Keys to Species in the *eminulus*, *gregarius*, *lugens* and *mendax* Species Groups (Diptera : Chironomidae). *Annals of the Entomological Society of America* **96:** 265–328.

Ekrem, T. & Willassen, E. (2004) Exploring Tanytarsini relationships (Diptera : Chironomidae) using mitochondrial COII gene sequences. *Insect Systematics & Evolution* **35:** 263–276.
Ekrem, T., Willassen, E. & Stur, E. (2010) Phylogenetic utility of five genes for dipteran phylogeny: A test case in the Chironomidae leads to generic synonymies. *Molecular Phylogenetics and Evolution* **57:** 561–571.
Epler, J.H., Ekrem, T. & Cranston, P.S. (2013) The larvae of Chironominae (Diptera: Chironomidae) of the Holarctic region—keys and diagnoses. In: Cederholm L, ed. Chironomidae of the Holarctic Region: Keys and Diagnoses, Part 1: Larvae. Lund, Sweden: Insect Systematics and Evolution, Supplement **66:** 387–556.
Freeman, P. (1958) A study of the Chironomidae (Diptera) of Africa South of the Sahara. Part IV. *Bulletin of the British Museum (Natural History). Entomology* **6:** 263–363.
Garber, M., Grabherr, M.G., Guttman, M. & Trapnell, C. (2011) Computational methods for transcriptome annotation and quantification using RNA-seq. *Nature Methods* **8:** 469–477.
Ghonaim, M., Ali, A. & Salem, M. (2004) *Tanytarsus* (Diptera : Chironomidae) from Egypt with description of a new species. *Florida Entomologist* **87:** 571–575.
Gibson, J.F., Skevington, J.H. & Kelso, S. (2010) Placement of Conopidae (Diptera) within Schizophora based on mtDNA and nrDNA gene regions. *Molecular Phylogenetics and Evolution* **56:** 91–103.
Giłka, W. & Paasivirta, L. (2007) Two new species of the genus *Tanytarsus* van der Wulp (Diptera: Chironomidae) from Fennoscandia. In: Andersen T, ed. Contributions to the systematics and ecology of aquatic Diptera–A tribute to Ole A. Sæther. Columbus, Ohio: The Caddis Press. 107–113.
Giłka, W. & Paasivirta, L. (2008) On the systematics of the tribe Tanytarsini (Diptera: Chironomidae) - three new species from Finland. *Entomologica Fennica* **19:** 41–48.
Giłka, W. & Paasivirta, L. (2009) Evaluation of diagnostic characters of the *Tanytarsus chinyensis* group (Diptera: Chironomidae), with description of a new species from Lapland. *Zootaxa* **2197:** 31–42.
Giłka, W. & Zakrzewska, M. (2013) A contribution to the systematics of Neotropical *Tanytarsus* van der Wulp: first descriptions from Ecuador (Diptera: Chironomidae: Tanytarsini). *Zootaxa* **3619:** 453–459.
Glover, B. (1973) The Tanytarsini (Diptera: Chironomidae) of Australia. *Australian Journal of Zoology Supplementary Series* **21:** 403–478.
Goodwin, S., McPherson, J.D. & McCombie, W.R. (2016) Coming of age: ten years of next-generation sequencing technologies. *Nature Reviews Genetics* **17:** 333–351.
Hash, J.M., Heraty, J.M. & Brown, B.V. (2017) Phylogeny, host association and biogeographical patterns in the diverse millipede-parasitoid genus *Myriophora* Brown (Diptera: Phoridae). *Cladistics***:** 10.1111/cla.12189.
Hirvenoja, M. (1961) Description of the larvae of *Corynocera ambigua* Zett.(Dipt., Chironomidae) and its relation to the subfossil species *Dryadotanytarsus edentulus* Anders. and *D. duffi* Deevey. *Annales Entomologici Fennici* **27:** 105–110.
Holt, B.G., Lessard, J.P., Borregaard, M.K., Fritz, S.A., Araujo, M.B., Dimitrov, D., Fabre, P.H., Graham, C.H., Graves, G.R., Jonsson, K.A., Nogues-Bravo, D., Wang, Z., Whittaker, R.J., Fjeldsa, J. & Rahbek, C. (2013) An update of Wallace's zoogeographic regions of the world. *Science* **339:** 74–78.
Kjer, K.M., Carle, F.L., Litman, J. & Ware, J. (2006) A molecular phylogeny of Hexapoda. *Arthropod Systematics & Phylogeny* **64:** 35–44.
Kutty, S.N., Pape, T., Wiegmann, B.M. & Meier, R. (2010) Molecular phylogeny of the Calyptratae (Diptera: Cyclorrhapha) with an emphasis on the superfamily Oestroidea

and the position of Mystacinobiidae and McAlpine's fly. *Systematic Entomology* **35:** 614–635.
Lanfear, R., Calcott, B., Ho, S.Y.W. & Guindon, S. (2012) PartitionFinder: Combined Selection of Partitioning Schemes and Substitution Models for Phylogenetic Analyses. *Molecular Biology and Evolution* **29:** 1695–1701.
Langton, P.H. (1991) A key to pupal exuaviae of West Palaearctic Chironomidae. Langton.
Lin, X.L., Stur, E. & Ekrem, T. (2015) Exploring genetic divergence in a species-rich insect genus using 2790 DNA Barcodes. *PloS One* **10:** e0138993.
Lin, X.L., Stur, E. & Ekrem, T. (submitted) DNA barcodes and morphology reveal new semi-cryptic species of Chironomidae (Diptera). *Insect Systematics & Evolution*.
Lindeberg, B. (1963) Taxonomy, biology and biometry of *Tanytarsus curticornis* Kieff. and *T. brundini* n. sp. (Dipt., Chironomidae). *Annales Entomologici Fennici* **29:** 118–130.
Lindeberg, B. (1967) Sibling species delimitation in the *Tanytarsus lestagei* aggregate Diptera, Chironomidae. *Annales Zoologici Fennici* **4:** 45–86.
Maddison, W. & Maddison, D. (2010) Mesquite: a modular system for evolutionary analysis. 2011; Version 2.75. *Available at: mesquiteproject. org/mesquite/download/download. html*.
Mardis, E.R. (2008) Next-generation DNA sequencing methods. *Annual Review of Genomics and Human Genetics* **9:** 387–402.
Metzker, M.L. (2010) Sequencing technologies—the next generation. *Nature Reviews Genetics* **11:** 31–46.
Misof, B., Liu, S., Meusemann, K., Peters, R.S., Donath, A., Mayer, C., Frandsen, P.B., Ware, J., Flouri, T. & Beutel, R.G. (2014) Phylogenomics resolves the timing and pattern of insect evolution. *Science* **346:** 763–767.
Montes, C., Cardona, A., Jaramillo, C., Pardo, A., Silva, J.C., Valencia, V., Ayala, C., Pérez-Angel, L.C., Rodriguez-Parra, L.A., Ramirez, V. & Niño, H. (2015) Middle Miocene closure of the Central American Seaway. *Science* **348:** 226–229.
Moulton, J.K. & Wiegmann, B.M. (2004) Evolution and phylogenetic utility of CAD (rudimentary) among Mesozoic-aged Eremoneuran Diptera (Insecta). *Molecular Phylogenetics and Evolution* **31:** 363–378.
Nei, M. & Kumar, S. (2000) Molecular Evolution and Phylogenetics. Oxford University Press, Oxford. pp. 333.
Petersen, F.T., Meier, R., Kutty, S.N. & Wiegmann, B.M. (2007) The phylogeny and evolution of host choice in the Hippoboscoidea (Diptera) as reconstructed using four molecular markers. *Molecular Phylogenetics and Evolution* **45:** 111–122.
Pinder, L.C.V. (1982) *Virgatanytarsus* new genus - for the "*triangularis*" group of the genus *Tanytarsus* van der Wulp (Diptera: Chironomidae). *Spixiana* **5:** 31–34.
Pinder, L.C.V. (1986) The pupae of Chironominae (Diptera: Chironomidae) of the Holarctic region – keys and diagnoses. In: Wiederholm, T. (Ed.), Chironomidae of the Holarctic Region. Keys and Diagnoses. Part 2. Pupae. *Insect Systematics & Evolution* **28:** 299–456.
Rambaut, A., Suchard, M.A., Xie, D. & Drummond, A.J. (2014) Tracer v1.6, Available from http://beast.bio.ed.ac.uk/Tracer.
Ratnasingham, S. & Hebert, P.D.N. (2007) BOLD: The Barcode of Life Data System (www.barcodinglife.org). *Molecular Ecology Notes* **7:** 355–364.
Ratnasingham, S. & Hebert, P.D.N. (2013) A DNA-based registry for all animal species: the barcode index number (BIN) system. *PloS One* **8:** e66213.
Regier, J.C., Shultz, J.W., Ganley, A.R., Hussey, A., Shi, D., Ball, B., Zwick, A., Stajich, J.E., Cummings, M.P. & Martin, J.W. (2008) Resolving arthropod phylogeny:

exploring phylogenetic signal within 41 kb of protein-coding nuclear gene sequence. *Systematic Biology* **57:** 920–938.
Reiss, F. & Fittkau, E.J. (1971) Taxonomie und Ökologie europäisch verbreiteter *Tanytarsus*-Arten (Chironomidae, Diptera). *Archiv für Hydrobiologie, Supplement* **40:** 75–200.
Roback, S.S. (1975) A new subgenus and species of the genus *Tanytarsus* (Chironomidae: Chironominae: Tanytarsini). *Proceedings of the Academy of Natural Sciences of Philadelphia* **127:** 71–80.
Rogers, J. & Wall, R. (1980) A mechanism for RNA splicing. *Proceedings of the National Academy of Sciences* **77:** 1877–1879.
Ronquist, F., Teslenko, M., van der Mark, P., Ayres, D.L., Darling, A., Höhna, S., Larget, B., Liu, L., Suchard, M.A. & Huelsenbeck, J.P. (2012) MrBayes 3.2: efficient bayesian phylogenetic inference and model choice across a large model space. *Systematic Biology* **61:** 539–542.
Sæther, O.A. (1969) Some Nearctic Pondonominae, Diamesinae, and Orthocladiinae (Diptera: Chironomidae). *Bulletin of the Fisheries Research Board of Canada* **170:** 1–154.
Sæther, O.A. (1979) Underlying synapomorphies and anagenetic analysis. *Zoologica Scripta* **8:** 305–312.
Sanseverino, A.M. (2006) A review of the genus *Tanytarsus* van der Wulp, 1874 (Insecta, Diptera, Chironomidae) from the Neotropical region. *Dissertation zur Erlangung des Doktorgrades der Fakultät für Biologie der Ludwig-Maximilians-Universität, München***:** pp. 306.
Sanseverino, A.M. & Fittkau, E.J. (2006) Four new species of *Tanytarsus* van der Wulp, 1874 (Diptera : Chironomidae) from South America. *Zootaxa* **1162:** 1–18.
Sanseverino, A.M. & Trivinho-Strixino, S. (2010) New species of *Tanytarsus* van der Wulp (Diptera: Chironomidae) from São Paulo State, Brazil. *Neotropical Entomology* **39:** 67–82.
Sanseverino, A.M., Trivinho-Strixino, S. & Nessimian, J.L. (2010) Taxonomic status of *Nimbocera* Reiss, 1972, a junior synonym of *Tanytarsus* van der Wulp, 1874 (Diptera: Chironomidae). *Zootaxa* **2359:** 43–57.
Sanseverino, A.M. & Wiedenbrug, S. (2000) Description of the pupa of *Tanytarsus cuieirensis* Fittkau & Reiss (Insecta, Diptera, Chironomidae). *Spixiana* **23:** 207–210.
Sanseverino, A.M., Wiedenbrug, S. & Fittkau, E. (2002) *Marauia* group: a new species group in the genus *Tanytarsus* van der Wulp, 1874, from the Neotropics (Diptera, Chironomidae). *Studia dipterologica* **9:** 453–468.
Sasa, M. (1980) Studies on chironomid midges of the Tama River. Part 2. Description of 20 species of Chironominae recovered from a tributary. *Research Report from the National Institute for Environmental Studies, Japan* **13:** 9–107.
Sasa, M. & Kawai, K. (1987) Studies on chironomid midges of Lake Biwa (Diptera, Chironomidae). *Lake Biwa Research Institute, Otsu, Japan* **3:** 1–119.
Säwedal, L. (1981) Amazonian Tanytarsini II. Description of *Caladomyia* n. gen. and eight new species (Diptera: Chironomidae). *Insect Systematics & Evolution* **12:** 123–143.
Scholz, M.B., Lo, C.C. & Chain, P.S.G. (2012) Next generation sequencing and bioinformatic bottlenecks: the current state of metagenomic data analysis. *Current Opinion in Biotechnology* **23:** 9–15.
Ståhls, G., Hippa, H., Rotheray, G., Muona, J. & Gilbert, F. (2003) Phylogeny of Syrphidae (Diptera) inferred from combined analysis of molecular and morphological characters. *Systematic Entomology* **28:** 433–450.
Stamatakis, A. (2006) RAxML-VI-HPC: maximum likelihood-based phylogenetic analyses with thousands of taxa and mixed models. *Bioinformatics* **22:** 2688–2690.

Stamatakis, A. (2014) RAxML version 8: a tool for phylogenetic analysis and post-analysis of large phylogenies. *Bioinformatics* **30:** 1312–1313.
Stur, E. & Ekrem, T. (2011) Exploring unknown life stages of Arctic Tanytarsini (Diptera: Chironomidae) with DNA barcoding. *Zootaxa* **2743:** 27–39.
Su, K.F.Y., Narayanan Kutty, S. & Meier, R. (2008) Morphology versus molecules: the phylogenetic relationships of Sepsidae (Diptera: Cyclorrhapha) based on morphology and DNA sequence data from ten genes. *Cladistics* **24:** 902–916.
Sublette, J. & Sasa, M. (1994) Chironomidae collected in Onchocerciasis endemic areas of Guatemala (Insecta, Diptera). *Spixiana Supplement* **20:** 1–60.
Swofford, D.L. (2002) PAUP*: Phylogenetic Analysis Using Parsimony (* and Other Methods), Version 4.0 b10. *Sinauer Associates. Sunderland, MA*.
Tachi, T. (2013) Molecular phylogeny and host use evolution of the genus *Exorista* Meigen (Diptera: Tachinidae). *Molecular Phylogenetics and Evolution* **66:** 401–411.
Tachi, T. & Shima, H. (2010) Molecular phylogeny of the subfamily Exoristinae (Diptera, Tachinidae), with discussions on the evolutionary history of female oviposition strategy. *Systematic Entomology* **35:** 148–163.
Tamura, K., Stecher, G., Peterson, D., Filipski, A. & Kumar, S. (2013) MEGA6: molecular evolutionary genetics analysis version 6.0. *Molecular Biology and Evolution* **30:** 2725–2729.
Trivinho-Strixino, S. (2012) A systematic review of Neotropical *Caladomyia* SÄWEDAL (Diptera: Chironomidae). *Zootaxa* **3495:** 1–41.
Trivinho-Strixino, S. & Strixino, G. (2007) A new Neotropical species of *Tanytarsus* van der Wulp, 1874 (Diptera : Chironomidae), with an unusual anal process. *Zootaxa* **1654:** 61–67.
Trivinho-Strixino, S., Wiedenbrug, S. & da Silva, F.L. (2015) New species of *Tanytarsus* van der Wulp (Diptera: Chironomidae: Tanytarsini) from Brazil. *European Journal of Environmental Sciences* **5:** 92–100.
Vaidya, G., Lohman, D.J. & Meier, R. (2011) SequenceMatrix: concatenation software for the fast assembly of multi-gene datasets with character set and codon information. *Cladistics* **27:** 171–180.
van Dijk, E.L., Auger, H., Jaszczyszyn, Y. & Thermes, C. (2014) Ten years of next-generation sequencing technology. *Trends in Genetics* **30:** 418–426.
Vinogradova, E.M., Riss, H.W. & Spies, M. (2009) New species of *Tanytarsus* van der Wulp, 1874 (Diptera: Chironomidae) from Central America. *Aquatic Insects* **31:** 11–17.
Virgilio, M., Jordaens, K., Verwimp, C., White, I.M. & De Meyer, M. (2015) Higher phylogeny of frugivorous flies (Diptera, Tephritidae, Dacini): Localised partition conflicts and a novel generic classification. *Molecular Phylogenetics and Evolution* **85:** 171–179.
Wagner, C.E., Keller, I., Wittwer, S., Selz, O.M., Mwaiko, S., Greuter, L., Sivasundar, A. & Seehausen, O. (2013) Genome-wide RAD sequence data provide unprecedented resolution of species boundaries and relationships in the Lake Victoria cichlid adaptive radiation. *Molecular Ecology* **22:** 787–798.
Wallace, A.R. (1876) The geographical distribution of animals: with a study of the relations of living and extinct faunas as elucidating the past changes of the Earth's surface: MacMillan and Co., London, United Kingdom.
Whiting, M.F., Carpenter, J.C., Wheeler, Q.D. & Wheeler, W.C. (1997) The Strepsiptera problem: phylogeny of the holometabolous insect orders inferred from 18S and 28S ribosomal DNA sequences and morphology. *Systematic Biology* **46:** 1–68.

Winterton, S.L., Hardy, N.B., Gaimari, S.D., Hauser, M., Hill, H.N., Holston, K.C., Irwin, M.E., Lambkin, C.L., Metz, M.A. & Turco, F. (2016) The phylogeny of stiletto flies (Diptera: Therevidae). *Systematic Entomology* **41:** 144–161.
Winterton, S.L. & Ware, J.L. (2015) Phylogeny, divergence times and biogeography of window flies (Scenopinidae) and the therevoid clade (Diptera: Asiloidea). *Systematic Entomology* **40:** 491–519.
Wulp, F.M. (1874) Dipterologische aanteekeningen. *Tijdschrift voor Entomologie* **17:** 109–148.
Xi, Z.X., Liu, L. & Davis, C.C. (2016) The Impact of Missing Data on Species Tree Estimation. *Molecular Biology and Evolution* **33:** 838–860.
Xia, X.H. (2013) DAMBE5: a comprehensive software package for data analysis in molecular biology and evolution. *Molecular Biology and Evolution* **30:** 1720–1728.
Xia, X.H. & Lemey, P. (2009) Assessing substitution saturation with DAMBE. *The phylogenetic handbook: a practical approach to DNA and protein phylogeny* **2:** 615–630.
Xia, X.H., Xie, Z., Salemi, M., Chen, L. & Wang, Y. (2003) An index of substitution saturation and its application. *Molecular Phylogenetics and Evolution* **26:** 1–7.
Yu, Y., Harris, A. & He, X.J. (2010) S-DIVA (Statistical Dispersal-Vicariance Analysis): a tool for inferring biogeographic histories. *Molecular Phylogenetics and Evolution* **56:** 848–850.
Yu, Y., Harris, A.J., Blair, C. & He, X.J. (2015) RASP (Reconstruct Ancestral State in Phylogenies): A tool for historical biogeography. *Molecular Phylogenetics and Evolution* **87:** 46–49.
Zakrzewska, M. & Giłka, W. (2013) In the Eocene, the extant genus *Caladomyia* occurred in the Palaearctic (Diptera: Chironomidae: Tanytarsini). *Polish Journal of Entomology/Polskie Pismo Entomologiczne* **82:** 397–403.
Zetterstedt, J.W. (1838) Dipterologia Scandinaviae, Sectio Tertia [Section 3] Diptera. Insecta lapponica. Leipzig. 477–868.

Figure captions

Figure 1. Maximum likelihood tree based on the concatenated DNA dataset (18S, AATS1, CAD1, CAD4, PGD, TPI, 4281 characters) of *Tanytarsus* sensu lato. Support number refers to posterior probability over 0.95 + ML bootstrap value over 70% / MP bootstrap value over 70%.

Figure 2. Clade A of maximum likelihood tree based on the concatenated DNA dataset (18S, AATS1, CAD1, CAD4, PGD, TPI, 4281 characters) of *Tanytarsus* sensu lato. Support number refers to posterior probability over 0.95 + ML bootstrap value over 70% / MP bootstrap value over 70%.

Figure 3. Clade B of maximum likelihood tree based on the concatenated DNA dataset (18S, AATS1, CAD1, CAD4, PGD, TPI, 4281 characters) of *Tanytarsus* sensu lato. Support number refers to posterior probability over 0.95 + ML bootstrap value over 70% / MP bootstrap value over 70%.

Figure 4. Clade C of maximum likelihood tree based on the concatenated DNA dataset (18S, AATS1, CAD1, CAD4, PGD, TPI, 4281 characters) of *Tanytarsus* sensu lato. Support number refers to posterior probability over 0.95 + ML bootstrap value over 70% / MP bootstrap value over 70%.

Figure 5. Hypothesized event-based ancestral area reconstruction of *Tanytarsus* as inferred by S-DIVA analyses based on the updated Wallace's zoogeographical regions. Pie diagrams show the ancestral distributions estimated for internal nodes of the phylogeny of *Tanytarsus* by S-DIVA. Blue circles indicate dispersal events, green circles indicate vicariance events. The letter A = Afrotropical region; B = Neotropical region; C = Australian region; D = Oriental region; E = Palearctic region; F = Nearctic region; G = Sino-Japanese region; H = Panamanian region; I = Saharo-Arabian region.

Figure 6. Hypothesized event-based ancestral area reconstruction of *Tanytarsus* as inferred by S-DIVA analyses based on the traditional Wallace's zoogeographical regions. Pie diagrams show the ancestral distributions estimated for internal nodes of the phylogeny of *Tanytarsus* by S-DIVA. Blue circles indicate dispersal events, green circles indicate vicariance events. The letter A = Afrotropical region; B = Neotropical region; C = Australian region; D = Oriental region; E = Palearctic region; F = Nearctic region.

Figure 7. Hypothesized event-based ancestral area reconstruction of *Tanytarsus* as inferred by S-DIVA analyses based on the Bănărescu's zoogeographical regions. Pie diagrams show the ancestral distributions estimated for internal nodes of the phylogeny of *Tanytarsus* by S-DIVA. Blue circles indicate dispersal events, green circles indicate vicariance

events. The letter A = Afrotropical region; B = Neotropical region; C = Australian region; D = Oriental region; E = Holarctic region.

Figure 1

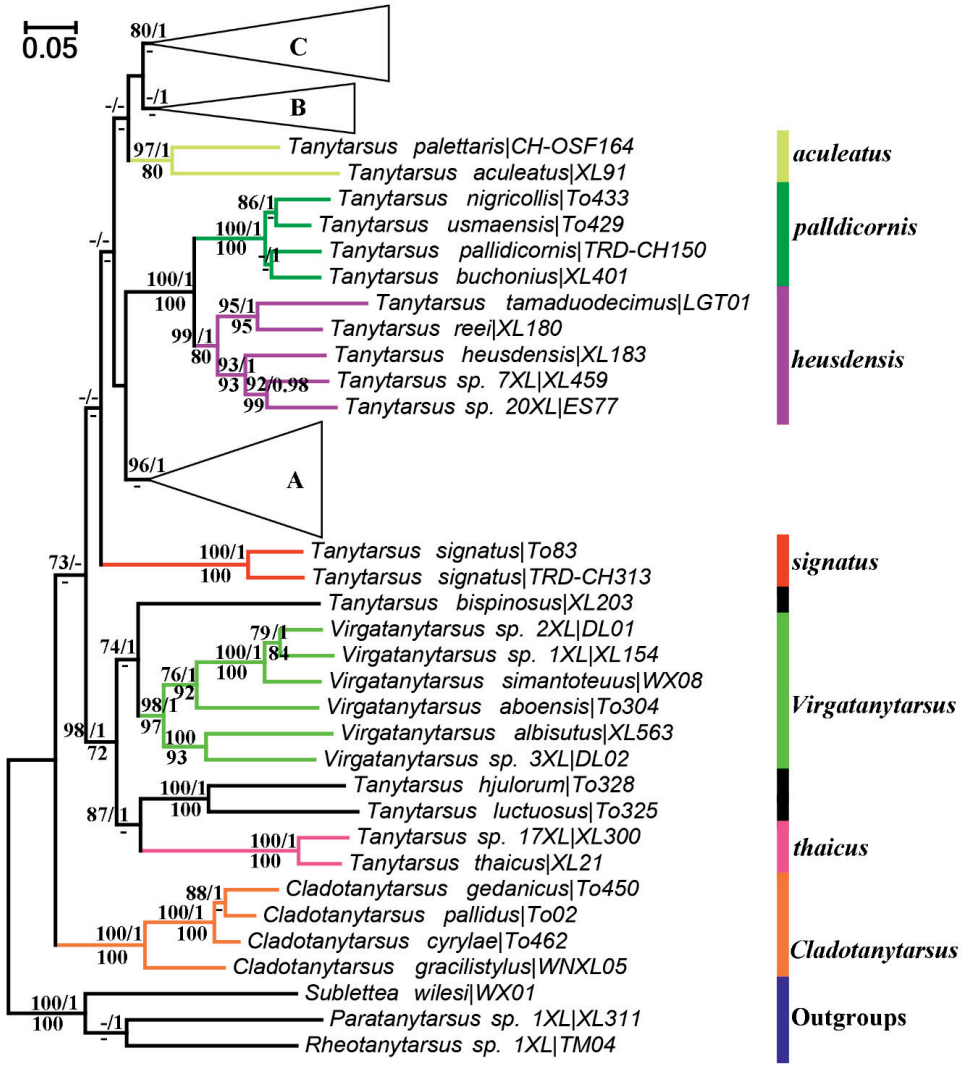
0.05
C
B
A
Tanytarsus palettaris|CH-OSF164
Tanytarsus aculeatus|XL91
Tanytarsus nigricollis|To433
Tanytarsus usmaensis|To429
Tanytarsus pallidicornis|TRD-CH150
Tanytarsus buchonius|XL401
Tanytarsus tamaduodecimus|LGT01
Tanytarsus reei|XL180
Tanytarsus heusdensis|XL183
Tanytarsus sp. 7XL|XL459
Tanytarsus sp. 20XL|ES77
Tanytarsus signatus|To83
Tanytarsus signatus|TRD-CH313
Tanytarsus bispinosus|XL203
Virgatanytarsus sp. 2XL|DL01
Virgatanytarsus sp. 1XL|XL154
Virgatanytarsus simantoteuus|WX08
Virgatanytarsus aboensis|To304
Virgatanytarsus albisutus|XL563
Virgatanytarsus sp. 3XL|DL02
Tanytarsus hjulorum|To328
Tanytarsus luctuosus|To325
Tanytarsus sp. 17XL|XL300
Tanytarsus thaicus|XL21
Cladotanytarsus gedanicus|To450
Cladotanytarsus pallidus|To02
Cladotanytarsus cyrylae|To462
Cladotanytarsus gracilistylus|WNXL05
Sublettea wilesi|WX01
Paratanytarsus sp. 1XL|XL311
Rheotanytarsus sp. 1XL|TM04
aculeatus
palldicornis
heusdensis
signatus
Virgatanytarsus
thaicus
Cladotanytarsus
Outgroups

Figure 2

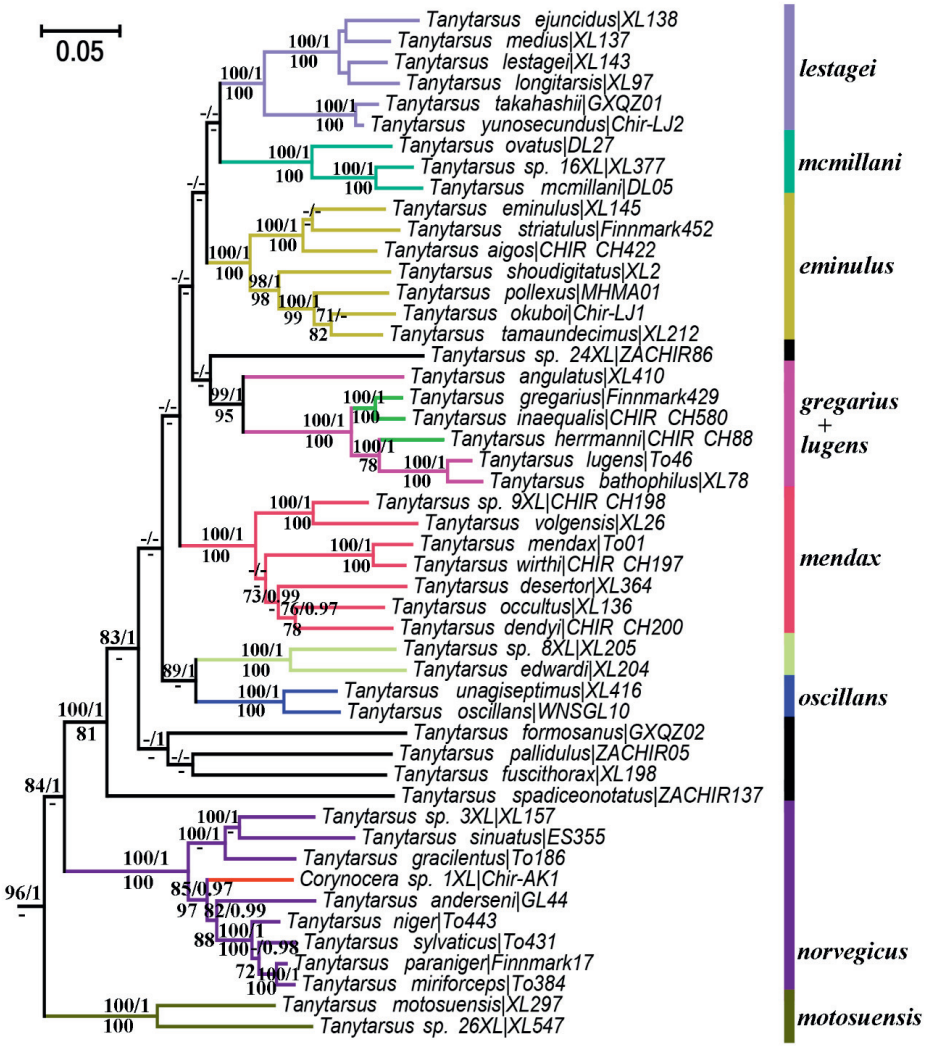
0.05
Tanytarsus ejuncidus|XL138
Tanytarsus medius|XL137
Tanytarsus lestagei|XL143
Tanytarsus longitarsis|XL97
Tanytarsus takahashii|GXQZ01
Tanytarsus yunosecundus|Chir-LJ2
Tanytarsus ovatus|DL27
Tanytarsus sp. 16XL|XL377
Tanytarsus mcmillani|DL05
Tanytarsus eminulus|XL145
Tanytarsus striatulus|Finnmark452
Tanytarsus aigos|CHIR CH422
Tanytarsus shoudigitatus|XL2
Tanytarsus pollexus|MHMA01
Tanytarsus okuboi|Chir-LJ1
Tanytarsus tamaundecimus|XL212
Tanytarsus sp. 24XL|ZACHIR86
Tanytarsus angulatus|XL410
Tanytarsus gregarius|Finnmark429
Tanytarsus inaequalis|CHIR CH580
Tanytarsus herrmanni|CHIR CH88
Tanytarsus lugens|To46
Tanytarsus bathophilus|XL78
Tanytarsus sp. 9XL|CHIR CH198
Tanytarsus volgensis|XL26
Tanytarsus mendax|To01
Tanytarsus wirthi|CHIR CH197
Tanytarsus desertor|XL364
Tanytarsus occultus|XL136
Tanytarsus dendyi|CHIR CH200
Tanytarsus sp. 8XL|XL205
Tanytarsus edwardi|XL204
Tanytarsus unagiseptimus|XL416
Tanytarsus oscillans|WNSGL10
Tanytarsus formosanus|GXQZ02
Tanytarsus pallidulus|ZACHIR05
Tanytarsus fuscithorax|XL198
Tanytarsus spadiceonotatus|ZACHIR137
Tanytarsus sp. 3XL|XL157
Tanytarsus sinuatus|ES355
Tanytarsus gracilentus|To186
Corynocera sp. 1XL|Chir-AK1
Tanytarsus anderseni|GL44
Tanytarsus niger|To443
Tanytarsus sylvaticus|To431
Tanytarsus paraniger|Finnmark17
Tanytarsus miriforceps|To384
Tanytarsus motosuensis|XL297
Tanytarsus sp. 26XL|XL547
lestagei
mcmillani
eminulus
gregarius + lugens
mendax
oscillans
norvegicus
motosuensis

Figure 3

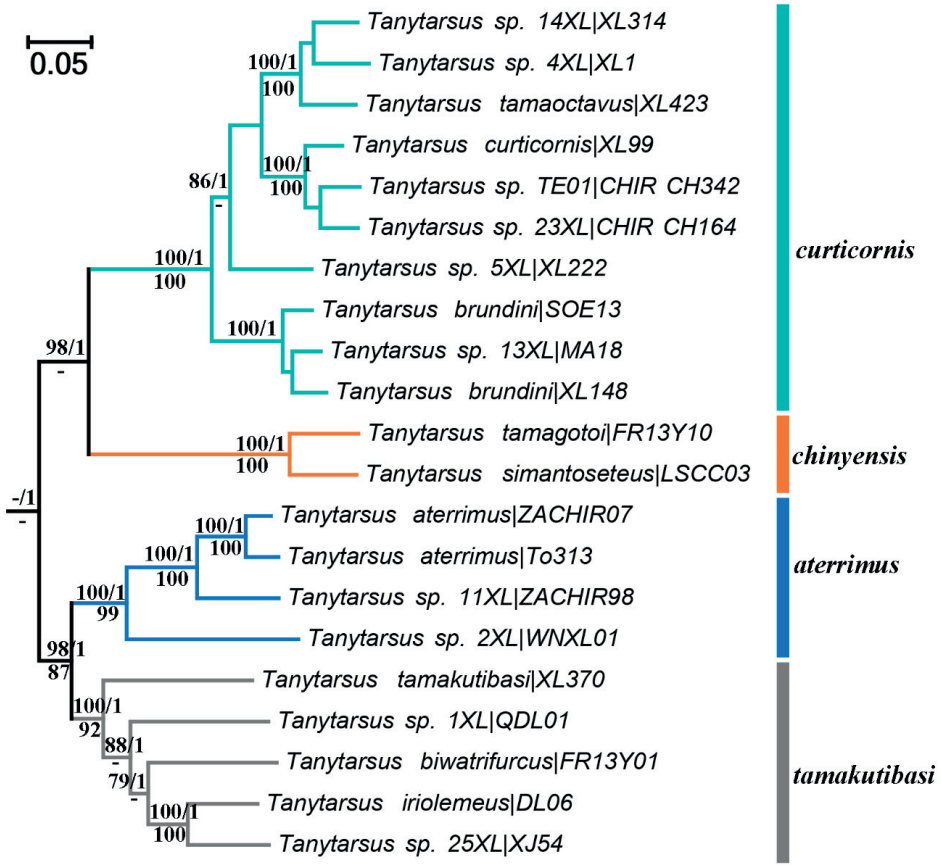
0.05
Tanytarsus sp. 14XL|XL314
Tanytarsus sp. 4XL|XL1
Tanytarsus tamaoctavus|XL423
Tanytarsus curticornis|XL99
Tanytarsus sp. TE01|CHIR CH342
Tanytarsus sp. 23XL|CHIR CH164
Tanytarsus sp. 5XL|XL222
Tanytarsus brundini|SOE13
Tanytarsus sp. 13XL|MA18
Tanytarsus brundini|XL148
Tanytarsus tamagotoi|FR13Y10
Tanytarsus simantoseteus|LSCC03
Tanytarsus aterrimus|ZACHIR07
Tanytarsus aterrimus|To313
Tanytarsus sp. 11XL|ZACHIR98
Tanytarsus sp. 2XL|WNXL01
Tanytarsus tamakutibasi|XL370
Tanytarsus sp. 1XL|QDL01
Tanytarsus biwatrifurcus|FR13Y01
Tanytarsus iriolemeus|DL06
Tanytarsus sp. 25XL|XJ54
curticornis
chinyensis
aterrimus
tamakutibasi

Figure 4

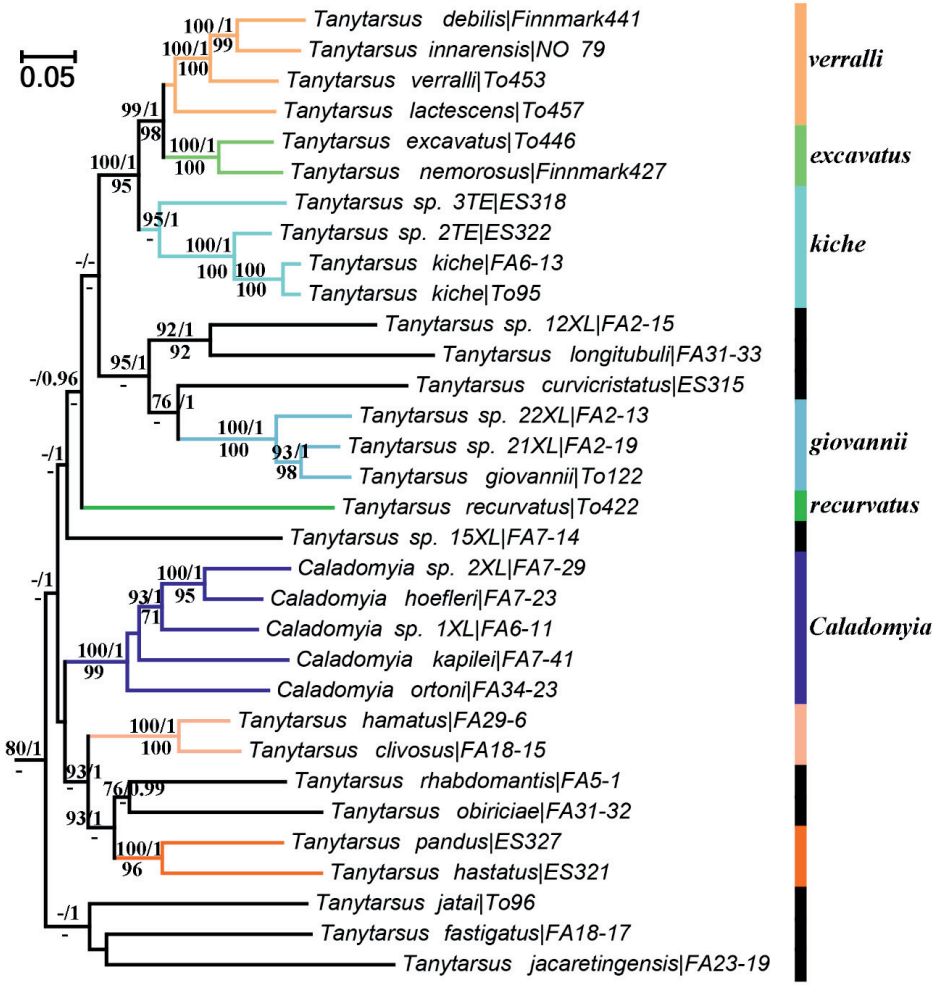
0.05
Tanytarsus debilis|Finnmark441
Tanytarsus innarensis|NO 79
Tanytarsus verralli|To453
Tanytarsus lactescens|To457
Tanytarsus excavatus|To446
Tanytarsus nemorosus|Finnmark427
Tanytarsus sp. 3TE|ES318
Tanytarsus sp. 2TE|ES322
Tanytarsus kiche|FA6-13
Tanytarsus kiche|To95
Tanytarsus sp. 12XL|FA2-15
Tanytarsus longitubuli|FA31-33
Tanytarsus curvicristatus|ES315
Tanytarsus sp. 22XL|FA2-13
Tanytarsus sp. 21XL|FA2-19
Tanytarsus giovannii|To122
Tanytarsus recurvatus|To422
Tanytarsus sp. 15XL|FA7-14
Caladomyia sp. 2XL|FA7-29
Caladomyia hoefleri|FA7-23
Caladomyia sp. 1XL|FA6-11
Caladomyia kapilei|FA7-41
Caladomyia ortoni|FA34-23
Tanytarsus hamatus|FA29-6
Tanytarsus clivosus|FA18-15
Tanytarsus rhabdomantis|FA5-1
Tanytarsus obiriciae|FA31-32
Tanytarsus pandus|ES327
Tanytarsus hastatus|ES321
Tanytarsus jatai|To96
Tanytarsus fastigatus|FA18-17
Tanytarsus jacaretingensis|FA23-19
verralli
excavatus
kiche
giovannii
recurvatus
Caladomyia

Figure 5

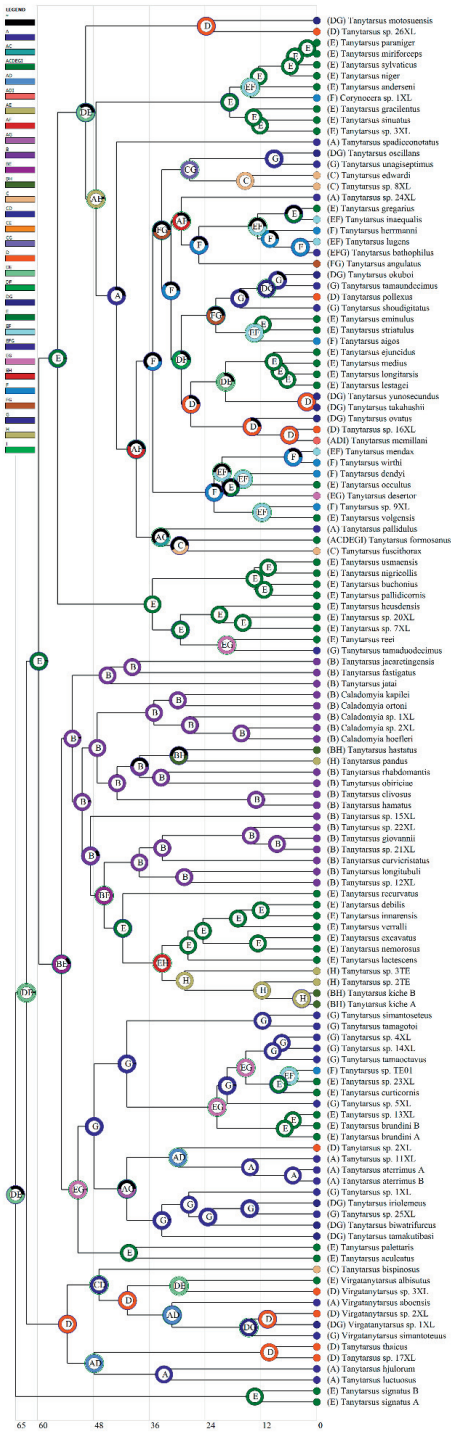
(DG) Tanytarsus motosuensis
(D) Tanytarsus sp. 26XL
(F) Tanytarsus paramiger
(E) Tanytarsus miriforceps
(E) Tanytarsus sylvaticus
(E) Tanytarsus niger
(E) Tanytarsus andersoni
(F) Corynoecera sp. 1XL
(E) Tanytarsus gracilentus
(E) Tanytarsus sinuatus
(F) Tanytarsus sp. 3XL
(A) Tanytarsus spadiconotatus
(DG) Tanytarsus oscillans
(G) Tanytarsus unagiseptimus
(C) Tanytarsus edwardi
(C) Tanytarsus sp. 8XL
(A) Tanytarsus sp. 24XL
(E) Tanytarsus gregarius
(EF) Tanytarsus inaequalis
(F) Tanytarsus herrmanni
(EF) Tanytarsus ligens
(EFG) Tanytarsus bathophilus
(FG) Tanytarsus angulatus
(DG) Tanytarsus okuboi
(G) Tanytarsus tamaundecimus
(D) Tanytarsus pollexus
(G) Tanytarsus shoudigitatus
(E) Tanytarsus eminulus
(E) Tanytarsus striatulus
(F) Tanytarsus nigos
(E) Tanytarsus ejuncidus
(E) Tanytarsus medius
(E) Tanytarsus longitarsis
(E) Tanytarsus lestagei
(DG) Tanytarsus yunosecundus
(DG) Tanytarsus takahashii
(DG) Tanytarsus ovatus
(D) Tanytarsus sp. 16XL
(AD) Tanytarsus mcmillani
(EF) Tanytarsus mendax
(F) Tanytarsus wirthi
(F) Tanytarsus dendyi
(E) Tanytarsus occultus
(EG) Tanytarsus desertor
(F) Tanytarsus sp. 9XL
(E) Tanytarsus volgensis
(A) Tanytarsus pallidulus
(ACDEGI) Tanytarsus formosanus
(C) Tanytarsus fasciithorax
(E) Tanytarsus usmaensis
(E) Tanytarsus nigricollis
(E) Tanytarsus buchonius
(F) Tanytarsus pallidicornis
(E) Tanytarsus heusdensis
(E) Tanytarsus sp. 20XL
(E) Tanytarsus sp. 7XL
(F) Tanytarsus reei
(G) Tanytarsus tamaduodecimus
(B) Tanytarsus jacuticotigensis
(B) Tanytarsus fastigatus
(B) Tanytarsus jutai
(B) Caladomyia kapilei
(B) Caladomyia orteei
(B) Caladomyia sp. 1XL
(B) Caladomyia sp. 2XL
(B) Caladomyia hoefleri
(BH) Tanytarsus hastatus
(H) Tanytarsus pandus
(B) Tanytarsus rhabdomantis
(B) Tanytarsus obiriciae
(B) Tanytarsus clivosus
(B) Tanytarsus hamatus
(B) Tanytarsus sp. 15XL
(B) Tanytarsus sp. 22XL
(B) Tanytarsus giovanni
(B) Tanytarsus sp. 21XL
(B) Tanytarsus curvicrisatus
(B) Tanytarsus longilubuli
(B) Tanytarsus sp. 12XL
(E) Tanytarsus recurvatus
(E) Tanytarsus debilis
(F) Tanytarsus innarensis
(F) Tanytarsus verralli
(E) Tanytarsus excavatus
(E) Tanytarsus nemorosus
(E) Tanytarsus lactescens
(H) Tanytarsus sp. 3TE
(H) Tanytarsus sp. 2TE
(BH) Tanytarsus kiche B
(BH) Tanytarsus kiche A
(G) Tanytarsus simantoseteus
(G) Tanytarsus tamagotoi
(G) Tanytarsus sp. 4XL
(G) Tanytarsus sp. 14XL
(G) Tanytarsus tamaoctavus
(F) Tanytarsus sp. TE01
(E) Tanytarsus sp. 23XL
(E) Tanytarsus curticornis
(G) Tanytarsus sp. 5XL
(E) Tanytarsus sp. 13XL
(E) Tanytarsus brundini B
(E) Tanytarsus brundini A
(D) Tanytarsus sp. 2XL
(A) Tanytarsus sp. 11XL
(A) Tanytarsus aterrimus A
(A) Tanytarsus aterrimus B
(G) Tanytarsus sp. 1XL
(DG) Tanytarsus iriolemeus
(G) Tanytarsus sp. 25XL
(DG) Tanytarsus biwatrifurcus
(DG) Tanytarsus tamakulibasi
(E) Tanytarsus palettaris
(E) Tanytarsus aculeatus
(C) Tanytarsus bispinosus
(E) Virgatanytarsus albisutus
(D) Virgatanytarsus sp. 3XL
(A) Virgatanytarsus aboensis
(D) Virgatanytarsus sp. 2XL
(DG) Virgatanytarsus sp. 1XL
(G) Virgatanytarsus simantoteus
(D) Tanytarsus thaicus
(D) Tanytarsus sp. 17XL
(A) Tanytarsus hjulorum
(A) Tanytarsus luctuosus
(E) Tanytarsus signatus B
(E) Tanytarsus signatus A
65
60
48
36
24
12
0

Figure 6

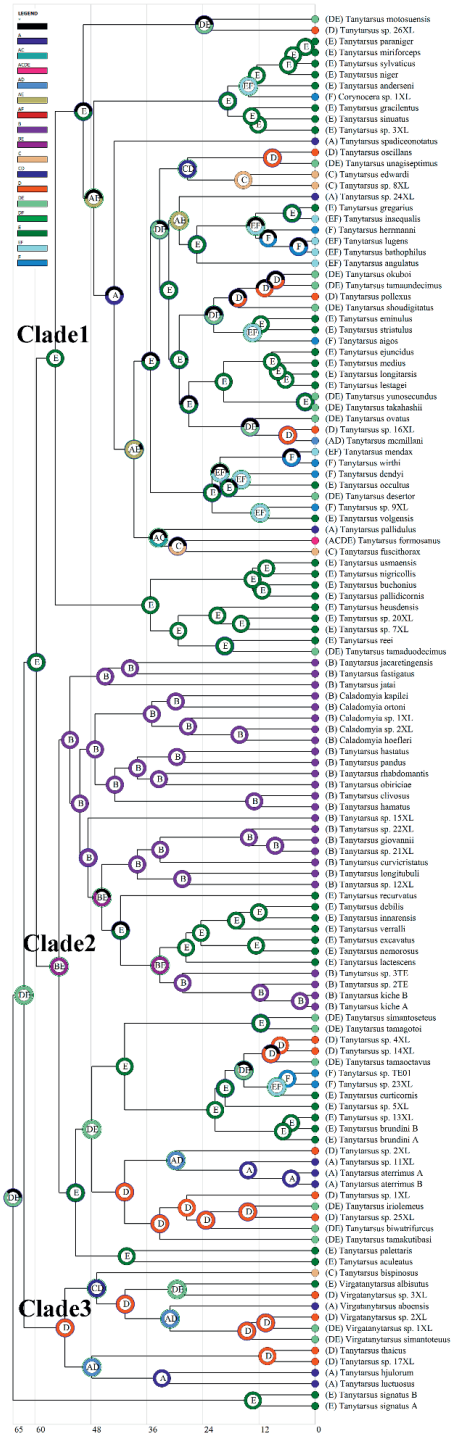
Clade1
Clade2
Clade3
(DE) Tanytarsus motosuensis
(D) Tanytarsus sp. 26XL
(E) Tanytarsus paramiger
(E) Tanytarsus mirifoceps
(E) Tanytarsus sylvaticus
(E) Tanytarsus niger
(E) Tanytarsus andersoni
(F) Corynocera sp. 1XL
(E) Tanytarsus gracilentus
(E) Tanytarsus sinuatus
(E) Tanytarsus sp. 3XL
(A) Tanytarsus spadiceonotatus
(D) Tanytarsus oscillans
(DE) Tanytarsus unagiseptimus
(C) Tanytarsus edwardi
(C) Tanytarsus sp. 8XL
(A) Tanytarsus sp. 24XL
(E) Tanytarsus gregarius
(EF) Tanytarsus inaequalis
(F) Tanytarsus hermanni
(EF) Tanytarsus lugens
(EF) Tanytarsus bathophilus
(EF) Tanytarsus angulatus
(DE) Tanytarsus okuboi
(DE) Tanytarsus tamaundecimus
(D) Tanytarsus pollexus
(DE) Tanytarsus shoudigitatus
(E) Tanytarsus eminulus
(E) Tanytarsus strantulus
(F) Tanytarsus aigos
(E) Tanytarsus ejuncidus
(E) Tanytarsus modius
(E) Tanytarsus longitarsis
(E) Tanytarsus leistagei
(DE) Tanytarsus yunosecundus
(DE) Tanytarsus takahashii
(DE) Tanytarsus ovatus
(D) Tanytarsus sp. 16XL
(AD) Tanytarsus mcmillani
(EF) Tanytarsus mendax
(F) Tanytarsus wirthi
(F) Tanytarsus dendyi
(E) Tanytarsus oculatus
(DE) Tanytarsus desertor
(F) Tanytarsus sp. 9XL
(E) Tanytarsus volgensis
(A) Tanytarsus pallidulus
(ACDE) Tanytarsus formosanus
(C) Tanytarsus fuscithorax
(E) Tanytarsus usmaensis
(E) Tanytarsus nigricollis
(E) Tanytarsus buchanius
(E) Tanytarsus pallidicornis
(F) Tanytarsus heusdensis
(E) Tanytarsus sp. 20XL
(E) Tanytarsus sp. 7XL
(E) Tanytarsus ree
(DE) Tanytarsus tamaduodecimus
(B) Tanytarsus jacaretingensis
(B) Tanytarsus fastigatus
(B) Tanytarsus jatai
(B) Caladomyia kapilei
(B) Caladomyia ortoni
(B) Caladomyia sp. 1XL
(B) Caladomyia sp. 2XL
(B) Caladomyia hoefleri
(B) Tanytarsus hastatus
(B) Tanytarsus pandus
(B) Tanytarsus rhabdomantis
(B) Tanytarsus obiriciae
(B) Tanytarsus clivosus
(B) Tanytarsus hanantus
(B) Tanytarsus sp. 15XL
(B) Tanytarsus sp. 22XL
(B) Tanytarsus giovannii
(B) Tanytarsus sp. 21XL
(B) Tanytarsus curviceristatus
(B) Tanytarsus longitibuli
(B) Tanytarsus sp. 12XL
(E) Tanytarsus recurvatus
(E) Tanytarsus debilis
(E) Tanytarsus inaraensis
(E) Tanytarsus verralli
(E) Tanytarsus excavatus
(E) Tanytarsus nemorosus
(E) Tanytarsus lactescens
(B) Tanytarsus sp. 3TF
(B) Tanytarsus sp. 2TE
(B) Tanytarsus kiche B
(B) Tanytarsus kiche A
(DE) Tanytarsus simuntoseteus
(DE) Tanytarsus tamagotoi
(D) Tanytarsus sp. 4XL
(D) Tanytarsus sp. 14XL
(DE) Tanytarsus tamaoctavus
(F) Tanytarsus sp. TE01
(F) Tanytarsus sp. 23XL
(E) Tanytarsus curticornis
(E) Tanytarsus sp. 5XL
(E) Tanytarsus sp. 13XL
(E) Tanytarsus brundini B
(E) Tanytarsus brundini A
(D) Tanytarsus sp. 2XL
(A) Tanytarsus sp. 11XL
(A) Tanytarsus aterrimus A
(A) Tanytarsus aterrimus B
(D) Tanytarsus sp. 1XL
(DE) Tanytarsus iriolemeus
(D) Tanytarsus sp. 25XL
(DE) Tanytarsus biwatrifurcus
(DE) Tanytarsus tamakutibasi
(E) Tanytarsus palettaris
(E) Tanytarsus aculeatus
(C) Tanytarsus bispinosus
(E) Virgatanytarsus albisutus
(D) Virgatanytarsus sp. 3XL
(A) Virgatanytarsus aboensis
(D) Virgatanytarsus sp. 2XL
(DE) Virgatanytarsus sp. 1XL
(DE) Virgatanytarsus simantoteuus
(D) Tanytarsus thaicus
(D) Tanytarsus sp. 17XL
(A) Tanytarsus hjulorum
(A) Tanytarsus luctuosus
(E) Tanytarsus signatus B
(E) Tanytarsus signatus A
65
60
48
36
24
12
0

Figure 7

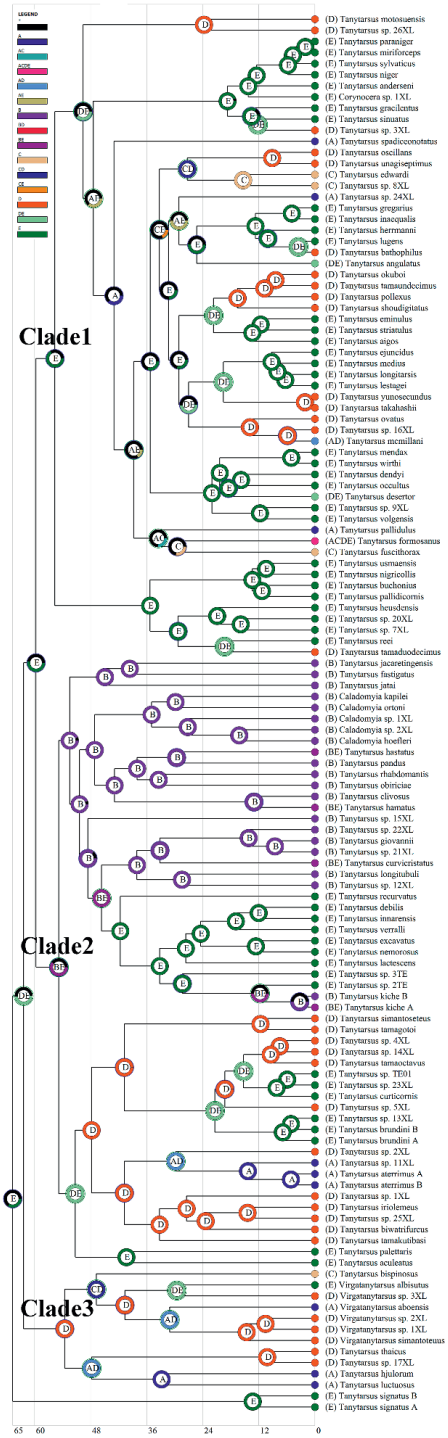
Clade1
Clade2
Clade3
(D) Tanytarsus motosuensis
(D) Tanytarsus sp. 26XL
(E) Tanytarsus paraniger
(E) Tanytarsus mirifonceps
(F) Tanytarsus sylvaticus
(E) Tanytarsus niger
(E) Tanytarsus anderseni
(E) Corynocera sp. 1XL
(E) Tanytarsus gracilentus
(E) Tanytarsus sinuatus
(D) Tanytarsus sp. 3XL
(A) Tanytarsus spadiceonotatus
(D) Tanytarsus oscillans
(D) Tanytarsus unagisepinus
(C) Tanytarsus edwardi
(C) Tanytarsus sp. 8XL
(A) Tanytarsus sp. 24XL
(E) Tanytarsus gregarius
(E) Tanytarsus inaequalis
(E) Tanytarsus herrmanni
(F) Tanytarsus lugens
(D) Tanytarsus bathophilus
(DE) Tanytarsus angulatus
(D) Tanytarsus okuboi
(D) Tanytarsus tamaundecimus
(D) Tanytarsus pollexus
(D) Tanytarsus shoudigitatus
(E) Tanytarsus eminulus
(E) Tanytarsus striatulus
(E) Tanytarsus aigos
(E) Tanytarsus ejuncidus
(E) Tanytarsus medina
(E) Tanytarsus longitarsis
(F) Tanytarsus lestagei
(D) Tanytarsus yunosecundus
(D) Tanytarsus takahashii
(D) Tanytarsus ovatus
(D) Tanytarsus sp. 16XL
(AD) Tanytarsus mcmillani
(E) Tanytarsus mendax
(E) Tanytarsus wirthi
(E) Tanytarsus dendyi
(E) Tanytarsus occultus
(DE) Tanytarsus desertor
(E) Tanytarsus sp. 9XL
(E) Tanytarsus volgensis
(A) Tanytarsus pallidulus
(ACDE) Tanytarsus formosanus
(C) Tanytarsus fuscithorax
(E) Tanytarsus usmaensis
(E) Tanytarsus nigricollis
(E) Tanytarsus buchonius
(E) Tanytarsus pallidicornis
(E) Tanytarsus heusdensis
(E) Tanytarsus sp. 20XL
(E) Tanytarsus sp. 7XL
(E) Tanytarsus reei
(D) Tanytarsus tanaduodecimus
(B) Tanytarsus jacaretingensis
(B) Tanytarsus fastigatus
(B) Tanytarsus jatai
(B) Caladomyia kapilei
(B) Caladomyia ortoni
(B) Caladomyia sp. 1XL
(B) Caladomyia sp. 2XL
(B) Caladomyia hoefleri
(BE) Tanytarsus hastatus
(B) Tanytarsus pandus
(B) Tanytarsus rhabdomantis
(B) Tanytarsus obiriciae
(B) Tanytarsus clivosus
(BE) Tanytarsus hamatus
(B) Tanytarsus sp. 15XL
(B) Tanytarsus sp. 22XL
(B) Tanytarsus giovannii
(B) Tanytarsus sp. 21XL
(BE) Tanytarsus curviceristatus
(B) Tanytarsus longitubuli
(B) Tanytarsus sp. 12XL
(E) Tanytarsus recurvatus
(E) Tanytarsus debilis
(E) Tanytarsus innaensis
(E) Tanytarsus verralli
(E) Tanytarsus excavatus
(E) Tanytarsus nemorosus
(E) Tanytarsus lactescens
(E) Tanytarsus sp. 3TE
(E) Tanytarsus sp. 2TE
(B) Tanytarsus kiche B
(BE) Tanytarsus kiche A
(D) Tanytarsus simantoeteus
(D) Tanytarsus tamagotoi
(D) Tanytarsus sp. 4XL
(D) Tanytarsus sp. 14XL
(D) Tanytarsus tamaoctavus
(E) Tanytarsus sp. TF01
(E) Tanytarsus sp. 23XL
(E) Tanytarsus curticornis
(D) Tanytarsus sp. 5XL
(E) Tanytarsus sp. 13XL
(E) Tanytarsus brundini B
(E) Tanytarsus brundini A
(D) Tanytarsus sp. 2XL
(A) Tanytarsus sp. 11XL
(A) Tanytarsus aterrimus A
(A) Tanytarsus aterrimus B
(D) Tanytarsus sp. 1XL
(D) Tanytarsus iriolemeus
(D) Tanytarsus sp. 25XL
(D) Tanytarsus biwantifurcus
(D) Tanytarsus tamakubbasi
(E) Tanytarsus paletturis
(E) Tanytarsus aculeatus
(C) Tanytarsus bispinosus
(E) Virgatanytarsus albisutus
(D) Virgatanytarsus sp. 3XL
(A) Virgatanytarsus aboensis
(D) Virgatanytarsus sp. 2XL
(D) Virgatanytarsus sp. 1XL
(D) Virgatanytarsus simantoteus
(D) Tanytarsus thaicus
(D) Tanytarsus sp. 17XL
(A) Tanytarsus hjulorum
(A) Tanytarsus luctuosus
(E) Tanytarsus signatus B
(E) Tanytarsus signatus A
65
60
48
36
24
12
0

Supporting information

File S1. The aligned sequences for each gene used for phylogenetic analyses.

File S2. BEAST divergence time estimates tree with node age. Nodes on the chronogram represent means of the probability distributions for node ages with time interval for 95% probability of actual age represented as coloured bars. Timescale units are in millions of years, with the estimated age for a divergence given on each node.

File S3. BEAST divergence time estimates tree with 95% height range. Timescale units are in millions of years, with the estimated age for a divergence given on each node.

File S2

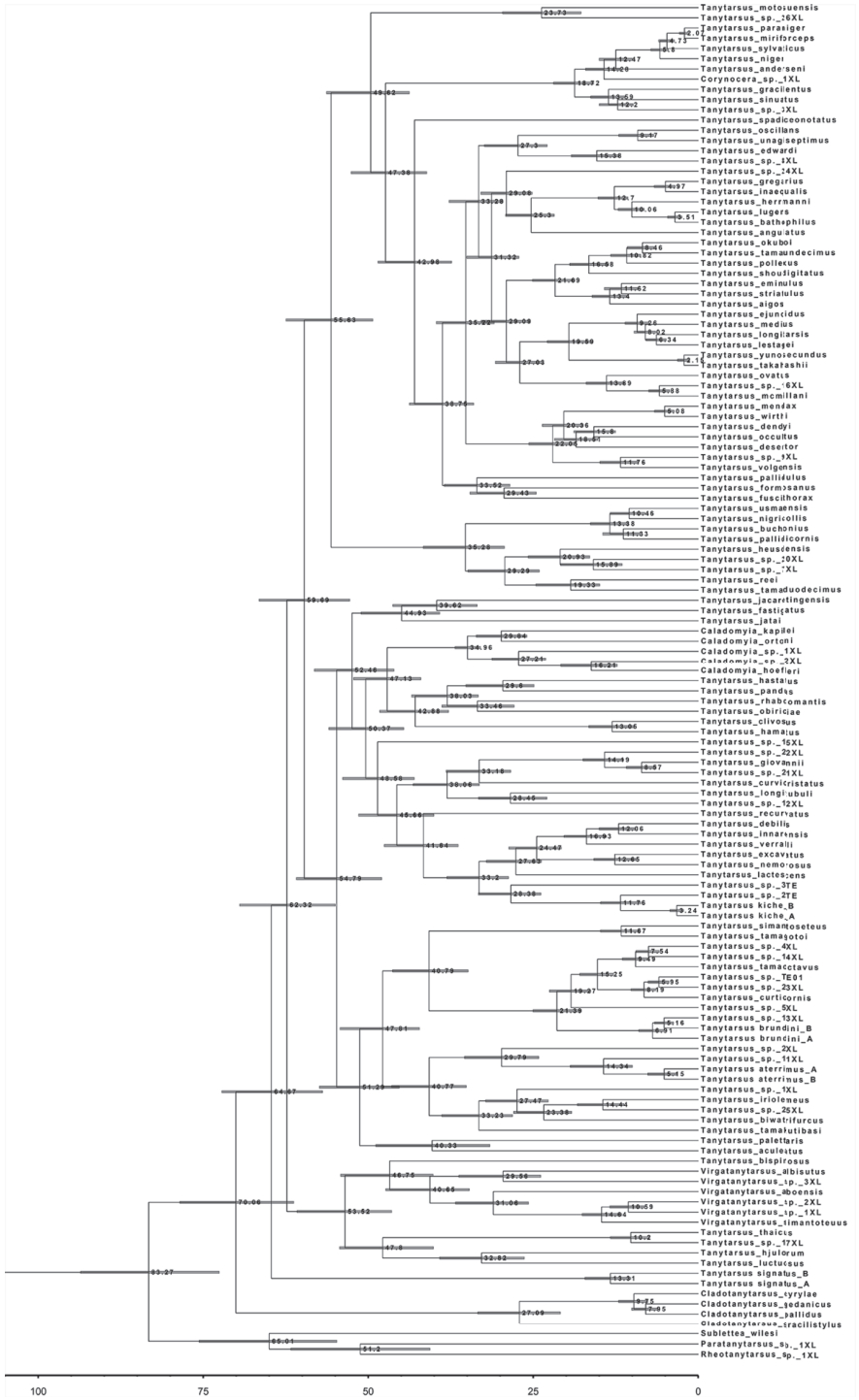
Tanytarsus_motosuensis
Tanytarsus_sp._16XL
Tanytarsus_parasiger
Tanytarsus_mirifrceps
Tanytarsus_sylvaicus
Tanytarsus_nigei
Tanytarsus_andersoni
Corynocera_sp._1XL
Tanytarsus_gracilentus
Tanytarsus_sinuatus
Tanytarsus_sp._13XL
Tanytarsus_spadiconotatus
Tanytarsus_oscillans
Tanytarsus_unagiseptimus
Tanytarsus_edwardi
Tanytarsus_sp._1XL
Tanytarsus_sp._24XL
Tanytarsus_gregarius
Tanytarsus_inaequalis
Tanytarsus_herrmanni
Tanytarsus_lugens
Tanytarsus_bathophilus
Tanytarsus_anguiatus
Tanytarsus_okuboi
Tanytarsus_tamaundecimus
Tanytarsus_pollexus
Tanytarsus_shoulighitatus
Tanytarsus_eminulus
Tanytarsus_striaiulus
Tanytarsus_aigos
Tanytarsus_ejuncidus
Tanytarsus_mediis
Tanytarsus_longiarsis
Tanytarsus_lestagei
Tanytarsus_yunoiecundus
Tanytarsus_takazashii
Tanytarsus_ovatis
Tanytarsus_sp._16XL
Tanytarsus_mcmillani
Tanytarsus_menéax
Tanytarsus_wirthi
Tanytarsus_dendyi
Tanytarsus_occultus
Tanytarsus_deserior
Tanytarsus_sp._1XL
Tanytarsus_volgensis
Tanytarsus_pallidulus
Tanytarsus_formosanus
Tanytarsus_fuscithorax
Tanytarsus_usmaensis
Tanytarsus_nigricollis
Tanytarsus_buchonius
Tanytarsus_pallidicornis
Tanytarsus_heuscensis
Tanytarsus_sp._20XL
Tanytarsus_sp._7XL
Tanytarsus_reei
Tanytarsus_tamaduodecimus
Tanytarsus_jacarettingensis
Tanytarsus_fastigatus
Tanytarsus_jatai
Caladomyia_kapilei
Caladomyia_ortoni
Caladomyia_sp._1XL
Caladomyia_sp._2XL
Caladomyia_hoefleri
Tanytarsus_hastatus
Tanytarsus_pandus
Tanytarsus_rhabdomantis
Tanytarsus_obiriciae
Tanytarsus_clivosus
Tanytarsus_hamatus
Tanytarsus_sp._15XL
Tanytarsus_sp._22XL
Tanytarsus_giovanni
Tanytarsus_sp._21XL
Tanytarsus_curvicristatus
Tanytarsus_longitubuli
Tanytarsus_sp._12XL
Tanytarsus_recurvatus
Tanytarsus_debilis
Tanytarsus_innarensis
Tanytarsus_verralli
Tanytarsus_excavatus
Tanytarsus_nemorosus
Tanytarsus_lactescens
Tanytarsus_sp._3TE
Tanytarsus_sp._2TE
Tanytarsus kiche_B
Tanytarsus kiche_A
Tanytarsus_simantoseteus
Tanytarsus_tamagotoi
Tanytarsus_sp._4XL
Tanytarsus_sp._14XL
Tanytarsus_tamacetavus
Tanytarsus_sp._TE01
Tanytarsus_sp._23XL
Tanytarsus_curticornis
Tanytarsus_sp._5XL
Tanytarsus_sp._13XL
Tanytarsus brundini_B
Tanytarsus brundini_A
Tanytarsus_sp._2XL
Tanytarsus_sp._11XL
Tanytarsus aterrimus_A
Tanytarsus aterrimus_B
Tanytarsus_sp._1XL
Tanytarsus_trioleneus
Tanytarsus_sp._25XL
Tanytarsus_biwatrifurcus
Tanytarsus_tamalutibasi
Tanytarsus_palettaris
Tanytarsus_aculeatus
Tanytarsus_bispirosus
Virgatanytarsus_albisutus
Virgatanytarsus_sp._3XL
Virgatanytarsus_aboensis
Virgatanytarsus_sp._2XL
Virgatanytarsus_sp._1XL
Virgatanytarsus_simantoteuus
Tanytarsus_thaicus
Tanytarsus_sp._17XL
Tanytarsus_hjulorum
Tanytarsus_luctuosus
Tanytarsus signatus_B
Tanytarsus signatus_A
Cladotanytarsus_syrylae
Cladotanytarsus_sedanicus
Cladotanytarsus_pallidus
Cladotanytarsus_gracilistylus
Sublettea_wilesi
Paratanytarsus_sp._1XL
Rheotanytarsus_sp._1XL
100
75
50
25
0

File S3

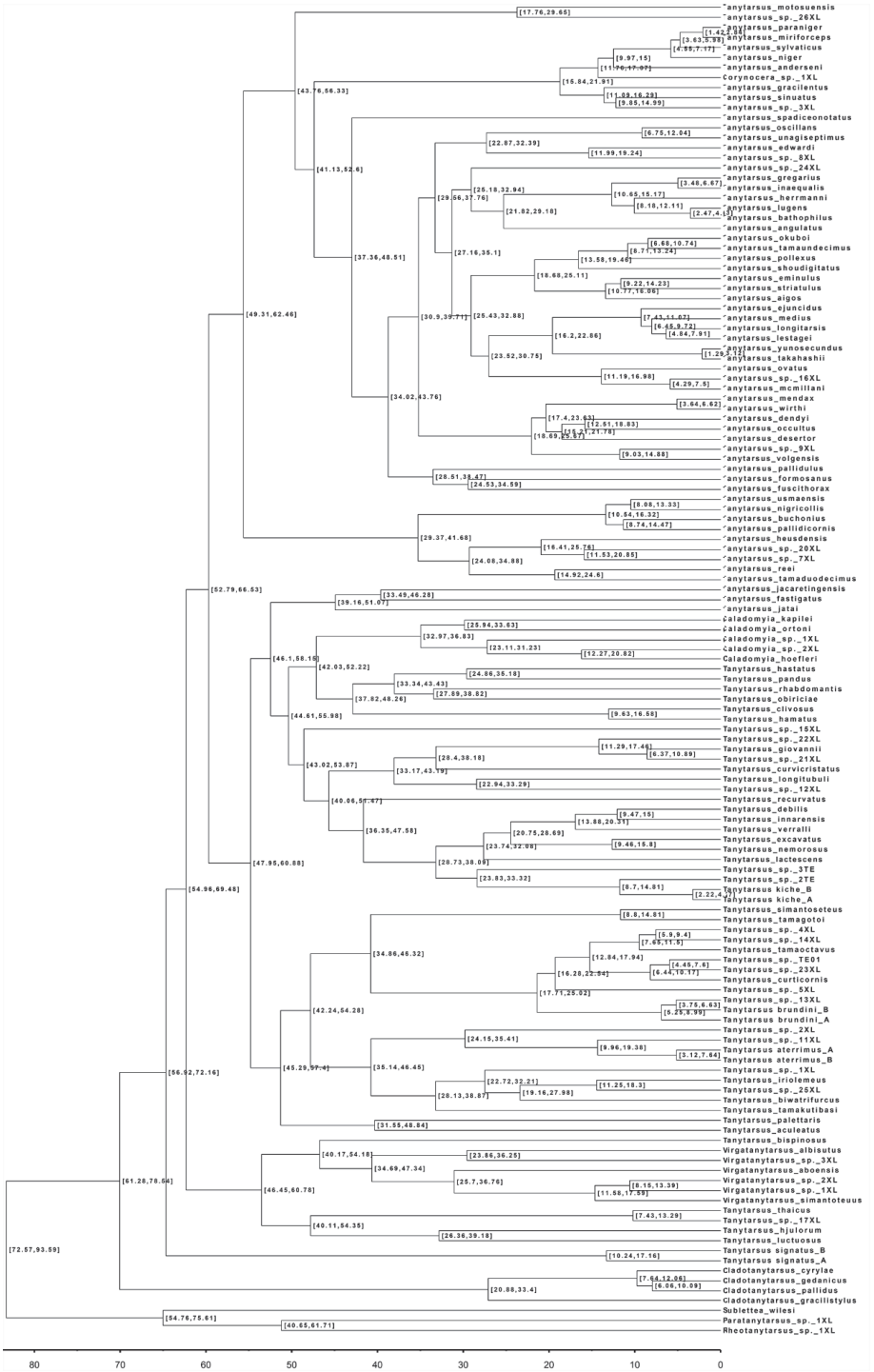
anytarsus_motosuensis
anytarsus_sp._26XL
anytarsus_paraniger
anytarsus_miriforceps
anytarsus_sylvaticus
anytarsus_niger
anytarsus_anderseni
Corynocera_sp._1XL
anytarsus_gracilentus
anytarsus_sinuatus
anytarsus_sp._3XL
anytarsus_spadiceonotatus
anytarsus_oscillans
anytarsus_unagiseptimus
anytarsus_edwardi
anytarsus_sp._8XL
anytarsus_sp._24XL
anytarsus_gregarius
anytarsus_inaequalis
anytarsus_herrmanni
anytarsus_lugens
anytarsus_bathophilus
anytarsus_angulatus
anytarsus_okuboi
anytarsus_tamaundecimus
anytarsus_pollexus
anytarsus_shoudigitatus
anytarsus_eminulus
anytarsus_striatulus
anytarsus_aigos
anytarsus_ejuncidus
anytarsus_medius
anytarsus_longitarsis
anytarsus_lestagei
anytarsus_yunosecundus
anytarsus_takahashii
anytarsus_ovatus
anytarsus_sp._16XL
anytarsus_mcmillani
anytarsus_mendax
anytarsus_wirthi
anytarsus_dendyi
anytarsus_occultus
anytarsus_desertor
anytarsus_sp._9XL
anytarsus_volgensis
anytarsus_pallidulus
anytarsus_formosanus
anytarsus_fuscithorax
anytarsus_usmaensis
anytarsus_nigricollis
anytarsus_buchonius
anytarsus_pallidicornis
anytarsus_heusdensis
anytarsus_sp._20XL
anytarsus_sp._7XL
anytarsus_reei
anytarsus_tamaduodecimus
anytarsus_jacaretingensis
anytarsus_fastigatus
anytarsus_jatai
Caladomyia_kapilei
Caladomyia_ortoni
Caladomyia_sp._1XL
Caladomyia_sp._2XL
Caladomyia_hoefleri
Tanytarsus_hastatus
Tanytarsus_pandus
Tanytarsus_rhabdomantis
Tanytarsus_obiriciae
Tanytarsus_clivosus
Tanytarsus_hamatus
Tanytarsus_sp._15XL
Tanytarsus_sp._22XL
Tanytarsus_giovannii
Tanytarsus_sp._21XL
Tanytarsus_curvicristatus
Tanytarsus_longitubuli
Tanytarsus_sp._12XL
Tanytarsus_recurvatus
Tanytarsus_debilis
Tanytarsus_innarensis
Tanytarsus_verralli
Tanytarsus_excavatus
Tanytarsus_nemorosus
Tanytarsus_lactescens
Tanytarsus_sp._3TE
Tanytarsus_sp._2TE
Tanytarsus kiche_B
Tanytarsus kiche_A
Tanytarsus_simantoseteus
Tanytarsus_tamagotoi
Tanytarsus_sp._4XL
Tanytarsus_sp._14XL
Tanytarsus_tamaoctavus
Tanytarsus_sp._TE01
Tanytarsus_sp._23XL
Tanytarsus_curticornis
Tanytarsus_sp._5XL
Tanytarsus_sp._13XL
Tanytarsus brundini_B
Tanytarsus brundini_A
Tanytarsus_sp._2XL
Tanytarsus_sp._11XL
Tanytarsus aterrimus_A
Tanytarsus aterrimus_B
Tanytarsus_sp._1XL
Tanytarsus_irioiomeus
Tanytarsus_sp._25XL
Tanytarsus_biwatrifurcus
Tanytarsus_tamakutibasi
Tanytarsus_palettaris
Tanytarsus_aculeatus
Tanytarsus_bispinosus
Virgatanytarsus_albisutus
Virgatanytarsus_sp._3XL
Virgatanytarsus_aboensis
Virgatanytarsus_sp._2XL
Virgatanytarsus_sp._1XL
Virgatanytarsus_simantoteuus
Tanytarsus_thaicus
Tanytarsus_sp._17XL
Tanytarsus_hjulorum
Tanytarsus_luctuosus
Tanytarsus signatus_B
Tanytarsus signatus_A
Cladotanytarsus_cyrylae
Cladotanytarsus_gedanicus
Cladotanytarsus_pallidus
Cladotanytarsus_gracilistylus
Sublettea_wilesi
Paratanytarsus_sp._1XL
Rheotanytarsus_sp._1XL
80
70
60
50
40
30
20
10
0

Table S1. The final dataset for phylogenetic analyses, with BOLD Sample ID and lengths (bp) of each amplified gene

Species	Sample ID	18S	AATS1	CAD1	CAD4	PGD	TPI
Caladomyia hoefleri	FA7-23	939	403	N/C	846	748	438
Caladomyia kapilei	FA7-41	939	405	N/C	846	744	437
Caladomyia ortoni	FA34-23	940	401	897	846	748	438
Caladomyia sp. 1XL	FA6-11	940	405	876	847	748	439
Caladomyia sp. 2XL	FA7-29	940	395	886	841	742	N/C
Cladotanytarsus cyrylae	To462	926	404	883	836	742	438
Cladotanytarsus gedanicus	To450	925	385	886	829	743	413
Cladotanytarsus gracilistylus	WNXL05	939	402	878	846	744	439
Cladotanytarsus pallidus	To02	N/C	404	810	814	741	439
Corynocera sp. 1XL	Chir-AK1	941	405	876	847	748	439
Paratanytarsus sp. 1XL	XL311	921	403	900	847	748	N/C
Rheotanytarsus	TM04	940	405	901	845	747	432
Sublettea wilesi	WX01	937	405	895	847	748	413
Tanytarsus aculeatus	XL91	944	405	909	847	N/C	439
Tanytarsus aigos	CHIR_CH422	936	405	905	847	748	439
Tanytarsus anderseni	GL44	941	405	908	847	748	415
Tanytarsus angulatus	XL410	926	405	909	847	748	439
Tanytarsus aterrimus	To313	N/C	408	N/C	N/C	743	410
Tanytarsus aterrimus	ZACHIR07	940	341	N/C	N/C	738	439
Tanytarsus bathophilus	XL78	939	405	908	847	748	439
Tanytarsus bispinosus	XL203	943	404	903	846	748	439
Tanytarsus biwatrifurcus	FR13Y01	939	403	887	847	747	N/C
Tanytarsus brundini	SOE13	N/C	408	909	N/C	745	N/C
Tanytarsus brundini	XL148	939	408	909	839	744	436
Tanytarsus buchonius	XL401	939	407	909	N/C	743	434
Tanytarsus clivosus	FA18-15	939	405	903	845	721	437
Tanytarsus curticornis	XL99	939	404	908	843	748	N/C
Tanytarsus curvicristatus	ES315	924	384	896	847	748	439
Tanytarsus debilis	Finnmark441	938	401	870	847	748	437
Tanytarsus dendyi	CHIR_CH200	940	405	908	847	748	413
Tanytarsus desertor	XL364	940	404	791	840	748	419
Tanytarsus edwardi	XL204	938	404	909	845	747	439
Tanytarsus ejuncidus	XL138	939	405	909	847	746	439
Tanytarsus eminulus	XL145	938	401	907	846	745	411
Tanytarsus excavatus	To446	938	403	864	843	748	438
Tanytarsus fastigatus	FA18-17	940	403	906	841	745	439
Tanytarsus formosanus	GXQZ02	940	406	869	845	747	439
Tanytarsus fuscithorax	XL198	940	404	888	847	747	439

Tanytarsus giovannii	To122	N/C	404	897	847	739	409
Tanytarsus gracilentus	To186	939	405	818	847	746	439
Tanytarsus gregarius	Finnmark429	939	402	907	847	747	424
Tanytarsus hamatus	FA29-6	939	405	903	846	745	439
Tanytarsus hastatus	ES321	936	404	909	844	748	410
Tanytarsus herrmanni	CHIR_CH88	939	405	907	847	746	439
Tanytarsus heusdensis	XL183	939	387	886	N/C	748	406
Tanytarsus hjulorum	To328	923	395	874	825	747	439
Tanytarsus inaequalis	CHIR_CH580	919	405	908	847	715	439
Tanytarsus innarensis	NO 79	938	405	909	847	746	438
Tanytarsus iriolemeus	DL06	925	404	888	847	748	421
Tanytarsus jacaretingensis	FA23-19	942	404	909	N/C	748	439
Tanytarsus jatai	To96	924	405	845	847	748	439
Tanytarsus kiche	FA6-13	938	405	899	845	748	439
Tanytarsus kiche	To95	920	405	816	824	748	438
Tanytarsus lactescens	To457	938	405	848	830	748	397
Tanytarsus lestagei	XL143	938	400	900	847	748	414
Tanytarsus longitarsis	XL97	938	405	908	847	748	439
Tanytarsus longitubuli	FA31-33	940	405	905	847	748	438
Tanytarsus luctuosus	To325	917	405	909	847	748	439
Tanytarsus lugens	To46	926	404	908	847	N/C	439
Tanytarsus mcmillani	DL05	939	401	894	847	707	409
Tanytarsus medius	XL137	940	403	909	847	748	439
Tanytarsus mendax	To01	926	404	835	847	746	438
Tanytarsus miriforceps	To384	941	374	909	844	748	439
Tanytarsus motosuensis	XL297	940	403	909	847	747	439
Tanytarsus nemorosus	Finnmark427	938	408	896	847	748	N/C
Tanytarsus niger	To443	941	401	901	839	748	334
Tanytarsus nigricollis	To433	939	405	899	843	747	432
Tanytarsus obiriciae	FA31-32	939	98	908	847	747	119
Tanytarsus occultus	XL136	939	402	909	847	748	438
Tanytarsus okuboi	Chir-LJ1	937	405	874	847	747	439
Tanytarsus oscillans	WNSGL10	938	403	881	840	744	439
Tanytarsus ovatus	DL27	939	382	873	847	743	432
Tanytarsus palettaris	CH-OSF164	946	408	909	847	748	439
Tanytarsus pallidicornis	TRD-CH150	939	405	909	N/C	723	439
Tanytarsus pallidulus	ZACHIR05	939	404	908	847	724	439
Tanytarsus pandus	ES327	941	408	874	847	748	439
Tanytarsus paraniger	Finnmark17	940	401	907	847	743	439
Tanytarsus pollexus	MHMA01	939	405	819	847	747	439
Tanytarsus recurvatus	To422	938	405	909	847	746	N/C
Tanytarsus reei	XL180	938	405	897	N/C	748	438
Tanytarsus rhabdomantis	FA5-1	938	401	901	847	746	437
Tanytarsus shoudigitatus	XL2	940	405	897	846	748	439
Tanytarsus signatus	To83	941	382	901	842	747	439

Tanytarsus signatus	TRD-CH313	941	405	903	842	748	439
Tanytarsus simantoseteus	LSCC03	922	402	874	847	747	438
Tanytarsus sinuatus	ES355	939	405	892	847	743	439
Tanytarsus sp. 11XL	ZACHIR98	940	N/C	879	N/C	739	439
Tanytarsus sp. 12XL	FA2-15	939	405	906	N/C	748	439
Tanytarsus sp. 13XL	MA18	940	408	907	844	747	439
Tanytarsus sp. 14XL	XL314	940	405	909	828	745	439
Tanytarsus sp. 15XL	FA7-14	943	404	909	849	747	433
Tanytarsus sp. 16XL	XL377	938	403	735	841	744	435
Tanytarsus sp. 17XL	XL300	945	405	909	847	746	396
Tanytarsus sp. 1XL	QDL01	939	405	815	847	742	439
Tanytarsus sp. 20XL	ES77	939	408	909	N/C	748	0
Tanytarsus sp. 21XL	FA2-19	939	404	902	847	748	439
Tanytarsus sp. 22XL	FA2-13	944	364	903	847	748	N/C
Tanytarsus sp. 23XL	CHIR_CH164	939	405	909	845	747	439
Tanytarsus sp. 24XL	ZACHIR86	940	405	906	846	748	439
Tanytarsus sp. 25XL	XJ54	939	395	900	839	748	257
Tanytarsus sp. 26XL	XL547	N/C	404	865	847	748	432
Tanytarsus sp. 2TE	ES322	938	377	902	N/C	743	437
Tanytarsus sp. 2XL	WNXL01	938	408	877	N/C	747	438
Tanytarsus sp. 3TE	ES318	938	381	909	847	745	439
Tanytarsus sp. 3XL	XL157	939	405	868	845	748	439
Tanytarsus sp. 4XL	XL1	939	398	892	844	743	439
Tanytarsus sp. 5XL	XL222	940	403	909	837	744	439
Tanytarsus sp. 7XL	XL459	939	N/C	899	N/C	731	439
Tanytarsus sp. 8XL	XL205	940	403	909	847	747	432
Tanytarsus sp. 9XL	CHIR_CH198	938	405	908	847	748	384
Tanytarsus spadiceonotatus	ZACHIR137	940	402	897	N/C	745	439
Tanytarsus sp. TE01	CHIR_CH342	939	405	874	846	745	N/C
Tanytarsus striatulus	Finnmark452	938	394	900	847	746	N/C
Tanytarsus sylvaticus	To431	941	405	881	847	748	439
Tanytarsus takahashii	GXQZ01	939	405	898	N/C	720	438
Tanytarsus tamaduodecimus	LGT01	938	388	893	N/C	748	438
Tanytarsus tamagotoi	FR13Y10	942	404	509	847	748	439
Tanytarsus tamakutibasi	XL370	929	397	792	842	734	N/C
Tanytarsus tamaoctavus	XL423	926	405	892	847	748	435
Tanytarsus tamaundecimus	XL212	938	400	909	847	748	439
Tanytarsus thaicus	XL21	949	404	903	847	748	N/C
Tanytarsus unagiseptimus	XL416	939	402	609	846	747	439
Tanytarsus usmaensis	To429	939	405	886	845	748	439
Tanytarsus verralli	To453	938	380	904	842	748	439
Tanytarsus volgensis	XL26	939	403	883	847	748	438
Tanytarsus wirthi	CHIR_CH197	940	405	908	847	748	439

Tanytarsus yunosecundus	Chir-LJ2	940	405	887	846	748	439
Virgatanytarsus aboensis	To304	942	401	814	846	747	417
Virgatanytarsus albisutus	XL563	943	405	908	826	747	439
Virgatanytarsus simantoteuus	WX08	944	405	895	847	747	439
Virgatanytarsus sp. 1XL	XL154	944	405	894	847	748	439
Virgatanytarsus sp. 2XL	DL01	945	392	867	838	748	437
Virgatanytarsus sp. 3XL	DL02	943	405	877	835	748	439

Table S2. Informative sites, and average nucleotide composition in the aligned nuclear gene sequences.

Gene	Nucleotide position	Informative sites	T(%)	C(%)	A(%)	G(%)	AT(%)	GC(%)
18S	All	136(100%)	28.3	17.2	29.2	25.2	57.5	42.5
AATS1	1st	46(26.3%)	23.7	20.4	23.5	32.4	47.2	52.8
	2nd	24(12.2%)	28.5	15.9	33.6	22.0	62.1	37.9
	3nd	127(64.5%)	35.4	22.2	21.8	20.6	57.2	42.8
	All	197(100%)	29.2	19.5	26.3	25.0	55.5	44.5
CAD1	1st	103(23.3%)	21.1	18.7	30.9	29.3	52.0	48.0
	2nd	52(11.7%)	28.0	18.8	35.3	17.9	63.3	36.7
	3nd	288(65.0%)	37.5	18.6	26.0	17.9	63.5	36.5
	All	443(100%)	28.8	18.7	30.7	21.7	59.5	40.5
CAD4	1st	89(21.7%)	21.7	12.1	32.6	33.6	54.3	45.7
	2nd	53(12.9%)	31.8	17.3	34.9	16.0	66.7	33.3
	3nd	268(65.4%)	34.5	19.9	25.6	20.0	40.1	39.9
	All	410(100%)	29.3	16.4	31.1	23.2	60.4	39.6
PGD	1st	53(17.3%)	20.1	17.5	29.2	33.2	49.3	50.7
	2nd	21(6.9%)	29.7	20.6	30.8	18.9	60.5	39.5
	3nd	232(75.8%)	30.4	28.0	21.1	20.5	51.5	48.5
	All	306(100%)	26.7	22.0	27.1	24.2	53.8	46.2
TPI	1st	54(24.0%)	17.3	14.9	21.0	46.8	38.3	61.7
	2nd	29(12.9%)	31.3	27.9	25.1	15.7	56.4	43.6
	3nd	142(63.1%)	35.3	26.7	22.3	15.7	57.6	42.4
	All	225(100%)	27.9	23.2	22.8	26.1	50.7	49.3

Doctoral theses in Biology
Norwegian University of Science and Technology
Department of Biology

Year	Name	Degree	Title
1974	Tor-Henning Iversen	Dr. philos Botany	The roles of statholiths, auxin transport, and auxin metabolism in root gravitropism
1978	Tore Slagsvold	Dr. philos Zoology	Breeding events of birds in relation to spring temperature and environmental phenology
1978	Egil Sakshaug	Dr. philos Botany	"The influence of environmental factors on the chemical composition of cultivated and natural populations of marine phytoplankton"
1980	Arnfinn Langeland	Dr. philos Zoology	Interaction between fish and zooplankton populations and their effects on the material utilization in a freshwater lake
1980	Helge Reinertsen	Dr. philos Botany	The effect of lake fertilization on the dynamics and stability of a limnetic ecosystem with special reference to the phytoplankton
1982	Gunn Mari Olsen	Dr. scient Botany	Gravitropism in roots of *Pisum sativum* and *Arabidopsis thaliana*
1982	Dag Dolmen	Dr. philos Zoology	Life aspects of two sympartic species of newts (*Triturus, Amphibia*) in Norway, with special emphasis on their ecological niche segregation
1984	Eivin Røskaft	Dr. philos Zoology	Sociobiological studies of the rook *Corvus frugilegus*
1984	Anne Margrethe Cameron	Dr. scient Botany	Effects of alcohol inhalation on levels of circulating testosterone, follicle stimulating hormone and luteinzing hormone in male mature rats
1984	Asbjørn Magne Nilsen	Dr. scient Botany	Alveolar macrophages from expectorates – Biological monitoring of workers exosed to occupational air pollution. An evaluation of the AM-test
1985	Jarle Mork	Dr. philos Zoology	Biochemical genetic studies in fish
1985	John Solem	Dr. philos Zoology	Taxonomy, distribution and ecology of caddisflies (*Trichoptera*) in the Dovrefjell mountains
1985	Randi E. Reinertsen	Dr. philos Zoology	Energy strategies in the cold: Metabolic and thermoregulatory adaptations in small northern birds
1986	Bernt-Erik Sæther	Dr. philos Zoology	Ecological and evolutionary basis for variation in reproductive traits of some vertebrates: A comparative approach
1986	Torleif Holthe	Dr. philos Zoology	Evolution, systematics, nomenclature, and zoogeography in the polychaete orders *Oweniimorpha* and *Terebellomorpha*, with special reference to the Arctic and Scandinavian fauna
1987	Helene Lampe	Dr. scient Zoology	The function of bird song in mate attraction and territorial defence, and the importance of song repertoires
1987	Olav Hogstad	Dr. philos Zoology	Winter survival strategies of the Willow tit *Parus montanus*
1987	Jarle Inge Holten	Dr. philos Botany	Autecological investigations along a coust-inland transect at Nord-Møre, Central Norway

1987	Rita Kumar	Dr. scient Botany	Somaclonal variation in plants regenerated from cell cultures of *Nicotiana sanderae* and *Chrysanthemum morifolium*
1987	Bjørn Åge Tømmerås	Dr. scient Zoology	Olfaction in bark beetle communities: Interspecific interactions in regulation of colonization density, predator - prey relationship and host attraction
1988	Hans Christian Pedersen	Dr. philos Zoology	Reproductive behaviour in willow ptarmigan with special emphasis on territoriality and parental care
1988	Tor G. Heggberget	Dr. philos Zoology	Reproduction in Atlantic Salmon (*Salmo salar*): Aspects of spawning, incubation, early life history and population structure
1988	Marianne V. Nielsen	Dr. scient Zoology	The effects of selected environmental factors on carbon allocation/growth of larval and juvenile mussels (*Mytilus edulis*)
1988	Ole Kristian Berg	Dr. scient Zoology	The formation of landlocked Atlantic salmon (*Salmo salar* L.)
1989	John W. Jensen	Dr. philos Zoology	Crustacean plankton and fish during the first decade of the manmade Nesjø reservoir, with special emphasis on the effects of gill nets and salmonid growth
1989	Helga J. Vivås	Dr. scient Zoology	Theoretical models of activity pattern and optimal foraging: Predictions for the Moose *Alces alces*
1989	Reidar Andersen	Dr. scient Zoology	Interactions between a generalist herbivore, the moose *Alces alces*, and its winter food resources: a study of behavioural variation
1989	Kurt Ingar Draget	Dr. scient Botany	Alginate gel media for plant tissue culture
1990	Bengt Finstad	Dr. scient Zoology	Osmotic and ionic regulation in Atlantic salmon, rainbow trout and Arctic charr: Effect of temperature, salinity and season
1990	Hege Johannesen	Dr. scient Zoology	Respiration and temperature regulation in birds with special emphasis on the oxygen extraction by the lung
1990	Åse Krøkje	Dr. scient Botany	The mutagenic load from air pollution at two work-places with PAH-exposure measured with Ames Salmonella/microsome test
1990	Arne Johan Jensen	Dr. philos Zoology	Effects of water temperature on early life history, juvenile growth and prespawning migrations of Atlantic salmion (*Salmo salar*) and brown trout (*Salmo trutta*): A summary of studies in Norwegian streams
1990	Tor Jørgen Almaas	Dr. scient Zoology	Pheromone reception in moths: Response characteristics of olfactory receptor neurons to intra- and interspecific chemical cues
1990	Magne Husby	Dr. scient Zoology	Breeding strategies in birds: Experiments with the Magpie *Pica pica*
1991	Tor Kvam	Dr. scient Zoology	Population biology of the European lynx (*Lynx lynx*) in Norway
1991	Jan Henning L'Abêe Lund	Dr. philos Zoology	Reproductive biology in freshwater fish, brown trout *Salmo trutta* and roach *Rutilus rutilus* in particular
1991	Asbjørn Moen	Dr. philos Botany	The plant cover of the boreal uplands of Central Norway. I. Vegetation ecology of Sølendet nature reserve; haymaking fens and birch woodlands
1991	Else Marie Løbersli	Dr. scient Botany	Soil acidification and metal uptake in plants
1991	Trond Nordtug	Dr. scient Zoology	Reflectometric studies of photomechanical adaptation in superposition eyes of arthropods

1991	Thyra Solem	Dr. scient Botany	Age, origin and development of blanket mires in Central Norway
1991	Odd Terje Sandlund	Dr. philos Zoology	The dynamics of habitat use in the salmonid genera *Coregonus* and *Salvelinus*: Ontogenic niche shifts and polymorphism
1991	Nina Jonsson	Dr. philos Zoology	Aspects of migration and spawning in salmonids
1991	Atle Bones	Dr. scient Botany	Compartmentation and molecular properties of thioglucoside glucohydrolase (myrosinase)
1992	Torgrim Breiehagen	Dr. scient Zoology	Mating behaviour and evolutionary aspects of the breeding system of two bird species: the Temminck's stint and the Pied flycatcher
1992	Anne Kjersti Bakken	Dr. scient Botany	The influence of photoperiod on nitrate assimilation and nitrogen status in timothy (*Phleum pratense* L.)
1992	Tycho Anker-Nilssen	Dr. scient Zoology	Food supply as a determinant of reproduction and population development in Norwegian Puffins *Fratercula arctica*
1992	Bjørn Munro Jenssen	Dr. philos Zoology	Thermoregulation in aquatic birds in air and water: With special emphasis on the effects of crude oil, chemically treated oil and cleaning on the thermal balance of ducks
1992	Arne Vollan Aarset	Dr. philos Zoology	The ecophysiology of under-ice fauna: Osmotic regulation, low temperature tolerance and metabolism in polar crustaceans.
1993	Geir Slupphaug	Dr. scient Botany	Regulation and expression of uracil-DNA glycosylase and O^6-methylguanine-DNA methyltransferase in mammalian cells
1993	Tor Fredrik Næsje	Dr. scient Zoology	Habitat shifts in coregonids.
1993	Yngvar Asbjørn Olsen	Dr. scient Zoology	Cortisol dynamics in Atlantic salmon, *Salmo salar* L.: Basal and stressor-induced variations in plasma levels ans some secondary effects.
1993	Bård Pedersen	Dr. scient Botany	Theoretical studies of life history evolution in modular and clonal organisms
1993	Ole Petter Thangstad	Dr. scient Botany	Molecular studies of myrosinase in Brassicaceae
1993	Thrine L. M. Heggberget	Dr. scient Zoology	Reproductive strategy and feeding ecology of the Eurasian otter *Lutra lutra*.
1993	Kjetil Bevanger	Dr. scient Zoology	Avian interactions with utility structures, a biological approach.
1993	Kåre Haugan	Dr. scient Botany	Mutations in the replication control gene trfA of the broad host-range plasmid RK2
1994	Peder Fiske	Dr. scient Zoology	Sexual selection in the lekking great snipe (*Gallinago media*): Male mating success and female behaviour at the lek
1994	Kjell Inge Reitan	Dr. scient Botany	Nutritional effects of algae in first-feeding of marine fish larvae
1994	Nils Røv	Dr. scient Zoology	Breeding distribution, population status and regulation of breeding numbers in the northeast-Atlantic Great Cormorant *Phalacrocorax carbo carbo*
1994	Annette-Susanne Hoepfner	Dr. scient Botany	Tissue culture techniques in propagation and breeding of Red Raspberry (*Rubus idaeus* L.)
1994	Inga Elise Bruteig	Dr. scient Botany	Distribution, ecology and biomonitoring studies of epiphytic lichens on conifers

1994	Geir Johnsen	Dr. scient Botany	Light harvesting and utilization in marine phytoplankton: Species-specific and photoadaptive responses
1994	Morten Bakken	Dr. scient Zoology	Infanticidal behaviour and reproductive performance in relation to competition capacity among farmed silver fox vixens, *Vulpes vulpes*
1994	Arne Moksnes	Dr. philos Zoology	Host adaptations towards brood parasitism by the Cockoo
1994	Solveig Bakken	Dr. scient Botany	Growth and nitrogen status in the moss *Dicranum majus* Sm. as influenced by nitrogen supply
1994	Torbjørn Forseth	Dr. scient Zoology	Bioenergetics in ecological and life history studies of fishes.
1995	Olav Vadstein	Dr. philos Botany	The role of heterotrophic planktonic bacteria in the cycling of phosphorus in lakes: Phosphorus requirement, competitive ability and food web interactions
1995	Hanne Christensen	Dr. scient Zoology	Determinants of Otter *Lutra lutra* distribution in Norway: Effects of harvest, polychlorinated biphenyls (PCBs), human population density and competition with mink *Mustela vision*
1995	Svein Håkon Lorentsen	Dr. scient Zoology	Reproductive effort in the Antarctic Petrel *Thalassoica antarctica*; the effect of parental body size and condition
1995	Chris Jørgen Jensen	Dr. scient Zoology	The surface electromyographic (EMG) amplitude as an estimate of upper trapezius muscle activity
1995	Martha Kold Bakkevig	Dr. scient Zoology	The impact of clothing textiles and construction in a clothing system on thermoregulatory responses, sweat accumulation and heat transport
1995	Vidar Moen	Dr. scient Zoology	Distribution patterns and adaptations to light in newly introduced populations of *Mysis relicta* and constraints on Cladoceran and Char populations
1995	Hans Haavardsholm Blom	Dr. philos Botany	A revision of the *Schistidium apocarpum* complex in Norway and Sweden
1996	Jorun Skjærmo	Dr. scient Botany	Microbial ecology of early stages of cultivated marine fish; inpact fish-bacterial interactions on growth and survival of larvae
1996	Ola Ugedal	Dr. scient Zoology	Radiocesium turnover in freshwater fishes
1996	Ingibjørg Einarsdottir	Dr. scient Zoology	Production of Atlantic salmon (*Salmo salar*) and Arctic charr (*Salvelinus alpinus*): A study of some physiological and immunological responses to rearing routines
1996	Christina M. S. Pereira	Dr. scient Zoology	Glucose metabolism in salmonids: Dietary effects and hormonal regulation
1996	Jan Fredrik Børseth	Dr. scient Zoology	The sodium energy gradients in muscle cells of *Mytilus edulis* and the effects of organic xenobiotics
1996	Gunnar Henriksen	Dr. scient Zoology	Status of Grey seal *Halichoerus grypus* and Harbour seal *Phoca vitulina* in the Barents sea region
1997	Gunvor Øie	Dr. scient Botany	Eevalution of rotifer *Brachionus plicatilis* quality in early first feeding of turbot *Scophtalmus maximus* L. larvae
1997	Håkon Holien	Dr. scient Botany	Studies of lichens in spurce forest of Central Norway. Diversity, old growth species and the relationship to site and stand parameters

1997	Ole Reitan	Dr. scient Zoology	Responses of birds to habitat disturbance due to damming
1997	Jon Arne Grøttum	Dr. scient Zoology	Physiological effects of reduced water quality on fish in aquaculture
1997	Per Gustav Thingstad	Dr. scient Zoology	Birds as indicators for studying natural and human-induced variations in the environment, with special emphasis on the suitability of the Pied Flycatcher
1997	Torgeir Nygård	Dr. scient Zoology	Temporal and spatial trends of pollutants in birds in Norway: Birds of prey and Willow Grouse used as
1997	Signe Nybø	Dr. scient Zoology	Impacts of long-range transported air pollution on birds with particular reference to the dipper *Cinclus cinclus* in southern Norway
1997	Atle Wibe	Dr. scient Zoology	Identification of conifer volatiles detected by receptor neurons in the pine weevil (*Hylobius abietis*), analysed by gas chromatography linked to electrophysiology and to mass spectrometry
1997	Rolv Lundheim	Dr. scient Zoology	Adaptive and incidental biological ice nucleators
1997	Arild Magne Landa	Dr. scient Zoology	Wolverines in Scandinavia: ecology, sheep depredation and conservation
1997	Kåre Magne Nielsen	Dr. scient Botany	An evolution of possible horizontal gene transfer from plants to sail bacteria by studies of natural transformation in *Acinetobacter calcoacetius*
1997	Jarle Tufto	Dr. scient Zoology	Gene flow and genetic drift in geographically structured populations: Ecological, population genetic, and statistical models
1997	Trygve Hesthagen	Dr. philos Zoology	Population responces of Arctic charr (*Salvelinus alpinus* (L.)) and brown trout (*Salmo trutta* L.) to acidification in Norwegian inland waters
1997	Trygve Sigholt	Dr. philos Zoology	Control of Parr-smolt transformation and seawater tolerance in farmed Atlantic Salmon (*Salmo salar*) Effects of photoperiod, temperature, gradual seawater acclimation, NaCl and betaine in the diet
1997	Jan Østnes	Dr. scient Zoology	Cold sensation in adult and neonate birds
1998	Seethaledsumy Visvalingam	Dr. scient Botany	Influence of environmental factors on myrosinases and myrosinase-binding proteins
1998	Thor Harald Ringsby	Dr. scient Zoology	Variation in space and time: The biology of a House sparrow metapopulation
1998	Erling Johan Solberg	Dr. scient Zoology	Variation in population dynamics and life history in a Norwegian moose (*Alces alces*) population: consequences of harvesting in a variable environment
1998	Sigurd Mjøen Saastad	Dr. scient Botany	Species delimitation and phylogenetic relationships between the Sphagnum recurvum complex (Bryophyta): genetic variation and phenotypic plasticity
1998	Bjarte Mortensen	Dr. scient Botany	Metabolism of volatile organic chemicals (VOCs) in a head liver S9 vial equilibration system in vitro
1998	Gunnar Austrheim	Dr. scient Botany	Plant biodiversity and land use in subalpine grasslands. – A conservtaion biological approach
1998	Bente Gunnveig Berg	Dr. scient Zoology	Encoding of pheromone information in two related moth species
1999	Kristian Overskaug	Dr. scient Zoology	Behavioural and morphological characteristics in Northern Tawny Owls *Strix aluco*: An intra- and interspecific comparative approach

1999	Hans Kristen Stenøien	Dr. scient Botany	Genetic studies of evolutionary processes in various populations of nonvascular plants (mosses, liverworts and hornworts)
1999	Trond Arnesen	Dr. scient Botany	Vegetation dynamics following trampling and burning in the outlying haylands at Sølendet, Central Norway
1999	Ingvar Stenberg	Dr. scient Zoology	Habitat selection, reproduction and survival in the White-backed Woodpecker *Dendrocopos leucotos*
1999	Stein Olle Johansen	Dr. scient Botany	A study of driftwood dispersal to the Nordic Seas by dendrochronology and wood anatomical analysis
1999	Trina Falck Galloway	Dr. scient Zoology	Muscle development and growth in early life stages of the Atlantic cod (*Gadus morhua* L.) and Halibut (*Hippoglossus hippoglossus* L.)
1999	Marianne Giæver	Dr. scient Zoology	Population genetic studies in three gadoid species: blue whiting (*Micromisistius poutassou*), haddock (*Melanogrammus aeglefinus*) and cod (*Gradus morhua*) in the North-East Atlantic
1999	Hans Martin Hanslin	Dr. scient Botany	The impact of environmental conditions of density dependent performance in the boreal forest bryophytes *Dicranum majus*, *Hylocomium splendens*, *Plagiochila asplenigides*, *Ptilium crista-castrensis* and *Rhytidiadelphus lokeus*
1999	Ingrid Bysveen Mjølnerød	Dr. scient Zoology	Aspects of population genetics, behaviour and performance of wild and farmed Atlantic salmon (*Salmo salar*) revealed by molecular genetic techniques
1999	Else Berit Skagen	Dr. scient Botany	The early regeneration process in protoplasts from *Brassica napus* hypocotyls cultivated under various g-forces
1999	Stein-Are Sæther	Dr. philos Zoology	Mate choice, competition for mates, and conflicts of interest in the Lekking Great Snipe
1999	Katrine Wangen Rustad	Dr. scient Zoology	Modulation of glutamatergic neurotransmission related to cognitive dysfunctions and Alzheimer's disease
1999	Per Terje Smiseth	Dr. scient Zoology	Social evolution in monogamous families:
1999	Gunnbjørn Bremset	Dr. scient Zoology	Young Atlantic salmon (*Salmo salar* L.) and Brown trout (*Salmo trutta* L.) inhabiting the deep pool habitat, with special reference to their habitat use, habitat preferences and competitive interactions
1999	Frode Ødegaard	Dr. scient Zoology	Host spesificity as parameter in estimates of arhrophod species richness
1999	Sonja Andersen	Dr. scient Zoology	Expressional and functional analyses of human, secretory phospholipase A2
2000	Ingrid Salvesen	Dr. scient Botany	Microbial ecology in early stages of marine fish: Development and evaluation of methods for microbial management in intensive larviculture
2000	Ingar Jostein Øien	Dr. scient Zoology	The Cuckoo (*Cuculus canorus*) and its host: adaptions and counteradaptions in a coevolutionary arms race
2000	Pavlos Makridis	Dr. scient Botany	Methods for the microbial econtrol of live food used for the rearing of marine fish larvae
2000	Sigbjørn Stokke	Dr. scient Zoology	Sexual segregation in the African elephant (*Loxodonta africana*)
2000	Odd A. Gulseth	Dr. philos Zoology	Seawater tolerance, migratory behaviour and growth of Charr, (*Salvelinus alpinus*), with emphasis on the high Arctic Dieset charr on Spitsbergen, Svalbard

2000	Pål A. Olsvik	Dr. scient Zoology	Biochemical impacts of Cd, Cu and Zn on brown trout (*Salmo trutta*) in two mining-contaminated rivers in Central Norway
2000	Sigurd Einum	Dr. scient Zoology	Maternal effects in fish: Implications for the evolution of breeding time and egg size
2001	Jan Ove Evjemo	Dr. scient Zoology	Production and nutritional adaptation of the brine shrimp *Artemia* sp. as live food organism for larvae of marine cold water fish species
2001	Olga Hilmo	Dr. scient Botany	Lichen response to environmental changes in the managed boreal forset systems
2001	Ingebrigt Uglem	Dr. scient Zoology	Male dimorphism and reproductive biology in corkwing wrasse (*Symphodus melops* L.)
2001	Bård Gunnar Stokke	Dr. scient Zoology	Coevolutionary adaptations in avian brood parasites and their hosts
2002	Ronny Aanes	Dr. scient Zoology	Spatio-temporal dynamics in Svalbard reindeer (*Rangifer tarandus platyrhynchus*)
2002	Mariann Sandsund	Dr. scient Zoology	Exercise- and cold-induced asthma. Respiratory and thermoregulatory responses
2002	Dag-Inge Øien	Dr. scient Botany	Dynamics of plant communities and populations in boreal vegetation influenced by scything at Sølendet, Central Norway
2002	Frank Rosell	Dr. scient Zoology	The function of scent marking in beaver (*Castor fiber*)
2002	Janne Østvang	Dr. scient Botany	The Role and Regulation of Phospholipase A_2 in Monocytes During Atherosclerosis Development
2002	Terje Thun	Dr. philos Biology	Dendrochronological constructions of Norwegian conifer chronologies providing dating of historical material
2002	Birgit Hafjeld Borgen	Dr. scient Biology	Functional analysis of plant idioblasts (Myrosin cells) and their role in defense, development and growth
2002	Bård Øyvind Solberg	Dr. scient Biology	Effects of climatic change on the growth of dominating tree species along major environmental gradients
2002	Per Winge	Dr. scient Biology	The evolution of small GTP binding proteins in cellular organisms. Studies of RAC GTPases in *Arabidopsis thaliana* and the Ral GTPase from *Drosophila melanogaster*
2002	Henrik Jensen	Dr. scient Biology	Causes and consequenses of individual variation in fitness-related traits in house sparrows
2003	Jens Rohloff	Dr. philos Biology	Cultivation of herbs and medicinal plants in Norway – Essential oil production and quality control
2003	Åsa Maria O. Espmark Wibe	Dr. scient Biology	Behavioural effects of environmental pollution in threespine stickleback *Gasterosteus aculeatur* L.
2003	Dagmar Hagen	Dr. scient Biology	Assisted recovery of disturbed arctic and alpine vegetation – an integrated approach
2003	Bjørn Dahle	Dr. scient Biology	Reproductive strategies in Scandinavian brown bears
2003	Cyril Lebogang Taolo	Dr. scient Biology	Population ecology, seasonal movement and habitat use of the African buffalo (*Syncerus caffer*) in Chobe National Park, Botswana
2003	Marit Stranden	Dr. scient Biology	Olfactory receptor neurones specified for the same odorants in three related Heliothine species (*Helicoverpa armigera, Helicoverpa assulta* and *Heliothis virescens*)
2003	Kristian Hassel	Dr. scient Biology	Life history characteristics and genetic variation in an expanding species, *Pogonatum dentatum*

2003	David Alexander Rae	Dr. scient Biology	Plant- and invertebrate-community responses to species interaction and microclimatic gradients in alpine and Artic environments
2003	Åsa A Borg	Dr. scient Biology	Sex roles and reproductive behaviour in gobies and guppies: a female perspective
2003	Eldar Åsgard Bendiksen	Dr. scient Biology	Environmental effects on lipid nutrition of farmed Atlantic salmon (*Salmo Salar* L.) parr and smolt
2004	Torkild Bakken	Dr. scient Biology	A revision of Nereidinae (Polychaeta, Nereididae)
2004	Ingar Pareliussen	Dr. scient Biology	Natural and Experimental Tree Establishment in a Fragmented Forest, Ambohitantely Forest Reserve, Madagascar
2004	Tore Brembu	Dr. scient Biology	Genetic, molecular and functional studies of RAC GTPases and the WAVE-like regulatory protein complex in *Arabidopsis thaliana*
2004	Liv S. Nilsen	Dr. scient Biology	Coastal heath vegetation on central Norway; recent past, present state and future possibilities
2004	Hanne T. Skiri	Dr. scient Biology	Olfactory coding and olfactory learning of plant odours in heliothine moths. An anatomical, physiological and behavioural study of three related species (*Heliothis virescens, Helicoverpa armigera* and *Helicoverpa assulta*)
2004	Lene Østby	Dr. scient Biology	Cytochrome P4501A (CYP1A) induction and DNA adducts as biomarkers for organic pollution in the natural environment
2004	Emmanuel J. Gerreta	Dr. philos Biology	The Importance of Water Quality and Quantity in the Tropical Ecosystems, Tanzania
2004	Linda Dalen	Dr. scient Biology	Dynamics of Mountain Birch Treelines in the Scandes Mountain Chain, and Effects of Climate Warming
2004	Lisbeth Mehli	Dr. scient Biology	Polygalacturonase-inhibiting protein (PGIP) in cultivated strawberry (*Fragaria* x *ananassa*): characterisation and induction of the gene following fruit infection by *Botrytis cinerea*
2004	Børge Moe	Dr. scient Biology	Energy-Allocation in Avian Nestlings Facing Short-Term Food Shortage
2005	Matilde Skogen Chauton	Dr. scient Biology	Metabolic profiling and species discrimination from High-Resolution Magic Angle Spinning NMR analysis of whole-cell samples
2005	Sten Karlsson	Dr. scient Biology	Dynamics of Genetic Polymorphisms
2005	Terje Bongard	Dr. scient Biology	Life History strategies, mate choice, and parental investment among Norwegians over a 300-year period
2005	Tonette Røstelien	PhD Biology	Functional characterisation of olfactory receptor neurone types in heliothine moths
2005	Erlend Kristiansen	Dr. scient Biology	Studies on antifreeze proteins
2005	Eugen G. Sørmo	Dr. scient Biology	Organochlorine pollutants in grey seal (*Halichoerus grypus*) pups and their impact on plasma thyrid hormone and vitamin A concentrations
2005	Christian Westad	Dr. scient Biology	Motor control of the upper trapezius
2005	Lasse Mork Olsen	PhD Biology	Interactions between marine osmo- and phagotrophs in different physicochemical environments
2005	Åslaug Viken	PhD Biology	Implications of mate choice for the management of small populations

2005	Ariaya Hymete Sahle Dingle	PhD Biology	Investigation of the biological activities and chemical constituents of selected *Echinops* spp. growing in Ethiopia
2005	Anders Gravbrøt Finstad	PhD Biology	Salmonid fishes in a changing climate: The winter challenge
2005	Shimane Washington Makabu	PhD Biology	Interactions between woody plants, elephants and other browsers in the Chobe Riverfront, Botswana
2005	Kjartan Østbye	Dr. scient Biology	The European whitefish *Coregonus lavaretus* (L.) species complex: historical contingency and adaptive radiation
2006	Kari Mette Murvoll	PhD Biology	Levels and effects of persistent organic pollutans (POPs) in seabirds, Retinoids and α-tocopherol – potential biomakers of POPs in birds?
2006	Ivar Herfindal	Dr. scient Biology	Life history consequences of environmental variation along ecological gradients in northern ungulates
2006	Nils Egil Tokle	PhD Biology	Are the ubiquitous marine copepods limited by food or predation? Experimental and field-based studies with main focus on *Calanus finmarchicus*
2006	Jan Ove Gjershaug	Dr. philos Biology	Taxonomy and conservation status of some booted eagles in south-east Asia
2006	Jon Kristian Skei	Dr. scient Biology	Conservation biology and acidification problems in the breeding habitat of amphibians in Norway
2006	Johanna Järnegren	PhD Biology	Acesta Oophaga and Acesta Excavata – a study of hidden biodiversity
2006	Bjørn Henrik Hansen	PhD Biology	Metal-mediated oxidative stress responses in brown trout (*Salmo trutta*) from mining contaminated rivers in Central Norway
2006	Vidar Grøtan	PhD Biology	Temporal and spatial effects of climate fluctuations on population dynamics of vertebrates
2006	Jafari R Kideghesho	PhD Biology	Wildlife conservation and local land use conflicts in western Serengeti, Corridor Tanzania
2006	Anna Maria Billing	PhD Biology	Reproductive decisions in the sex role reversed pipefish *Syngnathus typhle*: when and how to invest in reproduction
2006	Henrik Pärn	PhD Biology	Female ornaments and reproductive biology in the bluethroat
2006	Anders J. Fjellheim	PhD Biology	Selection and administration of probiotic bacteria to marine fish larvae
2006	P. Andreas Svensson	PhD Biology	Female coloration, egg carotenoids and reproductive success: gobies as a model system
2007	Sindre A. Pedersen	PhD Biology	Metal binding proteins and antifreeze proteins in the beetle *Tenebrio molitor* - a study on possible competition for the semi-essential amino acid cysteine
2007	Kasper Hancke	PhD Biology	Photosynthetic responses as a function of light and temperature: Field and laboratory studies on marine microalgae
2007	Tomas Holmern	PhD Biology	Bushmeat hunting in the western Serengeti: Implications for community-based conservation
2007	Kari Jørgensen	PhD Biology	Functional tracing of gustatory receptor neurons in the CNS and chemosensory learning in the moth *Heliothis virescens*
2007	Stig Ulland	PhD Biology	Functional Characterisation of Olfactory Receptor Neurons in the Cabbage Moth, (*Mamestra brassicae* L.) (Lepidoptera, Noctuidae). Gas Chromatography

			Linked to Single Cell Recordings and Mass Spectrometry
2007	Snorre Henriksen	PhD Biology	Spatial and temporal variation in herbivore resources at northern latitudes
2007	Roelof Frans May	PhD Biology	Spatial Ecology of Wolverines in Scandinavia
2007	Vedasto Gabriel Ndibalema	PhD Biology	Demographic variation, distribution and habitat use between wildebeest sub-populations in the Serengeti National Park, Tanzania
2007	Julius William Nyahongo	PhD Biology	Depredation of Livestock by wild Carnivores and Illegal Utilization of Natural Resources by Humans in the Western Serengeti, Tanzania
2007	Shombe Ntaraluka Hassan	PhD Biology	Effects of fire on large herbivores and their forage resources in Serengeti, Tanzania
2007	Per-Arvid Wold	PhD Biology	Functional development and response to dietary treatment in larval Atlantic cod *(Gadus morhua* L.) Focus on formulated diets and early weaning
2007	Anne Skjetne Mortensen	PhD Biology	Toxicogenomics of Aryl Hydrocarbon- and Estrogen Receptor Interactions in Fish: Mechanisms and Profiling of Gene Expression Patterns in Chemical Mixture Exposure Scenarios
2008	Brage Bremset Hansen	PhD Biology	The Svalbard reindeer (*Rangifer tarandus platyrhynchus*) and its food base: plant-herbivore interactions in a high-arctic ecosystem
2008	Jiska van Dijk	PhD Biology	Wolverine foraging strategies in a multiple-use landscape
2008	Flora John Magige	PhD Biology	The ecology and behaviour of the Masai Ostrich (Struthio camelus massaicus) in the Serengeti Ecosystem, Tanzania
2008	Bernt Rønning	PhD Biology	Sources of inter- and intra-individual variation in basal metabolic rate in the zebra finch, (*Taeniopygia guttata*)
2008	Sølvi Wehn	PhD Biology	Biodiversity dynamics in semi-natural mountain landscapes - A study of consequences of changed agricultural practices in Eastern Jotunheimen
2008	Trond Moxness Kortner	PhD Biology	"The Role of Androgens on previtellogenic oocyte growth in Atlantic cod (*Gadus morhua*): Identification and patterns of differentially expressed genes in relation to Stereological Evaluations"
2008	Katarina Mariann Jørgensen	Dr. scient Biology	The role of platelet activating factor in activation of growth arrested keratinocytes and re-epithelialisation
2008	Tommy Jørstad	PhD Biology	Statistical Modelling of Gene Expression Data
2008	Anna Kusnierczyk	PhD Biology	*Arabidopsis thaliana* Responses to Aphid Infestation
2008	Jussi Evertsen	PhD Biology	Herbivore sacoglossans with photosynthetic chloroplasts
2008	John Eilif Hermansen	PhD Biology	Mediating ecological interests between locals and globals by means of indicators. A study attributed to the asymmetry between stakeholders of tropical forest at Mt. Kilimanjaro, Tanzania
2008	Ragnhild Lyngved	PhD Biology	Somatic embryogenesis in *Cyclamen persicum*. Biological investigations and educational aspects of cloning
2008	Line Elisabeth Sundt-Hansen	PhD Biology	Cost of rapid growth in salmonid fishes

2008	Line Johansen	PhD Biology	Exploring factors underlying fluctuations in white clover populations – clonal growth, population structure and spatial distribution
2009	Astrid Jullumstrø Feuerherm	PhD Biology	Elucidation of molecular mechanisms for pro-inflammatory phospholipase A2 in chronic disease
2009	Pål Kvello	PhD Biology	Neurons forming the network involved in gustatory coding and learning in the moth *Heliothis virescens:* Physiological and morphological characterisation, and integration into a standard brain atlas
2009	Trygve Devold Kjellsen	PhD Biology	Extreme Frost Tolerance in Boreal Conifers
2009	Johan Reinert Vikan	PhD Biology	Coevolutionary interactions between common cuckoos *Cuculus canorus* and *Fringilla* finches
2009	Zsolt Volent	PhD Biology	Remote sensing of marine environment: Applied surveillance with focus on optical properties of phytoplankton, coloured organic matter and suspended matter
2009	Lester Rocha	PhD Biology	Functional responses of perennial grasses to simulated grazing and resource availability
2009	Dennis Ikanda	PhD Biology	Dimensions of a Human-lion conflict: Ecology of human predation and persecution of African lions (*Panthera leo*) in Tanzania
2010	Huy Quang Nguyen	PhD Biology	Egg characteristics and development of larval digestive function of cobia (*Rachycentron canadum*) in response to dietary treatments - Focus on formulated diets
2010	Eli Kvingedal	PhD Biology	Intraspecific competition in stream salmonids: the impact of environment and phenotype
2010	Sverre Lundemo	PhD Biology	Molecular studies of genetic structuring and demography in *Arabidopsis* from Northern Europe
2010	Iddi Mihijai Mfunda	PhD Biology	Wildlife Conservation and People's livelihoods: Lessons Learnt and Considerations for Improvements. Tha Case of Serengeti Ecosystem, Tanzania
2010	Anton Tinchov Antonov	PhD Biology	Why do cuckoos lay strong-shelled eggs? Tests of the puncture resistance hypothesis
2010	Anders Lyngstad	PhD Biology	Population Ecology of *Eriophorum latifolium*, a Clonal Species in Rich Fen Vegetation
2010	Hilde Færevik	PhD Biology	Impact of protective clothing on thermal and cognitive responses
2010	Ingerid Brænne Arbo	PhD Medical technology	Nutritional lifestyle changes – effects of dietary carbohydrate restriction in healthy obese and overweight humans
2010	Yngvild Vindenes	PhD Biology	Stochastic modeling of finite populations with individual heterogeneity in vital parameters
2010	Hans-Richard Brattbakk	PhD Medical technology	The effect of macronutrient composition, insulin stimulation, and genetic variation on leukocyte gene expression and possible health benefits
2011	Geir Hysing Bolstad	PhD Biology	Evolution of Signals: Genetic Architecture, Natural Selection and Adaptive Accuracy
2011	Karen de Jong	PhD Biology	Operational sex ratio and reproductive behaviour in the two-spotted goby (*Gobiusculus flavescens*)
2011	Ann-Iren Kittang	PhD Biology	*Arabidopsis thaliana* L. adaptation mechanisms to microgravity through the EMCS MULTIGEN-2 experiment on the ISS:– The science of space experiment integration and adaptation to simulated microgravity

2011	Aline Magdalena Lee	PhD Biology	Stochastic modeling of mating systems and their effect on population dynamics and genetics
2011	Christopher Gravningen Sørmo	PhD Biology	Rho GTPases in Plants: Structural analysis of ROP GTPases; genetic and functional studies of MIRO GTPases in Arabidopsis thaliana
2011	Grethe Robertsen	PhD Biology	Relative performance of salmonid phenotypes across environments and competitive intensities
2011	Line-Kristin Larsen	PhD Biology	Life-history trait dynamics in experimental populations of guppy (*Poecilia reticulata*): the role of breeding regime and captive environment
2011	Maxim A. K. Teichert	PhD Biology	Regulation in Atlantic salmon (*Salmo salar*): The interaction between habitat and density
2011	Torunn Beate Hancke	PhD Biology	Use of Pulse Amplitude Modulated (PAM) Fluorescence and Bio-optics for Assessing Microalgal Photosynthesis and Physiology
2011	Sajeda Begum	PhD Biology	Brood Parasitism in Asian Cuckoos: Different Aspects of Interactions between Cuckoos and their Hosts in Bangladesh
2011	Kari J. K. Attramadal	PhD Biology	Water treatment as an approach to increase microbial control in the culture of cold water marine larvae
2011	Camilla Kalvatn Egset	PhD Biology	The Evolvability of Static Allometry: A Case Study
2011	AHM Raihan Sarker	PhD Biology	Conflict over the conservation of the Asian elephant (*Elephas maximus*) in Bangladesh
2011	Gro Dehli Villanger	PhD Biology	Effects of complex organohalogen contaminant mixtures on thyroid hormone homeostasis in selected arctic marine mammals
2011	Kari Bjørneraas	PhD Biology	Spatiotemporal variation in resource utilisation by a large herbivore, the moose
2011	John Odden	PhD Biology	The ecology of a conflict: Eurasian lynx depredation on domestic sheep
2011	Simen Pedersen	PhD Biology	Effects of native and introduced cervids on small mammals and birds
2011	Mohsen Falahati-Anbaran	PhD Biology	Evolutionary consequences of seed banks and seed dispersal in *Arabidopsis*
2012	Jakob Hønborg Hansen	PhD Biology	Shift work in the offshore vessel fleet: circadian rhythms and cognitive performance
2012	Elin Noreen	PhD Biology	Consequences of diet quality and age on life-history traits in a small passerine bird
2012	Irja Ida Ratikainen	PhD Biology	Foraging in a variable world:adaptions to stochasticity
2012	Aleksander Handå	PhD Biology	Cultivation of mussels (*Mytilus edulis):*Feed requirements, storage and integration with salmon (*Salmo salar*) farming
2012	Morten Kraabøl	PhD Biology	Reproductive and migratory challenges inflicted on migrant brown trour (*Salmo trutta* L) in a heavily modified river
2012	Jisca Huisman	PhD Biology	Gene flow and natural selection in Atlantic salmon
	Maria Bergvik	PhD Biology	Lipid and astaxanthin contents and biochemical post-harvest stability in *Calanus finmarchicus*
2012	Bjarte Bye Løfaldli	PhD Biology	Functional and morphological characterization of central olfactory neurons in the model insect *Heliothis virescens*.

2012	Karen Marie Hammer	PhD Biology	Acid-base regulation and metabolite responses in shallow- and deep-living marine invertebrates during environmental hypercapnia
2012	Øystein Nordrum Wiggen	PhD Biology	Optimal performance in the cold
2012	Robert Dominikus Fyumagwa	Dr. Philos Biology	Anthropogenic and natural influence on disease prevalence at the human –livestock-wildlife interface in the Serengeti ecosystem, Tanzania
2012	Jenny Bytingsvik	PhD Biology	Organohalogenated contaminants (OHCs) in polar bear mother-cub pairs from Svalbard, Norway. Maternal transfer, exposure assessment and thyroid hormone disruptive effects in polar bear cubs
2012	Christer Moe Rolandsen	PhD Biology	The ecological significance of space use and movement patterns of moose in a variable environment
2012	Erlend Kjeldsberg Hovland	PhD Biology	Bio-optics and Ecology in *Emiliania huxleyi* Blooms: Field and Remote Sensing Studies in Norwegian Waters
2012	Lise Cats Myhre	PhD Biology	Effects of the social and physical environment on mating behaviour in a marine fish
2012	Tonje Aronsen	PhD Biology	Demographic, environmental and evolutionary aspects of sexual selection
	Bin Liu	PhD Biology	Molecular genetic investigation of cell separation and cell death regulation in *Arabidopsis thaliana*
2013	Jørgen Rosvold	PhD Biology	Ungulates in a dynamic and increasingly human dominated landscape – A millennia-scale perspective
2013	Pankaj Barah	PhD Biology	Integrated Systems Approaches to Study Plant Stress Responses
2013	Marit Linnerud	PhD Biology	Patterns in spatial and temporal variation in population abundances of vertebrates
2013	Xinxin Wang	PhD Biology	Integrated multi-trophic aquaculture driven by nutrient wastes released from Atlantic salmon (*Salmo salar*) farming
2013	Ingrid Ertshus Mathisen	PhD Biology	Structure, dynamics, and regeneration capacity at the sub-arctic forest-tundra ecotone of northern Norway and Kola Peninsula, NW Russia
2013	Anders Foldvik	PhD Biology	Spatial distributions and productivity in salmonid populations
2013	Anna Marie Holand	PhD Biology	Statistical methods for estimating intra- and inter-population variation in genetic diversity
2013	Anna Solvang Båtnes	PhD Biology	Light in the dark – the role of irradiance in the high Arctic marine ecosystem during polar night
2013	Sebastian Wacker	PhD Biology	The dynamics of sexual selection: effects of OSR, density and resource competition in a fish
2013	Cecilie Miljeteig	PhD Biology	Phototaxis in *Calanus finmarchicus* – light sensitivity and the influence of energy reserves and oil exposure
2013	Ane Kjersti Vie	PhD Biology	Molecular and functional characterisation of the IDA family of signalling peptides in *Arabidopsis thaliana*
2013	Marianne Nymark	PhD Biology	Light responses in the marine diatom *Phaeodactylum tricornutum*
2014	Jannik Schultner	PhD Biology	Resource Allocation under Stress - Mechanisms and Strategies in a Long-Lived Bird
2014	Craig Ryan Jackson	PhD Biology	Factors influencing African wild dog *(Lycaon pictus*) habitat selection and ranging behaviour: conservation and management implications

2014	Aravind Venkatesan	PhD Biology	Application of Semantic Web Technology to establish knowledge management and discovery in the Life Sciences
2014	Kristin Collier Valle	PhD Biology	Photoacclimation mechanisms and light responses in marine micro- and macroalgae
2014	Michael Puffer	PhD Biology	Effects of rapidly fluctuating water levels on juvenile Atlantic salmon (*Salmo salar* L.)
2014	Gundula S. Bartzke	PhD Biology	Effects of power lines on moose *(Alces alces)* habitat selection, movements and feeding activity
2014	Eirin Marie Bjørkvoll	PhD Biology	Life-history variation and stochastic population dynamics in vertebrates
2014	Håkon Holand	PhD Biology	The parasite *Syngamus trachea* in a metapopulation of house sparrows
2014	Randi Magnus Sommerfelt	PhD Biology	Molecular mechanisms of inflammation – a central role for cytosolic phospholiphase A2
2014	Espen Lie Dahl	PhD Biology	Population demographics in white-tailed eagle at an on-shore wind farm area in coastal Norway
2014	Anders Øverby	PhD Biology	Functional analysis of the action of plant isothiocyanates: cellular mechanisms and in vivo role in plants, and anticancer activity
2014	Kamal Prasad Acharya	PhD Biology	Invasive species: Genetics, characteristics and trait variation along a latitudinal gradient.
2014	Ida Beathe Øverjordet	PhD Biology	Element accumulation and oxidative stress variables in Arctic pelagic food chains: Calanus, little auks (alle alle) and black-legged kittiwakes (Rissa tridactyla)
2014	Kristin Møller Gabrielsen	PhD Biology	Target tissue toxicity of the thyroid hormone system in two species of arctic mammals carrying high loads of organohalogen contaminants
2015	Gine Roll Skjervø	Dr. philos Biology	Testing behavioral ecology models with historical individual-based human demographic data from Norway
2015	Nils Erik Gustaf Forsberg	PhD Biology	Spatial and Temporal Genetic Structure in Landrace Cereals
2015	Leila Alipanah	PhD Biology	Integrated analyses of nitrogen and phosphorus deprivation in the diatoms *Phaeodactylum tricornutum* and *Seminavis robusta*
2015	Javad Najafi	PhD Biology	Molecular investigation of signaling components in sugar sensing and defense in *Arabidopsis thaliana*
2015	Bjørnar Sporsheim	PhD Biology	Quantitative confocal laser scanning microscopy: optimization of in vivo and in vitro analysis of intracellular transport
2015	Magni Olsen Kyrkjeeide	PhD Biology	Genetic variation and structure in peatmosses (*Sphagnum*)
2015	Keshuai Li	PhD Biology	Phospholipids in Atlantic cod (*Gadus morhua* L.) larvae rearing: Incorporation of DHA in live feed and larval phospholipids and the metabolic capabilities of larvae for the de novo synthesis
2015	Ingvild Fladvad Størdal	PhD Biology	The role of the copepod *Calanus finmarchicus* in affecting the fate of marine oil spills
2016	Thomas Kvalnes	PhD Biology	Evolution by natural selection in age-structured populations in fluctuating environments
2016	Øystein Leiknes	PhD Biology	The effect of nutrition on important life-history traits in the marine copepod *Calanus finmarchicus*

2016	Johan Henrik Hårdensson Berntsen	PhD Biology	Individual variation in survival: The effect of incubation temperature on the rate of physiological ageing in a small passerine bird
2016	Marianne Opsahl Olufsen	PhD Biology	Multiple environmental stressors: Biological interactions between parameters of climate change and perfluorinated alkyl substances in fish
2016	Rebekka Varne	PhD Biology	Tracing the fate of escaped cod (*Gadus morhua* L.) in a Norwegian fjord system
2016	Anette Antonsen Fenstad	PhD Biology	Pollutant Levels, Antioxidants and Potential Genotoxic Effects in Incubating Female Common Eiders (*Somateria mollissima*)
2016	Wilfred Njama Marealle	PhD Biology	Ecology, Behaviour and Conservation Status of Masai Giraffe (***Giraffa camelopardalis tippelskirchi***) in Tanzania
2016	Ingunn Nilssen	PhD Biology	Integrated Enviromental Mapping and Monitoring: A Methodological approach for endusers.
2017	Konika Chawla	PhD Biology	Discovering, analysing and taking care of knowledge.
2017	Øystein Hjorthol Opedal	PhD Biology	The Evolution of Herkogamy: Pollinator Reliability, Natural Selection, and Trait Evolvability.
2017	Ane Marlene Myhre	PhD Biology	Effective size of density dependent populations in fluctuating environments
2017	Emmanuel Hosiana Masenga	PhD Biology	Behavioural Ecology of Free-ranging and Reintroduced African Wild Dog (Lycaon pictus) Packs in the Serengeti Ecosystem, Tanzania